



Cessna Aircraft Company Raytheon Missile Systems AIAA Foundation

The 2008 Cessna/Raytheon Missile Systems Design/Build/Fly Competition Flyoff was held at Cessna Field in Wichita, KS on the weekend of April 18-20, 2008. This was the 12th year the competition was held, and participation continued to increase from past years. A total of 60 teams submitted written reports to be judged. At least 51 teams attended the flyoff, 47 of which completed the technical inspection. Approximately 600 students, faculty, and guests were present. Near ideal weather allowed for non-stop flights to be conducted each day. Of the 166 official flight attempts, 55 resulted in a valid score. In almost every respect, the quality of the teams, their readiness to compete, and the execution of the flights was better than in any past flyoff. A historical perspective of participation is shown below.

The primary design objective for this year was to accommodate a random payload combination composed of passengers (1/2 liter water bottles) and cargo pallets (1/2 size bricks). A delivery flight was first required, where the airplane was flown with no payload. The flight score was determined by the number of laps flown in a five minute period, divided by the battery pack weight for that flight. For the payload flights, teams were assigned a payload manifest determined at random, and the payload loading was timed. The airplane then had to fly two laps of the course to make the score valid. The payload flight score was determined by the inverted product of the loading time, battery weight, and empty weight. Total flight score was the sum of the delivery flight score plus up to two payload flight scores. As usual, the total score is the product of the flight score and written report score. More details can be found at the competition website: <http://www.ae.uiuc.edu/aiaadbfbf>

The top places were taken by teams from two universities: Oklahoma State and U. Texas at Austin. OSU Team Black scored first place with an excellent written report score, very low System Weight, and two of the top three flight scores. UT Austin Team Hornworks scored second, and OSU Team Orange was third. The top report score of 98% was achieved by Wichita State University Team AeroShock, and the lowest System Weight was built by Massachusetts Institute of Technology Team Cardinal. The complete standings are listed in the table below.

We owe our thanks for the success of the DBF competition to the efforts of many volunteers from Cessna Aircraft, Raytheon Missile Systems, the Naval Research Lab, and the AIAA sponsoring technical committees: Applied Aerodynamics, Aircraft Design, Flight Test, and Design Engineering. These volunteers collectively set the rules for the contest, publicize the event, gather entries, judge the written reports, and organize the flyoff. Thanks also go to the Corporate Sponsors: the Raytheon Missile Systems, Cessna Aircraft, and the AIAA Foundation for their financial support. Special thanks go to Cessna Aircraft for hosting the flyoff this year.

AIAA/Cessna/RMS

Design/Build/Fly

2007-2008

AeroShock

Design Report



Department of Aerospace Engineering

Wichita State University

March 2008



Table of Contents

Acronyms, Abbreviations, and Symbols	4
<u>1.0 Executive Summary</u>	5
<u>2.0 Management Summary</u>	6
2.1 Design Team Composition and Responsibilities.....	6
2.2 Scheduling.....	7
<u>3.0 Conceptual Design</u>	8
3.1 Mission Requirements.....	8
3.2 Scoring Analysis.....	9
3.3 Design Objectives and Requirements.....	11
3.4 Conceptual Configurations.....	11
3.5 Selection Process	12
3.5.1 Aircraft Configuration	13
3.5.2 Empennage Configuration	13
3.5.3 Landing Gear Configuration.....	14
3.5.4 Battery Configuration	14
3.5.5 Payload Arrangement	15
3.6 Conclusion.....	16
<u>4.0 Preliminary Design</u>	17
4.1 Critical Design Parameters	17
4.1.1 Aerodynamic Parameters	17
4.1.2 Propulsion Parameters.....	18
4.2 Mission Model	18
4.3 Optimization Scheme	19
4.3.1 Aerodynamics Module.....	19
4.3.2 Propulsion Module	20
4.3.3 Performance Module.....	21
4.3.4 Stability and Control Module	21
4.3.5 Weight and Structures Module.....	22
4.3.6 Flight Score Module	22
4.4 Optimization Results	22
4.5 Aerodynamic Trade Studies.....	24
4.5.1 Stagger Analysis	25
4.6 Preliminary Lift and Drag Estimates.....	26
4.7 Propulsion Trade Studies.....	27
4.8 Stability and Control Analysis.....	28



4.8.1 Stability and Control Critical Parameters	28
4.8.2 Estimated Stability Characteristics	29
4.9 Structural Analysis	30
4.9.1 Critical Design Loads and Parameters	30
4.9.2 Structural Optimization.....	30
4.10 Aircraft Performance Predictions	32
4.11 Mission Performance Prediction	34
<u>5.0 Detail Design</u>	34
5.1 Propulsion System Selection and Performance.....	34
5.2 Control Sub-System Selection	35
5.3 Aircraft Sizing	35
5.4 Aircraft Weight and Balance.....	36
5.5 Flight and Mission Performance.....	36
5.6 Structural Design and Capabilities	37
5.7 Landing Gear Selection.....	38
5.8 Payload Solution	39
5.9 Drawing Package	39
<u>6.0 Manufacturing Plan</u>	44
6.1 Manufacturing Methods and Materials.....	44
6.2 Manufacturing Methods and Materials Figure of Merit	44
6.3 Construction Process	45
6.4 Manufacturing Schedule	47
<u>7.0 Testing Plan</u>	48
7.1 Structural Testing	48
7.2 Material Testing.....	49
7.3 Propeller Testing	49
7.4 Half-Scale Wind Tunnel Testing.....	50
7.5 Propulsion System Wind Tunnel Testing	50
7.6 Full Scale Wind Tunnel Testing	51
7.7 Flight Testing.....	52
<u>8.0 Performance Results</u>	54
8.1 Propulsion System Evaluation	54
8.2 Flight Testing Evaluation	54
8.3 Wind Tunnel Study and Evaluation of Complete Aircraft.....	55
8.4 Performance Results Summary	57
<u>9.0 References</u>	57



Acronyms, Abbreviations, and Symbols

α	Angle of Attack	L	Lift Force
β	Sideslip Angle	LAPS	Lap Number (Total)
δ_a	Aileron Deflection	L/D	Lift-to-Drag Ratio
δ_e	Elevator Deflection Angle	LT	Loading Time
δ_r	Rudder Deflection Angle	MAC	Mean Aerodynamic Center
AC	Aerodynamic Center	MDO	Multidisciplinary Optimization
AOA	Angle of Attack (also α)	NiCad	Nickel Cadmium
AR	Aspect Ratio	NiMH	Nickel Metal Hydride
BW₁	Battery Weight - Delivery Mission	p	Roll Rate
BW₂	Battery Weight - Payload Mission	q	Pitch Rate
C_D	Drag Coefficient	r	Yaw Rate
C_l	Rolling Coefficient	RAC	Rated Aircraft Cost
C_L	Lift Coefficient	Re	Reynolds Number
C_M	Pitching Moment Coefficient	RMS	Raytheon Missile Systems
C_n	Yawing Coefficient	RPM	Revolutions per Minute
C_y	Sideforce Coefficient	S_a	Aileron Area
CA	Cyanoacrylate Glue	S_e	Elevator Area
CAD	Computer Aided Design	S_r	Rudder Area
CG	Center of Gravity	S_T	Horizontal Stabilizer Area
D	Drag Force	S_V	Vertical Stabilizer Area
DBF	Design/Build/Fly	S	Wing Reference Area
FEM	Finite Element Method	S&C	Stability and Control
FOM	Figure of Merit	SW	System Weight
FS	Flight Score	T/O	Takeoff
GP	Gold Peak (Battery Manufacturer)	WSU	Wichita State University
I	Current	X_{ac}	Aerodynamic Center Location
K_v	RPM/Volt Motor Constant	X-wind	Crosswind



1.0 Executive Summary

This report details the design, testing, and manufacturing processes conducted by the Wichita State University (WSU) AeroShock team in preparation for the AIAA/Cessna/RMS student Design/Build/Fly competition. The primary objective is to maximize the total score, which is comprised of a report and flight score (FS). The FS consists of two unique missions to be completed in succession: Delivery and Payload. The Delivery Mission requires the airplane to maximize the number of laps within 5 minutes using the least amount of battery weight, whereas the Payload Mission involves minimizing system and battery weight along with payload loading time. The most important competition constraints are a 75-ft takeoff distance (which is the most critical performance leg), and a 4x5-ft dimension restriction (which limits the fuselage length and wing span combination). Score analysis shows that system and battery weight combine for 61% of the Total Score, making them the most critical design variables.

Several solution concepts are proposed with a balanced wing loading and thrust-to-weight ratio to meet the design objectives and requirements previously stated. These are: a Biplane (single), a Monoplane (twin), a Tandem (single), a Canard (twin), and a Flying Wing (single). A Figure of Merit (FOM) analysis selected a single-propeller biplane wing-body with a conventional tail, a conventional/tail-dragger landing gear, and a single-stack battery configuration.

The chosen aircraft has a low wing loading which reduces the amount of thrust and battery weight required to meet the takeoff distance. The conventional tail provides formidable stability characteristics at a low weight. The conventional landing gear is light and improves field length performance due to its inherent angle of attack (AOA). The single-stack battery configuration is chosen due to its high power to weight ratio. In addition, top loading is implemented to reduce loading times, and composite manufacturing is used to reduce system weight.

A Multidisciplinary Optimization (MDO) program analyzes different combinations of the critical design variables, which include: wing area, span and airfoil, motor, propeller, and battery selection. The wings are sized to a 4.83-ft wingspan, with a total wing area of 9.67 ft² and a SD7062 airfoil. An inverted NACA 2408 airfoil is selected for the horizontal tail, while a flat plate is used for the vertical. Propulsion optimization suggests that a NEU 1506/3Y motor geared 5.2:1 performs optimally for both missions. For the Delivery Mission, 12 Elite 1700 cells and an 18x10E propeller yield the highest score. On the other hand, 18 GP 2000 cells with a 19x10E propeller are optimal for the Payload Mission.

The following performance capabilities are predicted for the Delivery and Payload Missions, respectively: a takeoff distance of 46 / 71-ft, a stall speed of 22 / 35-ft/s, a cruise speed of 40 / 50-ft/s, and a maximum speed of 59 / 75-ft/s. AeroShock is expected to complete 3 laps in the Delivery Mission with a battery weight of 0.75-lb, for a score of 4 laps/lb. The Payload Mission RAC is 7.2 lb², with a battery weight of 1.5-lb. The loading time is estimated at 15 seconds on average, which yields a score of 0.0093 (lb²•sec)⁻¹ per flight.



2.0 Management Summary

The team organization is based on a hierarchical structure to encourage dynamic involvement among all the members.

2.1 Design Team Composition and Responsibilities

Team AeroShock consists of 14 WSU aerospace engineering students ranging from freshman to graduate. The team includes: 5 seniors, each with a primary and secondary design responsibility, 1 graduate student advisor, and 8 underclassmen who help with manufacturing, flight testing, and payload. Each senior student is assigned to a technical group based on his individual interests, knowledge, and experience. The organizational chart is shown in Figure 2.1.

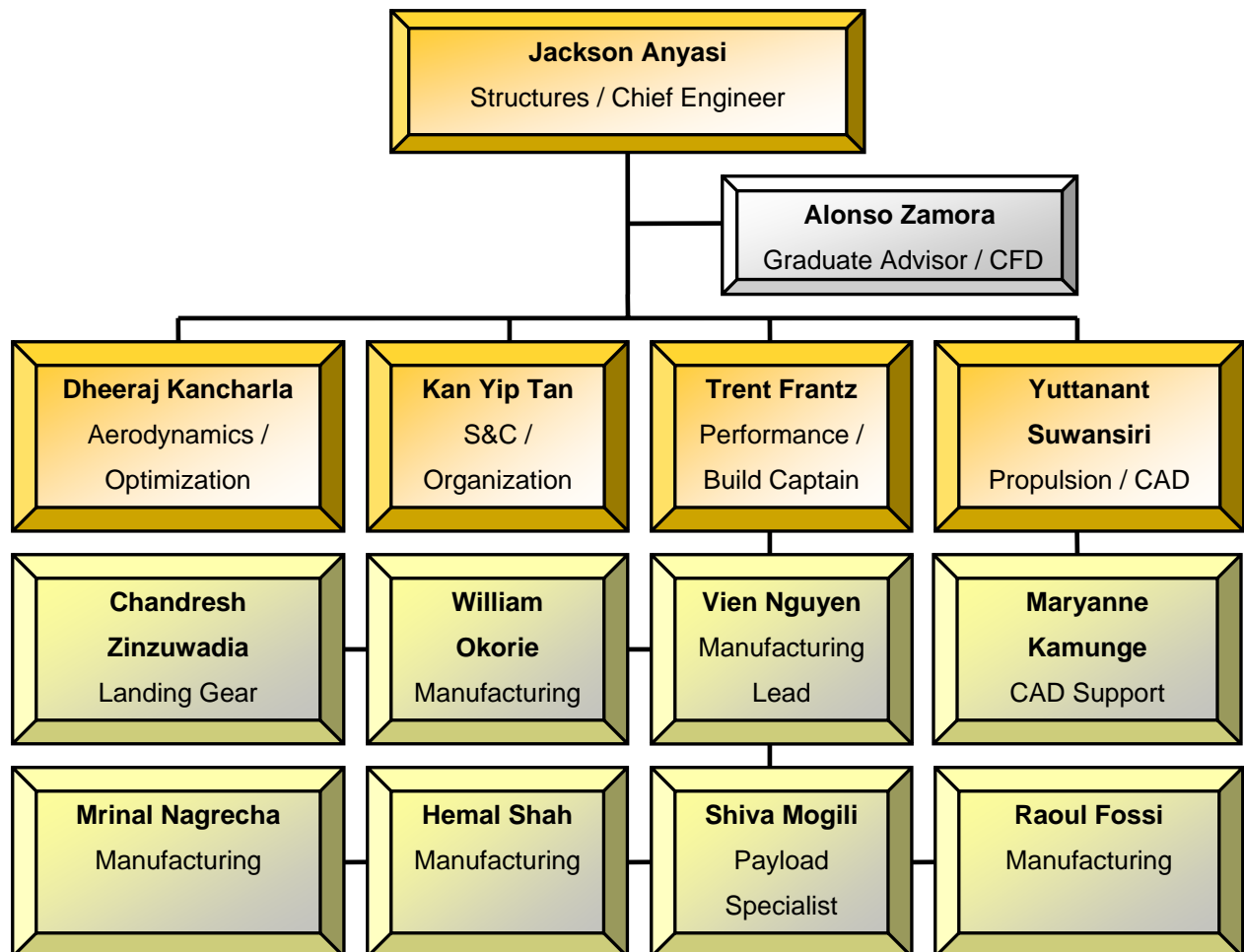


Figure 2.1 – Team Organization Chart



The Graduate advisor is a former member of the 2006/07 Wichita State DBF entry, “Shockin’ Surveyor”¹. He supervises design development, suggests improvements, and participates in the manufacturing and testing processes. The five main technical groups are:

- **Aerodynamics:** Responsible for aerodynamic force resolution, airfoil selection, wing sizing, wind tunnel testing, and programming for the Aerodynamics Module.
- **Propulsion:** In charge of propeller testing, coding for the Propulsion Module, and selection of components such as motor, batteries, and propellers. Also conducts wind tunnel testing on the optimized propulsion system to validate calculations.
- **Structures:** Responsible for laying out the overall aircraft’s internal and external design, selecting materials, and preparing a manufacturing scheme. Other responsibilities include structural and material testing.
- **S&C:** Acquires accurate weight estimates to assess longitudinal and lateral-directional stability. Other duties include: control surface sizing, servo selection, evaluation of X-wind capabilities, and investigation of dynamic stability modes.
- **Performance:** Evaluates the impact and interfacing of decisions made by other technical groups on the aircraft flying qualities, and suggests improvements to maximize the FS. Other tasks include coding and estimation of aircraft performance parameters for each flying mission, as well as the preparation of a detailed mission profile including time, current, and energy.

The senior student’s secondary roles are:

- **Chief Engineer:** Works dynamically among the other engineering groups to promote effective collaboration and to ensure a steady pace for the design effort.
- **Optimization:** Oversees MDO coding and all optimization efforts.
- **Organization:** Schedules team meetings, collaborates with undergraduate members, and monitors the overall design pace.
- **Build Captain:** Prepares the construction schedule, designates responsibilities, and oversees manufacturing efforts.
- **CAD Lead:** Responsible for organizing all Computer Aided Design (CAD) efforts.

2.2 Scheduling

The first team meeting occurred in August 2007. The design project was set to span over an 8-month period, and a competitive schedule was created and adopted with fixed dates and milestones. The following Gantt chart demonstrates the team schedule, showing planned and actual timing of the design, fabrication, and testing processes.

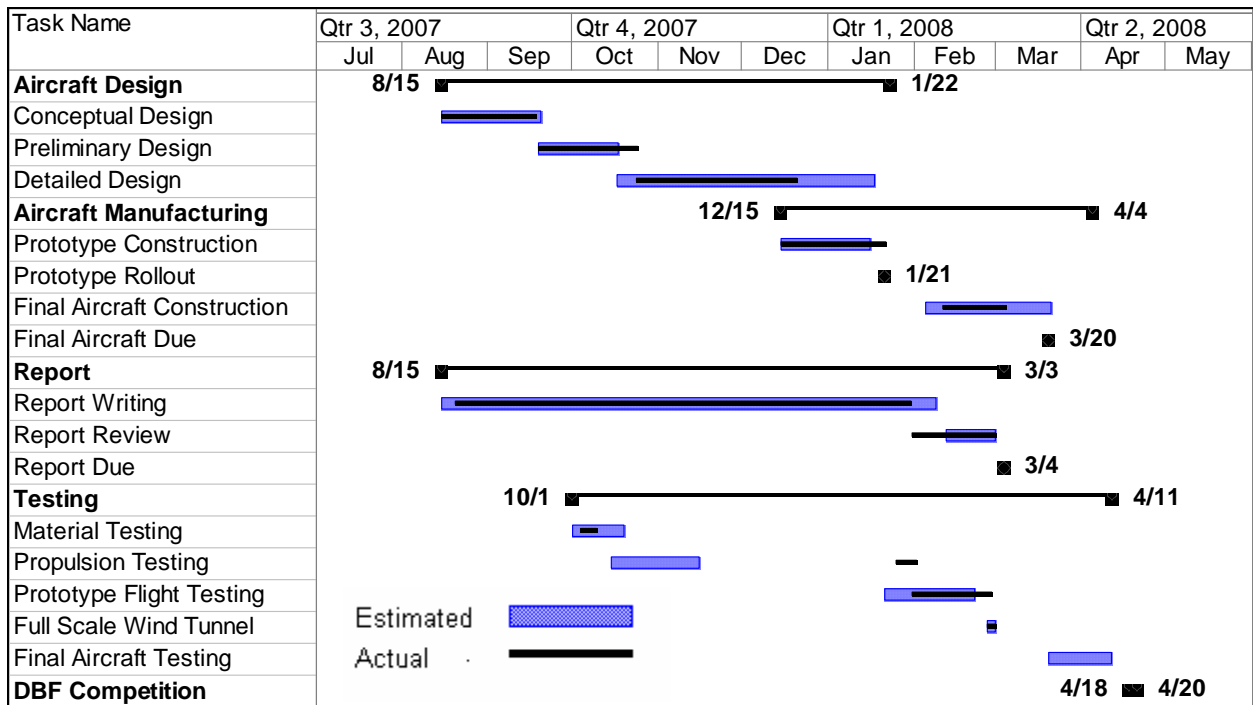


Figure 2.2 – Project Schedule

3.0 Conceptual Design

Conceptual design begins by identifying the mission requirements and details. The critical design variables and goals are selected to perform FOM analyses, and several aircraft configurations are proposed and evaluated. In addition, the basic propulsion system, payload, and landing gear configurations are also selected.

3.1 Mission Requirements

The competition score is directly proportional to the written report score and total FS, where the latter is the sum of the Delivery and Payload Mission scoring (50 and 100 points, respectively). Other competition requirements and specifications include:

- Size limitation of 4x5-ft.
- Maximum takeoff distance of 75-ft.
- Maximum battery weight of 4-lb.
- 40-Amp current limit.

- **Delivery Mission**

The airplane must fly empty while carrying all payload restraint components. The objective is to complete the course profile (Figure 3.1) as many times as possible within 5 minutes, while minimizing battery weight. Score is given by: **# Completed Laps / Battery Weight**. Maximum score is 50 points.

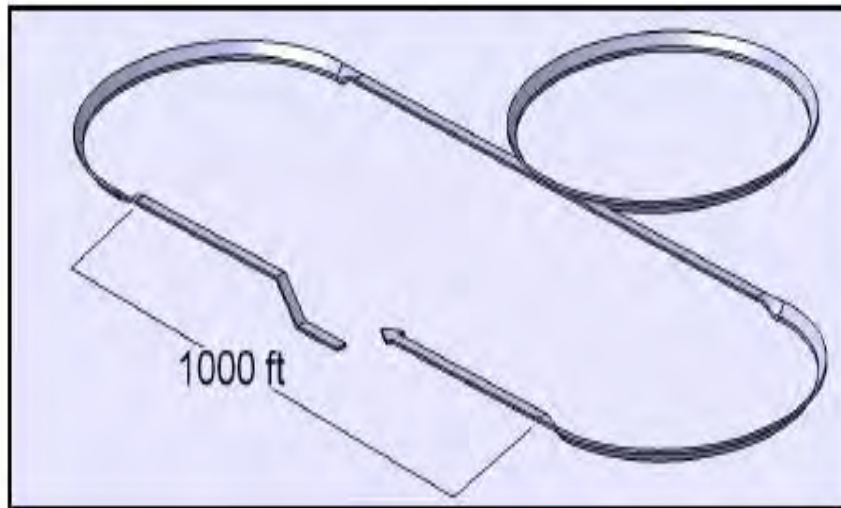


Figure 3.1 – Flight Course^{2, 1}

- **Payload Mission**

The team is timed to configure a given payload combination consisting of bottles and bricks (Table 3.1) with which the airplane must complete 2 course laps. The bottles have a maximum height of 8.5-in, and are fitted with a round or square collar (4-in diameter or 4x4-in maximum). They are ballasted with water to approximately 0.5-lb, which allows for center of gravity (CG) shifts during flight. The bricks are approximately 4x4x2-2/3-in and 1.8-lb each. In addition, the airplane is assigned a RAC (**System Weight x Battery Weight**), where **System Weight** is the airplane weight without payload or batteries. The score is inversely proportional to RAC and loading time ($1 / RAC \times Loading\ Time$). This mission can be completed twice for a score of 100 (50 each).

Option	Bottles	Bricks	Weight (lb)
1	10	1	6.8
2	3	3	6.9
3	14	0	7.0
4	7	2	7.1
5	0	4	7.2

Table 3.1 – Payload Combinations²

3.2 Scoring Analysis

A sensitivity study is conducted to evaluate the effects of mission scoring variables. Figure 3.2(a) shows Score vs. Battery Weight for the Delivery Mission. As battery weight increases, scoring becomes less sensitive to the number of laps completed. From this trend, it is evident that the maximum battery weight of 4-lb does not yield a competitive score.

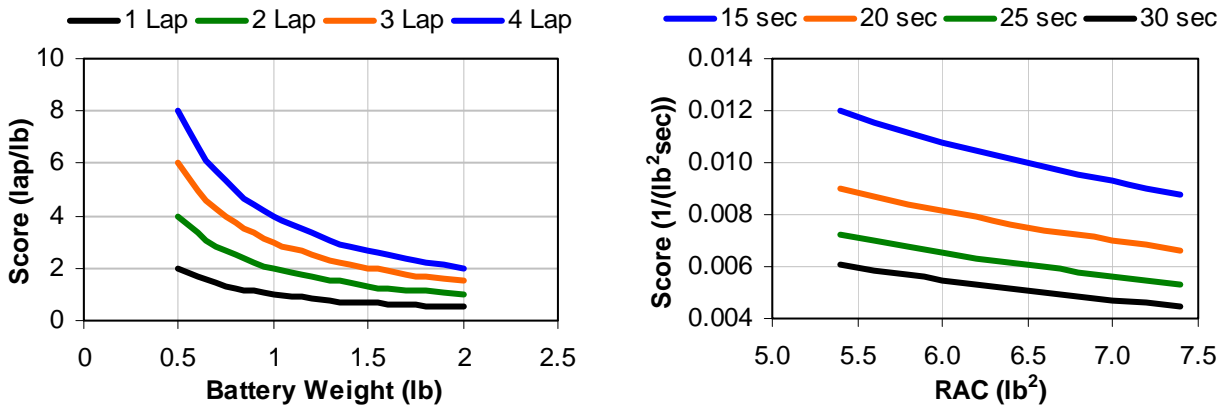


Figure 3.2 – (a) Score vs. Battery Weight for Delivery and (b) Score vs. RAC for Payload

Figure 3.2(b) shows Score vs. RAC for different loading times in the Payload Mission. Note that the change in score between 15 and 20 seconds is nearly identical to the difference between 20 to 25, and 25 to 30 seconds combined. As loading time increases, its effect on scoring diminishes rapidly. Further analysis is conducted by combining the individual mission score equations:

$$Score = \frac{LAPS}{BW_1} + \frac{2}{SW \cdot BW_2 \cdot LT} \quad \text{Equation 3.1}$$

Where LAPS is the total number of laps, SW is System Weight, LT is Loading Time, and BW_1 and BW_2 are Battery Weight for the Delivery and Payload Missions, respectively. Note that LT for each payload flight is assumed to be equal for this equation. Table 3.2 depicts the percentage influence on score for each variable.

Variable	Percentage Effect on Score
Battery Weight Payload (BW_2)	22.2%
System Weight (SW)	22.2%
Loading Time (LT)	22.2%
Battery Weight Delivery (BW_1)	16.7%
Number of Laps (LAPS)	16.7%

Table 3.2 – Variable Percentages

Initial inspection of Table 3.2 shows that SW, BW_2 , and LT have the same effect on score; however, the battery weight required is directly proportional to system weight. Also, the battery weight influence increases to 39% if it is combined for both missions. Consequently, battery and system weight can be considered the most influential factors in mission scoring.



The LT and LAPS variables both have a large degree of uncertainty. For example, although the number of laps completed depends on aerodynamic and performance parameters along with gross weight, it also depends on factors such as wind speed and direction. Therefore, environmental influences must be taken into account when predicting the mission profile and scoring. In regards to LT, any type of human factors, environmental influences, loading mechanism or aircraft failure could have a drastic effect. Since the time is recorded in seconds, the range of values could potentially be very large from one situation to another; much more than the range of weights or laps. Because of the unpredictable nature of this variable, special attention must be given to create a payload restraint system which is repeatable, reliable, and efficient for handling all types of payload combinations.

3.3 Design Objectives and Requirements

After conducting a scoring analysis and a competitive evaluation of past DBF airplanes, the team imposed the following design objectives and requirements.

- **Delivery Mission:** Complete at least 3 laps with less than 1-lb of battery weight.
- **Payload Mission:** Complete the 2 laps required with less than 1.5-lb of battery weight and a loading time under 15 seconds.
- **Wing Loading and Thrust-to-Weight Ratio:** Optimize the combination of wing loading and thrust-to-weight ratio to minimize battery weight, and to meet takeoff requirements (65 to 70-ft).
- **Manufacturing:** Produce a light aircraft structure (< 4.5-lb) with a high strength-to-weight ratio.
- **Payload Loading:** Implement top-loading to minimize loading time.
- **Payload Restraint:** Create a light and efficient loading mechanism to minimize time and system weight, and to maintain a consistent longitudinal CG for all payload combinations.

3.4 Conceptual Configurations

The following solution concepts are idealized with a balanced combination of wing loading and thrust-to-weight ratio to meet the design objectives and requirements previously stated.

- **Biplane (Single):** Low wing loading helps to reduce the amount of thrust and number of cells required to meet takeoff distance. The top wing spar location is a potential problem, as it could interfere with the payload bay.
- **Monoplane (Twin):** Higher wing loading and thrust-to-weight ratio than the Biplane concept. Relies on rapid acceleration to meet takeoff distance. It could require counter-rotating propellers and dihedral to maintain lateral-directional stability. Weight of two propulsion systems is a concern.
- **Tandem (Single):** Two wings are aligned in a negatively staggered configuration. Appropriate separation from the airplane CG could make a horizontal tail unnecessary. The takeoff field length is typically longer than that of a traditional monoplane or biplane concept.



- **Canard (Twin):** A lifting canard with multiple props is similar to a tandem concept, and has the same issues with takeoff distance. The motors can be placed on the canard wing tips along with the landing gear to merge stress concentration points and attempt to minimize structural weight.
- **Flying Wing (Single):** Takes advantage of payload bay width to increase available surface area and to lower wing loading. This configuration produces a considerable amount of induced drag due to its short aspect ratio. The necessary fuselage height to accommodate tall payload elements could present possible design complications.

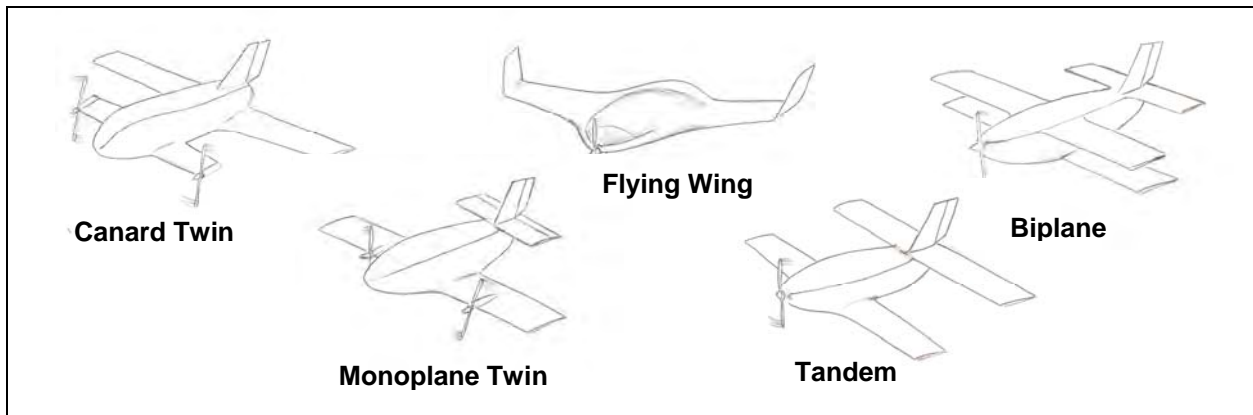


Figure 3.3 – Five Solution Concepts

3.5 Selection Process

The following Figures of Merit are assigned weighting factors and used to evaluate the proposed conceptual solutions and subsequent components using a five-point scale system (1-Inferior, 2-Weak, 3-Average, 4-Good, and 5-Superior).

- **Battery Weight:** A critical component of score for both missions.
- **System Weight:** Reducing system weight is critical to minimizing battery weight and the required lift coefficient for cruise.
- **Drag:** The amount of drag generated affects the number of laps for the Delivery Mission and the amount of energy required for both missions. In general, the more energy required, the heavier the battery.
- **Takeoff Distance:** A critical phase for both missions. The aircraft must takeoff within 75-ft.
- **Stability & Control:** It is desirable to have an aircraft with reliable S&C during takeoff, cruise, and landing. This is especially important considering the unpredictable nature of wind in Wichita.
- **Manufacturability:** Ease of manufacturability and reproducibility is important to minimize downtime after a crash event.



3.5.1 Aircraft Configuration

The proposed solution concepts are evaluated based on the previous Figures of Merit.

Figure of Merit	Weight (%)	Biplane Single	Monoplane Twin	Tandem Single	Canard Twin	Flying Wing Single
Battery Weight	25	4	3	4	3	4
System Weight	25	3	3	4	3	3
Drag	15	3	4	3	3	2
Takeoff Distance	15	4	3	2	2	2
Stability & Control	10	4	3	3	4	2
Manufacturability	10	3	3	3	3	2
Total	100	320	285	305	265	255

Table 3.3 – Aircraft Configuration Decision Matrix

From the decision matrix, the biplane is the most advantageous concept. It has a low wing loading to reduce the amount of thrust and battery weight required to meet the takeoff distance. In addition, it has adequate lateral-directional stability; an important factor when considering X-winds in Wichita. The only concern carried to preliminary design is the potential interference of the top wing spar with the payload bay.

3.5.2 Empennage Configuration

After selecting a biplane configuration, different types of empennage are investigated:






					
Figure of Merit	Weight (%)	Conventional	V-Tail	T-Tail	U-Tail
Stability & Control	40	4	2	4	3
System Weight	30	4	4	2	2
Drag	20	3	4	3	2
Manufacturing	10	5	3	2	3
Total FOM	100	390	310	300	310

Table 3.4 – Empennage Configuration Decision Matrix

- **Conventional:** A typical tail configuration that provides reliable and familiar S&C characteristics.
- **V-Tail:** Provides an opportunity to save weight since only two stabilizing surfaces are used. However, it is very susceptible to X-winds.



- **T-Tail:** Similar to conventional design, but the horizontal stabilizer is at the top of the vertical. This clears the horizontal from the wing wash and increases its effective angle of attack (AOA).
- **U-Tail:** Two vertical stabilizers are mounted on either side of a horizontal. This configuration can improve the efficiency of the horizontal since the verticals act as endplates. This is the heaviest configuration analyzed.

The conventional configuration is selected. It provides formidable stability characteristics at a lower weight than the T-tail and U-tail options, and adapts better to X-winds than a V-tail.

3.5.3 Landing Gear Configuration

The types of landing gear evaluated are:

- **Conventional:** The advantages of this configuration are: low drag (no nose-wheel) and an inherent AOA that assists short-field takeoffs. Ground handling capabilities are reduced.
- **Tricycle:** The most common type of landing gear. It has reliable ground handling capabilities, but it is heavier and produces more drag than the conventional.
- **Bicycle:** This type of gear has 4 wheels, one on the front, one aft of the main wings, and one on each wing. Drag, weight, and ground handling are significant drawbacks.


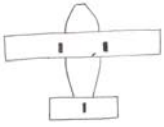
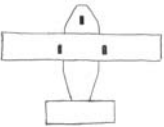
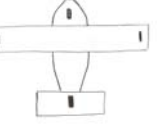
				
Figure of Merit	Weight (%)	Conventional	Tricycle	Bicycle
System Weight	50	4	3	2
Drag	20	4	3	2
Stability & Control	30	3	4	1
Total FOM	100	370	330	170

Table 3.5 – Landing Gear Configuration Decision Matrix

The conventional configuration is selected for its low weight and improved takeoff performance, at the minor expense of reduced ground handling capabilities.

3.5.4 Battery Configuration

Two different battery configurations are considered:

- **Single-Stack:** Arrangement where all the cells are placed in series in one or more packs. Battery weight is reduced in this configuration because fewer cells are required. A potential disadvantage is that the battery packs support the entire current drawn from the motor, which reduces their available voltage.



- **Double-Stack:** This configuration has two packs connected in parallel with each other. This arrangement is ideal for missions that demand a large energy capacity. However, the number of cells required is double that of a single-stack configuration.

Three additional Figures of Merit are added to determine the most competitive battery configuration.

- **Power:** Producing the largest amount of power with the least amount of cells is desirable.
- **Energy Available:** This is major concern for the Delivery Mission, since the number of laps directly depends on how much battery energy is available.
- **Efficiency:** This pertains to the discharge rate efficiency.


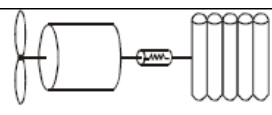
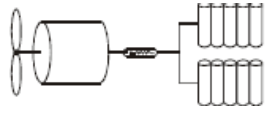
			
Figure of Merit	Weight (%)	Single-Stack	Double-Stack
Battery Weight	40	5	3
Power	30	4	3
Energy Available	15	3	4
Efficiency	15	3	3
Total FOM	100	410	315

Table 3.6 –Battery Configuration Decision Matrix

Although the double-stack provides more energy, the single-stack battery configuration is ultimately chosen based on its superior power-to-weight ratio.

3.5.5 Payload Arrangement

The last study during conceptual design investigates different ways to arrange the 5 possible payload combinations (Table 3.1). It is desired to maintain a constant CG location for all the combinations. After a preliminary screening process of basic concepts, the following arrangement options are considered for further study (Fig 3.4).

- **Option 1:** This is a symmetric system which allows for small taper angles. Although not readily apparent, this arrangement has a sizeable range of CG shift for various payload combinations.
- **Option 2:** This arrangement is the most compact of those considered. Due to lack of symmetry, the CG location varies significantly between combinations. Taper is allowed from one end only.
- **Option 3:** This is the narrowest of the options, which allows for a similarly narrow fuselage. However, the length may decrease ease of loading, and it may also require relatively large taper and upsweep angles, increasing drag. Although this arrangement is symmetric, payload balancing is a major concern.
- **Option 4:** This system is very similar to Option 1, except that it has slightly better stability characteristics and requires larger taper angles.



Three Figures of Merit for payload arrangement are considered:

- **Stability:** For consistent stability characteristics, it is desired to keep the payload CG as close as possible to the airplane CG for all the payload combinations.
- **Drag:** The width of the payload arrangement can determine the width of the fuselage. A narrow fuselage width provides less drag, while a wider fuselage will provide more drag. Also, some options better accommodate smaller taper and upsweep angles than others.
- **Ease of Loading:** Compact payload configurations require less movement of the individual's involved during loading, which will yield lower and more consistent loading times.

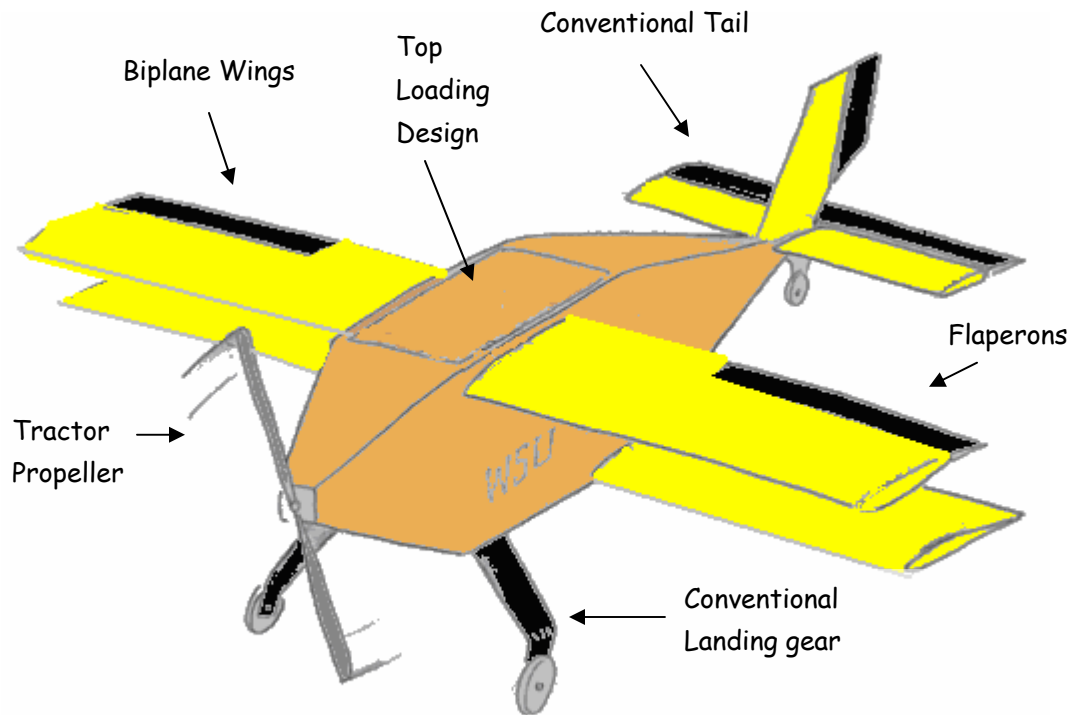
Figure of Merit		Option 1	Option 2	Option 3	Option 4
Stability	50	2	3	1	4
Drag	30	4	2	5	3
Ease of Loading	20	3	4	2	3
Total FOM	100	280	290	240	350

Figure 3.4 – Payload Configuration Decision Matrix

Option 4 is chosen based on results from stability analysis and the flexibility of fuselage tapering.

3.6 Conclusion

Upon conducting an analysis of mission requirements and scoring, a series of FOM decision matrices are used to analyze a combination of primary configurations and subsequent systems. The selected concept is a single propeller biplane wing-body with a conventional tail, a conventional landing gear, and a single-stack battery configuration. A top loading configuration is identified as optimal for easy access to the payload bay. An appropriate payload configuration is chosen based on stability and drag concerns; the latter of which is expected to be significant due to the large base area required for the payload bay. The final conceptual design is shown in Fig. 3.5.



AEROSHOCK

Figure 3.5 – Final Conceptual Design

4.0 Preliminary Design

This section describes the critical design parameters, mission model, and optimization scheme. In addition, analysis is conducted among the 5 main technical groups, and preliminary results are obtained from each.

4.1 Critical Design Parameters

Primary aircraft optimization is centered on obtaining an optimal range of aerodynamic and propulsion design parameters which have the largest influence on scoring and performance.

4.1.1 Aerodynamic Parameters

- **Wing Area:** An important parameter for the short field takeoff requirement. Increasing the wing area reduces the wing loading and helps to reduce takeoff distance, but increases drag which affects the amount of energy required.
- **Wing Span:** The competition rules impose a limitation on wingspan and fuselage length by stipulating that the aircraft must fit in a 4x5-ft spot size. It is necessary to achieve an optimal combination of wing span and area that best fulfills these dimensional requirements.



- **Wing Airfoil:** Airfoil selection is also critical to minimize takeoff distance. A high lift airfoil improves takeoff performance, but creates a significant amount of drag during cruise. Alternatively, a balanced airfoil provides moderate lift coefficients and less cruise drag.

4.1.2 Propulsion Parameters

- **Motor Selection:** This is highly influenced by system weight and power requirements. Brushless motors are preferred to brushed due to their lower weight and greater efficiency.
- **Battery Selection and Number of Cells:** Battery weight has a direct effect on scoring. The battery capacity must be chosen to minimize weight, while maximizing the number of laps for the Delivery Mission. The number of cells used must be able to provide sufficient power for takeoff.
- **Propeller Selection:** The propeller is an important parameter that directly affects the aircraft's available power and the current drawn from the battery.

4.2 Mission Model

The missions are modeled using five different phases: takeoff, climb, 180-degree turn, 360-degree turn, and cruise.

- **Takeoff:** Ground roll is modeled using a trapezoidal integration method. The model assumes a full throttle setting, a rolling friction coefficient of 0.03, and a wind speed set to 0 mph. The takeoff AOA varies with increasing speed. It is initially set at 12 degrees, and incrementally decreases as the airplane accelerates to a 0-degree attitude.
- **Climb:** Full throttle is assumed during the climb leg to 50-ft. The horizontal distance is calculated to ensure that the airplane successfully reaches the desired altitude before the first 180-deg turn.
- **Cruise:** Level flight is modeled to find the necessary cruise speed. Full throttle is maintained in the Delivery Mission to maximize the number of laps, while throttle control is implemented in the Payload Mission to reduce the amount of current consumed and to save energy.
- **Turns:** The turn segments are estimated by calculating the maximum bank angle the airplane can sustain in a 180- and 360-degree level turn. A maximum turn radius of 175-ft is specified. The same throttle conditions used for cruise are employed for turns.

The model includes head and crosswind (X-wind) data³ in Wichita for the third week of April (Table 4.1). The east field at Cessna heads N-S.

Year	Mean / Max Wind Speed (mph)
2003	14 / 31
2004	19 / 31
2005	11 / 21
2006	14 / 29
2007	20 / 34

Table 4.1 – Wind Historical Information



4.3 Optimization Scheme

A Multidisciplinary Optimization (MDO) Code is created using FORTRAN 77 to integrate the following technical Modules: Aerodynamics, Propulsion, Performance, S&C, Weight & Structures, and Mission Scoring. The code analyzes numerous configurations and records the results for comparison. Critical design variables are selected based on these outputs. Figure 4.1 depicts the optimization flowchart.

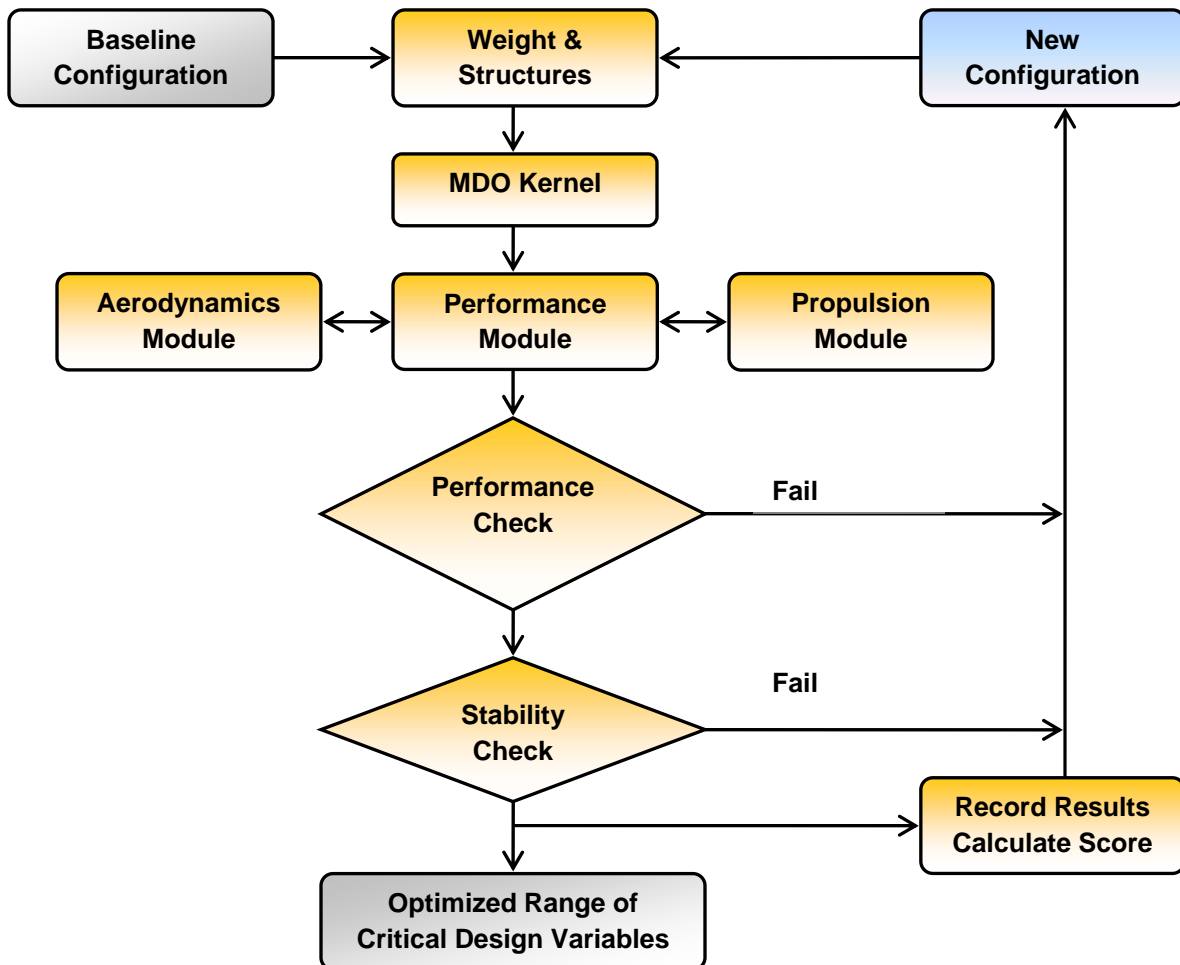


Figure 4.1 – Optimization Flowchart

4.3.1 Aerodynamics Module

This module calculates aerodynamic coefficients, Reynolds numbers, and aerodynamic forces for each external component. A complete drag build-up is implemented using the method outlined in Roskam⁴. Lift coefficients are calculated using the Prandtl lifting line theory and a biplane aspect ratio (AR) consistent with the definition from Hoerner⁵.



The module also compares four different airfoils: NACA 4415, Eppler 560, SD 7062, and Eppler 423. Figure 4.2 (a) and (b) show the lift-coefficient and drag polar curves for these airfoils obtained from XFOIL at a Reynolds number of 500,000. Estimates for the Oswald efficiency factor are initially based on data from WSU's previous DBF entry¹, and later validated through wind tunnel testing (Section 7.4).

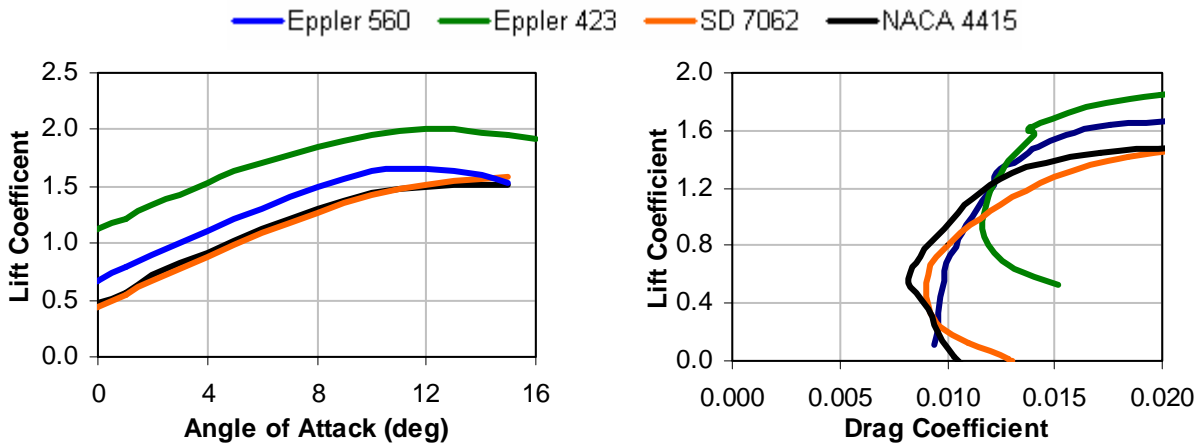


Figure 4.2 – (a) Airfoil Lift Curves and (b) Airfoil Drag Polar Curves

4.3.2 Propulsion Module

The Propulsion Module stores data for different motors, gear ratios, battery cells, and propellers. Subsequently, it calculates current, thrust, torque, and brake power for a given propulsion system configuration and flight speed. These values are used by the MDO kernel to evaluate the feasibility of numerous configurations in the Performance Module. Figure 4.3 shows the Propulsion Module flowchart.

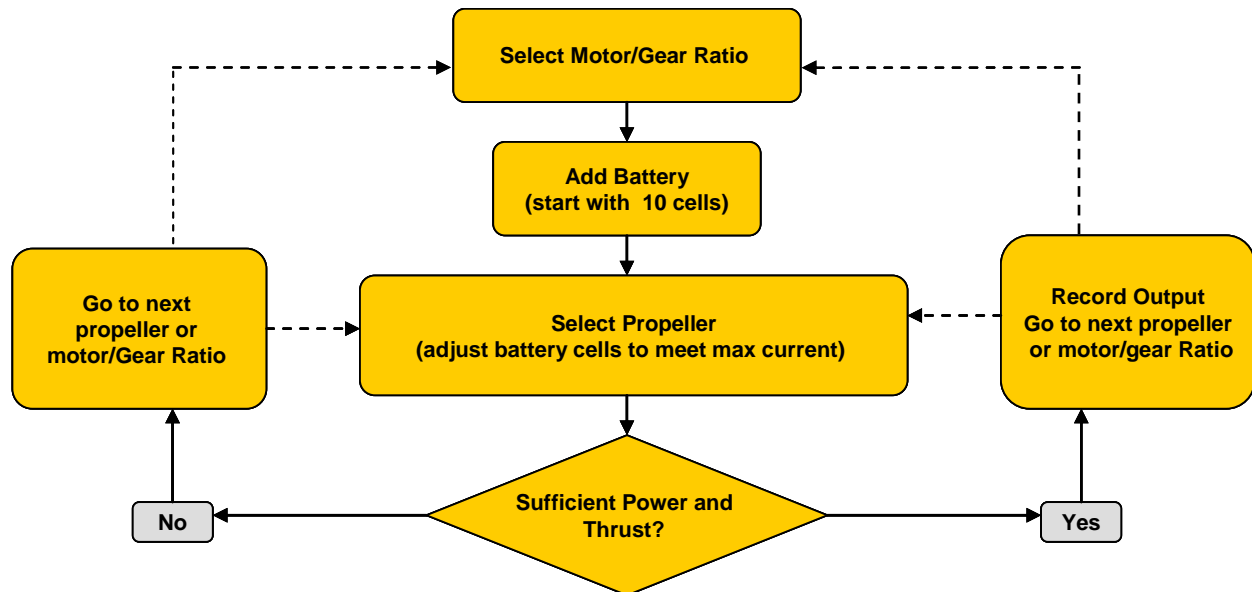


Figure 4.3 - Propulsion Module Flowchart



A preliminary screening process of historical data identifies the most efficient motors and batteries. Eight different motors (Table 4.2) are included into the module. Five NiMH battery cells are considered (Table 4.3) based on their superior capacity-to-weight ratio (energy density).

Motor	Kv (RPM/V)	Idle Current (A)	Resistance (Ω)	Weight (lb)
NEU 1506/3Y	1,700	1.2	0.0290	0.40
NEU 1509/2Y	1,820	1.5	0.0180	0.50
NEU 1512/3D	1,700	1.5	0.0120	0.64
NEU 1512/1.5Y	1,900	1.8	0.0090	0.64
NEU 1521/1.5D	1,860	3.5	0.0050	0.97
Hacker B50 10L	2,415	2.0	0.0103	0.69
Hacker B50 13L	1,858	1.3	0.0172	0.69
Hacker B50 9XL	1,753	1.4	0.0118	0.87

Table 4.2 - Motor Specifications

Battery Cell	Capacity (mAh)	Nominal Voltage (V)	Ri (m Ω)	Weight (lb)	Energy Density (mAh/lb)
IB 1400	1,350	1.1	4	0.060	23,333
Elite 1500	1,400	1.1	4	0.051	27,451
Elite 1700	1,600	1.1	4	0.063	25,396
GP 2000	1,850	1.1	4	0.080	23,125
Sanyo FAUP 1950	1,800	1.1	6	0.098	18,367

Table 4.3 – Battery Cell Properties

The criterion for propeller selection is based on the required power to takeoff within 75-ft. As a result, large diameters (17- to 20-in) and low pitches (10- to 12-in) are considered. These propellers are tested in a wind tunnel (Section 7.3) to obtain thrust, torque, and power coefficients. The maximum propeller size is set by the current limit and ground clearance.

4.3.3 Performance Module

The Performance Module analyzes each mission phase by solving the aircraft equations of motion⁶ and calculates total mission times based on the mission model described in Section 4.2. This module outputs variables including takeoff distance, rate of climb, cruise speed, rate of turn, turn radius, throttle setting, energy required, number of laps, and mission times, among others.

4.3.4 Stability and Control Module

The S&C Module assesses longitudinal and lateral-directional stability. It calculates static margin, along with the required tail area and control surface deflection for trimmed flight during takeoff and cruise. Airplane stability characteristics are estimated using a linear model outlined by Roskam⁴.



4.3.5 Weight and Structures Module

The primary function of this module is to generate a weight database of materials and components including battery cells and motors. The Euler-Bernoulli Beam Theory⁷ is used to size the wing spars and internal fuselage components. The aircraft structural weight is calculated based on the particular manufacturing method and materials selected for the wings, fuselage, and empennage (Section 6.0).

4.3.6 Flight Score Module

This module predicts a FS based on data output from other modules. The cost function (Eq. 4.1) includes the number of laps for the Delivery Mission, the system weight, and the battery weight for both missions. Loading time is not included as it is not a factor in the optimization of the critical design variables. This score is used to evaluate all the aircraft configurations that successfully pass the performance and stability requirements built into the code.

$$FS = \frac{LAPS}{BW_1} + \left(\frac{2}{SW \times BW_2} \right) \quad \text{Equation 4.1}$$

4.4 Optimization Results

The main tradeoff study to size the airplane's wings and to configure the propulsion system is related to the amount of energy (i.e. battery weight) required to complete both missions successfully. An MDO run is performed for the critical design parameters listed in Section 4.1 based on ranges determined from Conceptual Design and preliminary exploratory runs. The results demonstrate that there are multiple configurations which could achieve a high score. Table 4.4 lists several different competitive configurations obtained from the analysis. Some clear trends extracted from optimization are:

- Large wing spans and areas help to reduce the number of battery cells required.
- The SD 7062 and NACA 4415 consistently perform well for both missions. Therefore, it is not required to use a high lift airfoil (Eppler 423 and 560). This translates into reduced wing drag.
- The most suitable motor is the NEU 1506/3Y. It is the lightest available, and requires the least amount of current to provide adequate power.
- Only the APC 19x10E propeller can be used to successfully complete the Payload Mission without exceeding the 40-amp limit, while an 18x10 propeller provides adequate power for the Delivery Mission with less current drawn than the 19x10.
- Figure 4.4 (a) shows that the cruise speed is reduced as wing area increases. For the Delivery Mission, it is important to minimize cruise drag and to save energy by lowering the motor throttle setting.
- Figure 4.4 (b) suggests that configurations cruising from 26 to 30 ft/s need the least amount of energy to complete a single lap for the Delivery Mission. Low energy consumption facilitates the optimization of battery weight by using low capacity cells.



- Analysis of the Delivery Mission suggests that the wings can be sized from 7- to 10-ft² in order to achieve a cruise speed that minimizes energy consumption.
- Figure 4.5 suggests that a larger wing area does not necessarily imply a shorter takeoff distance for the Payload Mission (i.e. the wing loading cannot be arbitrarily lowered). A wing area between 7- and 10-ft² is also satisfactory for this case.

Case	Span (ft)	Wing Area (ft ²)	AR	Airfoil	Delivery Mission		Payload Mission	
					Propeller	Battery	Propeller	Battery
1	4.00	10.00	1.60	SD 7062	18x10	12 Elite 1700 (0.75-lb)	19x10	18 GP 2000 (1.52-lb)
2	4.25	8.50	2.13	SD 7062	18x10			
3	4.25	8.50	2.13	NACA 4415	18x10			
4	4.50	9.00	2.25	SD 7062	18x10			
5	4.75	7.125	3.17	SD 7062	18x10			
6	4.75	7.125	3.17	NACA 4415	18x10			
7	4.75	9.50	2.38	SD 7062	18x10			
8	5.00	7.50	3.33	SD 7062	18x10			
9	5.00	7.50	3.33	NACA 4415	18x10			

Table 4.4 – Competitive Configurations

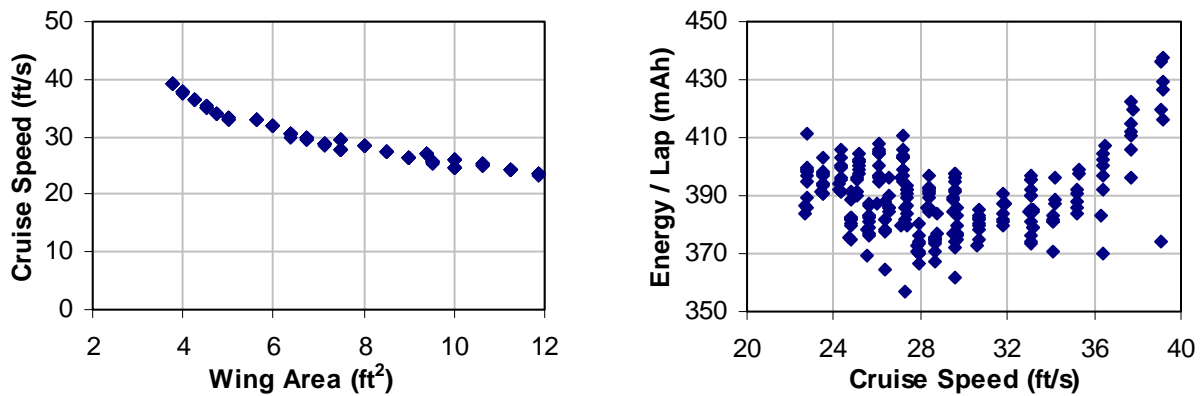


Figure 4.4 – Delivery Mission (a) Cruise Speed vs. Wing Area and (b) Energy/Lap vs. Cruise Speed

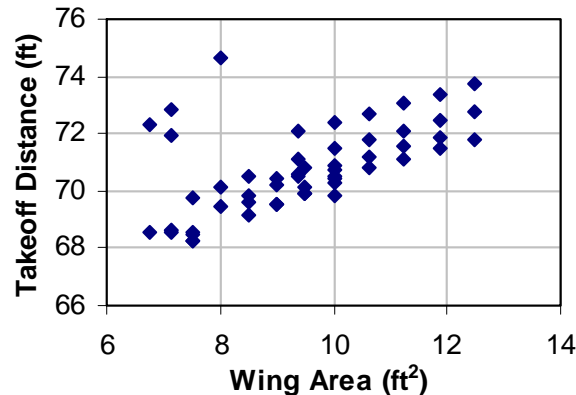


Figure 4.5 – Payload Mission Takeoff Distance vs. Wing Area



The following critical design parameters are selected based on the results and trends above. The configuration has a relatively large wing span and area, which most resembles case number 7. Based on the results from optimization, the largest possible wingspan is desirable; hence a maximum wingspan of 4.83-ft (58-in) is chosen to allow a 2-in tolerance from the 5-ft (60-in) geometric restriction.

Aerodynamic Parameters		Propulsion Parameters		
Item		Delivery	Payload	
Wing Airfoil	SD7062	NEU 1506/3Y		
Wing Chord (ft)	1.00	12 Elite 1700	18 GP 2000	
Wing Span (ft)	4.83	1,600		1,850
Wing Area (ft ²)	9.67	18X10E		19X10E

Tables 4.5 – Critical Design Parameter Selection

4.5 Aerodynamic Trade Studies

A FOM analysis is used to validate the airfoil selection from the optimization results with respect to parameters such as manufacturability and stall characteristics. The following Figures of Merit are used:

- **Delivery Performance (35%):** The airfoil must keep drag to a minimum.
- **Payload Performance (30%):** High lift is important to meet the required takeoff distance (75 ft).
- **Pitching Moment (25%):** Excessive negative pitching moments can create problems during the Payload Mission when the motor is full-throttled at takeoff (forcing the airplane to nose down).
- **Stall Characteristics (5%):** It is desirable to have a gentle stall.
- **Manufacturing (5%):** Airfoils with sharp trailing edges and under-camber are inherently difficult to manufacture.

Figure of Merit	Weight (%)	Eppler 423	Eppler 560	SD 7062	NACA 4415
Delivery Performance	35	2	3	4	5
Payload Performance	30	2	5	4	3
Pitching Moment	25	2	3	5	3
Stall Characteristics	5	4	3	2	4
Manufacturing	5	2	3	3	3
Total FOM	100	210	360	410	375

Table 4.6 – Airfoil Decision Matrix

The effects of decalage, wing twist, dihedral, taper, fuselage geometry, propeller location, and endplates are considered.

- **Decalage:** Increasing the top wing incidence can provide 1% higher efficiency⁵. However, this advantage does not outweigh the related manufacturing complexities.
- **Geometric and Aerodynamic Twist:** Twist helps increase the wing's span efficiency factor, thus improving its performance. It is not implemented due to manufacturing complexities.



- **Dihedral/Anhedral:** Dihedral is typically used to improve the aircraft's roll control. However, a biplane naturally has satisfactory roll behavior, therefore dihedral is unnecessary.
- **Wing Taper:** Taper increases the wing's AR, but decreases its area, affecting takeoff distance performance and battery optimization. Consequently, taper is not introduced.
- **Fuselage Geometry:** Flow visualization from half-scale wind tunnel testing (Section 7.4) showed excessive flow separation near the aft fuselage, which is tapered in all directions (as Figure 3.5 shows). As a result, taper angles are lowered and the empennage is raised to increase effectiveness.
- **Propeller Location:** The propeller is placed high on the nose to minimize slipstream blockage and to accelerate the flow on the fuselage's upper section.
- **Endplates (Wing Boxing):** A viable option to increase the effective AR is to box the wings. Figure 4.6 shows the lift coefficient increments and drag polar curves obtained from the half-scale wind tunnel test (Section 7.4). A penalty of using endplates is increased parasite drag; however they prove necessary to achieve the 2.5G loading requirement for the wing structure (Section 4.8). Another potential problem of wing boxing is the effect on lateral-directional stability.

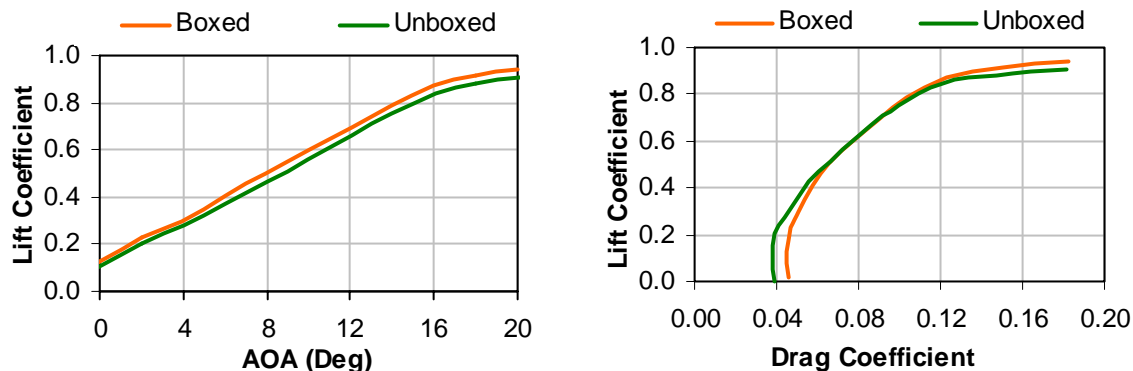


Figure 4.6 – Endplate Comparison: (a) Lift Coefficient vs. AOA and (b) Drag Polar Curves

4.5.1 Stagger Analysis

Stagger improves the efficiency of the biplane cell⁸ by reducing interference effects and trim drag⁹. A Computational Fluid Dynamics (CFD) analysis is performed to evaluate the impact of positive and negative stagger on the biplane cell's lift coefficients, and to study the flow characteristics. Fluent¹⁰, a commercial CFD package, is used to conduct the simulations. Unstructured computational grids are generated with a high grid density near the wing's surface ($Y^+ \sim 1$) to properly resolve the sub-viscous boundary layer, according to the specifications for the Spalart-Allmaras turbulence model¹⁰. The flow conservation equations (continuity, momentum, and energy), along with the integral equation for the turbulence scalar are solved with a 2nd-order coupled implicit upwind scheme.



A symmetry condition is used to truncate the domain in the spanwise direction, while a far field boundary condition (Mach = 0.045 and T = 300K) bounds the flow domain. All surfaces are modeled as no-slip. The results are post-processed in Fieldview.

Figure 4.6 shows (a) the pressure coefficient distribution for 4-in of positive stagger and (b) the lift coefficient curves for a 4-in positively and negatively stagger biplane cell. In general, the forward wing produces an average of 25% more lift for both cases. Positive stagger is introduced after analyzing the results from CFD and wind tunnel testing (Section 7.4). Based on the vertical distance between the wing chords, at least 4-in of stagger is recommended⁸.

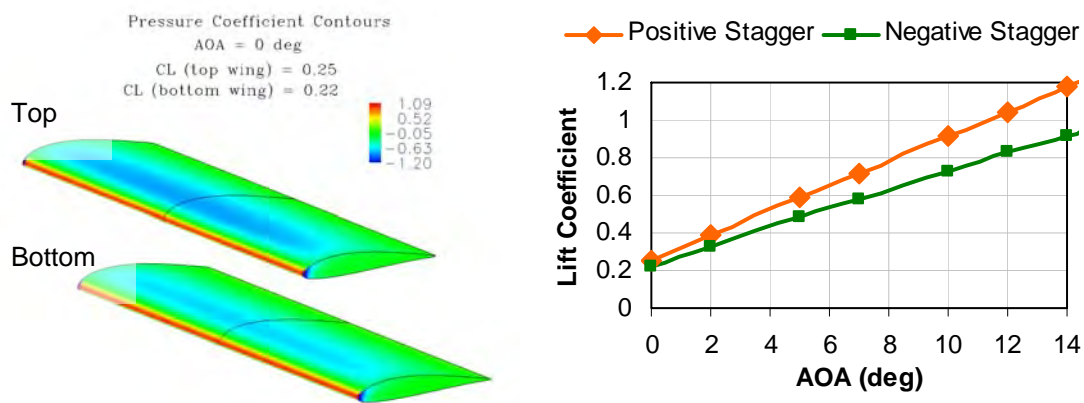


Figure 4.6 – (a) CFD Pressure Coefficient Distribution and (b) CFD Lift Curve Slopes

Airfoil: SD 7062, No Decalage, Span = 4.83-ft, $S_{ref} = 9.67\text{-ft}^2$, $Re = 300,000$

4.6 Preliminary Lift and Drag Estimates

Table 4.7 presents the preliminary aircraft parasite drag build-up, while Figure 4.7 shows the (a) Lift-to-Drag Curve and (b) Airplane Drag Polar.

Component	C_{D0}
Wings	0.0179
Fuselage	0.0260
Empennage	0.0050
Landing Gear	0.0081
Total	0.0570

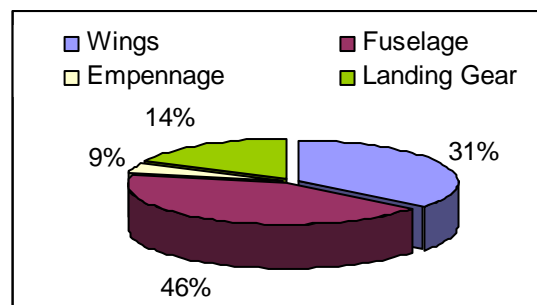


Table 4.7 – Parasite Drag Build-up

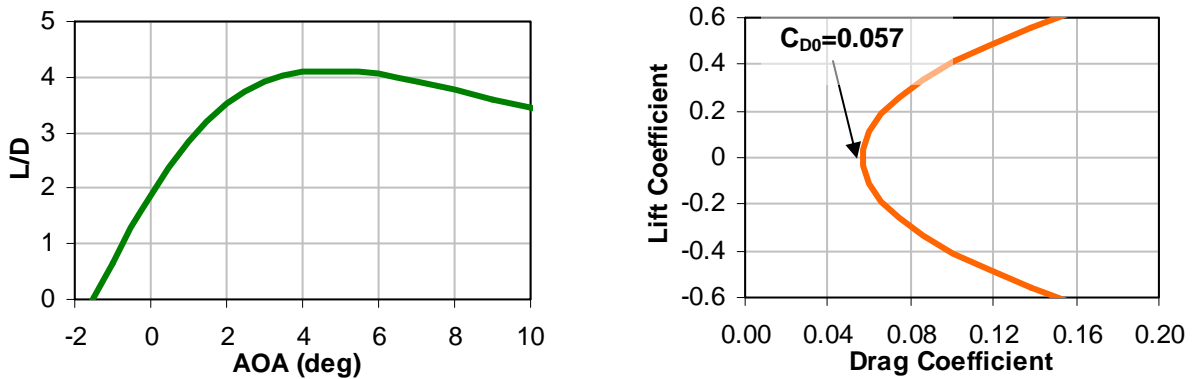


Figure 4.7 - (a) Airplane L/D Curve and (b) Airplane Drag Polar

4.7 Propulsion Trade Studies

The Optimization program predicted that the Delivery and Payload Missions can be completed with 12 Elite 1700 and 18 GP 2000 cells, respectively. Further trade studies are conducted to evaluate the effect of the discharge rate on the system performance. Table 4.8 shows the available voltage from different cell types at three different discharge rates. Figure 4.8 shows power available curves for these cells at various discharge levels. For the Delivery Mission, the curves for GP2000 and Elite 1700 overlap each other. In this case, the MDO program correctly selects Elite 1700 to minimize weight. On the other hand, the Payload Mission cannot be flown with Elite 1700 cells, as they cannot handle the predicted full throttle discharge rate (~35 Amps). This also confirms the MDO prediction that GP2000 must be used for the Payload Mission.

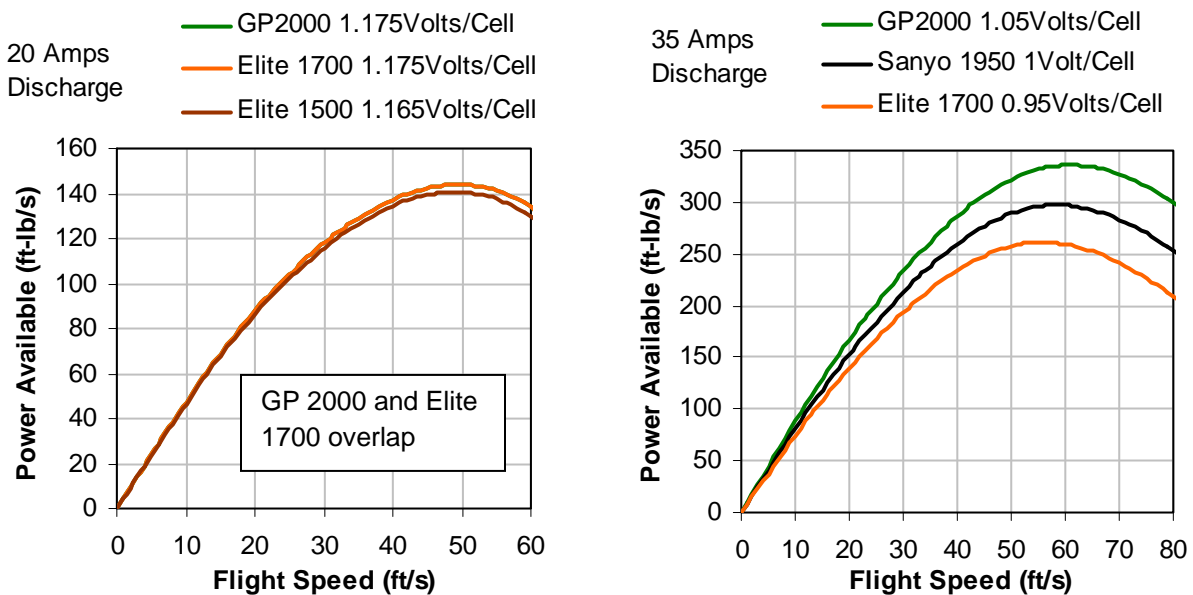


Figure 4.8 – Power Available Curves – (a) Delivery Mission, 12 cells @ 20 Amps and (b) Payload Mission, 18 cells @ 35 Amps



Voltage Cell	Discharge Levels		
	20 Amps	35 Amps	40 amps
Elite 1500	1.165 V	0.950 V	0.850 V
Elite 1700	1.175 V	0.950 V	0.900 V
GP 2000	1.175 V	1.050 V	1.050 V
Sanyo FAUP 1950	1.150 V	1.000 V	1.080 V

Table 4.8 – Cell’s Voltage at Various Discharge Rates

4.8 Stability and Control Analysis

The most important S&C tradeoff is the effect of stagger on the aircraft’s longitudinal stability. The Aerodynamics group recommends introducing at least 4-in of positive stagger to reduce interference effects along with a high motor location to minimize slipstream blockage. Therefore, an inverted tail with no incidence is introduced to counteract the expected large negative pitching moments, especially during the Payload Mission. Figure 4.9 shows a diagram of the primary forces and moments for such a configuration.

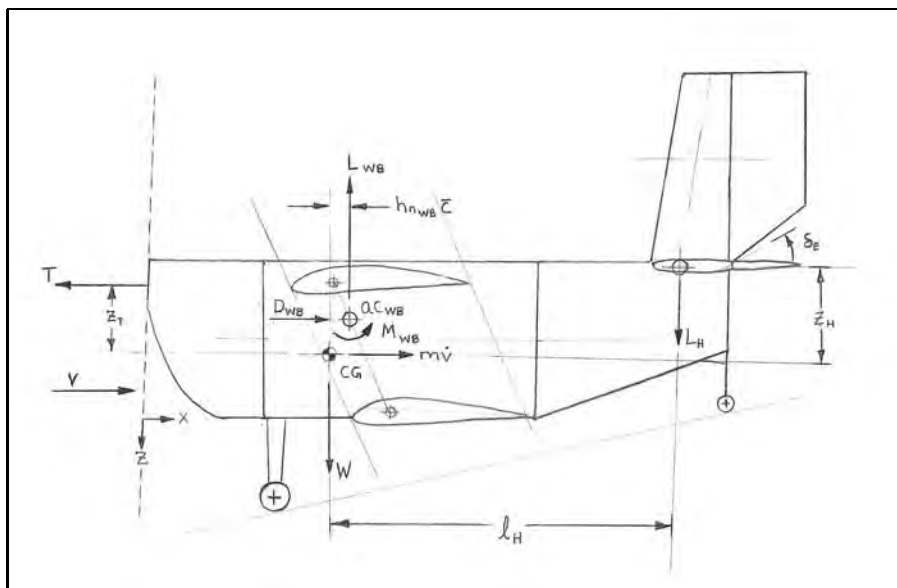


Figure 4.9 – 2D Longitudinal Stability Force and Moment Diagram at Cruise (AOA = 0-deg)

4.8.1 Stability and Control Critical Parameters

- **CG Location:** For the present biplane configuration, CFD analysis (Section 4.5.1) shows that the top wing produces an average of 25% more lift than the lower wing. An evaluation of pitching moments suggests that the CG must be placed forward of the aircraft mean aerodynamic center (MAC) to ensure adequate static margins.



- **Wing Location:** Ideally, it is desirable to place the top wing as forward as possible to clear it from the payload bay. However, a too far forward MAC reduces the longitudinal static margin because the CG cannot be moved forward as much.
- **Horizontal Tail Sizing:** The horizontal tail must be sized to achieve adequate pitch stiffness while minimizing trim drag. Different airfoils are evaluated and a NACA 2408 is selected due to its production of sufficient lift without incidence. Historical data from Raymer¹¹ and previous DBF teams is also used to guide the process and to determine acceptable volume coefficients. The horizontal tail volume coefficient is 0.32.
- **Vertical Tail Sizing:** The payload dimensions anticipate a large fuselage side area, which tends to affect the aircraft's lateral-directional stability. Therefore, it is necessary to use a large vertical tail that provides adequate yaw control. The same methods mentioned to size the horizontal tail are used for the vertical. The vertical tail volume coefficient is 0.03.
- **Control Surface Sizing:** Large control surfaces are considered to increase the aircraft maneuverability. Based on historical data, guidelines from Roskam⁴, and pilot feedback, the rudder and the elevator are sized to 50% of the vertical and horizontal tail, respectively. Flaperons are added on the top wing only to reduce weight and complexity. Based on historical data, Raymer¹¹ and Roskam⁴, the flaperons are sized to 62% of the span and 12% of the chord.

4.8.2 Estimated Stability Characteristics

The Stability & Control Module introduced in Section 4.3.4 is used to evaluate the aircraft's stability characteristics. As Table 4.9 shows, the aircraft CG is ahead of the MAC for both missions, which yields satisfactory static margins with 4-in of stagger. Figure 4.10 shows the longitudinal trim plots for takeoff and cruise conditions.

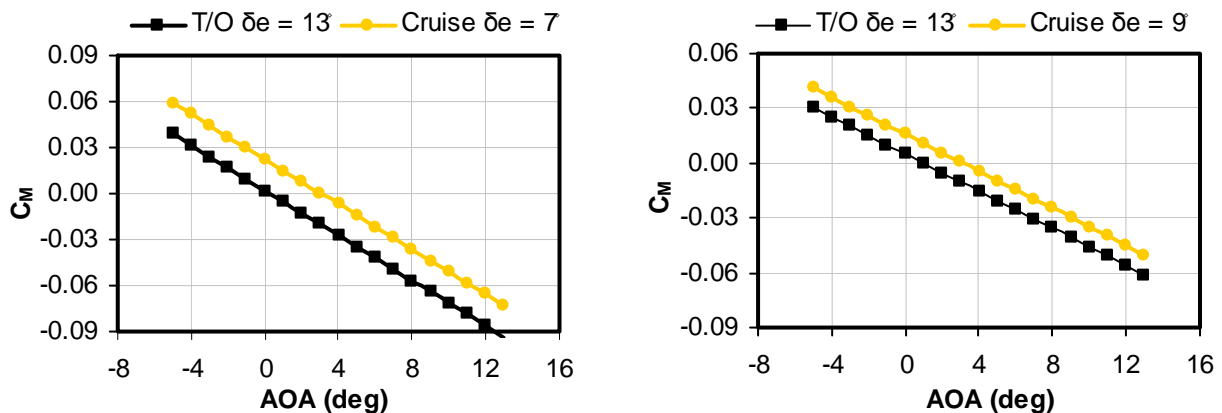


Figure 4.10 – Longitudinal Trim Plots for (a) Delivery Mission and (b) Payload Mission



	Delivery	Payload	Top Wing AC (in)	12.5
CG (in)	13.28	13.7 (avg.)	Bottom Wing AC (in)	16.5
Static Margin	12.50%	9.10% (avg.)	Aircraft MAC (in)	13.9

Table 4.9 – Static Margin Characteristics

The stability coefficients listed in Table 4.10 are initially calculated using methods from Roskam⁴ and Raymer¹¹. Wind Tunnel Testing (Section 7.6) provides more accurate estimates. The stability derivatives predict a stable airplane in both static and dynamic conditions. The X-wind capability, calculated using methods from Yechout and Morris¹², is 17.6 ft/s (12 mph).

C_{L0}	0.1116	$C_{M\delta\epsilon}$	1.0199	$C_{l\beta}$	-0.4870	$C_{n\beta}$	1.3636
$C_{L\alpha}$	3.2018	C_{Mq}	-2.5354	$C_{l\delta\alpha}$	0.8480	$C_{n\delta\alpha}$	-0.0126
$C_{L\delta\epsilon}$	0.2021	C_{y0}	-0.2865	$C_{l\delta r}$	0.0470	$C_{n\delta r}$	-0.0590
C_{M0}	8.4740	$C_{y\beta}$	-1.3751	C_{lr}	0.1121	C_{nr}	-0.0458
$C_{M\alpha}$	-0.4206	$C_{y\delta\alpha}$	-0.0550	C_{lp}	-0.6355	C_{np}	-0.0457

Table 4.10 – Stability Derivatives (1/rad) for Cruising Delivery Flight (AOA = 3 deg)

4.9 Structural Analysis

Structural analysis is conducted after identifying the material system and critical loading conditions.

4.9.1 Critical Design Loads and Parameters

The following parameters are critical for weight reduction and airframe integrity.

- **Manufacturing Process and Materials:** Investigation of alternative materials and construction methods are required to achieve the lightest possible aircraft (detailed in Section 6.0).
- **Top Wing Arrangement:** The restriction on top wing placement requires special structural considerations and analysis. The wings must be able to withstand a 2.5-G tip test.
- **Motor Mount:** It must be capable of distributing instantaneous motor loads (9-lb thrust and 12 in-lb torque) with a sufficient factor of safety.
- **Main Landing Gear Mount:** It must withstand a 5-G landing at full weight.

4.9.2 Structural Optimization

Structural optimization is paramount to reducing system and battery weight. The first study evaluates possible manufacturing techniques that could be used to build a light and reliable airplane. From analysis presented in Section 6.0, a hybrid composite method using fiberglass reinforced balsa is selected to construct a monocoque fuselage, while a balsa build-up approach is chosen for the wings and empennage.



The most important issue carried from conceptual design is the interference between the top wing spars and the payload bay. This can negatively impact loading time, and may provide a risk to the wing structure during payload handling. To circumvent these potential problems, it is determined necessary to avoid a continuous spar and to attach the top wing to the fuselage side-walls.

The proposed aircraft structure is analyzed numerically and experimentally. First, material properties for fiberglass reinforced balsa are obtained by conducting an MTS tensile test (Section 7.2). Next, a perfectly monocoque fuselage structure is modeled and solved in PATRAN/NASTRAN, a commercial finite element analysis package, to identify stress concentration points (the nose section is modeled without fillets for simplicity). Two critical loading scenarios are used: a 2.5-G load on the wing-fuselage attachment at maximum speed and throttle, and a 5-G landing at maximum weight. The first scenario is used to design proper reinforcements and load paths near the wing/fuselage connection and motor mount, while the second is used to design the main fuselage structure and landing gear mount.

The equivalent loads applied at the wing-fuselage attachment points on the fuselage model are calculated using Euler-Bernoulli Beam Theory⁶ with a triangular distributed loading of 8.75-lb and a 0.6 ft-lb torsional moment applied on each wing. The thrust loads are 9.5-lb and 12-in-lb at the motor mount location. Results yield maximum stresses of 625-psi located at the root chord of the top wing, and 3,500-psi located at the motor mount.

The 5-G landing scenario consists of a 70-lb landing load applied at the landing gear mount, shown in Figure 4.11. A maximum stress of 16,200-psi is obtained.

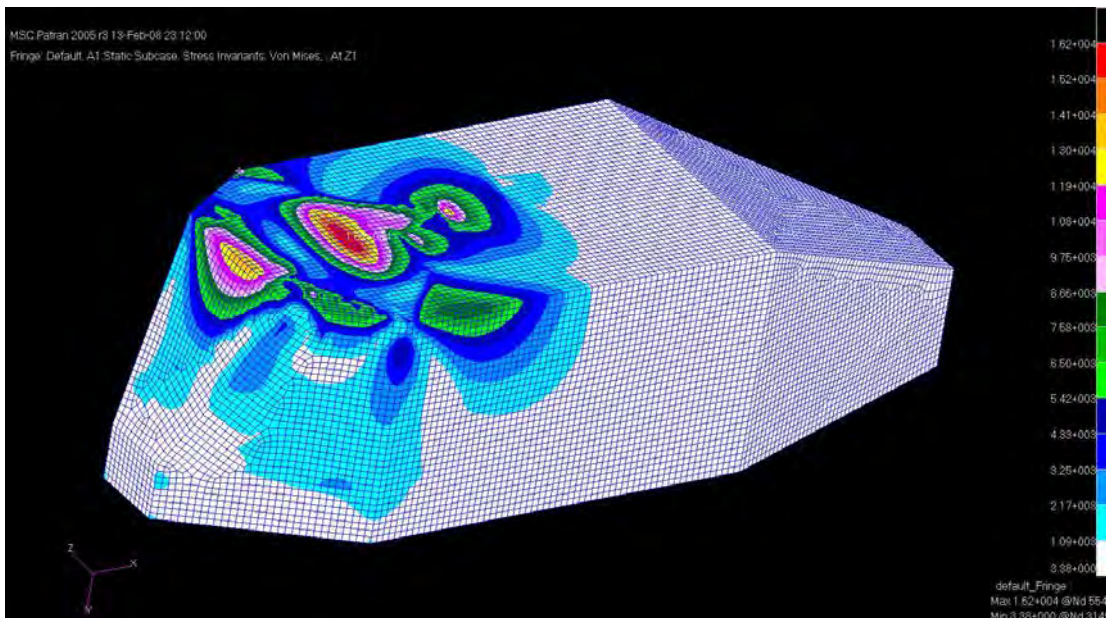


Figure 4.11 – FEM Results for a 5-G Landing at Maximum Weight



The results obtained from FEM analysis subsequently led to the design of appropriate load paths. As Figure 4.12 suggests, U-frames at the mid-fuselage section distribute landing loads, while longerons connect the main structure and reinforce the fuselage side panels. A motor mount and an aft bulkhead are used to support loads from the motor and empennage, which are transferred to the main structure via stringers. Once proper load paths are determined, calculations based on Euler-Bernoulli Beam Theory⁷ and Strength of Materials¹² are used to determine material and dimensions for the fuselage and wing's structure, which are documented in Sections 5.6 and 6.3.

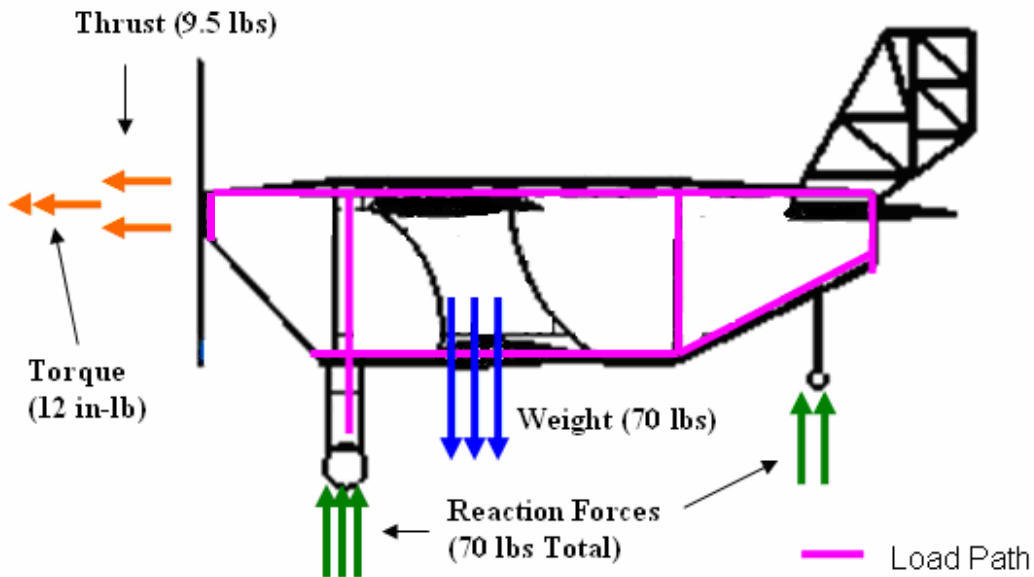


Figure 4.12 – Load Paths and Critical Loads

Internal fuselage attachment plates along with endplates are considered to reduce shear stresses and bending moments at the top wing roots. Experimental testing with a wiffle-tree apparatus evaluated the structural integrity of the proposed wing design (Section 7.1). Both wings were epoxy-glued to the fuselage walls. The experimental results showed that the system is capable of handling 2.6-G's, while deflections experienced at each wingtip were demonstrated to be approximately 2-in lower than predicted without endplates. The failure mode was compression buckling on the fuselage side panel. This outcome can be prevented if the low wing is not glued to the fuselage.

4.10 Aircraft Performance Predictions

Performance estimations are shown in Table 4.11. L/D versus Flight Speed and Power Available versus Power Required are shown for both missions in Figures 4.13 and 4.14, respectively. The cruise speed for the Delivery and Payload Missions are 40 ft/s and 50 ft/s, respectively. The maximum speeds are 59-ft/s and 75-ft/s for the Delivery and Payload Missions, respectively.



Basic Performance Parameters		Delivery Mission		Payload Mission	
$(L/D)_{max}$ (with flaps)	5.12	Max. Weight (lb)	5.75	Max. Weight (lb)	13.5
C_{Lmax} (12 deg)	1.0	Battery Weight (lb)	0.75	Battery Weight (lb)	1.50
C_{D0}	0.057	W / S (lb/ft ²)	0.60	W / S (lb/ft ²)	1.40
Oswald Efficiency Factor	0.77	T / W (takeoff)	0.87	T / W (takeoff)	0.67
Anticipated load factor	2.5	Cruise Speed (ft/s)	40.0	Cruise Speed (ft/s)	50.0
Rotation AOA (deg)	12	Stall Speed (ft/s)	22.0	Stall Speed (ft/s)	35.0
Rotation L/D (with flaps)	3.1	Takeoff distance (ft)	46.0	Takeoff distance (ft)	71.0

Table 4.11 – Aircraft Performance Predictions

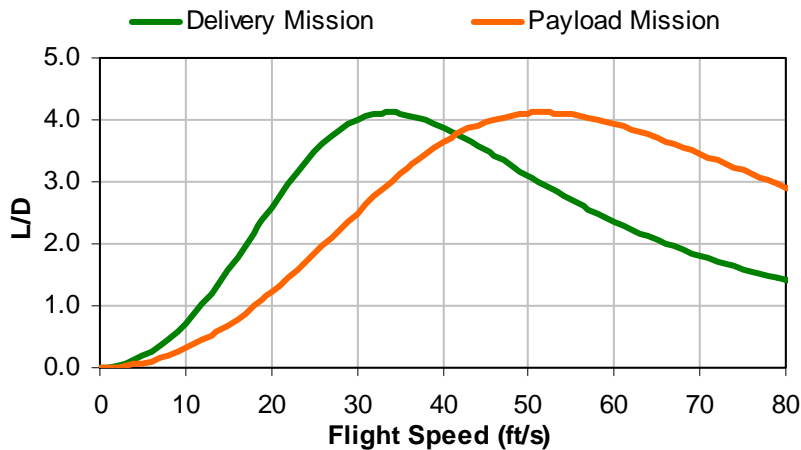


Figure 4.13 – L/D vs. Flight Speed

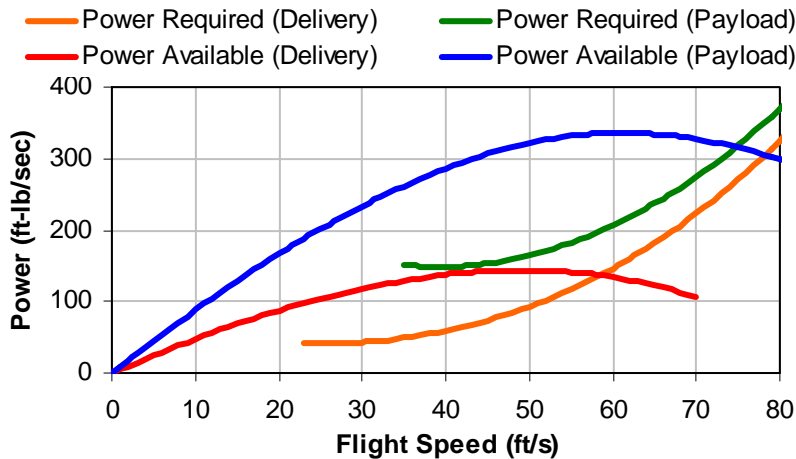


Figure 4.14 – Power Required vs. Flight Speed



4.11 Mission Performance Prediction

Table 4.12 shows current, energy, and time budgets for Delivery and Payload (max. wt.) Missions.

	Delivery Mission			Payload Mission		
	Current (Amps)	Time (sec)	Energy (mAh)	Current (Amps)	Time (sec)	Energy (mAh)
1st Lap						
Takeoff	24.0	2.3	14.7	40.5	4.3	47.8
Climb	23.8	4.7	30.8	40.1	8.1	90.0
Cruise (2000 ft)	19.4	47.0	252.1	35.8	35.8	355.5
180 turn (x 2)	18.9	21.0	109.7	38.1	19.7	212.8
Turn (360)	18.9	21.0	109.7	38.1	19.7	212.8
2nd Lap						
Cruise (2000 ft)	19.4	47.0	252.1	35.8	35.8	355.5
180 turn (x 2)	18.9	21.0	109.7	38.1	190.7	212.8
Turn (360)	18.9	21.0	109.7	38.1	190.7	212.8
3rd Lap	19.1(avg.)	89.0	477.8	-	-	-
Total	-	274.0	1,460.0	-	162.8	1,700.0
Available energy	-	-	1,600.0	-	-	1850.0
Excess Energy	-	-	260.0	-	-	150.0
Number of Laps	-	3	-	-	2	-

Table 4.12 – Current and Energy Budget for Delivery and Payload Missions

5.0 Detail Design

During detail design, all systems and components are selected and integrated. The aircraft structural characteristics and capabilities are finalized, and a complete aircraft sizing is expanded into a CAD loft depicting all features and dimensions. A weight and balance summary is compiled for each mission, including different payload combinations. Finally, flight and mission performance parameters are documented, along with the Rated Aircraft Cost for the Payload Mission.

5.1 Propulsion System Selection and Performance

The propulsion system components (Table 5.1) are selected based on data from Optimization Results (Section 4.4) and Propulsion Trade Studies (Section 4.7). The Opto-45 speed controller is chosen for its lightweight and its ability to handle high voltage. The batteries are located in front of the fore U-frames. Propulsion system performance predictions for this configuration are shown in Figure 5.1. The thrust values presented are validated experimentally in Section 8.0.

Propulsion Configuration		
Motor	NEU 1506/3Y geared 5.2:1	
Speed Controller	Opto-45	
	Delivery Mission	Payload Mission
Battery	12 Elite 1700	18 GP 2000
Propeller	APC 18x10E	APC 19x10E

Table 5.1 – Propulsion System Configuration

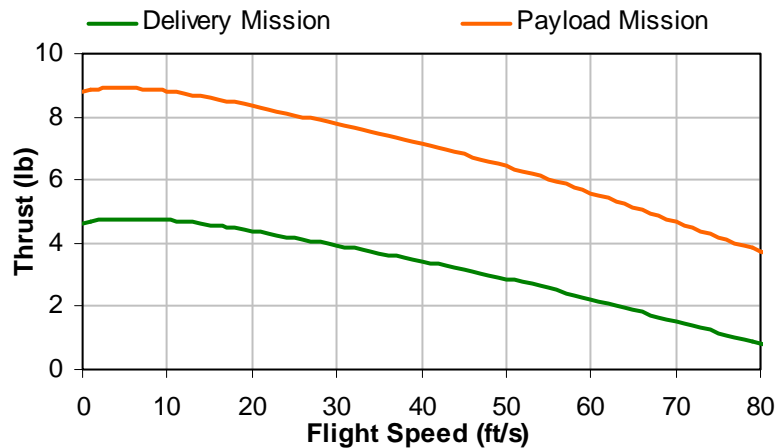


Figure 5.1 – Thrust vs. Flight Speed

5.2 Control Sub-System Selection

The control subsystems and selection justification are shown in Table 5.2. The elevator and rudder servos are located on the pressure side of the horizontal tail, on either side of the vertical. The flaperon servos are also placed on the top wing pressure side. The receiver battery is in front of the fore U-frames. The receiver is located behind the rear U-frames to minimize required wire length. Subsystem locations are shown in the Drawing Package (Section 5.9 – Systems Layout/Location).

Subsystem	Model	Weight (oz)	Selection Justification
Servos (4)	Hitec HS-85BB ⁺	0.67	Lightweight, Sufficient Torque
Receiver	JR R790UL 7-channel	0.42	Lightweight
Receiver Battery	JR Extra 1500	0.23	Lightweight, Adequate Capacity
Transmitter	JR X9303	N/A	Pilot Preference

Table 5.2 – Subsystem Selection and Justification

5.3 Aircraft Sizing

Fuselage					
Max Height (in)	10.5	Length (in)	39		
Maximum Diameter (in)	16.7	Landing Gear Height	6		
Base Diameter (in)	7.2	Aft upsweep (deg)	12		
Biplane Wings		Horizontal Tail		Vertical Tail	
Airfoil	SD 7062	Airfoil (inverted)	NACA 2408	Airfoil	Flat
Chord (in)	12	Chord (in)	10	Root Chord (in)	5
Span (in)	58	Span (in)	24	Tip Chord (in)	3
Area(in ²)	1392	Area (in ²)	240	Span (in)	12.5
Geometric AR	2.4	Aspect Ratio	2.4	Area (in ²)	81.3
Biplane AR	3.1	Incidence (deg)	0	Aspect Ratio	2.74
Stagger (in)	4	Volume Ratio	0.3	Volume Ratio	0.03
Aileron Chord (in)	1.7	Elevator Chord (in)	5	Rudder Chord (in)	5
Sa/S	0.04	Se/St	0.6	Sr/Sv	0.6

Table 5.3 – Aircraft Sizing



5.4 Aircraft Weight and Balance

Weight Build-Up		Delivery Mission		
Components	Weight (lb)			
Fuselage	1.30	Battery Weight (lb)	0.75	
Landing Gear	0.12	Gross Weight (lb)	5.55	
Payload Restraint	0.30	CG Location (in)	13.28	
Wings	1.40	Payload Mission		
Empennage	0.25	Battery Weight (lb)	1.5	
Servos	0.16	RAC (lb²)	7.2	
Receiver and Rx Battery	0.25	Payload Option	Gross Wt. (lb)	CG (in)
Wires, Bolts	0.31	14 bottles (7 lb)	13.3	13.70
Motor/Speed Controller	0.60	4 bricks (7.2 lb)	13.5	13.70
Propeller	0.10	10 bottles / 1 brick (6.8 lb)	13.1	13.73
System Weight	4.80	7 bottles / 2 bricks (7.1 lb)	13.4	13.70
		3 bottles / 3 bricks (6.9 lb)	13.2	13.68

Table 5.4 – (a) Weight Build-Up and (b) Mission Weight and Balance

5.5 Flight and Mission Performance

Table 5.5 lists some of the most important flight and mission performance parameters. In addition, Figure 5.2 shows the predicted (a) L/D curve and (b) drag polar for the final airplane with and without flaperon deflection.

Flight and Mission Performance				
		Delivery	Payload	
C_{D0}	0.057	Takeoff Distance (ft/s)	46	71
Oswald Efficiency Factor	0.77	Maximum Climb Rate (ft/min)	836	700
CL_{max} (No flaps)	1.01	Cruise Speed (ft/s)	40	50
L/D_{max} (No flaps)	4.10	Stall Speed (ft/s)	22	35
CL_{stall} (No Flaps)	1.23	Maximum Speed (ft/s)	59	75
CL_{max} (Flaps 15°)	1.34	Maximum Turn Rate (deg/min)	960	1188
L/D_{max} (Flaps 15°)	5.12	Max Load Factor	1.08	1.23

Table 5.5 – Flight and Mission Performance

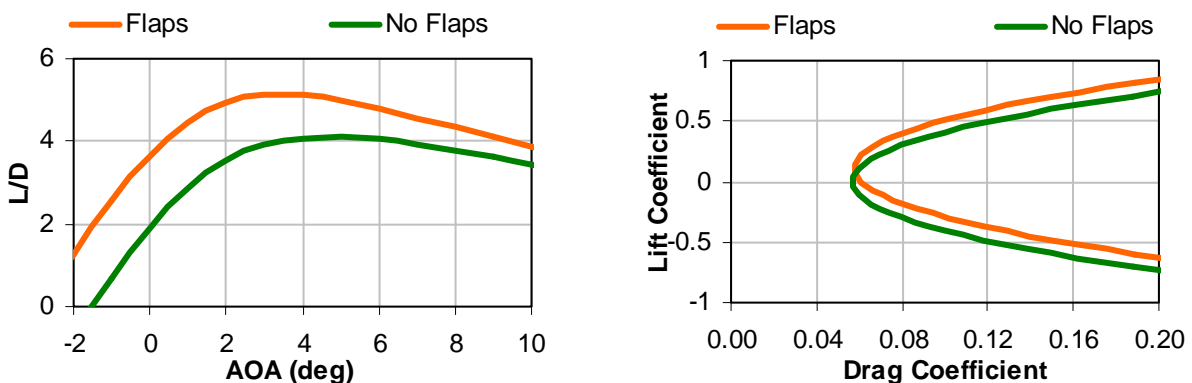


Figure 5.2 – Predicted Aerodynamic Performance



5.6 Structural Design and Capabilities

The aircraft structural design is based on the results from Structural Analysis (Section 4.9), and Manufacturing Methods and Materials FOM (Section 6.2).

The middle and aft fuselage skin is constructed by joining flat-plate sections of fiberglass reinforced balsa material. Four plywood U-frames (1/8-in thick) are attached to the side and bottom sections to reduce skin buckling and to efficiently transfer landing loads. Two plywood longerons (1/8-in thick) run across the base of the U-frames to stiffen the fuselage floor and to provide a resting platform for the payload bricks. An aft plywood bulkhead (1/8-in thick) is used to support the empennage load, which is transferred to the rear U-frames via 4 balsa stringers (1/4x1/4-in).

The nose is made using a molded method. This one piece structure better resists motor torque by providing improved shear flow. The motor is attached to the nose by a 5-ply plywood mount, which is connected to the main structure via 2 balsa stringers (1/4x1/4-in).

In addition, a 5-ply plywood mount attached between the two frontal U-frames supports the main landing loads, while a small 3-ply plywood mount attaches the secondary landing gear to the aft fuselage. The hatch is a composite laminate plate attached to the fuselage with Dubro™ hinges and light brass latches. Based on extended FEM analysis originally conducted in Section 4.9.2, the landing gear mount can support more than 5 G's with a safety factor of 1.2, and the nose/motor mount is designed for maximum propulsion loads of 14.25-lb and 18-in-lb which corresponds to a safety factor of 1.5. Figure 5.3 shows the fuselage structural layout.

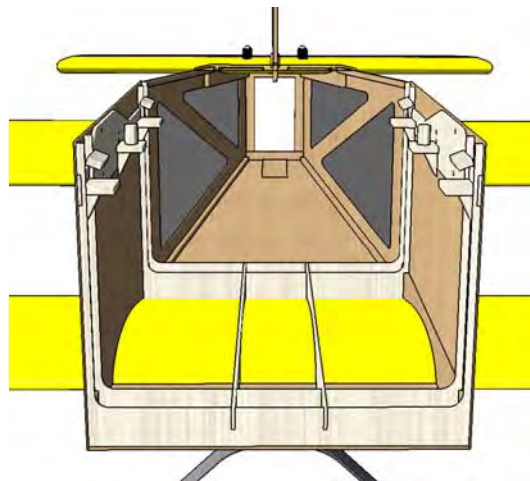


Figure 5.3 – Internal Fuselage Structural Layout

The top wing consists of 2 sections which are fixed to the fuselage side-walls by means of internal attachment plates. The top wing is framed by ribs and spaced with shear webs to improve bending rigidity and shear loading capabilities.



Five spruce spars span the wing: 1 at the leading edge, 2 at the quarter chord, and 2 at the trailing edge. The front-most spar is used to provide wing rigidity, the quarter chord spars handle bending loads, while the rear 2 handle torsional loads introduced from the flaperons. Based on structural testing results described in Sections 4.9.2 and 7.1, and FEM analysis, the top wing/fuselage connection is capable of supporting design loads up to 2.5 G's with a safety factor of 1.2.

The bottom wing consists of two joined wing sections and is attached to the fuselage floor by rubber bands strung across 2 dowel rods (1/4-in diameter balsa). The bottom wing has the same rib and shear plate configuration as the top wing. The main spar configuration is the same as the top wing, without the two trailing edge spars. In addition a spar which spans the fuselage's width is added to reinforce the joint between the two wing sections

Balsa sheeting is applied to the leading and trailing edge of both wings to preserve the airfoil shape. The wings are subsequently covered with Ultracote™ to create a light skin. Endplates connect the top and bottom wing to provide rigidity to the overall wing structure (Figure 5.4 (a)).

The horizontal stabilizer uses two spars to connect the ribs, similar to the top wing, and the vertical tail and rudder consists of a balsa truss structure (Figure 5.4 (b)). The empennage components are also covered with Ultracote™.

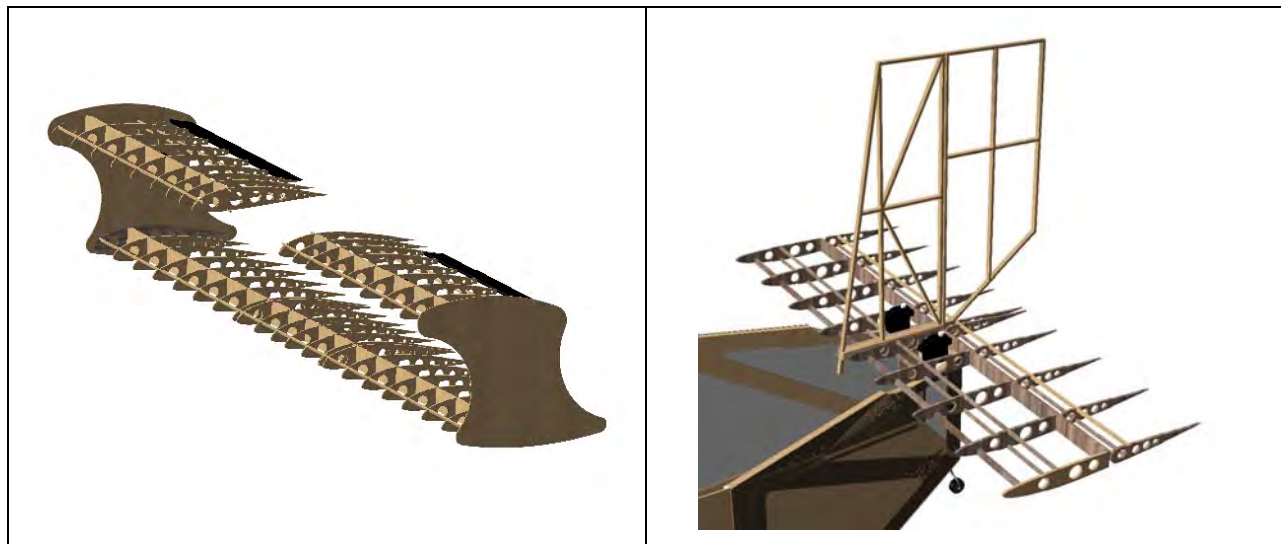


Figure 5.4 – Structural Layout of (a) Wings and (b) Empennage

5.7 Landing Gear Selection

For the primary landing gear, carbon fiber is selected over fiberglass and aluminum due to its high strength-to-weight ratio. The two options considered are:

- **Commercially Available:** Commercial landing gear comes in many different sizes and weights. These are usually built with a large factor of safety, which may be heavier than necessary.
- **Custom made:** The landing gear can be made exactly to the dimensions and mechanical properties desired. However, it is time consuming and requires a great deal of expertise.



The commercially available Graphtech RC 206 Banshee E3D carbon landing gear is selected over the custom gear option. It weighs only 1.9 ounces and provides a ground attitude of 12 degrees.

5.8 Payload Solution

The bottle restraint system is a speed-loader design made out of a fiberglass reinforced balsa plate with trap doors to secure the bottles by the neck (Figure 5.5 (a)).

Bottles that cannot be held by the neck due to a high collar location are first placed inside the aircraft, and then secured underneath by the bottle restraint. The bottle restraint rests on 6 brackets (3 on each side). The outermost brackets are covered with wood flaps to prevent vertical movement, and are attached to the fuselage sidewalls with CA hinges. The middle brackets on each side have a one-half inch diameter vertical dowel rod, which mates with holes drilled in the bottle restraint to prevent horizontal shifting. This fixture also increases the fuselage's structural rigidity by connecting the two fuselage sidewalls (Figure 5.5 (b)).

The bricks rest on top of the longerons, and are restrained by a balsa box-frame to prevent horizontal shifting. Cloth straps fitted with snap buttons are attached to either side of the box, and encircle the bricks to restrain them from vertical movement.

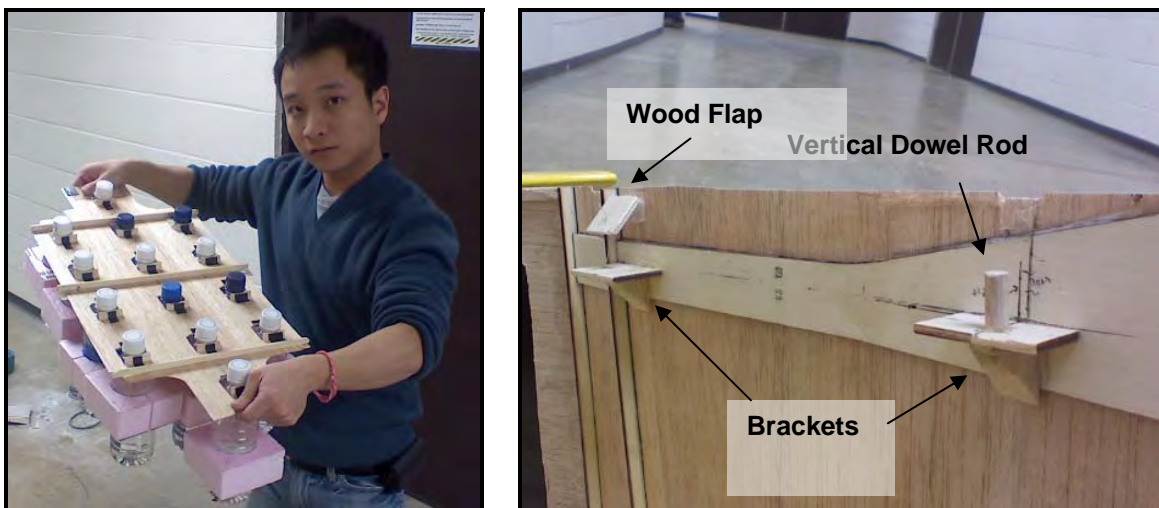


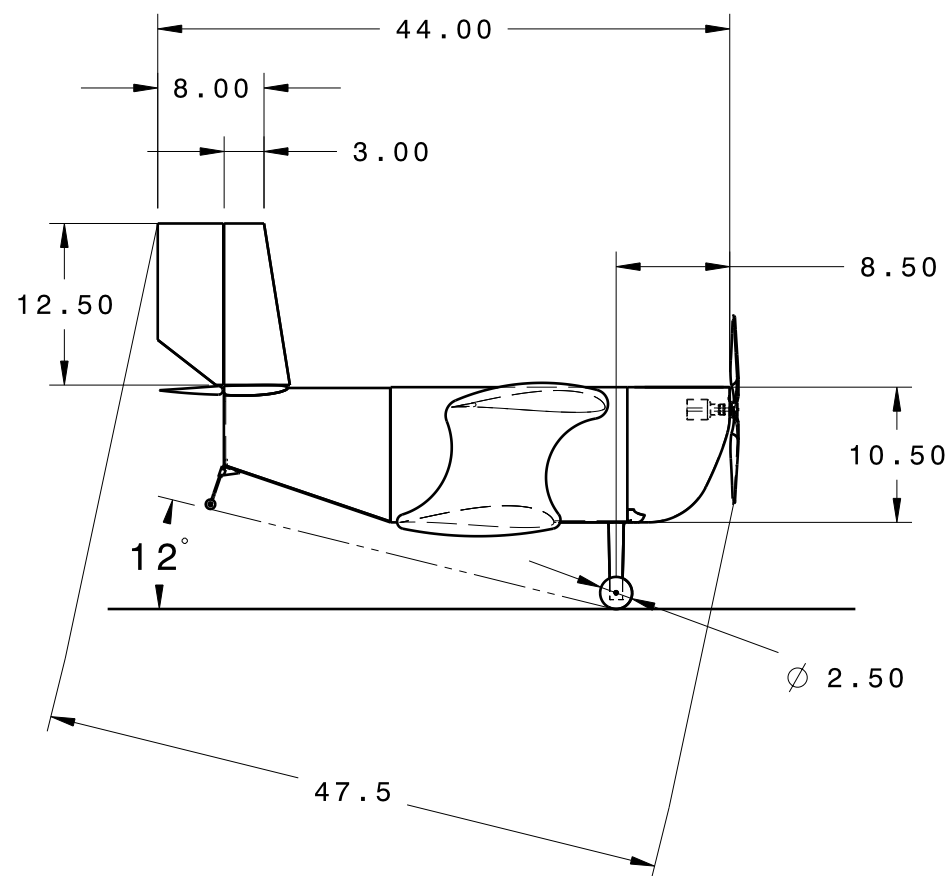
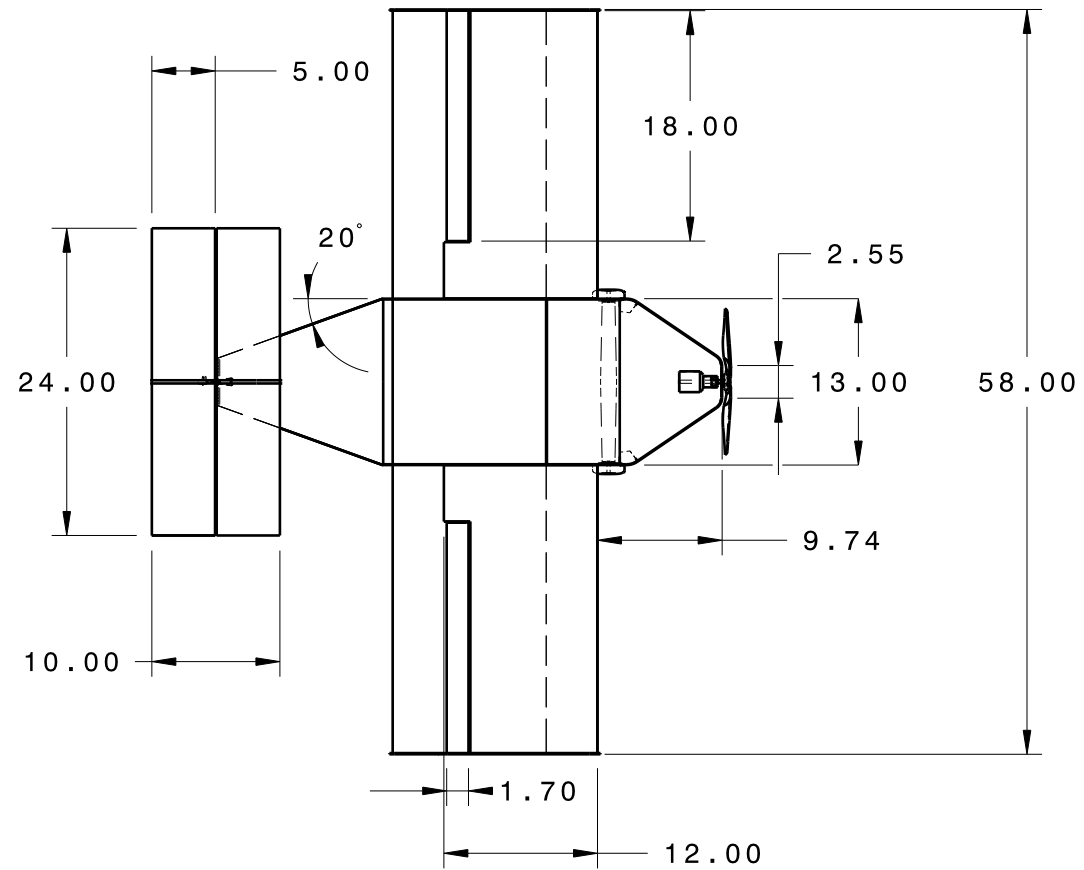
Figure 5.5 – (a) Bottle Restraint and (b) Bottle Restraint Attachment

5.9 Drawing Package

The drawing package, created using CATIA V5, includes the following drawings:

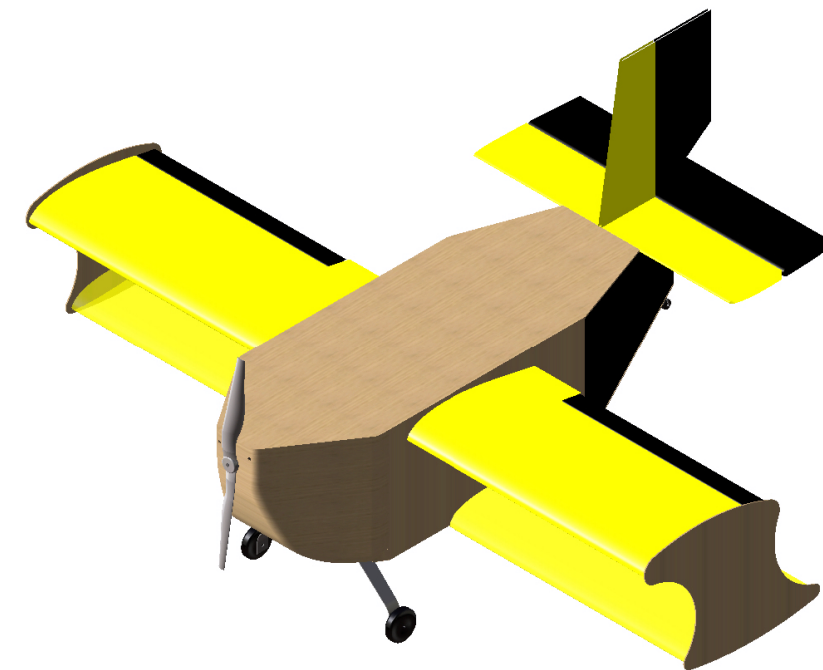
- Aircraft 3-view
- Structural Arrangement
- Systems Layout
- Payload System and Restraints

A

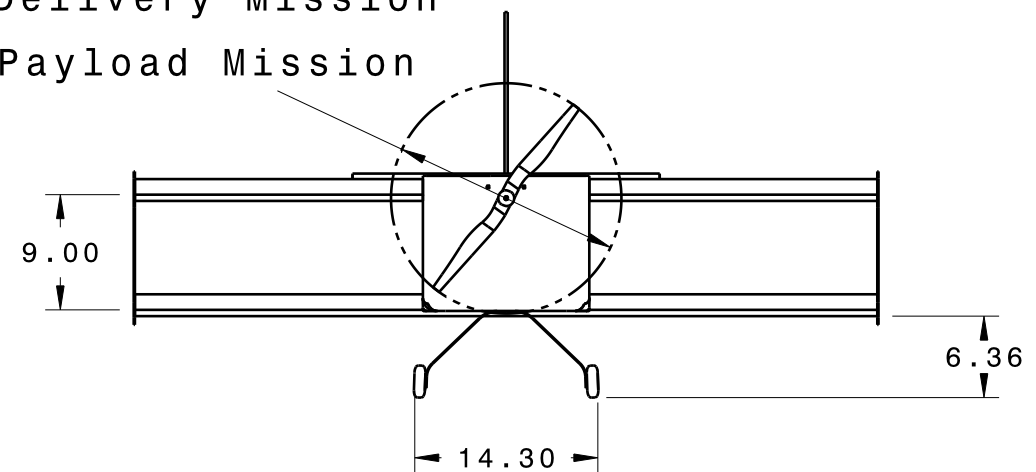


A

B



∅ 18.00 - Delivery Mission
 19.00 - Payload Mission

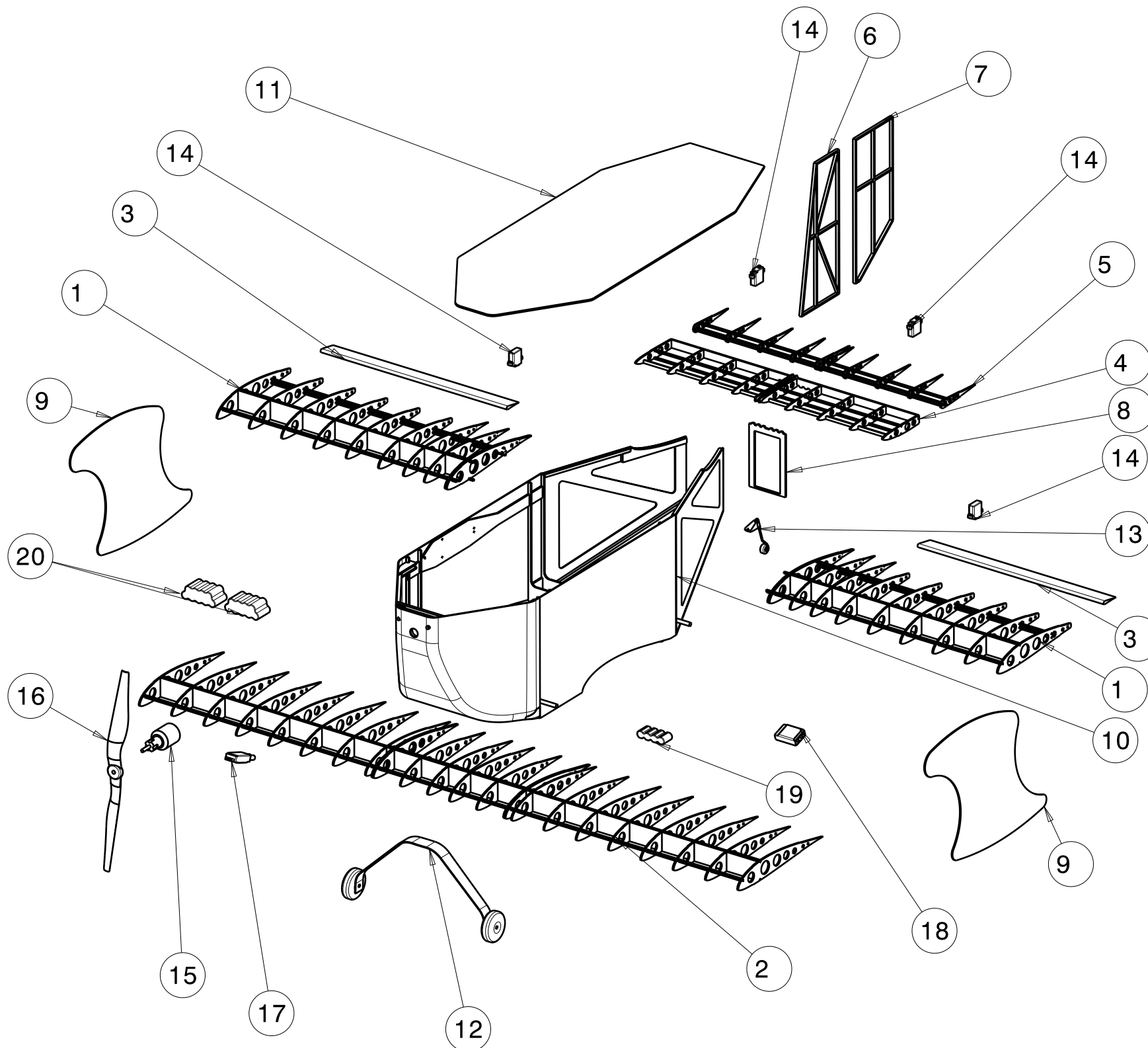


B

ALL DIMENSIONS IN INCHES		WICHITA STATE UNIVERSITY AeroShock		
DRAWN BY Y. SUWANSIRI		DRAWING TITLE AIRCRAFT 3-VIEW		
DATE 2/12/2008	CHECKED BY T. FRANTZ	DATE 2/26/2008	SIZE B	DRAWING NUMBER AS-1
DESIGNED BY AeroShock	DATE 11/12/2007	SCALE 1:15	SHEET 1/4	REV D

A

B



ITEM NO.	NAME	MATERIAL	QTY.
1	Top Wing Section	Balsa/Spruce	2
2	Bottom Wing	Balsa/Spruce	1
3	Flaperon	Balsa	2
4	Horizontal Stabilizer	Balsa/Spruce	1
5	Elevator	Balsa	1
6	Vertical Stabilizer	Balsa/Spruce	1
7	Rudder	Balsa	1
8	Aft Bulkhead	3-Ply Plywood	1
9	Endplate	Fiberglass/Balsa	2
10	Fuselage Assembly	Fiberglass/Balsa	1
11	Hatch	Fiberglass/Balsa	1
12	Main Landing Gear	Carbon Fiber	1
13	Trailing Gear	Aluminum Rod	1
14	Servo	Hitec HS-85 BB+	4
15	Motor	NEU 1506/3Y	1
16	Propeller	APC 18X10E/19X10E	1
17	Speed Controller	Opto 45	1
18	Receiver	JR R790UL	1
19	Receiver Battery	JR Extra 1500	1
20	System Battery Pack	9 GP2000/6 Elite 1700	2

ALL DIMENSIONS IN INCHES

WICHITA STATE UNIVERSITY
AeroShock

DRAWING TITLE

EXPLODED VIEW

DRAWN BY
Y. SUWANSIRIDATE
2/13/2008CHECKED BY
J. ANYASIDATE
2/26/2008DESIGNED BY
AeroShockDATE
11/12/2007SIZE
B

DRAWING NUMBER

AS-2

REV
B

SCALE 1:10

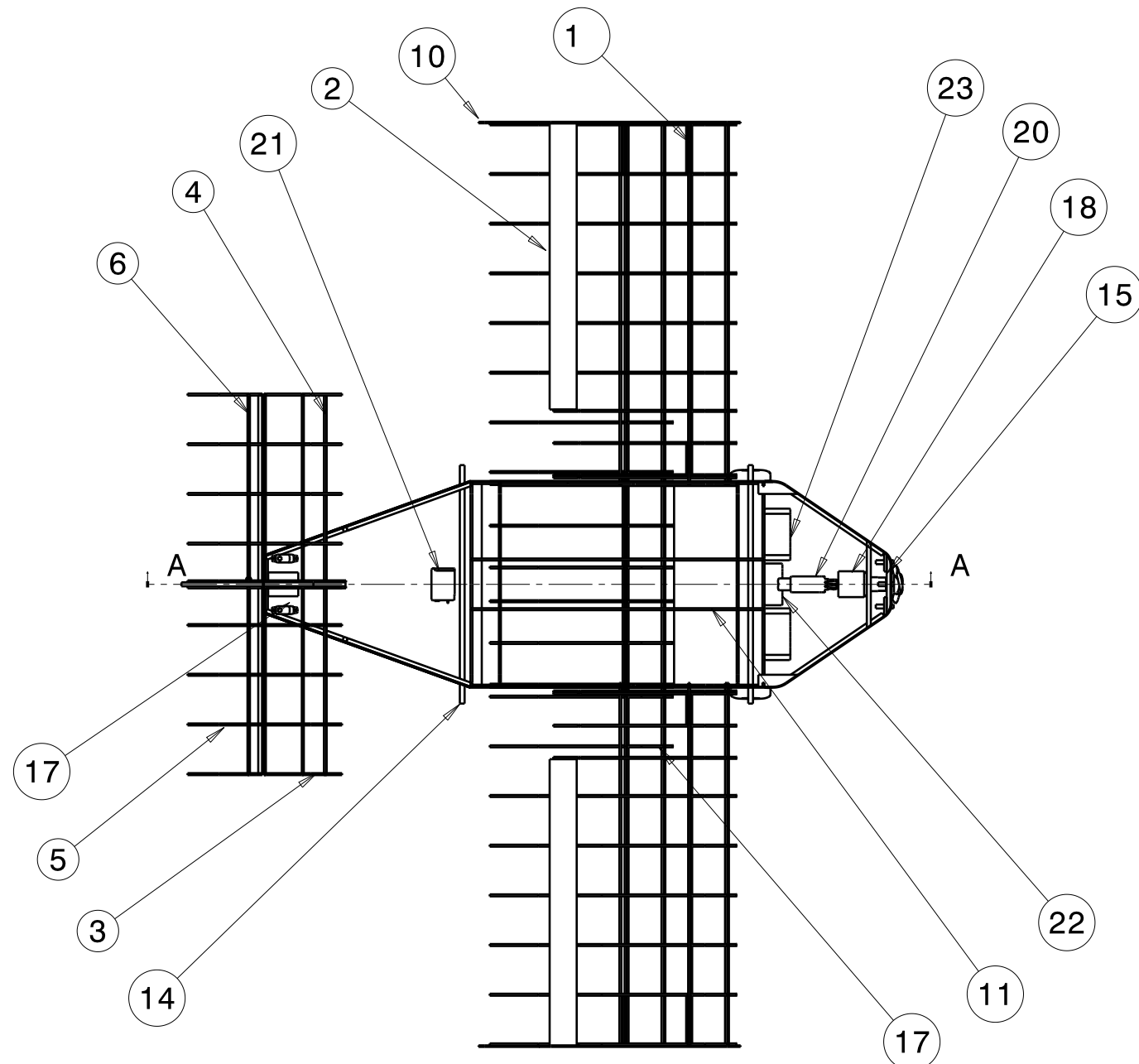
SHEET 2/4

A

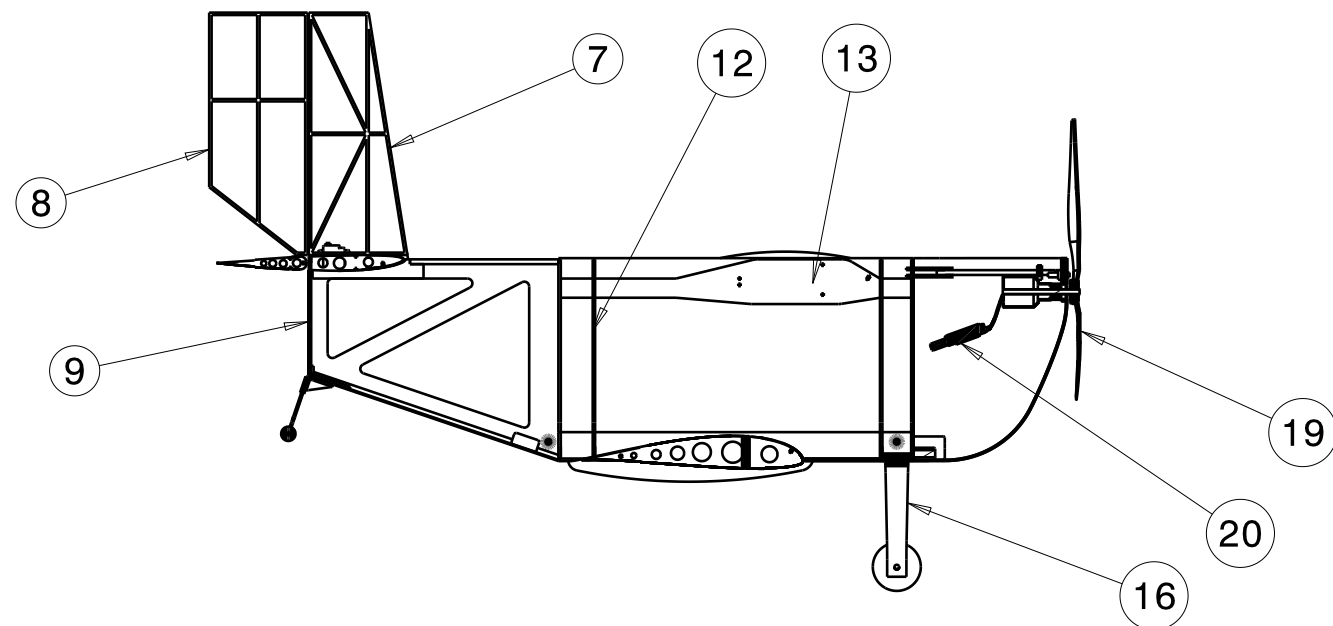
B

A

B



ITEM NO.	NAME	MATERIALS	QTY.
1	Wing Spar	Spruce	8
2	Flaperon	Balsa	2
3	Horizontal Stabilizer Rib	Balsa	10
4	Horizontal Stabilizer Spar	Spruce	2
5	Elevator Rib	Balsa	10
6	Elevator Spar	Spruce	2
7	Vertical Stabilizer	Balsa/Spruce	1
8	Rudder	Balsa	1
9	Aft Bulkhead	3-Ply Plywood	1
10	Endplate	Fiberglass-Balsa	2
11	Longeron	3-Ply Plywood	2
12	U-Frame	3-Ply Plywood	4
13	Wing Attachment	3-Ply Plywood	2
14	Dowel Rod	Wood	2
15	Motor Mount	3-Ply Plywood	1
16	Main Landing Gear	Carbon Fiber	1
17	Servo	Hitec HS-85 BB +	4
18	Motor	NEU 1506/3Y	1
19	Propeller	APC 18X10E/APC 19X10E	1
20	Speed Controller	Opto 45	1
21	Receiver	JR R790UL	1
22	Receiver Battery	JR Extra 1500	1
23	System Battery Pack	9 GP2000/6 Elite 1700	2



ALL DIMENSIONS IN INCHES		WICHITA STATE UNIVERSITY AeroShock		
DRAWN BY Y. SUWANSIRI		DRAWING TITLE Structural Arrangement & Systems Layout		
DATE 2/15/2008	CHECKED BY K. Y. TAN	DATE 2/26/2008	SIZE B	DRAWING NUMBER AS-3
DESIGNED BY AeroShock	DATE 11/12/2007	SCALE 1:10	SHEET 3/4	REV D

A

B



6.0 Manufacturing Plan

The type of manufacturing process chosen is affected by human and financial resources, along with aircraft weight and reparability issues. Therefore, it is important to properly select a procedure that takes all of these considerations into account.

6.1 Manufacturing Methods and Materials

Fuselage, wing, and empennage construction methods are evaluated using a FOM analysis. The methods considered are listed along with advantages and disadvantages.

- **Balsa Build-Up:** The structure consists primarily of a wooden frame. Parts can be laser cut for accurate dimensioning. The components are covered with Ultracote™ to provide an aerodynamic surface. This method can be structurally complicated and damages easily, however repair is relatively simple.
- **Lost Foam Composite:** A foam plug is created, and fiberglass and epoxy are laid on top of it and allowed to cure. After cure, the foam is dissolved using acetone. The result is a very lightweight structure. A new foam plug must be created each time a part is manufactured.
- **Foam Core Composite:** Same as the lost foam method, except the foam plug remains as a core.
- **Molded Composite:** The entire fuselage is created using a female mold. First, a foam plug is created to the desired shape of the fuselage. Next, a release agent is applied to the plug, and a female mold is created on top of it using thick fiberglass cloth. The resultant female mold possesses a smooth internal cavity to allow for the creation of a smooth external aircraft surface. This method requires many steps; however if performed correctly, the final product can be very light and strong.
- **Hybrid Composite:** This is a combination of composite manufacturing techniques which uses flat composite laminates for relatively flat sections, and a molded method for heavily contoured sections. This method requires less time than the molded method, and flat sections can be much more easily repaired than molded sections.

6.2 Manufacturing Methods and Materials Figure of Merit

The following five Figures of Merit are employed to select a proper manufacturing method.

- **Weight:** This factor is more significant for the fuselage than the wings or empennage; however it still remains a factor that cannot be neglected for any component.
- **Ease of Manufacturing:** This relates directly to the amount of time involved and the expertise necessary to build the part.
- **Precision:** This is more important for detailed components such as a wing or tail than a fuselage.
- **Cost:** This must always be considered for any manufacturing process.
- **Ease of Repair:** During the competition, field repair must be conducted reliably and efficiently.



- **Strength:** This factor can vary greatly between fuselage manufacturing methods, but not as much for wings and empennage construction.

Manufacturing Methods and Materials Figure of Merit							
Wings & Empennage	Figures of Merit	Weight (%)	Build-up	Foam Core	Lost Foam	Molded	Hybrid
	Weight	35	5	2	3	5	4
	Ease of Manufacturing	25	4	3	3	1	2
	Precision	20	3	4	4	4	4
	Cost	10	5	4	4	1	2
	Ease of Repair	10	3	3	2	2	3
	Total FOM	100	415	295	320	310	320
Fuselage	Weight (%)	Build-up	Foam Core	Lost Foam	Molded	Hybrid	
	Weight	35	5	2	3	5	5
	Ease of Manufacturing	15	4	3	3	1	2
	Strength	25	1	2	3	5	5
	Cost	10	5	4	4	1	2
	Ease of Repair	15	3	3	2	2	3
	Total FOM	100	355	250	295	355	395

Table 6.1 - Manufacturing Methods and Materials

A balsa build-up method is chosen for the wings and empennage, while a hybrid composite method is chosen for the fuselage.

After choosing a manufacturing method for the fuselage, it is necessary to choose a material which results in a lightweight, sufficiently rigid structure, which is durable and can be repaired between missions. Different materials considered include: carbon, Kevlar, and fiberglass, as well as fiberglass reinforced balsa. The fiberglass reinforced balsa construction method is determined to have the best combination of weight and stiffness qualities based on historical data and material properties. This construction method requires wet lay-up, since the balsa core would incinerate in an oven if prepreg were to be used.

6.3 Construction Process

- **Fuselage:** The main fuselage construction (middle and aft sections) begins by laying up flat plates consisting of 1 layer of 1/32-in contest grade balsa sandwiched between two layers of ½ oz/yd² fiberglass plain weave. Second, templates dimensioned in CAD are used to make section panels that are then joined with strips of thin fiberglass cloth and slow-set epoxy. The nose is created using a female molded method, as described in Section 6.1. Figure 6.1(b) shows the application of epoxy onto the nose's external fiberglass layer. The internal fuselage structure as described in Section 5.6 is shown in Figure 6.1 (c).



Figure 6.1—(a) Laminate Sheets, (b) Nose Lay-up, (c) Fuselage Structure, and (d) Final Fuselage

- **Wings:** The wings are made to the structural specifications of Section 5.6. The 2 top wing sections are attached to the fuselage by means of attachment plates made from 3-ply plywood. The top wing ribs (20) and shear plates (20) are made from 1/8-in thick balsa. All the spars for the top wing are made from 1/8x1/8-in spruce, except for the leading edge spar (1/8x1/4-in spruce). The bottom wing has 23 ribs and 26 shear plates. All spars for the bottom wing are 1/8x1/8-in spruce, except for the leading edge and the reinforcement spar (1/8x1/4-in spruce and 1/4x1/4-in spruce, respectively). The leading and trailing edge of the wing are sheathed with 1/32-in balsa. Finally, the two wings are joined by composite endplates (1/16 fiberglass-balsa sandwich) on the tips after installation on the fuselage.
- **Empennage:** The horizontal and vertical tails are created according to Section 5.6. The horizontal utilizes four 1/8x1/8-in spruce spars; two leading and two trailing. Slots located in the horizontal tail root mate with components of the vertical tail. A corrugated 1/8-in thick balsa adapter is attached to the trailing spars, which is mated with the aft bulkhead. The vertical tail and rudder consist of a truss structure created from 1/4x1/4-in balsa components.



- Payload Restraint:** This system is built according to the specifications outlined in Section 5.8. The bottle restraint is created from a 1/32-in composite laminate plate, with 1x3-in flaps to hold the bottle necks. Three 1/4x1/2-in balsa sticks run laterally along the top of the plate to provide extra rigidity. The brick holder is made from sections of 1/8-in balsa sheets cut to 1/2-in tall and 4-in wide, while the straps are 1/2x6-in nylon material.
- Assembled Prototype:**

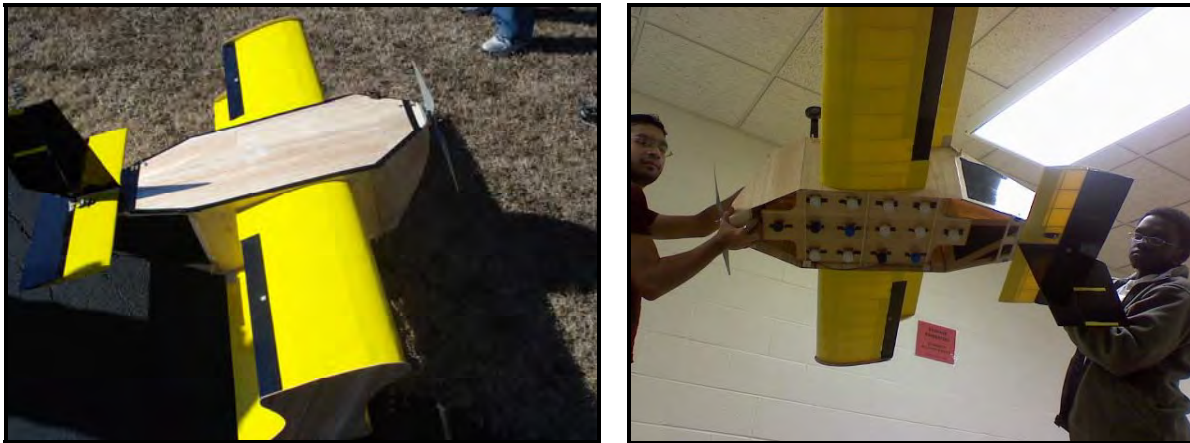


Figure 6.2 – (a) Assembled Aircraft and (b) Inverted Test with 14 Bottles Payload

6.4 Manufacturing Schedule

A detailed construction scheme is created to assist with the organization of manufacturing processes.

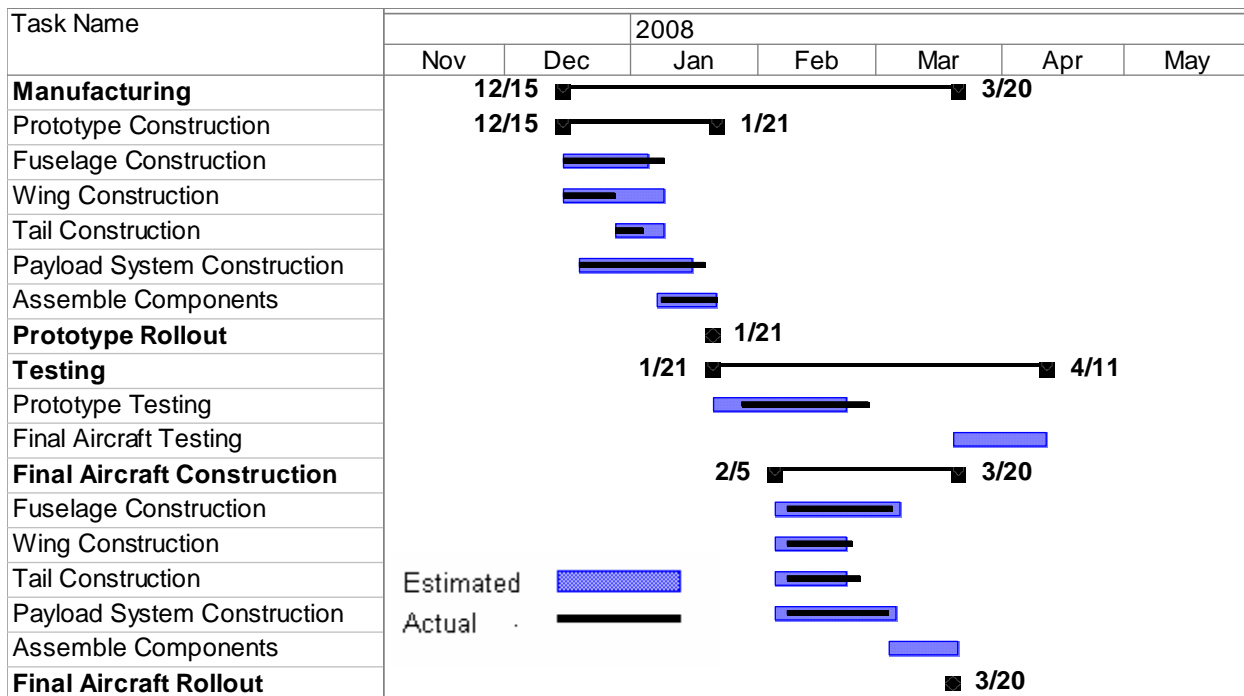


Figure 6.3 – Manufacturing Schedule



7.0 Testing Plan

A comprehensive plan is devised to systematize the team's testing schedule and milestones. Table 7.1 lists all the tests conducted and Figure 7.1 shows the testing schedule as it currently stands.

Date	Test	Objective
11/10/07 - 11/29/07	Structural Testing	Verify wing-fuselage structural integrity
10/22/07 - 10/23/07	Material Testing	Obtain composite material properties
10/18/07 - 10/21/07	Propeller testing	Obtain propeller coefficients
10/16/07 - 10/22/07	Half-Scale Wind Tunnel Test	Study concept aerodynamic performance
2/8/08 - 2/9/08	Propulsion Wind Tunnel Test	Verify propulsion system performance
2/26/08 – 2/28/08	Full Scale Wind Tunnel Test	Study aircraft aerodynamic performance
1/21/2008 – 4/11/2008	Flight Testing	Study aircraft flight performance

Table 7.1 – Testing

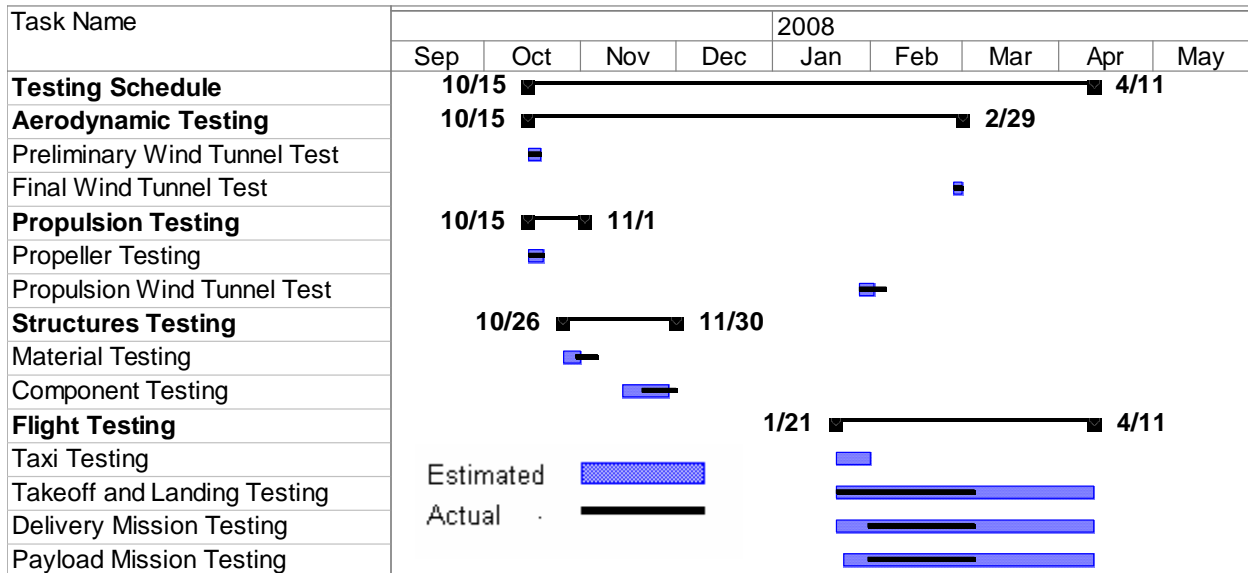


Figure 7.1 – Testing Schedule

7.1 Structural Testing

The top wing-fuselage configuration designed to facilitate loading requires structural verification to ensure an acceptable factor of safety. A wiffle-tree apparatus is used to simulate the effects of linear distributed loading along half of the wing-fuselage system. Incremental loading of 0.5-lb is applied until 18-lb is reached on both lower and upper wings (2.6 G's). Structural failure due to compression buckling occurs on the lower fuselage side wall shortly after the 18-lb loading was applied, while the wings remain intact. The indicated failure mode is not expected during flight.

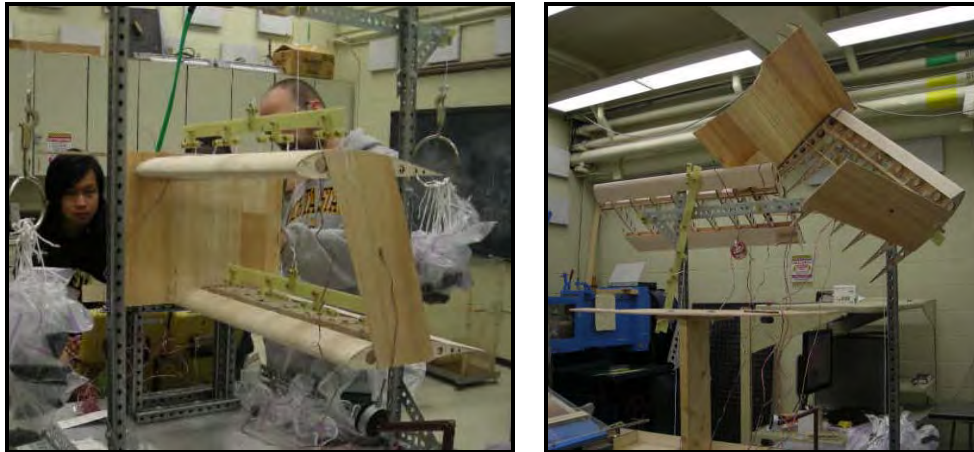


Figure 7.2 - Wing Structure Testing (a) During Test and (b) After Failure

7.2 Material Testing

Longitudinal and shear tensile testing is conducted on multiple fiberglass-balsa sandwich specimens to determine ultimate longitudinal strength and strain, ultimate shear strength and strain, and elastic and shear moduli. The resulting material properties are incorporated in the FEM analysis. A MTS tensile machine with a 200-lb load-cell was used for all tests. Figure 7.3 shows the test specimens and the apparatus during testing.



Figure 7.3 – (a) Prepared Specimens and (b) Testing in Progress

7.3 Propeller Testing

Wind tunnel testing is conducted to expand WSU's available propeller database.¹⁴ Figure 7.4 shows an APC 18x10E propeller mounted to a sting balance in the tunnel test section. The main output from the tests are propeller thrust, torque, and power coefficients, which are used in the MDO propulsion module.

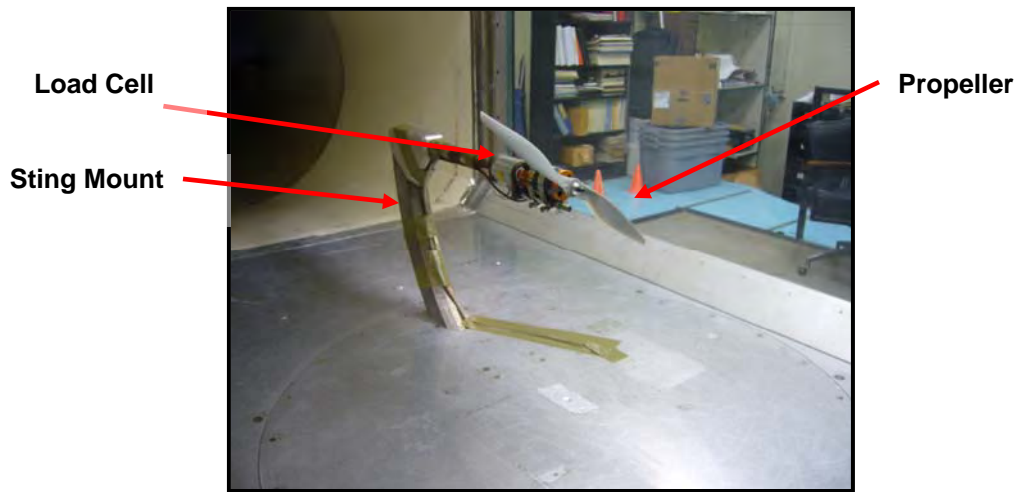


Figure 7.4 – Propeller in 3x4-ft Low Speed Wind Tunnel at Wichita State University

7.4 Half-Scale Wind Tunnel Testing

The 3x4-ft Low Speed Wind Tunnel at WSU is used to evaluate the proposed airplane configuration at the beginning of preliminary design. The test's primary goals are: to analyze the effects of endplates, stagger and aerodynamic wing interference. Some secondary goals include: visualization of flow separation at the aft fuselage and validation of methods and assumptions (e.g. Oswald Efficiency Factors) made based on the data available from the 2006/07 Wichita State DBF Team¹. The model shown in Figure 7.6 is attached inverted to a three component external balance. The data obtained from this test proved critical to the optimization process.

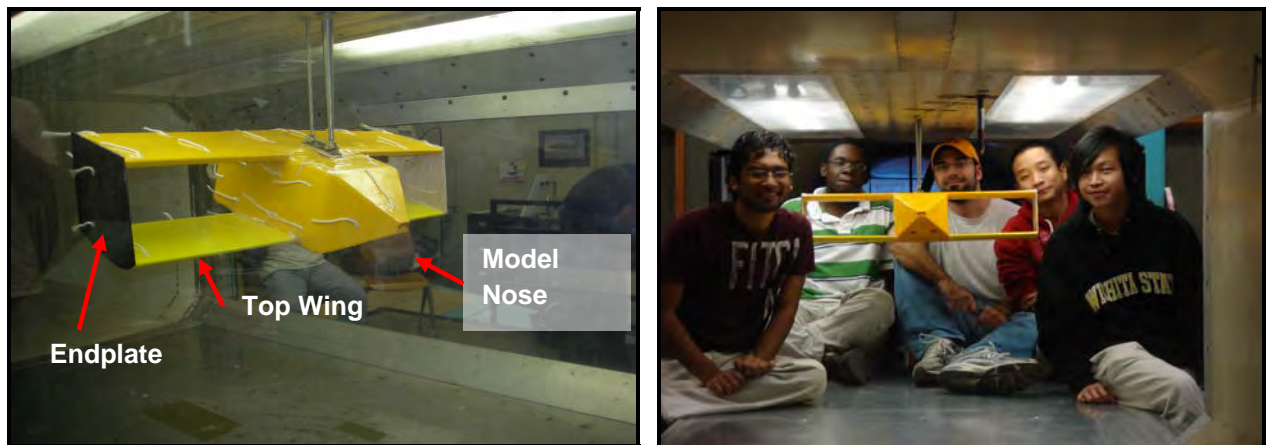


Figure 7.5 – (a) Test Model at High AOA and (b) Senior Design Team

7.5 Propulsion System Wind Tunnel Testing

The propulsion system selected in detail design is also tested at the WSU 3x4-ft Low Speed Wind Tunnel. The motor is mounted on a three component balance. Results are reported in Section 8.0.



Run #	Type	Battery Configuration
1	q-sweep	16 GP2000 (Exploratory Run)
2 - 6	q-sweep	12 GP2000 / 12 Elite1700 / 18 GP2000 / 10 Elite1500 / 16 GP2200

Table 7.1 Propulsion System Wind Tunnel Test Matrix

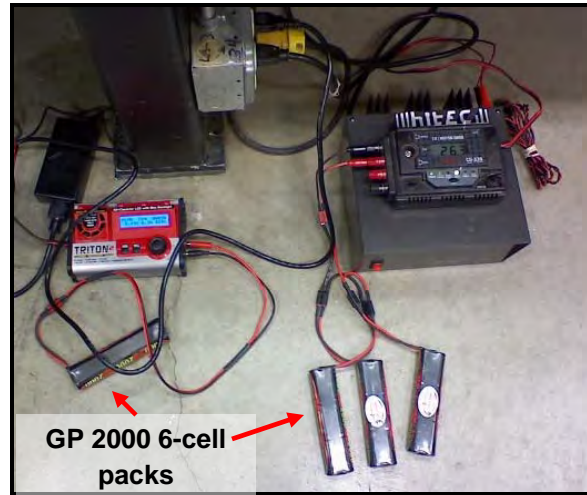
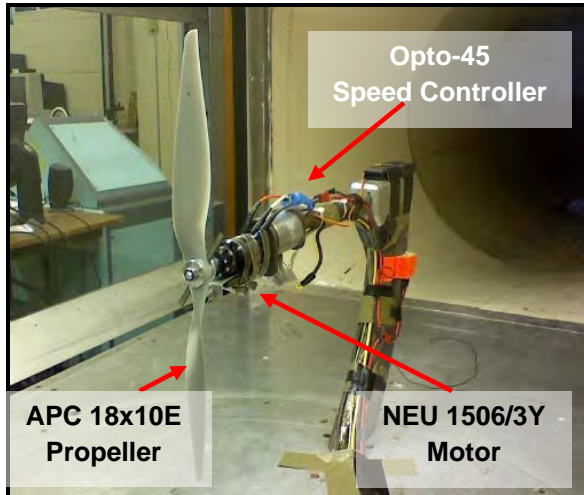


Figure 7.6 –Propulsion Test (a) Propeller, Motor & Related Components (b) Batteries and Chargers

7.6 Full Scale Wind Tunnel Testing

Wind tunnel testing is conducted in the 7x10-ft Low Speed Walter H. Beech Memorial Wind Tunnel at WSU to obtain reliable performance data that validate the airplane’s aerodynamic characteristics and performance predictions. Pilot feedback during flight testing also influenced the development of the test matrix, which is shown in Table 7.2. The aircraft prototype is mounted to a six component pyramidal external balance. Results from this test are reported in Section 8.0.

Run	Type	α (°)	β (°)	δe (°)	δr (°)	δa (°)
3001	Dynamic Tares	-2, 14, 1	0, 4, 8, 12	-	-	-
1001	Static Tares	-2, 14, 1	0, 4, 8, 12	-	-	-
01	α -sweep	-2,14,1	0	0	0	0
02	α -sweep	-2,14,2	0	0	0	Max
03-05	α -sweep	0, 8, 2	0	5, 10, Max	0	0
06-08	α -sweep	0, 8, 2	0	0	0	5, 10, Max
09-10	α -sweep	0, 8, 2	0	0	5, 10, Max	0
12-14	α -sweep	0, 8, 2	4, 8, 12	0	0	0
15	Power 10 Cells	0, 8, 2	0	0	0	0
16	Power 12 Cells	0, 8, 2	0	0	0	0
17	Repeat 01	-2,14,1	0	0	0	0
18	Smoke Flow Vis.	Variable	0	Variable	Variable	Variable

Table 7.2 Full-Scale Wind Tunnel Test Matrix

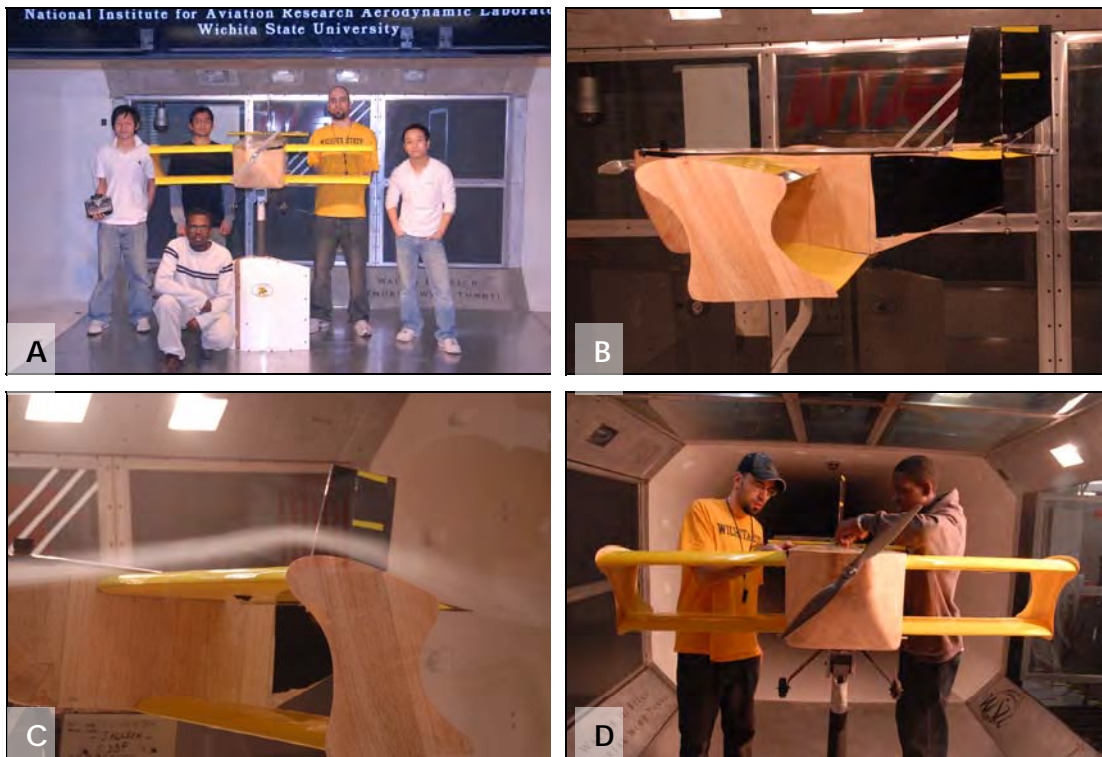


Figure 7.7 – (a) Senior Design Team, (b) Airplane Mounted, (c) Smoke Visualization, and (d) Set-up

7.7 Flight Testing

Flight testing began on January 26th, 2008. Table 7.3 shows the preflight checklist followed before each flight. Table 7.4 summarizes the Flight Test Plan. Figure 7.5 illustrates the airplane (a) during its maiden flight and (b) landing on the last flight to date.

Item	Description	Initial
Electrical System	Verify all wires are connected, check fuse	
Propulsion System	Batteries properly charged, motor and propeller secured	
C.G. Location	Payload and batteries are properly located and secured	
Payload Restraint	Verify restraint is correctly secured to the airframe	
Hatch	Closed and secured	
Structural Integrity	Wing tip test, landing gear properly secured	
Radio	Battery charged, range check (antenna down to 200-ft)	
Flight Controls	Correct, unrestricted range of movement	
Pilot Briefing	Describe flight profile and predict handling qualities	
Ground Run	Perform full-throttle run-up for 5 seconds	
Wind	Check wind speed and direction	

Table 7.3 – Preflight Checklist



Test #	Conditions	Acceptance Criteria
1	Taxi Test - Straight and 180° turns - Headwind, tailwind, X-wind	Aircraft controllable during entire taxi test. Turn radius not excessive.
2	- Straight ahead climb to 200-ft - Left and right 180° turns - Overhead pass - Normal Landing	Aircraft stable and controllable. Altitude maintained during turns. Control surface effective, but not overly sensitive.
3	- Takeoff, climb, cruise - Vary throttle settings - Slow Flight - Landing practice	Sustained flight with reduced throttle setting. No unstable behavior observed during slow flights or landings.
4	- Practice competition profile - Install 14 bottle payload and re-fly - Switch to 4 bricks payload and re-fly - Switch to 10 bottles and 1 brick and re-fly - Switch to 7 bottles and 2 bricks and re-fly - Switch to 3 bottles and 3 bricks and re-fly	Aircraft performance and stability satisfactory with payloads installed. Takeoff with 75-ft distance met for all payload combinations
5+	- Competition Practice - Cross and high wind practice	Able to handle X-winds greater than 10 mph and gusts above 20 mph.

Table 7.4 – Flight Test Plan and Checklist



Figure 7.8 – (a) Maiden Flight on Jan. 26th and (b) Sixth Flight on Feb. 29th



8.0 Performance Results

Predictions made in Section 5.0 are compared against demonstrated performance results obtained from the tests detailed in Section 7.0 for the propulsion system and the complete aircraft.

8.1 Propulsion System Evaluation

Propulsion wind tunnel testing (Section 7.5) confirms the system performance predictions. Figure 8.1 compares results between the propulsion code and the experimental data for: 12 cells with an 18 x 10 propeller, and 18 cells with a 19 x 10 propeller. The code predictions include the densities recorded during testing. The results are considered to be in excellent agreement. A special provision to the preflight checklist is added to ensure that the battery packs are properly charged. The difference between predicted and empirical values is approximately 3% for low speeds. Experimental uncertainties include wire resistance, lack of battery cooling, and the tunnel turbulence intensity, which is higher than the typical atmospheric value.

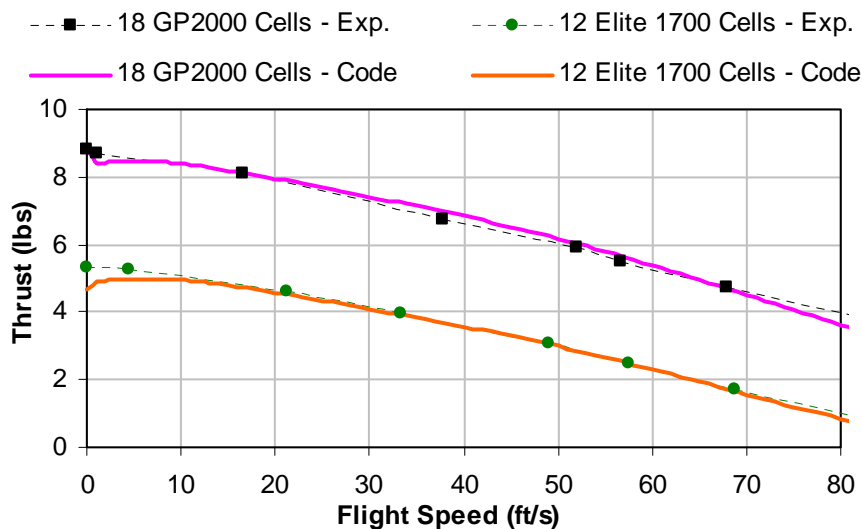


Figure 8.1 – Propulsion System Predictions vs. Experimental Data

8.2 Flight Testing Evaluation

Results and observations from flight testing are listed in Table 8.1, along with the team's testing evaluation and measures taken to improve the airplane. The most important problems found were related to the aircraft's stability. After the first flight, the entire S&C Module was revisited and updated to correctly account for the aircraft's MAC and CG locations. Next, flight testing with X-winds showed that the airplane has a tendency to sideslip into the wind due to the large amount of fuselage area behind the CG. Corrective measures are being considered at the present time. A flight-testing video database has been compiled and stored in the video-sharing website Youtube (Search: AeroShockWSU).



Flight No. – Description	Comments and/or Solutions
Flight #1 – Airplane was tail-heavy and could not be trimmed during flare with reduced power.	Mean AC was not properly predicted. S&C program was updated.
Flight #2 – Airplane experienced adverse yaw during turns. Control surface deflection was satisfactory.	Rudder and aileron were mixed to counteract adverse yaw. Pilot stated empty aircraft was overpowered with 12 cells.
Flight #3 – Empty airplane took-off at 36 ft with a 9-mph X-wind and 3-mph headwind.	Takeoff distance satisfactory for Delivery Mission. Airplane exhibited tendency to turn into the wind.
Flight #4 – Fast charged battery packs did not release power. Pilot quickly landed.	Further study confirmed that battery packs had not been properly trickle charged.
Flight #5 – Takeoff distance: 67-ft with 14 bottles (7.0 lbs payload) and no headwind.	First payload flight. Rudder and aileron mixing for turns allows fast 360-deg turns in 5 seconds.
Flight #6 – Second payload flight with same configuration.	Airplane veers to the left during takeoff due to motor torque. Pilot recommends more allowable rudder deflection.

Table 8.1 – Aircraft Performance Evaluation (Flight Testing)

8.3 Wind Tunnel Study and Evaluation of Complete Aircraft

As described in Section 7.6, the first prototype is subjected to full scale wind tunnel testing in order to corroborate the observations made during flight testing and to validate many aerodynamic performance parameters. Some important conclusions made after testing are:

- The Oswald Efficiency Factor was considerably under-predicted during design, which improved from the predicted 0.77 to 0.85. It is clear that the fuselage design improved from the half-scale wind tunnel test (Section 7.4) to the full-scale test.
- The aircraft zero-lift coefficient increased by 0.13 (from 0.11 to 0.24).
- The aircraft's parasite drag coefficient (C_{D0}) increased from 0.057 (Section 4.6) to 0.067. This was expected, as Roskam's drag built up method does not account for sharp corner edges.
- The increment in lift coefficient from flaperons on the top wing is correctly estimated.
- Results from Power-on runs show that the aircraft's lift coefficients improve as the amount of propeller rpm increases (See Figure 8.3).

The improvements in aerodynamic performance allow the team to re-evaluate the previously selected propulsion system. The MDO Modules, which have been updated with full-scale experimental data, suggest that the airplane can complete the Delivery Mission with 10 Elite 1500 cells, and the Payload Mission with either 16 GP2000 cells and a 19x10 propeller, or 14 GP2000 cells and a 20x10-in propeller. Figure 8.3 presents updated Power-Required curves for both missions and power-available curves for the previously mentioned propulsion system configurations, along with the ones selected during detail design.

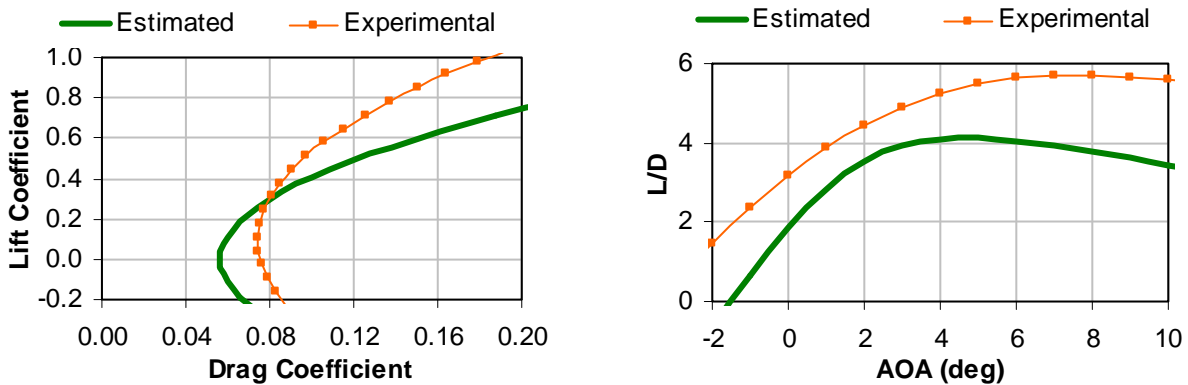


Figure 8.2 – (a) Drag Polar Curves (b) L/D Curves

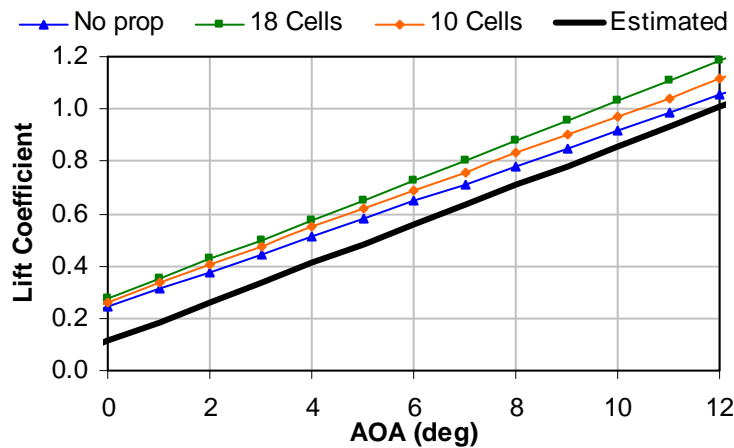


Figure 8.3 – Comparison of Lift Coefficients (Estimated vs. Experimental)

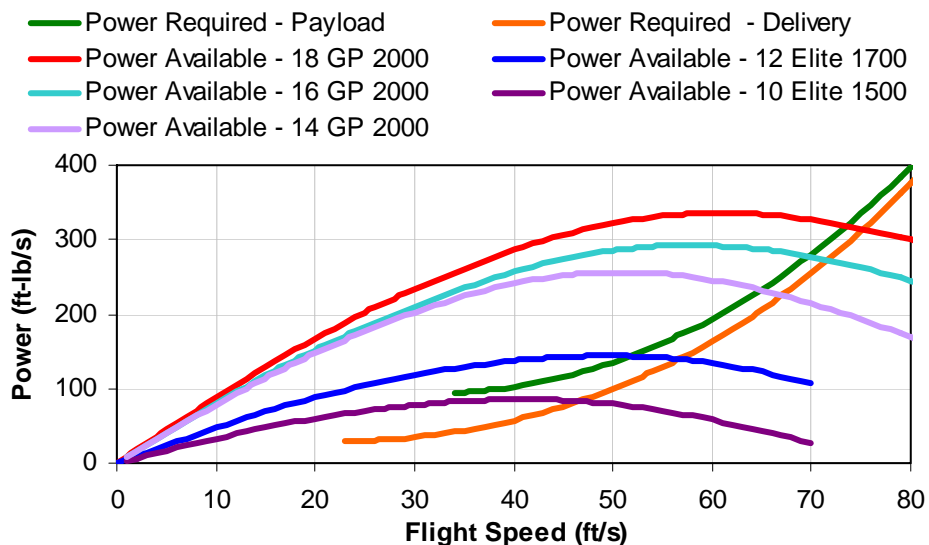


Figure 8.4 – Power Required and Power- Available Curves



8.4 Performance Results Summary

Table 8.2 summarizes some important performance parameters. Testing results have demonstrated that the overall aircraft design is on a steady pace for continuous improvement and refinement.

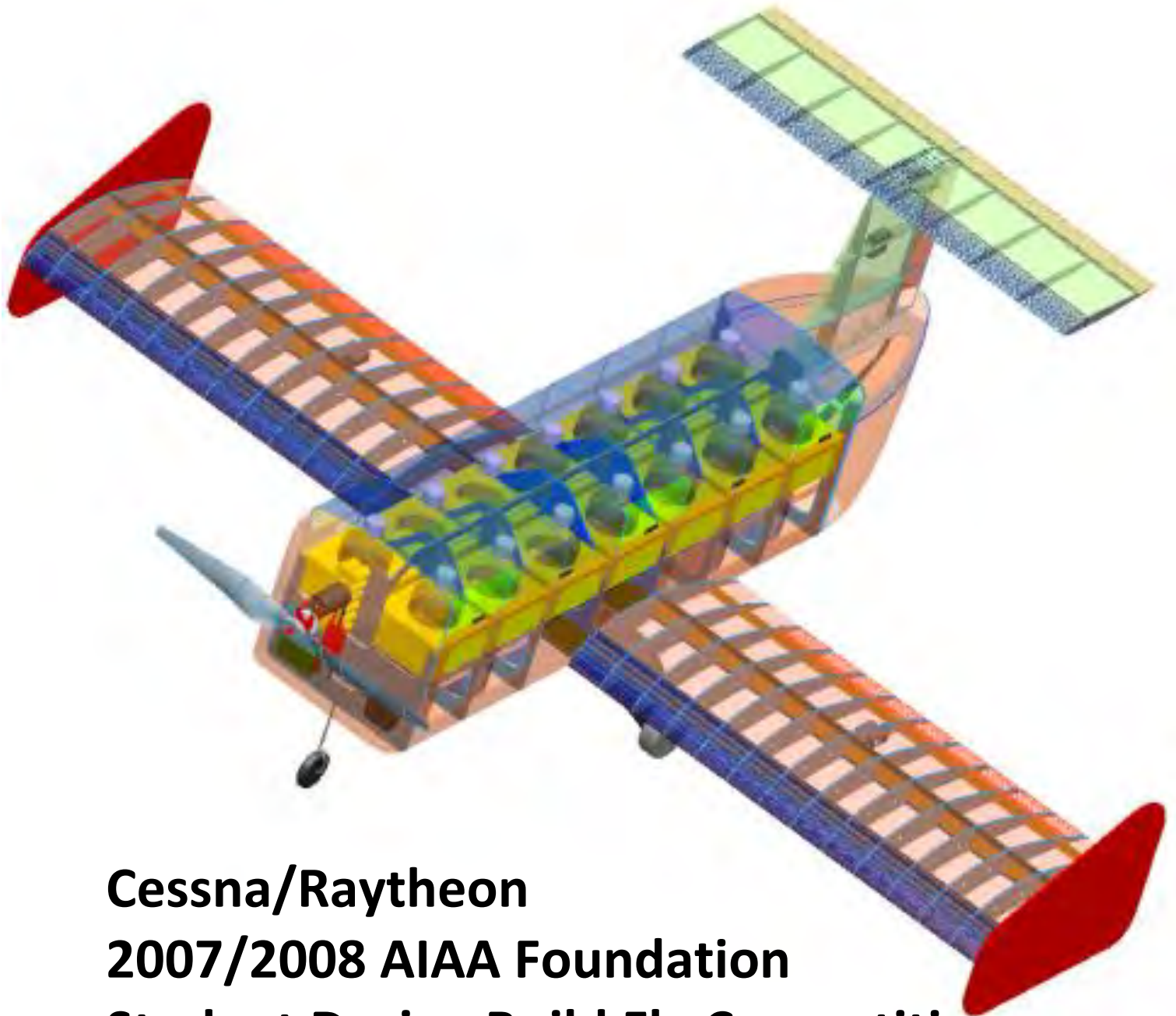
Criterion	Predicted	Tested	Method
Delivery Mission Takeoff Distance (ft)	46	36	Flight Testing
Payload Mission Takeoff Distance (ft)	71	67	Flight Testing
Delivery Mission Laps	3	3	Flight Testing
CL @ 12 degrees (max)	0.80	1.05	Full-Scale Wind Tunnel Test
CD0 @ Re = 300,000	0.057	0.066	Full-Scale Wind Tunnel Test
Delivery Mission Max. Power (ft-lb/s)	143.9	149.6	Propulsion Wind Tunnel Test
Payload Mission Max. Power (ft-lb/s)	335.8	323.4	Propulsion Wind Tunnel Test

Table 8.2 – Performance Evaluation Summary

9.0 References

- ¹Kamunge, S., McCrary, S., Munene, I., Smisor, D., and Zamora, A. Shockin' Surveyor, Design/Build/Fly Design Report, Wichita State University, Mar. 2007.
- ²"AIAA Design/Build/Fly Competition -2007/08 Rules", 7 Sept. 2007, <http://www.aiaadbf.org/>.
- ³"Wichita, Kansas." Weather Underground. Dec. 2007<<http://www.wunderground.com/US/KS/Wichita.html>>
- ⁴Roskam, J., Airplane Design – Part VI, Roskam Aviation and Engineering Corporation, 1989.
- ⁵Hoerner, S., Fluid-Dynamic Lift, Hoerner Fluid Dynamics, 1985.
- ⁶Anderson, J., Introduction to Flight, 5th Edition, McGraw-Hill, New York, 2004.
- ⁷Allen, D. and Haisler, W., Introduction to Aerospace Structural Analysis, John Wiley & Sons, 1985.
- ⁸Kang, H. et.al. "Aerodynamic Effects of End Plates on Biplane Wings", AIAA paper 2008-0317.
- ⁹Hoerner, S., Fluid-Dynamic Drag, Hoerner Fluid Dynamics, 1985.
- ¹⁰Fluent 6.3 User Guide, Fluent Inc., Lebanon, NH.
- ¹¹Raymer, D., Aircraft Design: A Conceptual Approach, 4th Edition, AIAA, Reston, Virginia, 2006.
- ¹²Yechout, T., Morris, S., Introduction to Aircraft Flight Mechanics: Performance, Static Stability, Dynamic Stability, and Classical Feedback Control, AIAA, Reston, Virginia, 2003.
- ¹³Hibbeler, R.C., Mechanics of Materials, 5th Edition, Prentice Hall, New Jersey, 2003.
- ¹⁴Merchant, M., and Miller, L.S., "Propeller Performance Measurement for Low Reynolds Number UAV Applications", AIAA paper 2006-1127, 2006.

Oklahoma State University Black Team



**Cessna/Raytheon
2007/2008 AIAA Foundation
Student Design Build Fly Competition**



1.0 Executive Summary	3
2.0 Management Summary	5
2.1 Team Objectives.....	5
2.2 Schedule and Planning.....	6
3.0 Conceptual Design.....	7
3.1 Mission Requirements (Problem Statement)	7
3.2 Mission Design Requirements.....	8
3.3 Weighting and Selection of Concepts/Configurations Considered	9
3.4 Integrating Concept Selections into a Full Aircraft Solution	17
3.5 Conceptual Design Summary	19
4.0 Preliminary Design.....	20
4.1 Description of Design/Analysis Methodology	20
4.2 Design and Sizing Trades	21
4.3 Mission Model (Capabilities and Uncertainties).....	22
4.4 Aerodynamic Sizing Trades	23
4.5 Stability Characteristics	25
4.6 Lift and Drag Estimations	27
4.7 Propulsion Sizing Trades.....	28
4.8 Structural Sizing Trades.....	30
4.9 Mission Performance Estimation.....	31
5.0 Detail Design	33
5.1 Dimensional Parameters	33
5.2 Structural Sub-System Characteristics/Capabilities	33
5.3 Systems and Sub-Systems.....	36
5.4 Weight and Balance for Final Design.....	38
5.5 Flight Performance Parameters	39
5.6 Rated Aircraft Cost	39
5.7 Mission Performance	39
5.8 Technical Drawing Package	40
6.0 Manufacturing Plan and Processes	46
6.1 Manufacturing Methods Selected for Major Components.....	46
6.2 Manufacturing Methods Selected for Full Assembly.....	47
6.3 Construction Schedule	48
6.4 Construction Costs.....	48
7.0 Testing Plan	49
7.1 Testing Objectives	49
7.2 Testing Schedule	50
7.3 Flight Check Lists	50
8.0 Performance Results	52
8.1 Key Subsystem Performance	52
8.2 Aircraft Performance.....	56
References	59

1.0 Executive Summary

In order to design, build, and fly an unmanned aerial vehicle to compete in AIAA's annual DBF contest, Oklahoma State University's Black Team developed an ambitious team strategy to ensure their aircraft was the best solution to the specified mission requirements. All sub-systems of the aircraft were designed and constructed in parallel by dividing the overall team into three technical teams—Aerodynamics, Propulsion, and Structures—that were in turn headed by a single chief engineer.

The team worked under an accelerated schedule and designed, manufactured, and tested an aircraft faster than any previous team in OSU history. Three overlapping phases guided the design process: Conceptual Design allowed the team to gain familiarity with the rules and determine the best general configuration for the aircraft, Preliminary Design focused on optimizing mission and sub-system performance, and Detail Design integrated all sub-systems into a final aircraft solution. After the design phases, the finalized aircraft was built using traditional construction methods and new methods developed specifically for the aircraft. Each key sub-system was manufactured and tested before constructing a full aircraft prototype. The initial prototype successfully completed its maiden flight and the aircraft solution was further improved after reviewing its performance during flight testing and mission simulations.

1.1 Design Summary

The basic aircraft configuration of the selected design is a monoplane with a five foot wingspan with endplates. Competition balsa and fiberglass were used to construct the main components of the aircraft, keeping the overall system light and stiff. *Microlite* coating is used on the skin of the T-tail empennage and wing. The landing gear consists of a carbon fiber bow as the main gear and a carbon tow strut for the front gear. An internal structure was designed to accommodate all possible payloads and cater to quick loading times while also adding strength to the aircraft's structure. Windows were cut from the outside hull of the aircraft to further reduce weight. All major sub-systems of the aircraft are integrated through one reinforced area that employs a dual-spar wing system to carry and appropriately transfer all loads from the wings and landing gear through the fuselage.

1.2 Key Mission Requirements

The selected aircraft is the best solution to the specified mission requirements because during the design process, key mission requirements were isolated and each design feature was keyed to perform well under all conditions. The contest consists of two missions. The aircraft must complete a Delivery Mission before a Payload Mission is attempted. Both missions share overall constraints and the aircraft design was sized appropriately to fit the defined constraints of the competition. The aircraft dimensions are restricted to a four by five foot box and trade studies showed that a five foot wingspan and a four foot fuselage would provide the best overall mission performance. The second constraint shared by both missions is that the aircraft must take-off within seventy-five feet. By minimizing system weight and choosing a high-lift airfoil, the aircraft could successfully meet take-off requirements for both missions.

1.3 Meeting Key Mission Requirements

The Delivery Mission requires the aircraft to fly laps around a specified course for up to five minutes. Its score is calculated by dividing the number of completed laps by the weight of batteries installed. The key requirements for the mission were identified based on the scoring function and resulted in the following considerations that allowed design features to be keyed to each identified requirement. These include: 1) Flying the mission efficiently, 2) Accounting for varying wind conditions, and 3) Reducing the power required to perform the mission. To fly the mission efficiently, endplates were attached to the aircraft's wings to improve its effective aspect ratio by 25%. To account for varying wind conditions, different battery packs were designed for low, medium, and high wind ranges. The power requirement of the aircraft was minimized by choosing batteries that resulted in the most efficient power output possible.

The Delivery Mission is worth up to 50 points, but the Payload Mission is flown twice for a total possible 100 points. The mission requires a ground crew to load a payload into the aircraft before the aircraft flies two laps around the course. This payload consist of one of five possible combinations of 0.5 lb water bottles and 1.8 lb clay bricks that add up to a total of about 7 lb. The payload is randomly assigned before each attempted flight and the aircraft design must accommodate for all five configurations. The aircraft design was keyed to this requirement because the plane uses an internal restraint system that accommodates for any payload combination. The restraint system carries the loads of the wings, fuselage and landing gear which allows for system weight reduction in the hull and other areas. The reduced system weight allows the aircraft to take-off with less power and reduces battery weight required for the mission. The score for the Delivery Mission is calculated based on loading time, system weight, and battery weight—all three of these scoring components experience an improved score due to the aircraft's internal structural characteristics.

1.4 Performance and Capabilities

Sub-system and overall aircraft performance were tested and improved to find an optimal configuration. Carbon fiber landing gear tests resulted in an ideal bow gear configuration of 0.32 lb that still provides a sufficient factor of safety. After experimenting with different loading strategies, the ground crew reduced loading time to an average of fifteen seconds. By doubling the restraint system as structural bulkheads, non-structural material was removed from the hull and resulted in an airframe of 1.62 lb. A dual-spar wing structure consisting of spruce and carbon fiber reduced wing weight to 0.71 lb. A Cl_{max} of about 1.75 allows the aircraft to take-off in 75 feet with payload and 5 mph wind using only 420 watts of power and 90 watts when empty. After testing motors, propellers, and batteries, a propulsion system of 0.7 lb was configured to allow successful missions with the least amount of battery weight possible. Total system weight of the aircraft is 3.8 lb and it finishes 3 laps in the Delivery Mission while using 0.3 lb of battery which results in a score of 10.0. The Payload Mission requires 0.6 lb of batteries for a total RAC of 2.31 and a mission score of 0.029. The team's competitive system solution is a result of keying each design feature to perform optimally while considering all specific mission requirements.



2.0 Management Summary

The 2008 Black team consisted of undergraduate Mechanical and Aerospace Engineering students from Oklahoma State University ranging from freshmen to seniors. In order to ensure productivity and communication among all members, the design team was organized into three specialty technical groups that were headed by a single chief engineer. The chief facilitated communication among the groups and delegated tasks to each of them. Group leads oversaw team member efforts to ensure to ensure deadlines set by the chief were met. Figure 1 displays the team personnel and their respective assignment areas.

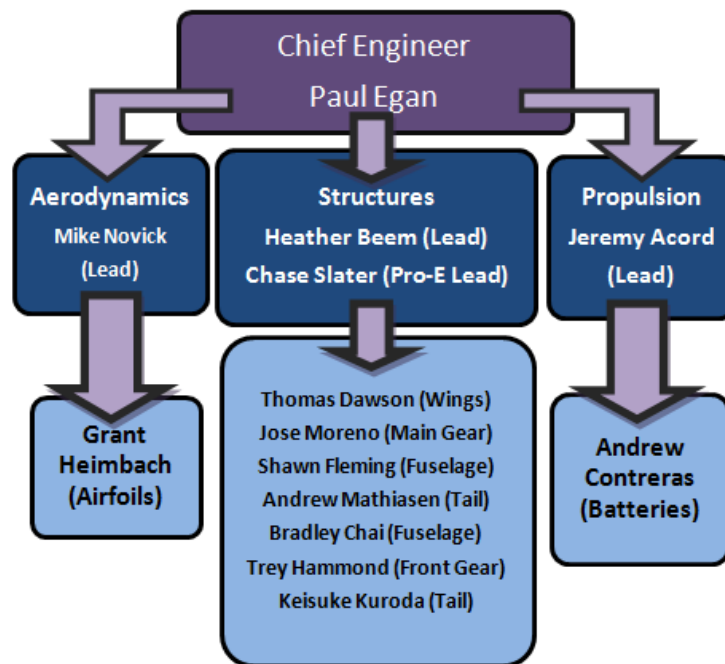


Figure 1: Team Structure

2.1 Team Objectives

Each team was assigned a set of responsibilities to fulfill over the course of the project:

- **Aerodynamics** – The initial responsibility of the Aerodynamics team was to decide the external configuration of the aircraft and optimize its performance in each mission. Considerations during the optimization procedure included aerodynamics, performance, stability, and control. This team was also responsible for conducting and reviewing flight tests.
- **Propulsion** – The Propulsion team was responsible for configuring and optimizing the propulsion system. Tasks included choosing a motor, batteries, propeller, gear box, and speed controller. Because battery weight was directly calculated in the score for both missions, this team propulsion optimized for the minimum amount of batteries to successfully complete each mission. They also conducted propeller and motor tests in the wind tunnel.



- Structures** – All members of the Structures team were involved in designing the payload system, performing structural analysis, and constructing the aircraft. Their primary optimization responsibility was to keep the system weight of the aircraft to a minimum while still safely fulfilling mission requirements safely. They also optimized loading time performance. The Structures team was headed by two leads: the overall lead worked on the written report and ensured all construction deadlines were met while the Pro-E lead completed all CAD drawings.

2.2 Schedule and Planning

The entire project took place over the course of four months and the team developed an accelerated, but achievable schedule to fit in this timeframe. Time periods for each phase of the project were planned and outlined in the Gantt chart below. The chart displays the planned dates for the design, fabrication, and testing processes in addition to the milestones reached by the team. The actual timing the team followed is plotted against the planned schedule to show how well the team maintained its projected timing.

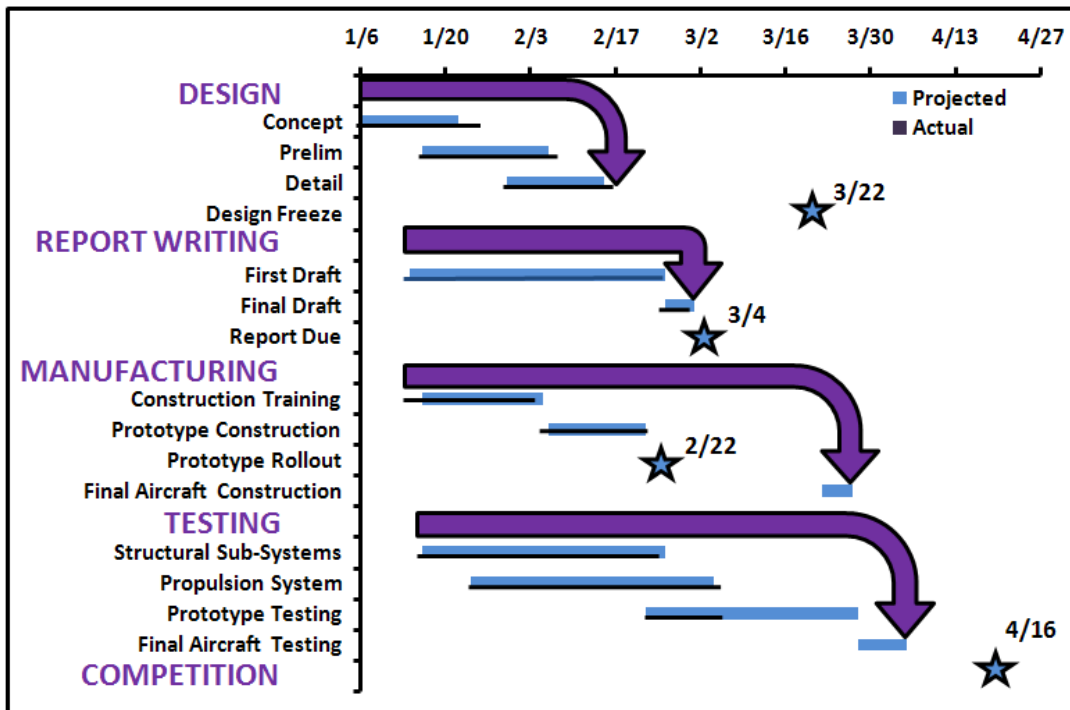


Figure 2: Project Schedule

The Gantt chart only gives a rough outline of construction and testing, but more detailed schedules were developed to better manage specific phases and are displayed in their respective sections of the report. Report writing and construction began in January. Because of this year's addition of the performance results section in the report, the team rolled-out a prototype earlier than any previous OSU team. This forced the schedule to become tight and constrained, but the team still met all deadlines.



3.0 Conceptual Design

The team initiated the conceptual design phase by becoming familiar with the contest rules and the overall mission goals. Aircraft design was guided by determining the key Figures of Merit (FOM) and using them with weighting factors to quantify the performance of each concept. Before any decisions could take place, the scoring mechanism and sensitivity were studied to help make intelligent design trade-offs and ensure the designed configuration scores high in both missions.

3.1 Mission Requirements (Problem Statement)

The ultimate team goal was to design an unmanned aerial vehicle (UAV) in the 2008 Cessna/Raytheon Student Design/Build/Fly competition in Wichita, Kansas. The aircraft must be capable of flying two different missions. The first (Delivery) mission, must be successfully completed before the second (Payload) mission may be attempted. The contest allows for five total flight attempts, but teams will only receive scores for their first successful delivery flight and their first two successful payload flights. Scores for a given mission are normalized against all scores from aircraft that complete the mission successfully. Each successful flight is worth up to 50 points for a maximum possible *Total Flight Score* of 150 points. The team's total score is calculated as: $SCORE = \text{Written Report Score} * \text{Total Flight Score}$.

The Rated Aircraft Cost (RAC) is calculated as $System_Weight * Battery_Weight$ with the following clarifications: (1) *System_Weight* is defined as an aircraft weight with no payload or batteries, but does include the weight of any/all payload insert/restraint components used in any mission. (2) *Battery_Weight* is the weight of the batteries flown on a given mission. Each mission has specific mission parameters, but they share a couple of restrictions: The aircraft must fit inside a box size of 4' by 5' when sitting on its landing gear at a normal ground altitude and must take off in 75'. Each lap of the course has a 1000' distance length-wise.

- Mission One: Delivery** – Teams select a battery pack upon entry of the staging box. Only the weight of the battery pack chosen is calculated for the this mission's score. There is no payload for this flight, but all restraint systems used in the payload mission must be present in the aircraft. The aircraft is allowed to fly laps around the course for up to five minutes. Time begins at the start of take-off, but landing time is not included. Only complete laps count towards the score which is calculated by the following expression: $\# \text{ Complete Laps} / \text{Battery_Weight}$.
- Mission Two: Payload** – The aircraft is required to fly with a payload for a distance of two laps. There is no time constraint, but the plane must successfully land on the runway. One of the five possible payload combinations will be assigned for the mission after batteries are chosen. The mission score is calculated by the expression $1 / (\text{Loading Time} * \text{RAC})$. Loading time is defined as the amount of time it takes the ground crew to load the payload into the aircraft.

3.1.1 Payload Mission Requirements

The five payload combinations consist of water bottles with collars to simulate passengers and clay bricks to emulate cargo pallets. Their total weight varies, but ranges from a nominal 6.8lb to 7.2lb. The combinations are:

- **14 passengers** (nominal 7lb)
- **10 passengers and 1 cargo pallet** (nominal 6.8lb)
- **7 passengers and 2 cargo pallets** (nominal 7.1lb)
- **3 passengers and 3 cargo pallets** (nominal 6.9lb)
- **4 cargo pallets** (nominal 7.2lb)

The payload combinations will be abbreviated in the following format for the rest of the report: # of passengers / # of cargo pallets. The 14 passenger configuration, for example, is 14/0. Bottle dimensions are approximately 2.5” in diameter and 8.5” in height. The collars are made out of Styrofoam and may be round (not to exceed 4” in diameter) or square (not to exceed 4”x4”). The volume of the bottle is 0.5L and will be filled with water until its weight is approximately 0.5lb. Collars are slipped over the bottles and may not overlap once the bottles are loaded. These collars may be located up to 1/8” from the bottom or top of the bottle and the passengers must remain upright during flight. Cargo pallets are US ½ size clay bricks and are approximately 4”x4”x2-2/3” and weigh about 1.8lb. During flight the cargo pallets may be oriented in any manner as long as they are properly restrained. All payload elements must remain safely restrained during flight and during a flip test. The latter consists of loading the aircraft and orienting the loading hatch towards the ground, and having the judges determine whether the payload is sufficiently secured.

3.2 Mission Design Requirements

All mission requirements were investigated and translated into design requirements.

Mission One: Delivery – The scoring equation for the delivery mission includes the number of laps flown and the battery weight of the system. By rewriting the equation in terms of design variables, the scoring function could operate according to variables that relate directly to airplane design. The only non-design variable left in the equation was the distance of one lap. The derived scoring function and design variable definitions are shown in Table 1 below.

Table 1: Delivery Mission Requirements and Design Variables

Delivery Mission Requirements	Design Variable Definitions:
Derived Scoring Function:	W_{batt} = Battery Weight W_{sys} = System Weight η = Propulsive Efficiency E_p = Energy Density per Battery Cell C_L/C_D = Lift to Drag Ratio for Entire Aircraft
$SCORE = \frac{\eta \cdot E_p \cdot \left(\frac{C_L}{C_D}\right)}{d_{lap} \cdot (W_{batt} \cdot W_{sys})}$	



By viewing the scoring equation in this form, the team could easily recognize important design variables and how the increase/decrease of each one affects score. For instance, variables in the numerator should be increased while variables in the denominator should be decreased.

Mission Two: Payload – The Payload Mission score can be derived in terms of design variables if RAC is rewritten in terms of *System_Weight* and *Battery_Weight* as shown in Table 2. The battery weight used to calculate the score for the Payload Mission is independent of the battery choice for the Delivery Mission. After reviewing this equation, it was found that the mission requirements involved variables for all technical teams to consider during the design process. The Aerodynamics team had to choose a light weight configuration that can take-off with minimal power requirements (so that battery weight stays at a minimum). The Propulsion team has to design an efficient system capable of using a low amount of batteries and the Structures team needed to concentrate on lowering system weight and ground crew loading time.

Table 2: Payload Mission Requirements and Design Variables

Payload Mission Requirements	Design Variable Definitions:
Derived Scoring Function:	Loadingtime = Time for Groundcrew to load aircraft
$\frac{1}{Loadingtime * W_{sys} * W_{batt_2}}$	W_{sys} = System Weight W_{batt} = Battery Weight

After writing all mission requirements in terms of design variables, it was found that both missions shared system weight and battery weight as key design requirements. After recognizing that lowering system weight and choosing a design that used batteries efficiently helped both missions' scores, the team chose to concentrate on designing for the Payload Mission. This Mission is worth 100 of the 150 total points and an aircraft that performs well in the Payload Mission should also perform well in the Delivery Mission.

3.3 Weighting and Selection of Concepts/Configurations Considered

After analyzing the mission design requirements the team performed a sensitivity and trade-off study and found that non-dimensionalized design trade-offs exist for each variable if nominal values are assumed. These nominal values are estimated based on the 2006 OSU DBF aircraft which had similar mission requirements. After assuming the mission performance of the aircraft would be close to a 15 second loading time, with a 4.5lb system weight and 0.8lb batteries for the Payload Mission, equal trade-offs were found: 2 seconds of loading time is equivalent to about 0.25 lb of system weight and 0.04lb of battery weight. By recognizing the importance of one second of loading time and the payload size the aircraft would have to accommodate, the team immediately began formulating payload accommodation concepts.



3.3.1 Payload Orientations Considered

The payload orientation inside the aircraft affects the cross-sectional area of the aircraft, the surface area and volume of the fuselage, and the center of gravity (CG). Because of the collars dimensions, the bottles may be considered to take up the same amount of floor space as a cargo pallet oriented with the 4"x4" side on the floor. This allowed for the creation of a "grid" design with all payload components considered as 4"x4" components. All ideas that considered making the plane height larger were displaced because the extra height would increase structural weight too much. Different ideas for organizing grid orientation are described and chosen as follows:

- **3x4 + 1x2 Grid** – The fuselage remains short in this configuration, but cross-sectional area is increased. The CG is difficult to balance between different payload configurations.
- **14x1 Grid** – This idea orients the aircraft diagonally in the box. It is efficient in terms of cross-sectional area, but increases the surface area of the fuselage. Because the aircraft is diagonal in the box, the chord size of the wing is limited and, as determined by the Aerodynamics team, planes with larger chords outperform configurations with limited chord size.
- **Diagonal Grid** – This encompasses several ideas investigated by the group to orient the grid with the components oriented at different angles. Every orientation considered increased the length and width of the payload system while also making the CG difficult to balance.
- **7x2 Grid** – The 7x2 grid was chosen because it provides the best balance of cross-sectional area and fuselage length, and it allows the payload CG to balance longitudinally between all different configurations, as shown in Figure 3 below.

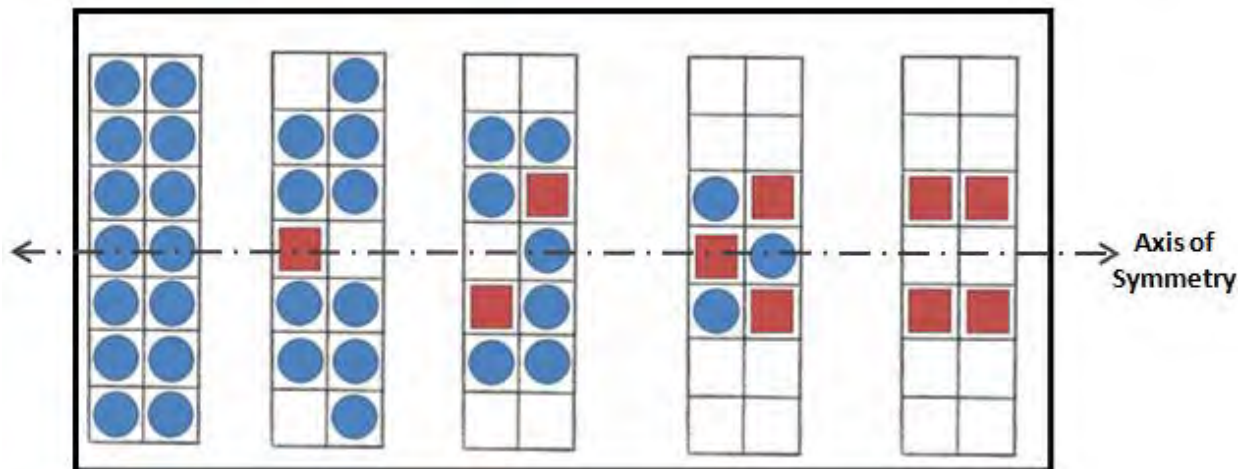


Figure 3: The Orientation of all payload combinations to balance CG (Blue Circles indicate bottle placement while red squares indicate brick placement)



3.3.2 Morphological Chart

The team's next step was to compile ideas for design components into a morphological chart. The morphological chart allowed the team to generate a large number of ideas quickly. All initial ideas were accepted, but some were discarded before the next phase because they would obviously not work. The morphological chart process allowed for two important steps in the conceptual design phase: (1) recognizing each technical team's specific considerations so other teams could accommodate for them and (2) immediately reducing concepts that definitely would not work so that time was not wasted later by quantifying these concepts in matrices.

Table 3: Morphological Chart

Design Component	Generated Concept					
Aircraft Configuration	Monoplane	Biplane	Blended	Delta	Tandem	Joined
Empennage	T-tail Bronco	H-Tail Canard	Cruciform Twin tail	Conventional None	Inverted V-Tail Boom Mounted	
Landing Gear	Tricycle	Single Main	Bicycle	Quad	Tail-Dragger	
Engine Placement	Single	Dual	Tractor	Pusher	Pod	
Payload Restraint	Egg Carton Elastic	Grid Clamps	Bag Velcro	Foam	Quick-Loader Peg Matrix	

3.3.3 Concept Weighting and Selection

After the team determined the most important concepts to evaluate, the concepts were further narrowed by using decision matrices and rating each idea against Figures of Merit (FOM). All FOMs were determined beforehand, although FOMs vary in how they apply to a particular concept.

Figures of Merit

The FOMs that are most important for consideration are those that affect the score directly. In the non-dimensional sensitivity, each of these FOMs was quantified to determine near equal trade-offs:

- **System Weight (0.25 lb)** – Used to evaluate how much a particular concept adds to the overall system weight. Weight not only affects the score, but also rate of climb and take-off distances.
- **Battery Weight (0.04 lb)** – Battery weight is the only FOM that is directly calculated in both mission scores. The amount of batteries increase as the power requirements of the aircraft increase. The propulsive efficiency of the aircraft also directly affects the number of batteries.
- **Loading time (1 s)** – Loading time is an FOM that seems to only limit ideas such as aircraft configuration choices because of dimension requirements. But some ideas could incorporate a restraint system with a fast loading time to increase structural integrity. Using more materials to restrain the payload adds more weight, but may reduce structural weight elsewhere.

RAC was not considered as a discrete FOM because it combines system weight and battery weight and is only directly calculated for the payload mission. The interaction between system weight and battery weight is complex, so each parameter was evaluated separately. The complexity arises when making decisions such as increasing system weight to increase lift to reduce the power required for take-

off (an example of this occurs when one compares a biplane and a monoplane). Other FOMs that did not directly calculate into the scoring function were also considered:

- **Manufacturability** – Used to determine how difficult a component is to construct and how much it costs. Also takes into account if a concept is structurally impossible.
- **Maintenance** –Affects how often the team may perform test flights and takes into account that if damage occurs at the competition, it must be repaired efficiently.
- **Strength** – Important for structural considerations to ensure all forces are distributed safely. If a concept was able to handle all loads without failure, it was given a positive score.
- **Ground/Air Stability and Control** – Affects aerodynamics of tail and aircraft configuration for stability and control. Also affects the structures team because all landing gear must handle safely on the ground. The aircraft should be able to consistently complete missions safely.
- **Drag** – If a concept increases drag, the aircraft flies less efficiently. As drag increases the aircraft must use more propulsive power which affects battery weight.
- **Take-off Distance** – The aircraft has to be able to take off in 75'. This FOM is important because if the aircraft is not able to take-off within mission constraints, it is awarded no score. In previous years, DBF aircraft have had a much larger available take-off length.
- **Power** – Determines how much power the aircraft has to take-off and cruise for each mission. Power also affects how well the aircraft climbs.

Each of these FOMs was weighted in concept matrices to quantify how well different concepts rated against each other in important categories. Each matrix isolated one aspect of aircraft design and compared several different possible solutions. Possible solutions were evaluated by giving them a score of 1, 0, or -1 for each weighted FOM. The total scores are summed after multiplying scores by their respective weight factor, and then compared to find the best concept. Because the grading mechanisms are carried out at a conceptual level, the grading system allows for generalities to be made about each concept according to the table below when assigning a score.

Table 4: Explanation of FOM Grading Scale

Score	How FOM Influences Concept Choice
1	FOM positively affects concept choice
0	Concept is not greatly influenced by FOM
-1	FOM negatively affects concept choice

3.3.4 Overall Aircraft Configuration

After the payload configuration and basic fuselage dimensions were determined, the Aerodynamics team knew the basic external shape of the aircraft and isolated aircraft configurations that accommodated for the shape. The FOMs and weighting factors were chosen to find structurally light weight solutions that

could still successfully compete in each mission. Also rated was the stability and control of each option because if the pilot can not consistently fly the aircraft, the plane may crash which results in a score of zero at the competition.





Aircraft Configuration					
Figure of Merit	Weight	Monoplane	Lifting Canard	Tandem Wing	Biplane
System Weight	4	0	-1	-1	0
Take-off Distance	2	0	0	1	1
Stability and Control	2	0	1	0	0
Manufacturability	1	1	0	-1	-1
Drag	1	0	-1	-1	-1
TOTAL	10	1	-3	-4	0

Figure 4: Aircraft Configuration Matrix

- **Monoplane** – The monoplane may be constructed as light weight and would perform well in both missions. It has stable handling qualities and OSU has a good history of building successful monoplanes. Monoplanes are the most versatile option for loading configurations.
- **Lifting Canard** – The lifting canard configuration incorporates two separate wing surfaces with the wing aft of the lifting canard. This configuration allows for more lift to be produced since there is the extra lifting surface at the front, but makes taking off difficult because the front surface stalls before the wing reaches maximum lift.
- **Tandem** – The tandem wing configuration is similar to that of the lifting canard. The main difference between the tandem wing and the lifting canard is that the tandem wing contains two equally sized wings in a line, providing more lift than the previous option, but it also loses some aerodynamic efficiency as the second wing lies within the downwash of the front wing.
- **Biplane** – The traditional biplane offers two vertically separated lifting surfaces. The configuration increases the construction complexity, but results in an efficient aircraft capable of short-takeoff. If the wings are constructed properly together, biplanes are light weight.

The biplane and monoplane configurations are both favorable from a basic conceptual view. In order to ensure the best solution was found, a simple preliminary analysis was performed for two variations of each configuration at three different wing areas. They were all evaluated at a wingspan of five feet because the optimization program used by the Aerodynamics team (explained in greater detail in Section 4.3) showed that the maximum possible wing span always achieved the highest overall mission score. The monoplane was evaluated with and without endplates while the biplane was evaluated with a nine inch gap between wings and an eighteen inch gap between wings. Endplates and a larger gap increase



the efficiency associated with a design. The results are shown in Figure 5.

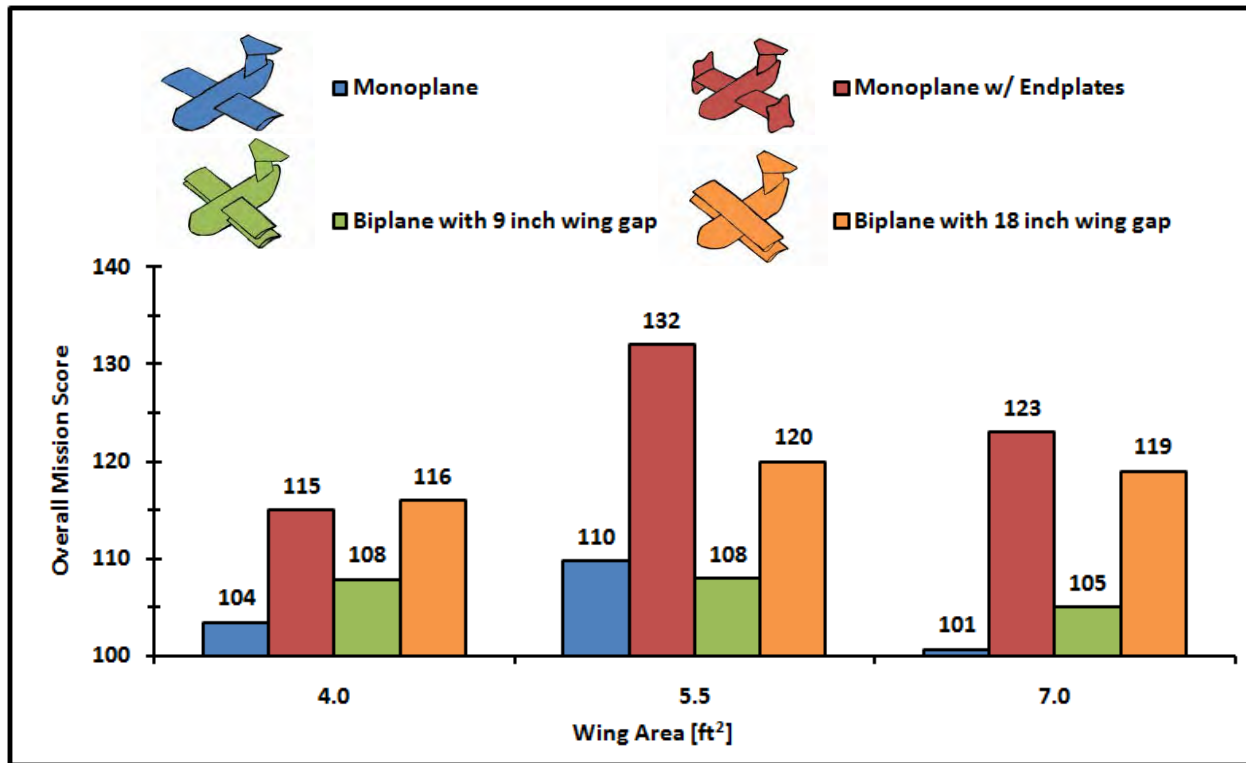


Figure 5: Conceptual Comparison of Scores Based on Aircraft Configuration

The results show that a monoplane with endplates at a wing area of about 5.5 ft² scored the highest and monoplanes with endplates consistently scored well in all configurations. The biplane with an 18” wing gap is the second highest scorer consistently, but the drawbacks associated with less loading location options also hurt its feasibility. The biplane with a 9” wing gap consistently scored almost 20% lower than the monoplane with endplates while a monoplane without endplates scored lowest.

3.3.5 Empennage Configuration

The best tail configuration for an aircraft should minimize system weight and drag. The tail should provide consistent stability and control and be easy to trim





Empennage					
Figure of Merit	Weight	Conventional	Cruciform	H-Tail	T-Tail
System Weight	4	0	-1	-1	0
Stability and Control	4	-1	1	1	1
Drag	2	0	-1	-1	-1
TOTAL	10	-4	-2	-1	2

Figure 6: Empennage Configuration Matrix



- **Conventional** – The conventional tail configuration consists of a mid-body elevator and a vertical stabilizer. The main problem with this concept is that the large cross-sectional area of the fuselage creates vortices that decrease tail effectiveness.
- **Cruciform** – The cruciform tail configuration is comprised of a stabilizer with the elevator mounted midway up. The cruciform provides a compromise between the greater effectiveness of the T-tail and downwash prone configuration of the conventional tail.
- **H-Tail** – The H-tail places the vertical stabilizers in an undisturbed airflow at high angles of attack. The rudders are able to maintain effectiveness in this configuration. The drawback is that too much extra weight is added to the tail.
- **T-Tail** – This configuration has the same vertical stabilizer as the conventional configuration but the horizontal elevator is placed on the top of the stabilizer, which increases structural weight, but allows for a smaller horizontal tail size because it is more effective. The T-tail was chosen because it offers a control surface that experiences less of the vortex created by the fuselage.

3.3.6 Landing Gear

Landing gear was primarily rated for allowing sufficient stability and control to safely take-off and land while also being light weight.

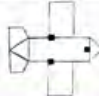
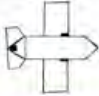
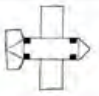
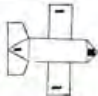
Landing Gear					
Figure of Merit	Weight	Tricycle	Tail Dragger	Quad	Single Main
Stability and Control	5	1	-1	0	-1
System Weight	3	0	1	-1	-1
Take-off Distance	2	0	1	-1	-1
TOTAL	10	5	0	-5	-10

Figure 7: Landing Gear Matrix

- **Tail Dragger:** The tail dragger allows for a more light weight landing gear to be built, but from OSU experience handles too dangerously to be considered as a feasible option.
- **Quad:** The quad design significantly increases contact area on the runway, providing better stability but considerably more weight than other designs.
- **Single Main:** Single main is an overlap of bicycle and tail dragger configurations, and is also difficult to control.
- **Tricycle:** Tricycle design creates substantial control stability through nose gear actuation. With only three wheels, it is a light weight option compared to four wheel landing gear configurations. It was chosen because it is the most well-rounded and reliable landing gear choice.



3.3.7 Payload Restraint

The importance of loading a restraint system quickly was the priority in this decision. The inclusion of any payload restraint mechanisms in the plane adds weight, but some configurations could also be doubled as structural support for the airframe. Any option capable of accomplishing this was positively rated in strength. System weight was a quantification of how much the restraining system itself weighed and manufacturability rated ease of construction.





Payload Restraints					
Figure of Merit	Weight	Peg Matrix	Thin-Walled Grid	Payload Bag	Sandwich
Loading Time	6	0	1	-1	-1
System Weight	4	1	0	1	1
Strength	3	0	1	0	0
Manufacturability	2	1	1	1	-1
TOTAL	15	6	11	0	-4

Figure 8: Payload Restraint Matrix

- Peg Matrix:** The peg matrix uses an arrangement of thin pegs placed in a pattern that creates enclosed compartments for the payload elements. The matrix can be easily built and have a low system weight, but makes accurate payload loading difficult because the pegs create a more confusing pattern when viewed from above than a grid system.
- Payload Bag:** The payload bag is the lightest weight option considered, but would be difficult to ensure that no payload collars overlap. No internal strength is added to the aircraft.
- Sandwich:** This idea uses two flat plates, between which the elements are squeezed together. The main problems are no lateral division is provided between elements and any bottles slightly shorter than others would not be adequately secured.
- Thin Walled Grid:** This system uses a series of walls to separate the payload elements. Due to the thinness of these components, system weight would be increased minimally while the fuselage received extra structure. This configuration is also loaded quickly and easily. The thin walled grid was chosen with the intent of doubling the grid system as internal structure.

3.3.8 Motor Placement

The first decision by the propulsion team was whether to pursue an aircraft with one motor/propeller or multiple motors and propellers. By adding additional motors, the system weight of the aircraft would increase even if they were lighter than a single motor because of extra structure required for mounting on the wings. If a single motor is capable of producing enough power for both missions, one motor would be the superior choice when considering RAC.



Using the single motor concept, a concept matrix with three different configurations to consider was evaluated. Power was given a high weight because it determines how well the aircraft performs during takeoff and climb. System weight was rated to determine how much weight the entire system would be as a result of the engine location.




Motor Placement				
Figure of Merit	Weight	Pusher	Tractor	Pod
Power	4	-1	1	1
System Weight	3	0	0	-1
Battery Weight	3	-1	1	0
TOTAL	10	-7	7	1

Figure 9: Motor Placement Matrix

- **Pusher:** Locating the propeller aft of the fuselage reduces the propeller efficiency and creates problems when rotating the aircraft at take-off.
- **Pod:** The benefits of using a pod concept can be characterized by adding flexibility in terms of propeller/motor placement, but the pod would substantially increase drag and add unwanted moment arms that could potentially overcomplicate the stability the aircraft.
- **Tractor:** A single tractor setup places the propeller/motor at the nose of the fuselage. This setup allows adequate airflow to the propeller. It was chosen because it is a balanced option that is capable of reaching thrust requirements and runs efficiently.

3.4 Integrating Concept Selections into a Full Aircraft Solution

After each technical team determined the best solutions for their specific sub-systems, the overall team met to determine how to fit together all of the chosen concepts to form a full aircraft.

3.4.1 Wing Placement

The height of wing placement was one of the first decisions that the Structures and Aerodynamics teams finalized after discussing basic trade-offs with each other. The Aerodynamics team found that a higher wing would help with stability. The Structures team preferred a low wing so that structural reinforcement around its attachment point would fall in the same area as the landing gear attachment point. Sharing the point of attachment would allow for a lower system weight since only one confined area would need to carry heavy loads. A high-wing would also disrupt the loading speed of the ground crew. It was decided that the increase in loading time and system weight would hurt the overall mission score more than the high-wing would benefit the aircraft's stability characteristics.



3.4.2 Structural Attachment and Loading

The wing/fuselage attachment was the next major decision considered. OSU has traditionally found success in a single wing spar, but due to the nature of the payload restraint system and the length of the aircraft, a quick analysis showed that for proper wing placement, a single spar would have to intersect with a payload element. To solve this problem, the concept that exploits the “rigid” payload restraints by doubling their function as structural bulkheads was expanded. A dual wing spar system could be integrated into this system of eight bulkheads, and one “sine.” By running spars directly under two of the bulkheads, loads would be transferred into the internal structure. Two spars also reduce resist wing torsion. By making the restraint a load-carrying structure, aircraft loads are distributed through the restraint itself, rather than through the skin of the aircraft—the traditionally used monocoque method. Drawings of each idea are shown below.

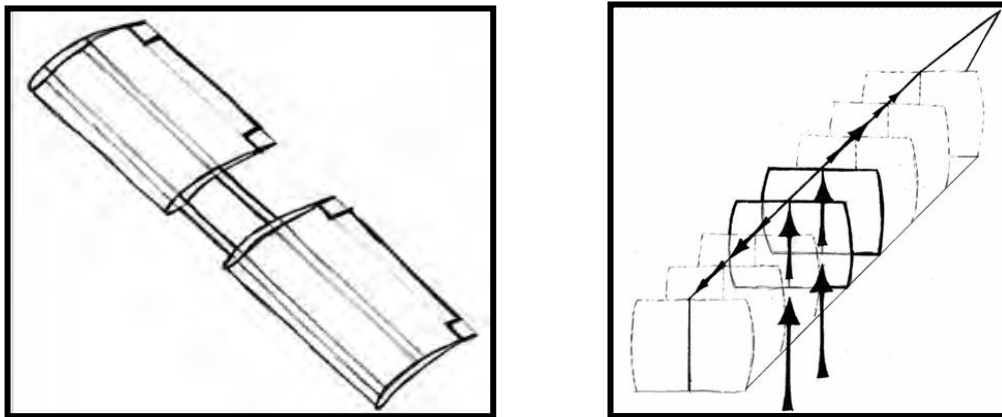


Figure 10: Dual Spar System and Internal System where all Loads are Carried

3.4.3 Landing Gear

Front and main gears were designed to be low weight, capable of absorbing shock, and strong. The main gear may be attached between the two bulkheads that carry all aircraft loads. The “J” shape of the front gear reduces stiffness, allowing it to absorb shock. The curves on the bow shaped main gear allows it to better absorb shock.

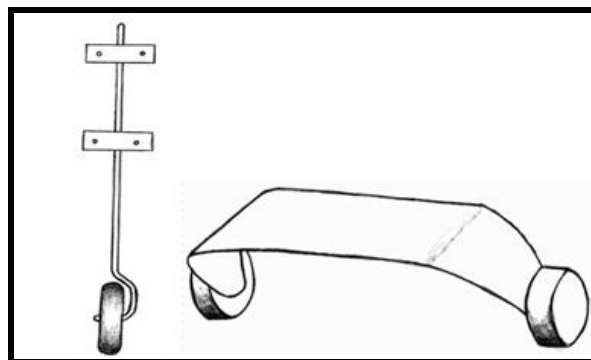


Figure 11: Landing Gear Concepts



3.5 Conceptual Design Summary

The following sketch displays the aircraft developed by the team during the Conceptual Design phase. A monoplane configuration was chosen with a 5' wingspan and large chord. The fuselage is designed to accommodate for a 2x7 "grid" configuration of payload elements, with the payload element dividers also serving as internal structure. Having sufficient internal structure allows for the removal of material from the outside hull, since the skin does not carry any major load. A dual spar system is used to support the wing. A T-tail provides stability and control to the airplane and a tricycle landing gear ensures stable ground handling. The design process accounted for all important mission parameters and intelligent trade-offs were made to ensure the aircraft remained competitive.

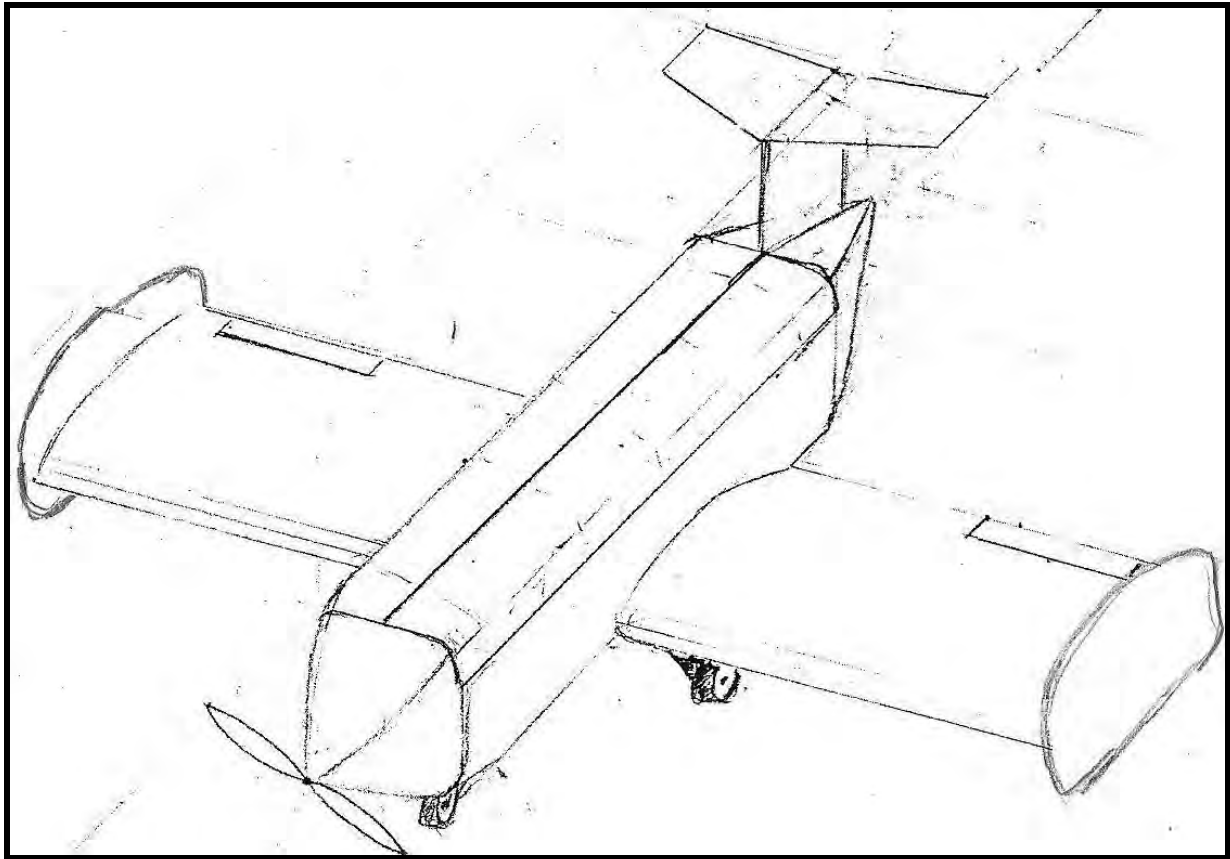


Figure 12: Final Conceptual Drawing of the Aircraft



4.0 Preliminary Design

The Preliminary Design Phase focused on optimizing the key sub-systems and the complete aircraft solution selected during the Conceptual Design Phase. The phase was initiated by deriving an easy-to-follow Design/Analysis Methodology that provides each technical team an effective way to optimize specific sub-systems while communicating with each other. Preliminary Design concludes by combining all optimized sub-systems to predict the mission performance of a complete aircraft.

4.1 Description of Design/Analysis Methodology

The flow chart below outlines the design/analysis methodology used in the Preliminary Design phase.

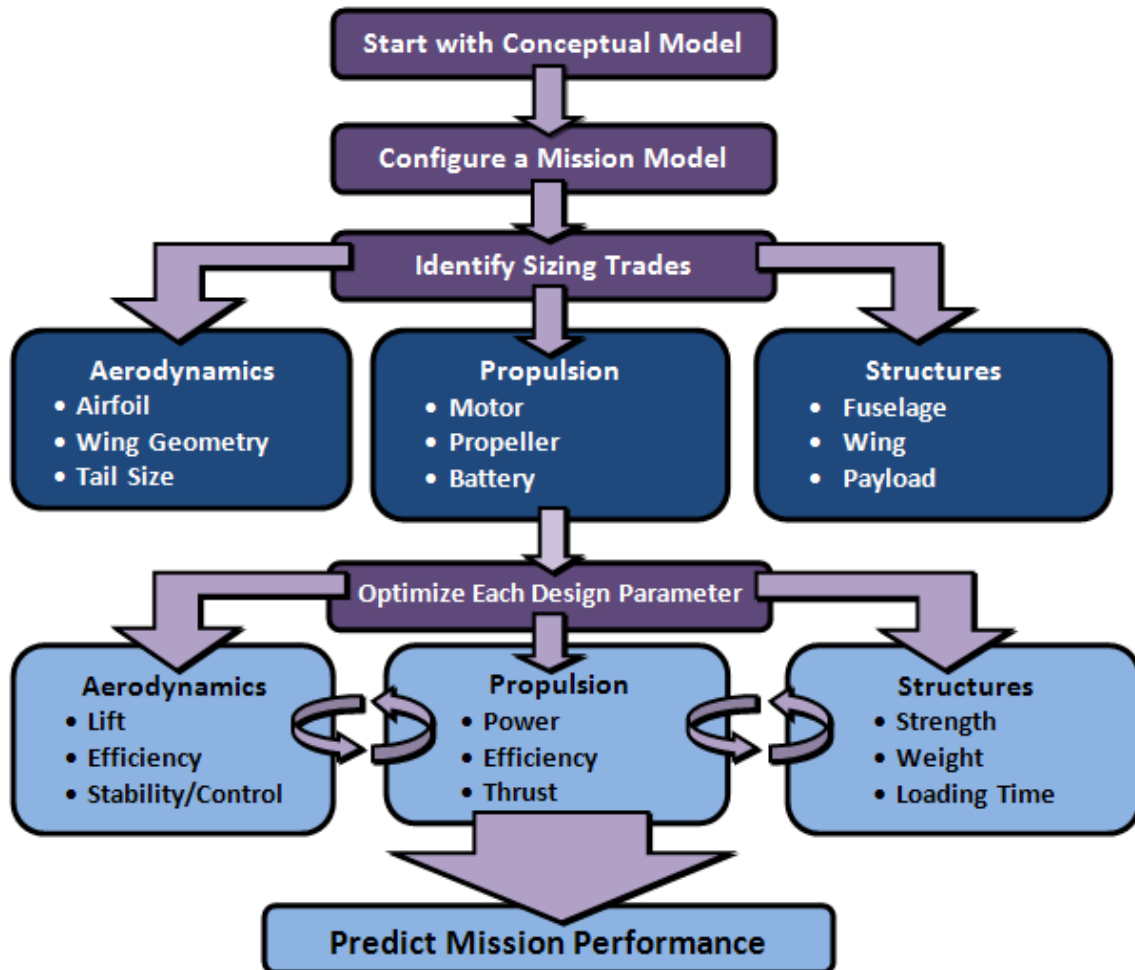


Figure 13: Preliminary Design/Analysis Flowchart

4.1.1 Description of Design Methodology

The first step in the Preliminary Design phase is reviewing the conceptual model of the aircraft selected during the Conceptual Design phase. Next, software developed by previous OSU DBF teams was modified to incorporate the mission model for this year's competition. The mission model considers all of the constraints of the competition and allows the user to vary uncertainties such as aircraft weight and wind. Design and sizing trades were identified by each technical team to ensure intelligent trade-offs

were made in all optimization decisions. After the design and sizing trade-offs were determined, each technical group optimized the aircraft by focusing on specific parameters needed to perform well in each mission. The optimization process was iterative and it was important for each technical team to communicate their designs' capabilities as often as possible. After all design parameters were narrowed, the technical teams worked together to predict the full mission performance of the aircraft.

4.1.2 Description of Design Analysis

The following tools were used by each technical team to analyze design and sizing trades:

- **Literature Study:** Texts (Referenced at the end of the paper) were studied to obtain equations determining efficiencies of different aircraft configurations and to learn structural theories.
- **Mathcad Aerodynamics Optimization:** A mission modeling program created by previous OSU DBF teams was modified to model uncertainties and design constraints for this year's contest.
- **X-Foil:** X-foil was used to generate lift and drag data for airfoils. Profill was to manipulate airfoil geometry and then the airfoil parameters were determined in X-foil
- **Mathcad Propulsion Simulation:** The program was created by previous OSU DBF teams. It allowed the propulsion team to input data for the motor, gear box, speed controller, batteries, and propeller, and then output aircraft performance data.
- **Excel Spreadsheets:** Excel spreadsheets were used by the structures team to model loads experienced by the fuselage, landing gear, and wing.
- **Prototype Experiments:** Prototypes of the loading system and structural components were created to determine their capabilities and design limitations.
- **Pro-Engineer (Pro-E):** Used to model parts of the aircraft before construction began. Pro-Mechanica may be used to conduct FEM analysis. Cutting out complex balsa shapes may be automated with a CNC milling machine, using coding from Pro-E.
- **Visio:** Used during design to create proposed drawings of trusses, the fuselage, and wing before detailing them in Pro-E.

4.2 Design and Sizing Trades

The first step outlined in the Preliminary Design methodology consists of isolating design parameters and evaluating trade-offs associated with each design and sizing choice.

4.2.1 Aerodynamic Design Parameters

- **Airfoil:** The 75' take-off constraint with full payload requires the aircraft to generate a large amount of lift. However, high lift airfoils usually have more parasite drag than lower lift airfoils. Choosing a high lift airfoil also makes construction more complex.
- **Wing Geometry:** The complete aircraft has to fit inside of a four by five foot box. The box size limits the wing span to four or five feet depending on the fuselage length. Wing sizing affects aspect ratio and wing area. A larger wing also increases system weight.



- **Empennage Size:** The tail should be large enough to stabilize the aircraft and trim at a low incidence angles. Increasing tail size increases weight, but a high incidence increases drag.

4.2.2 Propulsion Design Parameters

- **Motor:** Motors with greater power also weigh more. If the aircraft only requires a certain amount of power, extra power only adds unnecessary system weight
- **Propeller Selection:** A larger propeller is able to generate more thrust, but requires more current and power to turn. A larger current draw depletes battery energy faster.
- **Battery Selection:** Maximum current, energy density, and cell weight all affect battery performance. Adding more battery cells to a system increases voltage, power, and weight. Lighter batteries have lower capacities, and usually handle less current.

4.2.3 Structural Design Parameters

- **Wing/Fuselage:** Each structural system in the aircraft must remain low weight, but still provide enough strength to allow a sufficient safety factor for all flight conditions
- **Payload:** A larger payload accommodation area allows the loading crew to place payload elements quickly, but increases the size of the aircraft.

4.3 Mission Model (Capabilities and Uncertainties)

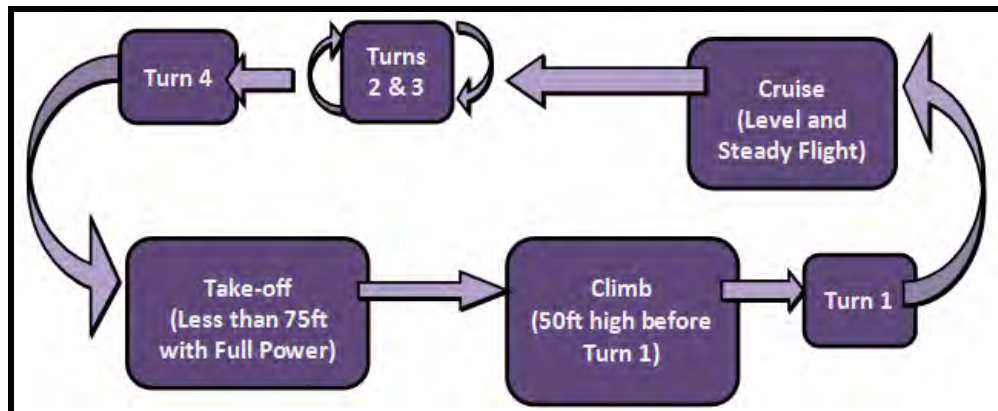


Figure 14: Assumptions Associated with Each Lap

An aerodynamic performance optimization program and a propulsion system modeling program are the primary design tools used by OSU DBF teams. Both are programmed in Mathcad and every year the programs are adapted to account for constraints and uncertainties associated with the current contest. The assumptions associated with one lap of each mission for this year's contest is shown in Figure 14. The purpose of the aerodynamic performance program is to use the mission model to design an aircraft that scores well in both missions under all conditions. The main uncertainty associated with the program is the assumption of a rubber propulsion system. To overcome this uncertainty, the propulsion team uses a dynamometer and propulsion system modeling program to verify the proposed capabilities needed in the propulsion system to confirm predictions. Another uncertainty occurs because values such as the

maximum lift coefficient for airfoil input is obtained using theoretical programs (X-foil). Actual lift and drag is affected by how well the structures team constructs the aircraft.

The optimization program allows the user to vary the wind conditions and account for uncertainties in weather conditions. It is important to consider uncertainties in the wind because a low wind hurts take-off performance while a high wind impedes cruise performance. The ability to vary uncertainties in the program allows the user to design an airplane that performs well under all wind conditions. Another uncertainty is the weight model which assumes a baseline weight that varies with wing area. Uncertainty exists in the aircraft weight until it is actually constructed and weighed.

Mission modeling was also performed for the ground portions of the mission. The contest rules state that the aircraft is between 10' and 50' away from the starting line and the loading crew. The uncertainty associated with distance changes the achievable loading time. The ground portions of the mission were modeled by constructing a prototype of the restraint system and performing ground crew time trials.

4.4 Aerodynamic Sizing Trades

During Conceptual Design, the aerodynamic optimization was used to select the monoplane with endplates over other aircraft concepts. The program was further used to compare plane placement within the box. It found that a 5' wing span scored better than a 5' fuselage (with a 4' wing). The latter design was heavier and less efficient, even though the longer fuselage helped control flow separation. The fuselage was then fixed with a cross-sectional area of 8.8"x9" which results in a C_{do} of about 0.25. When calculating score, results for a given study are normalized against the maximum predicted results (the same process used at the competition).

4.4.1 Airfoil Selection

Three types of airfoils were selected to find a general trend between the maximum lift coefficient of an airfoil compared to parasite drag and their effects on mission performance. High lift airfoils produce the most lift but also have the highest parasite drag coefficient. A high-lift airfoil performs better during take-off, but hurts the design during cruise performance. Low-lift airfoils behave in an opposite manner—they perform efficiently at cruise, but have trouble generating lift for take-off. A NACA6412, SD7032, and E423 were chosen to represent low, mid, and high-lift airfoils, respectively. The overall mission score was found by summing the normalized Delivery and Payload Mission score at high and low wind conditions.

Figure 15 on the following pages shows that the high-lift E423 outscored the other two options. The G23 airfoil was designed by blending characteristics of an E423, SD7032, and Wortman together to reduce C_{do} and increase $C_{L,max}$. The drag polar for the G23 and E423 is presented in Figure 15 and the G23 outperforms the E423 by achieving a higher maximum lift coefficient with a lower parasite drag.

OSU 2008 Black Team

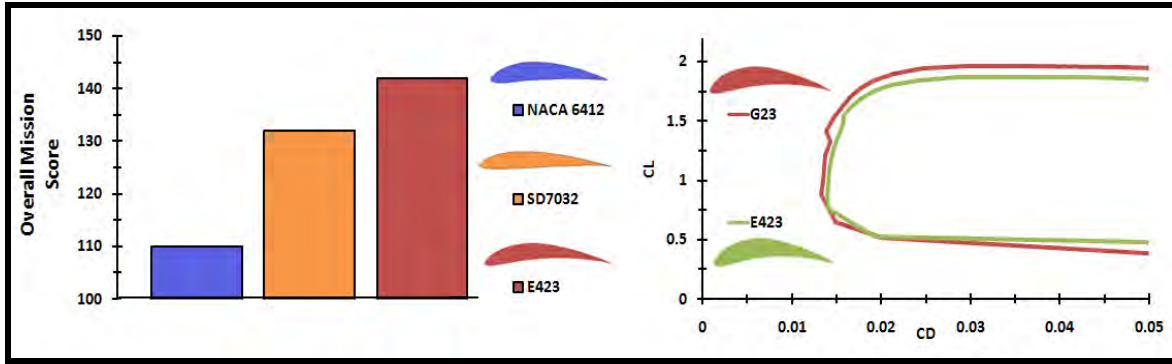


Figure 15: Airfoil Studies Conducted

4.4.2 Wing Sizing

Increase in wing area results in a larger chord and more lift at the expense of lower efficiency and higher weight. Using the optimization program, the wing area was varied at high and low winds for both missions. For the Delivery Mission, increasing the wing area resulted in a lower score while increasing wing area for the Payload Mission results in a higher score. A higher wind increased performance in the Payload Mission while hurting performance in the Delivery Mission. The overall Mission Score is plotted for both wind conditions and averaged in the figure below. The peak in the average line represents a choice for wing area that has a balanced performance between all wind conditions. The wing area chosen was 5.417ft² which gives a chord of 13in.

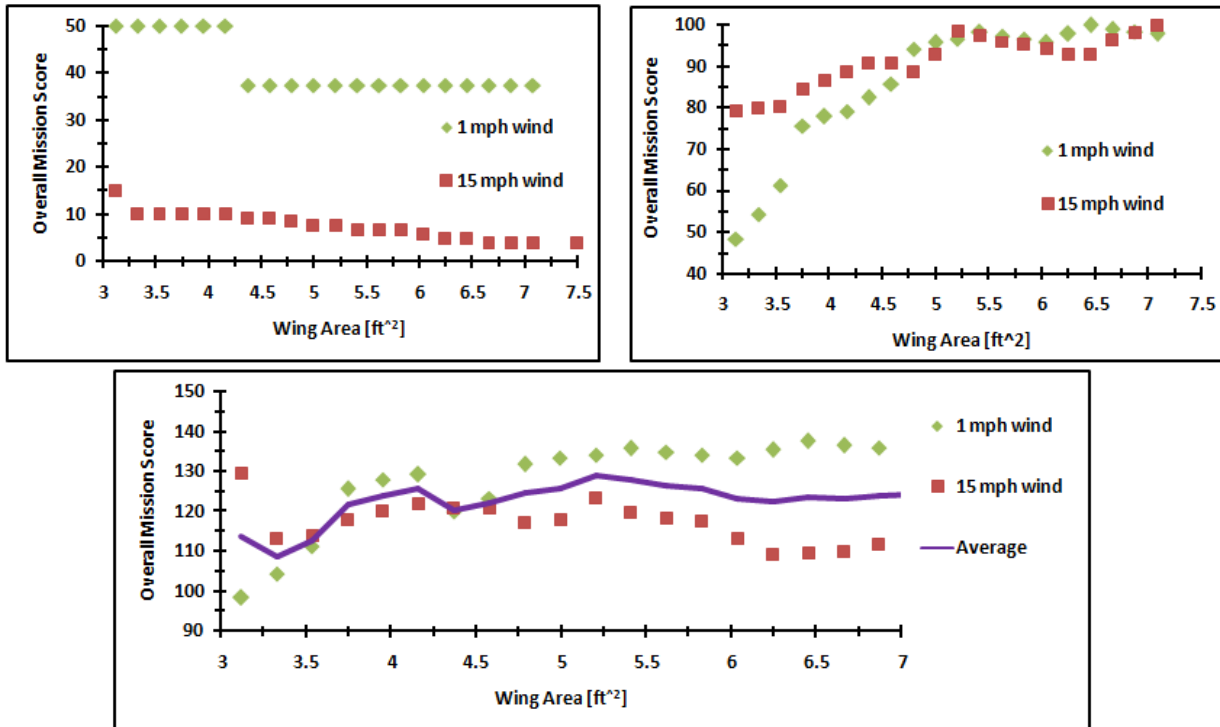


Figure 16: Mission Analysis to Size the Wing Area of the Aircraft



4.4.3 Endplate Sizing

The aircraft configuration study performed in Conceptual Design showed that adding endplates to a monoplane increased performance. Increasing endplate height results in a higher effective aspect ratio, but also increases induced drag and structural weight. The endplates were chosen to be 10" in height so they would not scrape the ground during take-off. They increase the effective aspect ratio by 25% without significantly increasing the skin-friction drag.

4.5 Stability Characteristics

4.5.1 Tail Sizing and Longitudinal Stability

Because tail sizing is an iterative process, a trade study was conducted to provide initial estimates for tail sizes and wing placement. A larger tail is trimmable at a lower incidence angle, but also adds structural weight. A 24" span and 7" chord was initially assumed for the horizontal tail size based on a historical study of previous DBF planes. A wing placement was also assumed in order to calculate its moment. A C_m vs. α curve was generated for each component in the entire aircraft. The left part of Figure 17 shows that the overall moment coefficient is zero at a 1 degree angle of attack. A C_m vs. α curve was then generated for different tail incidences to show they affect the moment coefficient of the entire aircraft. The graph on the right side of Figure 17 shows that a tail incidence of approximately -5 degrees trims the plane at a zero angle of attack. Drag vs. incidence of the tail was calculated, and the incidence did not add a substantial amount of drag to the tail. After determining the tail size, the wing was placed at 20.2" from the nose. With this wing placement, the static margin is about 20% and varies depending on payload configurations.

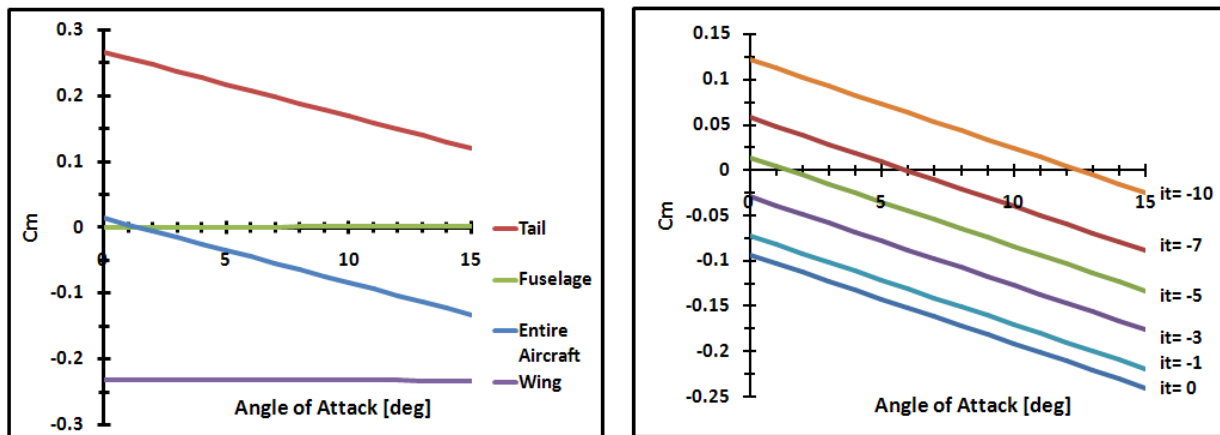


Figure 17: Trim plots for Tail Sizing

4.5.2 Longitudinal Static Stability and Control

The elevator size was determined by plotting different angles of elevator deflection against the moment coefficient of the plane. The sizing of the elevator determines the pitch capabilities of the aircraft. The elevator was sized at 18% of the tail surface and an elevator deflection plot (Figure 18) was used to determine whether the aircraft is trimmable at all angles of attack. The plot shows that a trim



angle of 11 degrees requires an elevator deflection of 10 degrees, which is acceptable amount because servos can easily deflect the elevator 20 degrees.

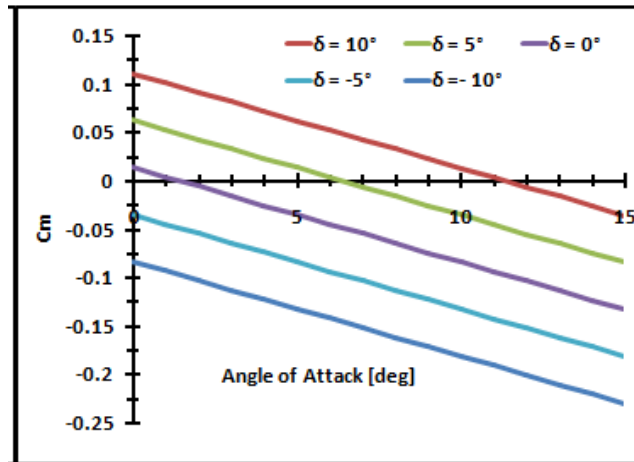


Figure 18: Elevator Deflection

4.5.3 Lateral Static Stability and Control

The vertical tail was sized to provide enough damping for directional flight modes. From Raymer (1999), a vertical tail volume of 0.04 was suggested for optimal flight characteristics. The aerodynamic center of the vertical tail was fixed because it must connect with the horizontal tail located at the end of the fuselage. A vertical tail with a semi-span of 8.5” and a root chord of 9.5” allows for adequate control. A rudder deflection of ± 20 degrees (at 20% of the vertical tail chord) was sufficient to counter all adverse yaw effects. OSU’s DBF pilot suggested designing the aircraft with a roll rate of approximately 60 degrees per second which allows the aircraft to easily perform routine banking maneuvers. Ailerons were sized at 18% of the total chord.

4.5.4 Dynamic Stability

Longitudinal Derivatives			Directional Derivatives		
X Force	Z Force	Pitching Moment	Y Force	Yawing Moment	Rolling Moment
$C_{X_u} = -0.039$	$C_{Z_u} = -1.701$	$C_{m_u} = 0$	$C_{Y_\beta} = -0.573$	$C_{n_\beta} = 0.146$	$C_{l_\beta} = -0.043$
$C_{X_\alpha} = 0.234$	$C_{Z_\alpha} = -4.883$	$C_{m_\alpha} = 0.568$	$C_{Y_p} = 0.000$	$C_{n_p} = -0.097$	$C_{l_p} = -0.932$
$C_{X_{\dot{\alpha}}} = 0.000$	$C_{Z_{\dot{\alpha}}} = -1.352$	$C_{m_{\dot{\alpha}}} = -2.314$	$C_{Y_r} = -0.017$	$C_{n_r} = -0.053$	$C_{l_r} = 0.219$
$C_{X_q} = 0.000$	$C_{Z_q} = 2.472$	$C_{m_q} = -4.230$	$C_{Y_{\delta a}} = 0.000$	$C_{n_{\delta a}} = -0.117$	$C_{l_{\delta a}} = 0.327$
$C_{\alpha_e} = 0.000$	$C_{Z_{\delta e}} = -0.325$	$C_{m_{\delta e}} = -0.556$	$C_{Y_{\delta r}} = 0.124$	$C_{n_{\delta r}} = -0.038$	$C_{l_{\delta r}} = -0.556$

Figure 19: Directional Stability Derivatives

Stability derivatives (Figure 19) for the aircraft were calculated using methods found in Nelson (1998). The derivatives show that the aircraft is stable for all longitudinal and lateral modes of flight. The effects



of endplates are not included in the calculations, but their presence should increase directional stability because they are placed behind the center of gravity of the aircraft.

The longitudinal and directional stability derivatives were used to calculate Eigenvalues for the aircraft. From the Eigenvalues the frequency and damping values were found. The Eigenvalues, frequency, and damping are plotted and tabulated below for each flight mode (Roll is not shown in the S-plot).

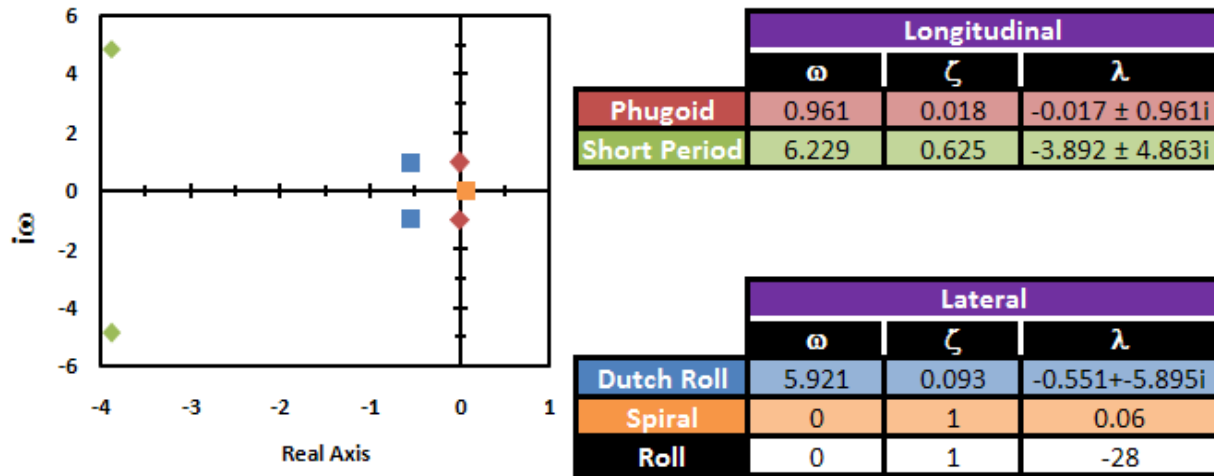


Figure 20: Dynamic Stability Eigenvalues

The Eigenvalues above suggest the aircraft has a low spiral mode. However, a control system analysis demonstrated that a pilot will easily counteract any spiral mode instability.

4.6 Lift and Drag Estimations

Parasite drag was found for each aircraft component that affects lift and drag characteristics. Interference drag is calculated based on the assumption that it increases the drag of the aircraft by 20%. All drag coefficients for the aircraft are shown in the table below and the percentage each component accounts for in relation to the total drag coefficient is displayed in the pie chart.

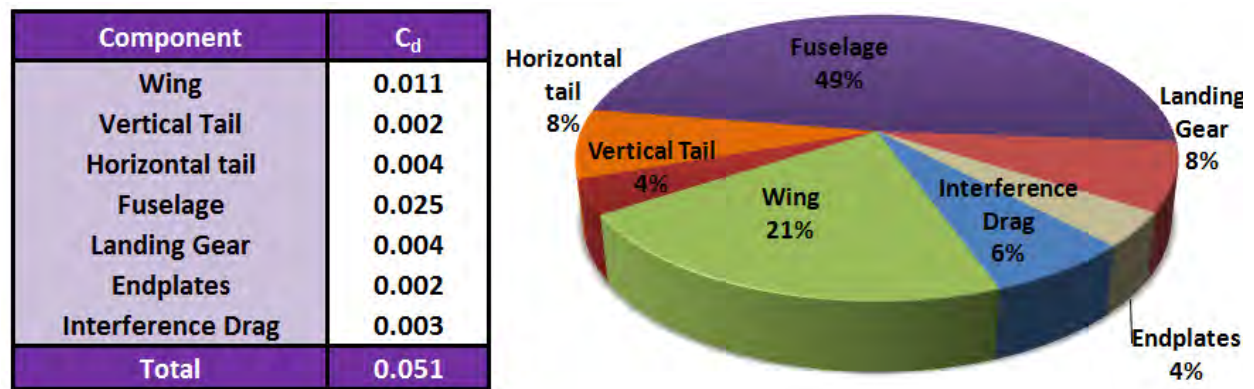


Figure 21: Drag Estimate for Entire Aircraft



Most of the drag for the aircraft is a result of the large fuselage cross-sectional area and cannot be decreased because the fuselage is already at the minimum cross-sectional area needed to restrain bottles. A high drag coefficient for the wing is caused because it is a high-lift airfoil, but this trade-off is required in order to achieve a 75' take-off.

L/D is plotted against angle of attack in Figure 22 and the drag polar for the entire aircraft is also shown. The maximum achievable L/D for the aircraft is 8.6, but for the Delivery Mission the aircraft flies at an 8.5 L/D and an 8.2 L/D for the Payload Mission. Higher L/D values allow the aircraft to fly more efficiently and over a further distance. Because the L/D flown for each mission is similar to the maximum L/D, it confirms that the tail and wing were trimmed properly. The lift and drag characteristics of the aircraft were found theoretically with X-foil, but the actual lift and drag of the aircraft is dependent on how well the structures team manufactures the shape of all of the external components.

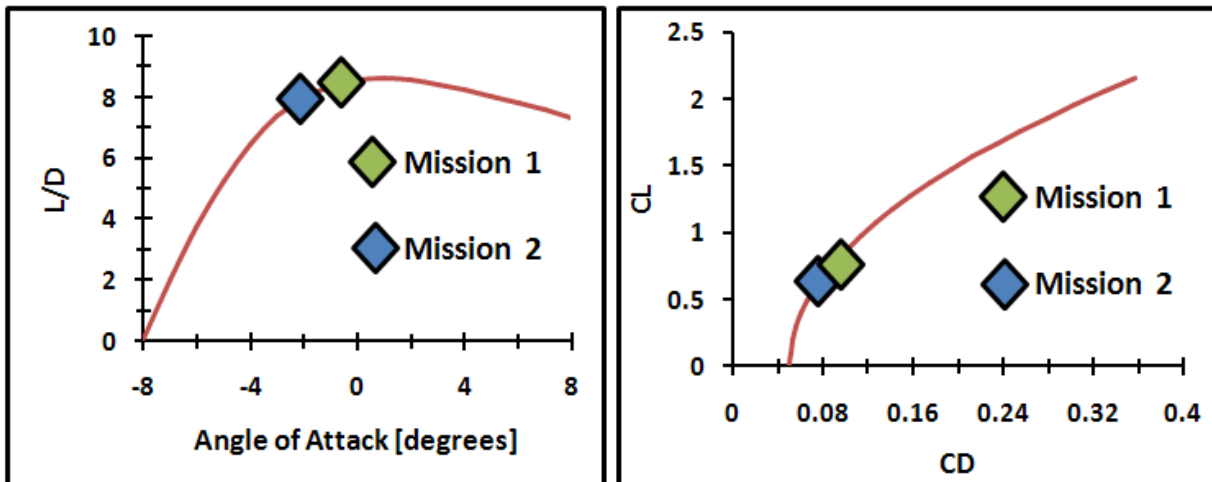


Figure 22: Drag Polar and CL/CD for entire Aircraft

4.7 Propulsion Sizing Trades

4.7.1 Motor and Gearbox Configuration

A propulsion power requirement of 450 Watts under worst case circumstances (no wind, Payload Mission) was estimated by the Aerodynamics mission modeling program. The power requirement in the mission modeling program assumes a rubber propulsion system so the propulsion team's first goal was to find a motor that matches the capabilities of the rubber system. Motors in the 200W to 700W range were benchmarked from a variety of different manufacturers. Motors with less than 450W were investigated because the amount of time that 450 Watts is required is so short (take-off and cruise) that motors with less power are feasible if cooled properly. Low power motors typically weigh less than high power motors. The K_v value of different motors was also investigated and affects how many RPM the motor operates at—inclusion of a gear box also adjusts RPM. Low power motors have better power to weight ratios than high power motors. Motors manufactured by Neu consistently had the best power to weight ratios. According to OSU history, Neu motors have been confirmed to operate within 5% of the



manufacturer’s specifications. Three series of Neu motors were investigated further: The 1105, 1107, and 1110 series which are rated for 350, 450, and 550 Watts of power, respectively.

To determine the best motor from all the series, the propulsion simulation program was used to compare how each motor performed by inputting their K_v , I_0 , and resistance parameters. Lower K_v motors with high gear ratios consistently outperformed all other motor configurations. The lower K_v allows more power to be used as torque which gives the plane a high amount of thrust, but forces it to fly slower. In terms of performance parameters (take-off distance, maximum climb angle, efficiency), the 1107 and 1110 series outperformed the 1105 motors. The 1105 motors are only rated to carry 350 Watts and were not able to utilize 450W of battery power as effectively as the other motors. A motor from the 1107 series was selected because 1107 series motors provided the same performance as the 1110 motors, but weighed less. The specific 1107 series motor was chosen based on running the propulsion simulation with differing battery and propeller inputs and selecting the motor with the best balance between power and efficiency while considering all mission parameters.

4.7.2 Batteries

Two different types of batteries are allowed at the competition, NiCad and NiMH. NiCad’s have better max current while NiMH’s have better energy density. Because battery weight is a variable directly calculated in RAC and Delivery Mission score, the energy density and efficiency for each battery type was investigated. The NiMH batteries were chosen over the NiCad batteries because higher energy densities allows for a lower required battery weight for each mission.

In order to choose the best batteries possible, the propulsion team built a test stand and measured different properties of batteries. These results are shown in the table below:

Cell	Weight (lb)	Capacity (mAh)	Resistance (Ohms)	Capacity/Weight (mAh/lb)	Max Current (Amps)	Max Specific Power (Watts/lb)
GP 2000	0.0772	1640	0.011	21254	30	338
Elite 2000	0.0772	1600	0.013	20736	30	349
Elite 1500	0.0507	1060	0.015	20905	25	407
CBP 300AA	0.0220	80	0.055	3629	8	272
KAN 700AAA	0.0287	460	0.033	16050	12	307
KAN 700AA	0.0331	490	0.031	14817	16	357
KAN 400AAA	0.0176	250	0.05	14175	9	382
KAN 160	0.0088	110	0.214	12474	3	189

Figure 23: Battery Data

Batteries were narrowed down initially based on capacity/weight values and their max specific power. The best batteries (Elite 2000, Elite 1500, KAN700AA) were further narrowed by comparing them in the mission modeling program. The results are shown in Figure 24. A trade-off exists between whether power is created by voltage or current. More current from the batteries allows for a larger propeller to be used, but as more current is drawn the battery voltage drops and power is provided less efficiently.

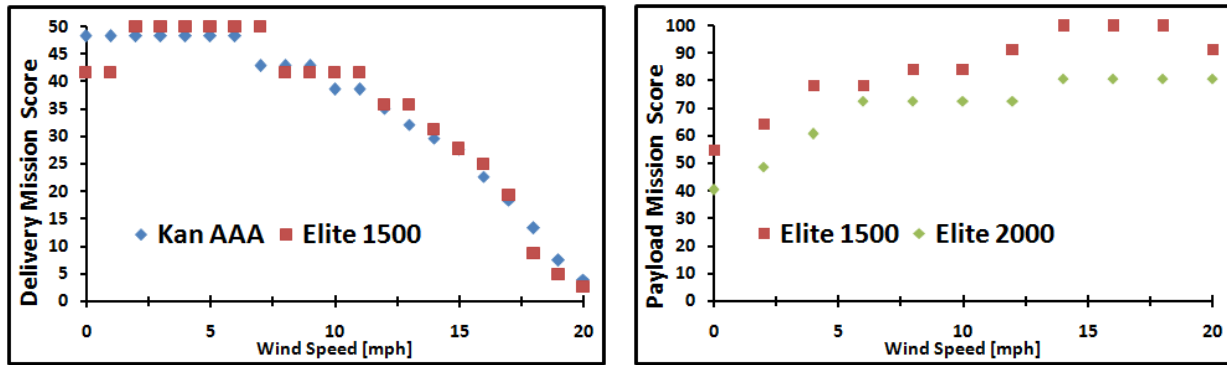


Figure 24: Battery Comparison Curves

The Aerodynamic mission modeling program shows that the Elite 1500 batteries provide the highest score for the Payload mission for all wind speeds and for a majority of speeds in the Delivery mission.

4.7.3 Propeller

Larger propellers provide more thrust, but draw more current from the batteries and are slightly heavier. The amount of current a propeller requires is reduced by choosing a motor with a low K_v value and a high gear ratio. The efficiency of the propeller is optimized by varying its pitch. Because of the high thrust requirements for take-off and climb in each mission, the highest diameter propeller possible was always selected.

4.8 Structural Sizing Trades

4.9.1 Fuselage

In the Conceptual Design phase, it was determined that the overall aircraft structure should force all loads through two bulkheads and further distribute loads along a spine that runs along the fuselage longitudinally. By modeling the fuselage as a T-shaped beam, an optimization program was created that calculated loads associated with the fuselage. A minimum bulkhead size was found to carry the highest possible load with the least amount of system weight. The spine was designed to be just tall enough to distribute loads across all bulkheads, with two of the bulkheads handling the majority of the load.

4.9.2 Wing

An excel program was created that allowed for the material and dimensions of a wing spar to vary according to user input. The spars were modeled as C-channels to allow for a simplified design model that still distributed loads efficiently. A bending and shear analysis determined that a 2.5g turn would be the worst load case scenario for the wing. The analysis showed that the spars would fail due to shear stress coupled with bending and the spar dimensions were varied until it was strong enough to survive a 2.5g turn with a 1.5 safety factor. Failure occurs at about 300psi, but according to the weight models in the mission modeling program, the wing never experiences more than 230psi during flight. Figure 25 shows the shear stress and bending stress experienced by the forward and aft wing spars during flight.

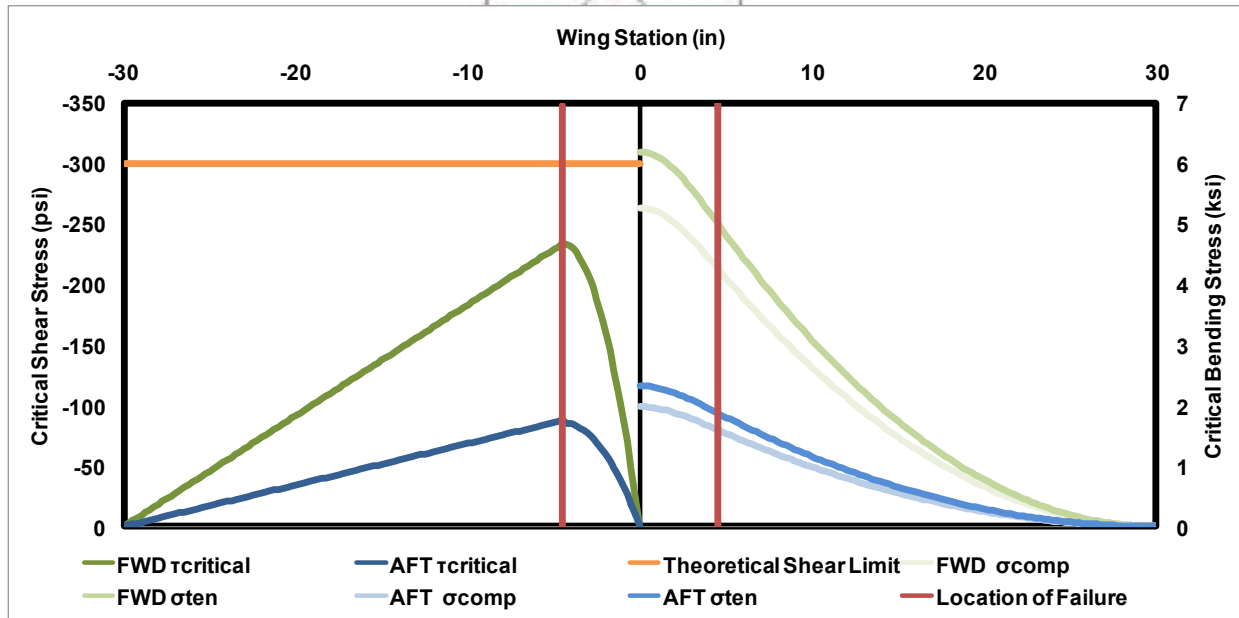


Figure 25: Wing Loading Predictions

The location of failure on the figure is where the wing mates with the fuselage, there is no line shown for bending stress failure because it is about twenty times higher than the wing ever experiences.

4.9 Mission Performance Estimation

4.9.1 Loading Time Performance Estimation

Experimental data was obtained to form decisions about loading process trade-offs. Uncertainty in the contest rules allows the distance between the aircraft and starting line at the contest to be any distance between 10' and 50'. A quick-loader was discarded as a viable option because one person from the team would have to run to the aircraft and retrieve the quick-loader before running to the payload station. In order to optimize loading times, the following three variables were isolated: 1) the spatial tolerance between payload elements, 2) the ground crew's loading method and 3) the hatch locking mechanisms. All tests were conducted using a loading distance of thirty feet.

1) A prototype restraint system was built with varying compartment sizes in order to find an optimal compartment size. Increasing spatial tolerance beyond 0.4" did not significantly improve loading times, but tolerances below 0.2" hurt times. A 0.3" inch tolerance in both directions was chosen for each payload compartment which results in a payload bay of 31". 2) Figure 26 displays recorded times when transporting each payload configuration with 2 and 3 people. Because it is difficult to hold any more than five bottles (five bottles are easily held as shown in Figure 26), the 14/0, 10/1, and 7/2 configurations worked better if three people retrieved the payload. 3) Loading times decreased if the hatches were easy to open and close quickly. The first latching method investigated required a sliding motion to lock the hatches, but a faster method was developed by using locks that allowed the hatches to drop into place effortlessly. Loading time improved when the two hatches used (a restraining hatch and an outer loading hatch) could both be opened using only one motion.

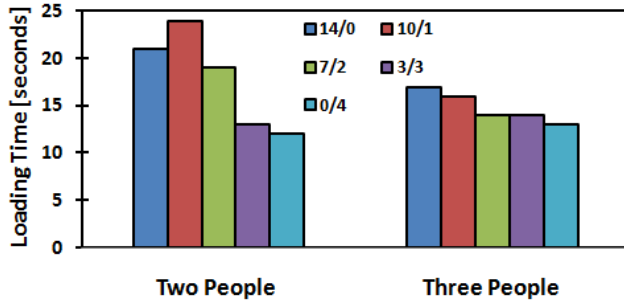


Figure 26: Payload Times with Different Strategies and Five Bottles easily Held by one Person
4.9.1 Aircraft Mission Performance Estimation

The mission modeling program assumes a weight of 4.7lb for the aircraft based on the wing area and is used to predict the flight performance of the aircraft for each mission. Figure 27a shows the estimated performance during the Delivery Mission with a 5 mph wind. Optimization showed that flying three laps at about 30 ft/s (just above stall velocity when wind is considered) provided the highest score. A projected battery weight of 0.4 lb gives a mission score of 7.5.

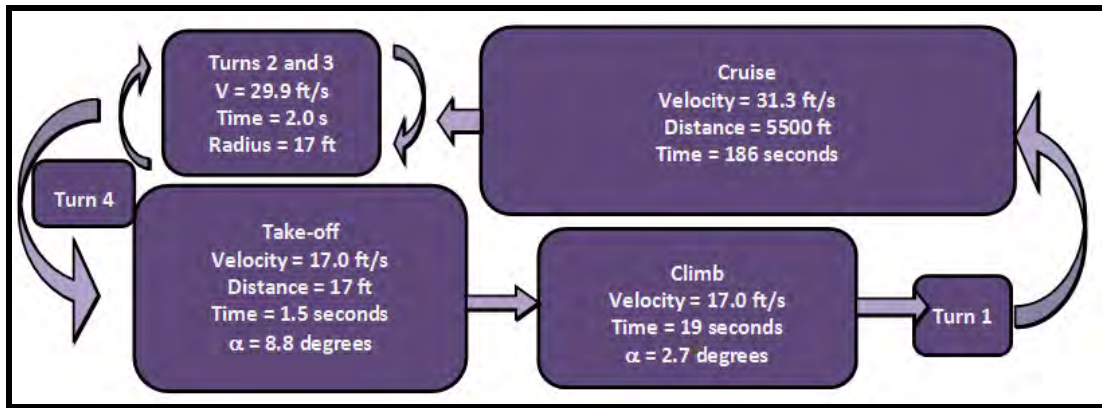


Figure 27a: Predicted Delivery Mission Performance

Figure 27b shows the aircraft performing the Payload Mission at a 5 mph wind with 0.6 lb of batteries. The RAC is predicted to be 2.82 and the mission score is 0.021 if loading time is 17 seconds.

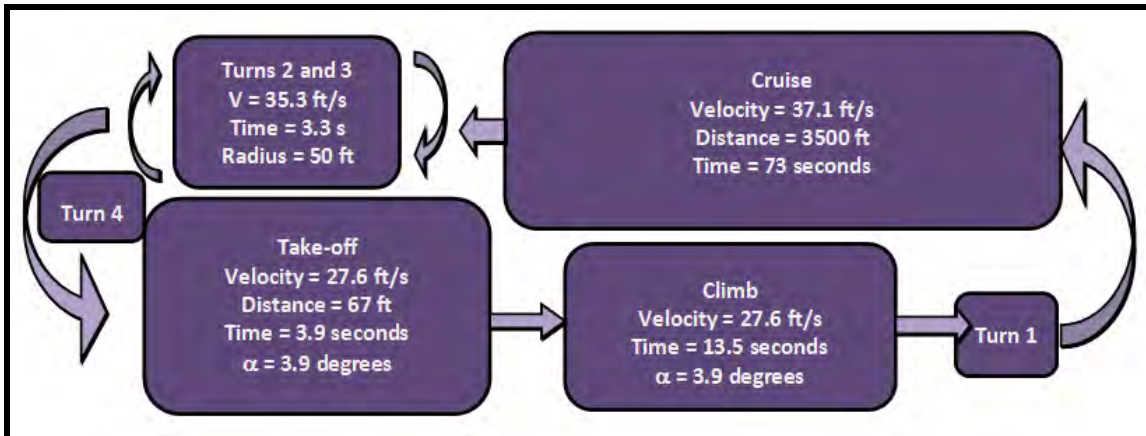


Figure 28b: Predicted Payload Mission Performance



5.0 Detail Design

The Detail Design Phase documents the characteristics and capabilities of the optimized aircraft design from the Preliminary Design Phase. The performance of all key sub-systems and the complete aircraft solution is predicted in this section of the report and compared against demonstrated results in Section 8: Performance Results.

5.1 Dimensional Parameters

The following table documents the dimensional parameters of the final design. The table shows the geometry of the fuselage, wing, and empennage.

Table 5: Dimensional Parameters

Dimensional Parameters							
Fuselage		Wing		Horizontal Stabilizer		Vertical Stabilizer	
Length [in]	48	Airfoil	G3	Airfoil	NACA 0009	Airfoil	NACA 0009
		Span [ft]	5	Span [ft]	2	Span [ft]	8.5
Width [in]	8.8	Chord [in]	13	Chord [in]	7	Root Chord [in]	9
		Area [ft ²]	5.417	Area [ft ²]	1.17	Area [ft ²]	0.472
Height [in]	9.5	Aspect Ratio	4.615	Incidence [deg]	-5	Aspect Ratio	4.25
		Incidence [deg]	2	Tail Volume	0.398	Tail Volume	0.04

5.2 Structural Sub-System Characteristics/Capabilities

5.2.1 Airframe

The outside hull and internal airframe structure are composed of 1/16" balsa and 0.7oz/yd² fiberglass with a cross-sectional area of 8.8" by 9.5"—the minimum size capable of fitting all payload configurations. Fuselage length is 46" and the internal restraint system is 31". A network of one spine and eight bulkheads make up the internal restraint system and evenly divide fourteen 4.3" by 4.3" compartments. All loads experienced by the fuselage are directed through the bulkheads. The outside hull is designed to carry a minimal load and is —windowed" with fiberglass to reduce weight. A primary characteristic of the fuselage is its T- beam shape (the bottom of the fuselage and the spine form a T) that is efficient in carrying both shear and bending forces.

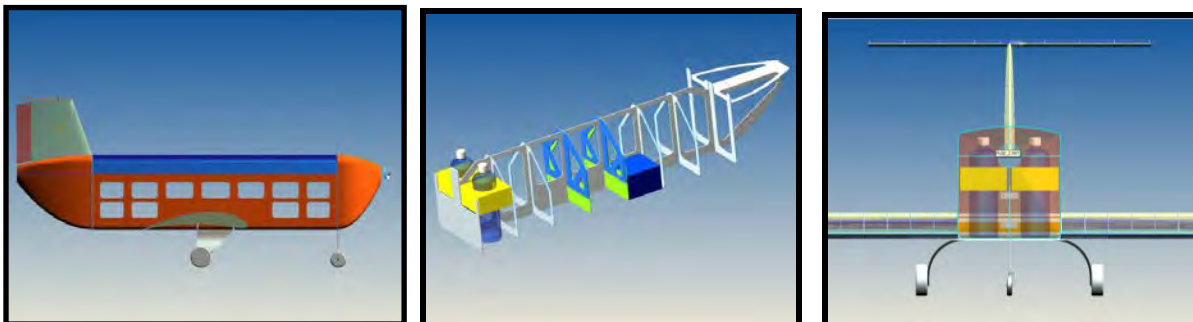


Figure 29: Outside Hull, Internal Frame, and Cross-sectional Area



5.2.2 Restraint System

A dual hatch system allows an inner-hatch to act as the payload restraint during check-in tests and an outer loading hatch to serve as a light weight external cover. The inner hatch is made of a fiberglass and balsa composite to retain stiffness and strength while the outer-hatch is constructed with *Microlite*. Both hatches overlap with each other and the inner-hatch forces the outer-hatch open during loading sequences. Loading time is decreased by the dual hatch characteristic and allows the ground crew to make only one movement to open both hatches, even though the hatches remain separate entities because they are not directly attached to each other. A balsa latching mechanism is used to attach the inner-hatch to the fuselage while the outer-hatch is connected to the fuselage with light-weight magnets. Bulkheads act as dividers between bottles and restrict their horizontal movement. The inner-hatch restrains the bottles in a vertical direction and four “dummy” pieces of balsa stored above the tail bulkhead are placed above bricks to restrict their vertical motion.

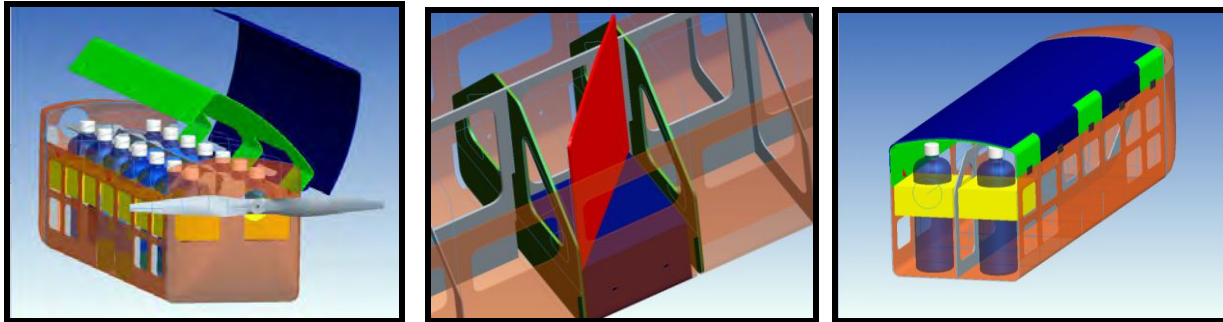


Figure 30: Restraint System and Hatch Mechanism

5.2.3 Wing

The wing is designed geometrically in the shape of the G23 airfoil with a 5' wing span and a chord size of 13". Two C-channel shaped spars connect the wing to the fuselage. The upper spar cap is a spruce beam reinforced with unidirectional carbon fiber. Carbon fiber increases the wing's strength and adds stiffness. The lower spar cap is characterized as a tension carrying member and is built with balsa. Ribs of the wing are made with 1/16" balsa and the ribs common to the control surface are cut at 80% of the chord length, with the trailing rib tips forming the control surface frame. Epoxy is used to strengthen the ribs that mate with the fuselage and the ribs that attach to each endplate. *Microlite* lines the top and bottom surfaces of the wings and a 1/32" balsa D-tube is used for the leading edge. The endplates are a fiberglass/balsa frame and extend 4" above and below the mid-point of the airfoil. Endplate size is limited due to rotation of the aircraft at take-off. The wing weighs 0.83lbs and is designed to fail due to shear at its root when a load of 13lb is applied to one of the wing tips. The design of the wing gives it the capability to survive the maximum load experienced by the wing during a 2.5g turn.

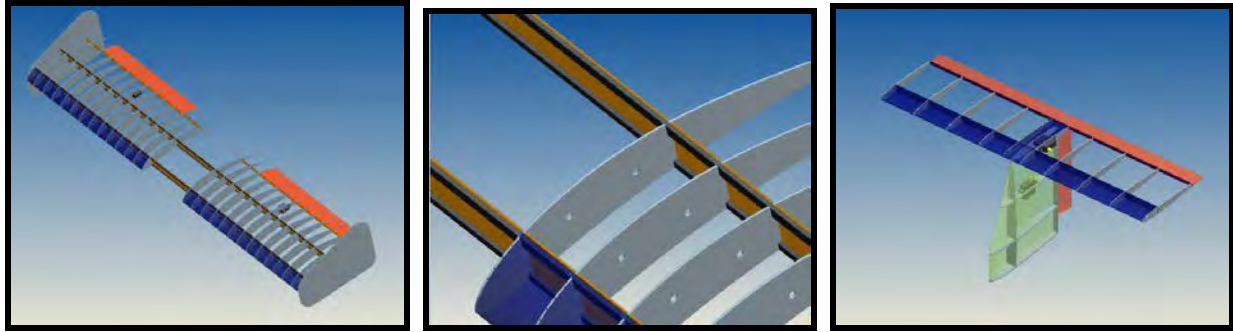


Figure 31: Dual Spar Wing and Empennage

5.2.4 Empennage

The vertical and horizontal tails weigh 0.24lb together, and the empennage spars consist of 1/16" fibreglassed balsa and the ribs are made of 1/32" balsa. Light CA hinges connect each control surface and *Microlite* covers the bottom and top skins of the horizontal tail.

5.2.5 Landing Gear

The front gear consists of a carbon fiber —Jshaped strut that weighs 0.12 lb. The front gear was designed to absorb half of the plane weight exerted from after a one foot drop and is attached to the nose bulkhead, which helps carry loads during landing. A bowed main gear built from carbon fiber absorbs the primary forces the aircraft experiences during landing. The main gear is constructed using ten plies of carbon fiber and 1/8" balsa and weighs 0.40lb. The main gear is rated to survive the entire aircraft's weight after a two foot drop. The landing gear touches the ground 4" below the aircraft and is 16" wide. Placement was decided by distributing 10% of the load to the nose gear and 90% to the main while sitting flat on the ground.

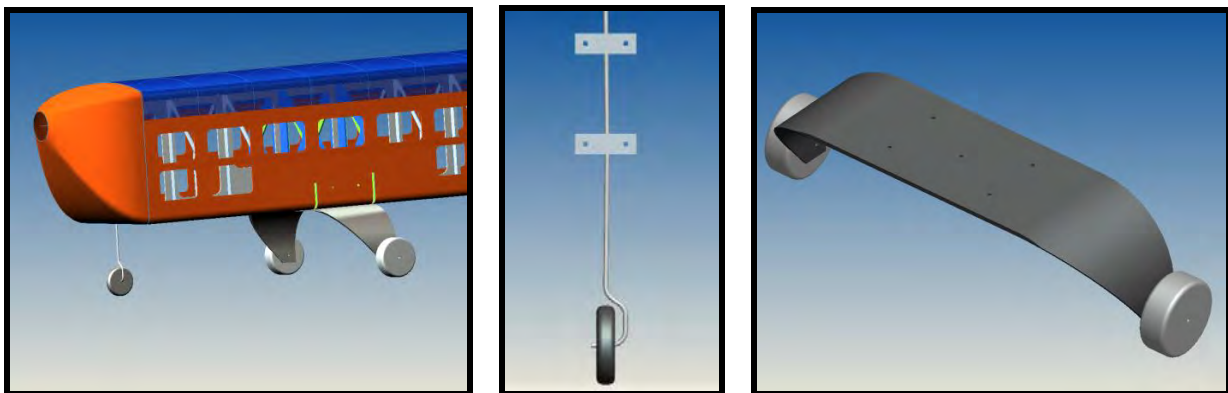


Figure 32: Landing Gear



5.3 Systems and Sub-Systems

5.3.1 Control Systems and Propulsion Sub-System Selection

The final configuration of all control systems and propulsive components is tabulated below:

Table 6: Control and System Selection

Systems Selection			
Control systems		Propulsion Components	
Radio	Spektrum DX-7	Motor	Neu 1107/2.5Y
Receiver	Spektrum AR-9000	Speed Controller	Kontronix Jaxx-40
Receiver Battery	4 x Kan400 AAA	Gear Ratio	6:1 MEC
Servos x4	HS-81	Battery	Elite 1500
Servos x1	HS-475	Propeller	APC 20x10 APC 18x10

The servos provide 36oz-in of torque—enough to rotate all control surfaces and nose gear for all expected mission conditions. Each mission utilizes a different propeller because of differing thrust and efficiency requirements. Batteries chosen for the receiver are the lightest batteries that will still provide adequate power. The speed controller was chosen for its efficiency and allowable current of 40 amps while the receiver was chosen based on historical OSU success.

5.3.2 Integrated Propulsion Sub-System Capabilities

With the propulsion components selected, the propulsion simulation program was used to model both missions. The simulation documents mission performance more accurately during the Detail Design Phase because a more precise system weight estimate replaces the assumed system weight from the mission modeling program. The simulation predicts the aircraft's performance by modeling take-off, cruise, and descent stages of each mission. The times spent in each flight phase were determined using the mission modeling optimization program and the thrust, power, and current values are documented at each point in time during the simulation. The Delivery mission was determined to require 2lb of thrust for take-off and 3.6 Watt hours of energy for the entire mission, as shown in the figure below.

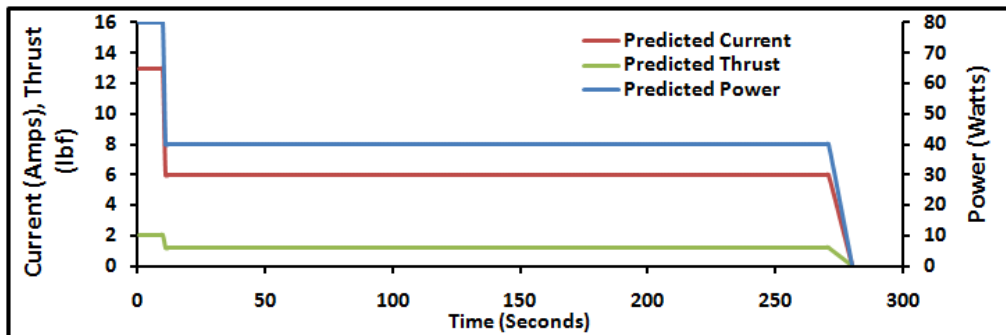


Figure 33: Delivery Mission Propulsion System Capabilities

The Payload mission requires about 5lb of thrust for take-off and 7.9 Watt hours of energy.

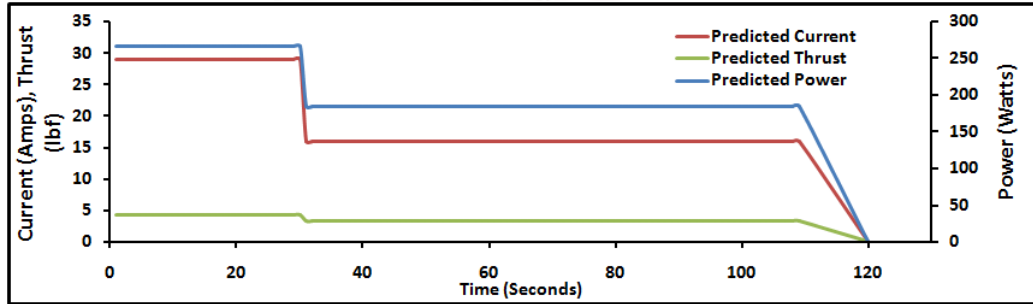


Figure 34: Payload Mission Propulsion System Capabilities

5.3.3 Battery Weight Selection

Battery weight required to complete each mission for all wind conditions is predicted more accurately since the weight of all components is known. Wind brackets for the Delivery Mission are also divided based on the number of laps the aircraft may complete for a given wind.

Delivery Mission			Payload Mission		
Wind Velocity	Number of Cells	Battery Weight	Wind Velocity	Number of Cells	Battery Weight
0 to 14	6	0.30	0 to 4	18	0.89
15 to 19	6	0.30	5 to 9	12	0.60
20 and above	10	0.50	10 and above	10	0.50

Figure 35: Batteries Used for All Wind Conditions

5.3.4 Sub-system Integration and Architecture

All propulsion system components are located in the nose of the fuselage. In order to assemble all propulsion components, the gear box and the motor are connected initially and the motor pinion is then meshed with the gear box spur. Two bolts run into the motor to connect it to the nose of the fuselage and the speed controller is wired into the back of the motor. The propeller is attached to the front of the nose.

Structural integration forces load paths to travel through a minimum area between the two main bulkheads. The dual spar wing system slides upwards into the fuselage and fits directly under two reinforced bulkheads. Four nylon bolts and Kevlar reinforcement are used to attach the main gear to the fuselage. The front gear is bolted to the front bulkhead. The tail is mounted to the back of the fuselage and a bulkhead in the tail structure absorbs loads and improves stiffness. All attachment points between the tail, the fuselage, and internal bulkheads are secured with epoxy and fiberglass.

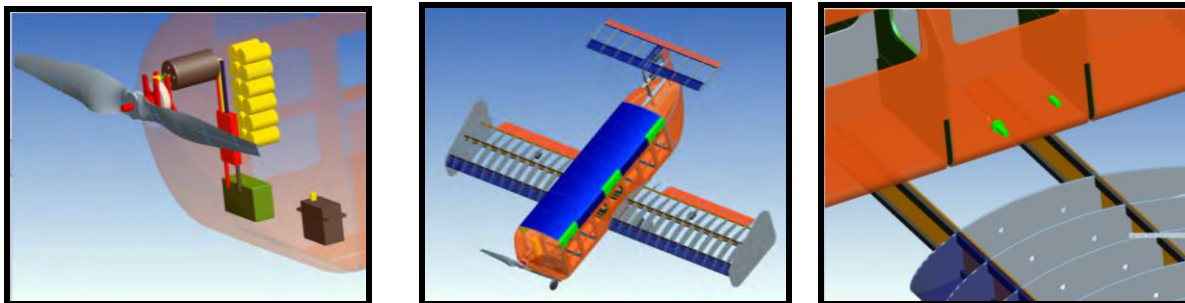


Figure 36: Sub-system Integration and Architecture



5.4 Weight and Balance for Final Design

5.4.1 Weight and Balance without considering Payload

The structural CG of the aircraft for both missions is tabulated below. Each mission has a different structural CG because the battery packs used for each mission are a different weight. Battery pack weight assumes the amount required for a 5-mph wind condition during flight. The pie chart shows the percentage each component takes up in comparison to the entire system weight.

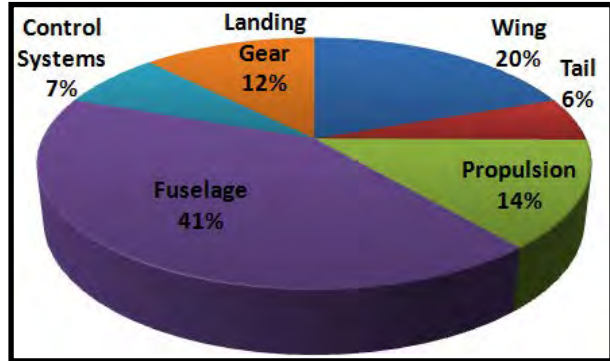


Table 7: Structural Weight and Balance

Weight and Balance			
Component	Weight [lb]	Distance [in]	Weight Moment [lb-in]
Wing	0.83	20.4	16.93
Tail	0.24	40.0	9.59
Propulsion	0.70	3.0	2.10
Fuselage	1.77	24.0	42.48
Main Gear	0.40	19.8	7.92
Front Gear	0.12	5.0	0.60
Mission 1 Batt	0.20	3.0	0.60
Mission 2 Batt	0.70	3.0	2.10
Delivery Mission			
Total Weight =	4.26	Total Weight Moment =	80.22
Structural CG=	20.26		
Payload Mission			
Total Weight =	4.76	Total Weight Moment =	81.72
Structural CG=	19.90		

5.4.2 Weight and Balance with all possible payloads

The aircraft's CG for each mission is shown below. The empty configuration applies to the Delivery Mission and the five payload configurations apply to the Payload Mission.

Table 8: Weight and Balance for All Possible Payload Configurations

Weight and Balance for Delivery and Payload Missions			
Payload Configuration	Payload Weight	CG	Static Margin
Empty	0	20.26	22.8%
14/0	7.0	19.92	16.7%
10/1	6.8	19.9	16.5%
7/2	7.1	19.93	17.0%
3/3	6.9	19.91	16.8%
0/4	7.2	19.94	18.2%



5.5 Flight Performance Parameters

Flight performance parameters are tabulated below for each mission at 5 mph. The difference in performance occurs because the total aircraft weight differs between flights.

Flight Performance Parameters			
General Aircraft Parameters			
C_{Lmax}	1.75	C_{Do}	0.051
Max C_L/C_D	8.6	e	0.9
Mission 1		Mission 2	
Max Climb Rate [ft/s]	4	Max Climb Rate [ft/s]	4.5
Max Climb Angle [deg]	4.2	Max Climb Angle [deg]	5.4
Stall Speed [ft/s]	18	Stall Speed [ft/s]	31.4
Max Speed [ft/s]	40	Max Speed [ft/s]	60
Take-off distance [ft]	17	Take-off distance [ft]	67
Max Power Required [W]	85	Max Power Required [W]	420
Turn Radius [ft]	17	Turn Radius [ft]	50
Roll Rate	58	Roll Rate	60
L/D During Cruise	8.5	L/D During Cruise	8.2

5.6 Rated Aircraft Cost

The RAC is calculated using the system weight documented in Section 5.4 and the documented battery weights for each wind condition are found in Section 5.3.3. Battery weight varies depending on the wind speed at the competition because the wind affects the aircraft's flight performance.

Table 9: RAC Estimate for All Wind Conditions

Wind Velocity	SYSTEM WEIGHT X W_{batt} = RAC		
0 to 4	4.26	0.89	3.80
5 to 9	4.26	0.60	2.53
10 and above	4.26	0.50	2.11

5.7 Mission Performance

Figure 26 shows a mission profile for the Delivery Mission with 5 mph wind, 3 laps completed, and 0.6 lb of batteries. Each stage of flight is represented and the important performance variables are tabulated.

	Take-off	Climb	Cruise	Descent
Power [Watts]	85	101	43	32
Efficiency	56.20%	54.70%	59.60%	65.20%
Thrust [lb]	2.21	2.42	1.46	0.32
Velocity [ft/s]	24	28	33	21
Distance [ft]	17	500	5800	87
Time [s]	1.3	18.4	195	14

Figure 37: Delivery Mission Flight Profile



The number of batteries and number of completed laps were varied with wind speed until the highest documented score was found for each wind condition (Figure 37). Score varies because the propulsive efficiency drops as aircraft speed increases in order to overcome increasing wind velocities.

DELIVERY MISSION			
Wind Velocity	Nlaps	÷ Wbatt	= Score
0 to 14	4	0.30	13.3
15 to 19	3	0.30	10.0
20 and above	2	0.50	4.0

Figure 38: Documented Delivery Mission Score

Figure 38's mission profile is for the Payload Mission at 5 mph wind with 0.6 lb of batteries.

	Take-off	Climb	Cruise	Descent
Power [Watts]	266	266	149	114
Efficiency	46.70%	46.70%	57.40%	66.40%
Thrust [lb]	4.35	4.35	2.85	0.41
Velocity [ft/s]	34	38	50	33
Distance [ft]	67	500	3700	129
Time [s]	3.7	12.8	75	13

Figure 39: Payload Mission Profile

The table below shows the highest possible score at each wind condition. Score increases with wind speed because faster winds improve take-off performance. At 10 mph the score does not increase further due to rate of climb limitations.

Table 10: Mission Performance

PAYLOAD MISSION			
Wind Velocity	1 ÷ (Loading Time * RAC)		= Score
1 to 4	17	3.80	0.015
5 to 9	17	2.53	0.023
10 and above	17	2.11	0.028

5.8 Technical Drawing Package

The drawing package includes a 3-view drawing with dimensions, a structural arrangement drawing (exploded view), two payload accommodation drawings, and a systems layout/location drawing.

OSU 2008 Black Team



See separate drawing package file for 3-view sketch

OSU 2008 Black Team



See separate drawing package file for structural arrangement drawing

OSU 2008 Black Team



See separate drawing package file for payload accommodation 1 drawing

OSU 2008 Black Team



See separate drawing package file for payload accommodation 2 drawing

OSU 2008 Black Team



See separate drawing package file for systems layout/location drawing

6.0 Manufacturing Plan and Processes

Several different construction methods for each subsystem were considered during the manufacturing phase of the project. Each technique varies in complexity and effectiveness and after investigating and comparing several methods, the construction of each subsystem and aircraft assembly was determined.

6.1 Manufacturing Methods Selected for Major Components

Construction methods for major components (the fuselage and wing) were determined initially and then construction methods for other sub-systems were evaluated. These methods were down-selected by weighting FOMs for different manufacturing processes. The following FOMs are used to evaluate construction methods:

- **RAC** – How the construction process affects the final weight of manufactured part
- **Building Time** – Time needed to construct a part
- **Ease of Construction** – Determines the complexity associated with a building method
- **Maintenance** – How easy it is to repair damaged parts
- **Cost** – How much materials/tooling cost for particular construction method

6.2.1 Fuselage Construction Selection Process and Results

Three methods were investigated to determine how to construct the fuselage. The methods were weighted to determine a quick way to build a fuselage that does not hurt performance or increase manufacturing costs.

Fuselage Construction		Foam Core	Plug Mold	CNC Mold
Figure of Merit	Weight			
RAC	5	-1	0	0
Building Time	5	1	0	-1
Ease of Construction	2	1	0	-1
Maintenance	2	-1	1	1
Cost	1	0	0	-1
TOTAL	15	0	2	-6

Figure 40: Construction methods investigated for Fuselage Manufacturing

- **Foam Core** – A foam core fuselage is constructed by cutting the shape of the fuselage from a large block of foam. Composite skins are laid up on top of the foam. The foam “core” is hollowed to allow for internal components and payload. Little tooling is required and construction is completed quickly. But the additional weight of the remaining foam core is unnecessary.
- **CNC Mold** – A CNC mill is used to machine master molds that are used to lay up composite structure. The CNC enables a precise mold to be built, but does not allow multiple team members to work on parts at the same time because there is only one CNC mill available in the lab.



- Plug Mold** – Similar to the foam core method, but uses the foam “plug” to produce a master mold from fiber glass layered with tool coat. A composite skin is then placed onto the master mold to produce the final part. Once a master mold is complete, construction lasts only a couple of days.

After the plug mold construction method was selected, the assembly of the fuselage with all other aircraft components was considered. It was determined that all internal components in the fuselage (bulkheads) and the tail would be attached to the fuselage with epoxy. Propulsive components are either bolted (motor/prop) or attached with velcro (batteries, receiver). The landing gear is bolted directly to the fuselage if nylon bolts, using nylon bolts and Kevlar reinforcement.

6.2.2 Wing Construction Selection Process and Results

Wing Construction		Mold	Traditional	Foam Core
Figure of Merit	Weight			
RAC	5	0	0	-1
Building Time	5	0	0	1
Ease of Construction	2	-1	0	0
Maintenance	2	0	-1	-1
Cost	1	-1	1	0
TOTAL	15	-3	-1	-2

Figure 41: Construction methods investigated for Wing manufacturing

- Mold** – A mold of the wing is constructed as a guide for the construction of the actual wing that is built using the skin as a starting point. The method requires a foam mold to be constructed initially, and construction is difficult because laying up the wing requires precision.
- Foam Core** – The same foam core method described for fuselage construction. The unnecessary weight associated with a completed part was the method’s main drawback.
- Traditional** – The traditional method requires the wing to be constructed using the ribs as a starting point. Typically, the ribs are aligned on a wing jig, and then the rest of the wing is built around them. Construction time is comparable to other methods and requires no mold.

Balsa ribs and *Microlite* skin were chosen as the best materials for traditional wing construction. Building the wings around two intact spars with the traditional method allows the wing to easily slide into the fuselage via holes and each spar is then epoxied to one of the two main bulkheads. Spars are built using carbon tow and balsa.

6.2 Manufacturing Methods Selected for Full Assembly

Other sub-system construction methods were selected based on the need to build and assemble prototypes quickly and efficiently. Once an initial mold is built, all parts laid up in the mold are constructed over the course of a couple days. Because the fuselage already required a mold, using a mold for other sub-systems did not add time to the overall assembly process. A skill level is assigned to each method



that helps determine where team members should work. Knowing the build time of each part helps the Structures lead create accurate manufacturing schedules.

Sub-System	Construction Method	Skill Level	Uses a Mold?	Build Time
Airframe	Foam Plug Mold	3	Yes	two days
Bulkheads	CNC	2	No	one day
Wing	Balsa with Fiberglass	2	No	three days
Front Gear	CNC Mold	1	Yes	two days
Main Gear	Foam Mold	1	Foam Mold	two days
Horizontal Tail	Balsa with Fiberglass	2	No	two days
Vertical Tail	Foam Plug Mold	3	Yes	two days
CAD Drawings	Pro-Engineer	3	No	two weeks

Figure 42: Table Documenting Methods used to construct each Sub-system

6.3 Construction Schedule

A detailed construction schedule was created to ensure the prototype was completed by the February 28 deadline. Because of the construction methods chosen, most components were built in parallel by the Structures team which allowed a one week construction time per aircraft after initial molds were made. The schedule includes all construction beginning with practice parts and ending with the final aircraft.

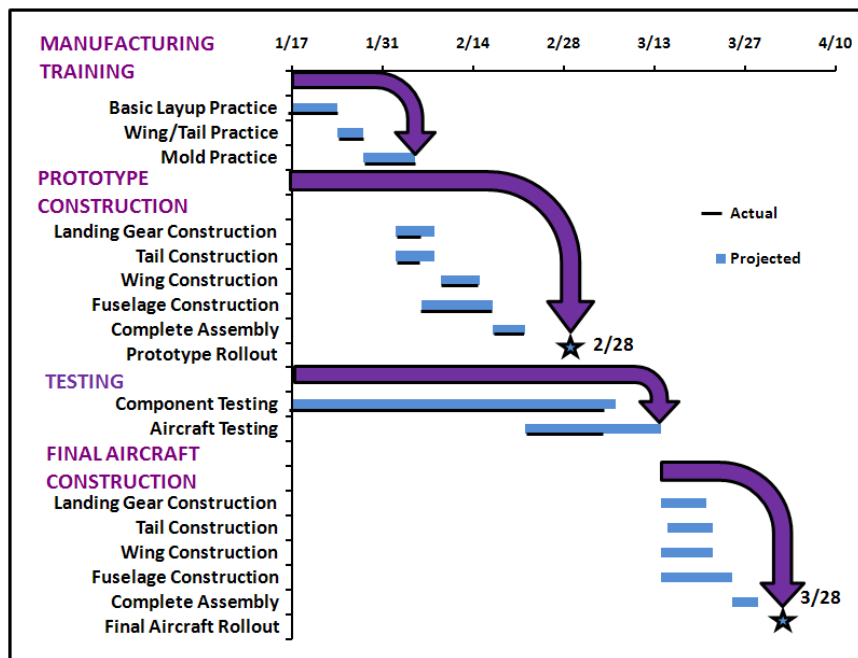


Figure 43: Construction Schedule

6.4 Construction Costs

After all materials were purchased for the construction of two prototypes and one competition aircraft, the costs were tabulated and graphed as shown below. Because of the construction methods chosen, the entire cost of the project was approximately \$4000—about \$1000 less than initially planned.

OSU 2008 Black Team

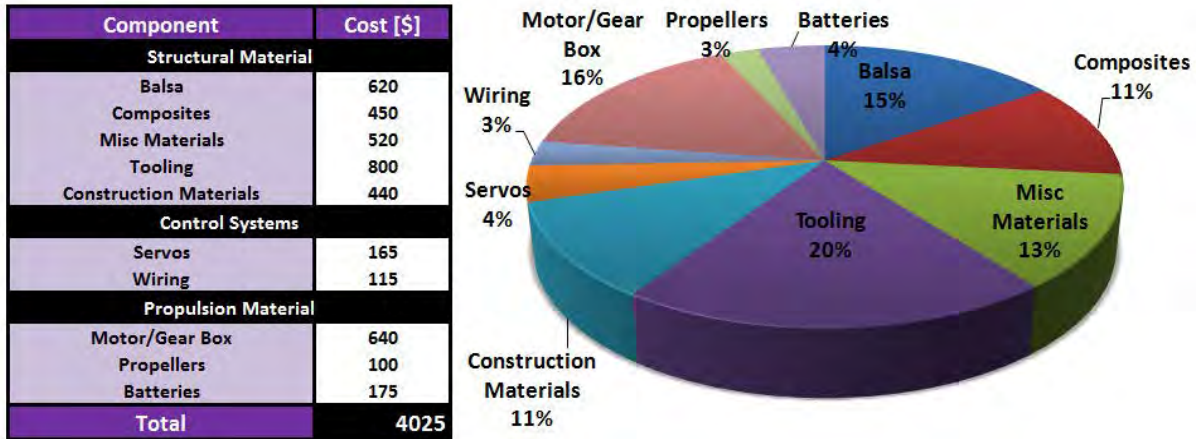


Figure 44: Costs for Two Prototype Aircraft and One Competition Aircraft

7.0 Testing Plan

A thorough testing plan was followed during the course of the project to ensure each designed sub-system operated at an optimal level. The results of the Preliminary and Detail Design sections only provide predictions for how the constructed aircraft may perform. Tests performed by the team were designed to challenge the documented results from the Detail Design phase by isolating variables that could be improved based on testing results.

7.1 Testing Objectives

Test objectives were created to help identify goals when testing each sub-system.

Sub-System Performance Test Objectives	
Test	Objective
Wing	Determine the strength needed in the spars for the highest load condition
Landing Gear	Test strength of landing gear to find the lightest landing gear that performs safely
Propeller and Motor	Optimize motor and propeller combination for best mission performance
Batteries	Tabulate the range of capacities for a given battery from a manufacturer
Airframe	Find how much structure may safely be removed from the outside hull
Hatches	Design the lightest weight hatch that still supports the payload
Airfoil	Experimentally find the C _{lmax} of the chosen airfoil
Payload	Test batteries to determine their efficiency and capacities

Figure 45: Testing Objectives for each Sub-system

Objectives were also identified to aid in the performance evaluation of the entire aircraft once all the sub-systems are integrated into a flight-ready prototype. Structural tests included a wing tip test and loading time trials were used to determine the best loading methods. The propulsion system tests determined the efficiency and power of the aircraft. Flight tests were used to evaluate the aircraft's stability and control characteristics, flight performance, mission performance, and RAC.



Table 11: Objectives Identified for Mission Performance

Aircraft Performance Test Objectives	
Test	Objective
Check-in Test	Ensure the aircraft is eligible for the competition by successfully completing all of the required check-in tests (spot size, payload accomodation, wing tip loading)
Taxi	Demonstrate the aircraft's ground handling stability under all conditions
Stability and Control	Watch aircraft during flight and speak with pilot to determine if it handles according to the pilots preference and determine if its stability and control is consistent
Propulsion	Determine whether the propulsion system utilizes power as designed
Mission Simulation	Determine how the aircraft scores in each mission compared to the prediction in Detail Design, score includes loading time, system weight, and flight performance

7.2 Testing Schedule

After the team isolated all important objectives for testing, test dates were planned and documented in a Gantt chart. By scheduling dates for testing, the team had deadlines to follow, such that and all sub-systems could be tested with enough time to use results to improve performance. All tests were placed in one of three categories so that each technical team could easily recognize their assigned test dates.

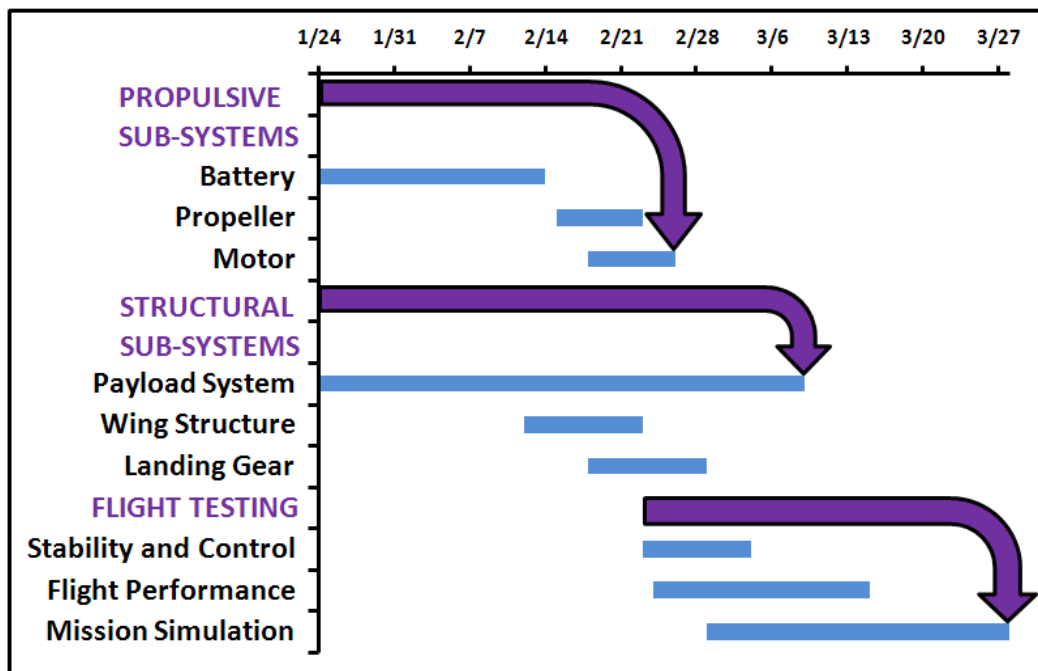


Figure 46: Testing Schedule

7.3 Flight Check Lists

The pre-flight checklist on the following page outlines procedures that remind the team which components of the aircraft to physically inspect before flight. The checklist also lists all electronics components and those team members who should be ready and attentive during flight tests.

Table 12: Pre-Flight Checklist

Pre-Flight Checklist		
Structural Integrity		
Visually and physically inspect each component for damage		
<input type="checkbox"/> Fuselage	<input type="checkbox"/> Horizontal Stabilizer	<input type="checkbox"/> Restraining Hatch
<input type="checkbox"/> Wing	<input type="checkbox"/> Vertical Stabilizer	<input type="checkbox"/> Loading Hatch
<input type="checkbox"/> Gear Wings	<input type="checkbox"/> Control Surfaces	<input type="checkbox"/> Spine Structure
<input type="checkbox"/> Landing Gear	<input type="checkbox"/> Internal Bulkheads	<input type="checkbox"/>
Attachment Points		
Ensure all connection points and internal components are secured		
<input type="checkbox"/> Motor	<input type="checkbox"/> Wires	<input type="checkbox"/> Control Surface Hinges
<input type="checkbox"/> Propellor	<input type="checkbox"/> Servos	<input type="checkbox"/> Landing Gear
<input type="checkbox"/> Batteries	<input type="checkbox"/> Payload	<input type="checkbox"/> Loading Hatch
Propulsion and Controls		
Make certain all electronics are operating safely		
<input type="checkbox"/> Batteries Charged	<input type="checkbox"/> Radio Fail safe	<input type="checkbox"/> 5 Second Throttle Run Up
<input type="checkbox"/> Servos Active (5)	<input type="checkbox"/> Unpowered Control Play	<input type="checkbox"/>
<input type="checkbox"/> Fail Safe Activated	<input type="checkbox"/> Powered Control Play	<input type="checkbox"/>
Final Pre-Flight Checks		
Check to make sure all persons present are attentive and aircraft is ready to fly		
<input type="checkbox"/> Fuse Properly Inserted	<input type="checkbox"/> Spotter Ready	<input type="checkbox"/> Final Visual Inspection
<input type="checkbox"/> Ground Crew Ready	<input type="checkbox"/> Pilot Ready	<input type="checkbox"/>

An additional checklist was created to help record data during each flight test. This list ensures that all important flight characteristics for each stage of flight are properly documented. The rightmost column on the checklist is to be filled out by each observer with their comments/data about each flight stage.

Table 13: Checklist for documenting important flight characteristics

Flight Test Data Recording CheckList		
Flight Stage	Parameters to Observe	Comments/Data
Taxi	Ground Control Tracks Straight Stability with Crosswind	
Take-Off	Take-off Speed Angle of Attack Ground Roll Acceleration Take-off Distance	
Climb	Climb Angle Power Used Altitude at First Pylon	
Cruise	Stability and Control Verify Cruise Speed Turning Rates Power Used Stall Speed Elevator Deflection	
Landing	Sink Rate Time to Stop Landing Impact	
Post-Flight	Battery Energy Used Check for Damages Retrieve Electronic Flight data	



8.0 Performance Results

Performance Testing was divided into two phases: 1) Sub system performance tested all structural and propulsive components and 2) Aircraft performance which was conducted with a complete prototype and determined how well the aircraft performed after all sub-systems were integrated. The Aircraft performance focused primarily on improving RAC, loading time, and mission scores.

8.1 Key Subsystem Performance

The testing procedures of four key-subsystems are presented in the following section. All other subsystems tested and how they improved is summarized in a table at the end of the section.

8.1.1 Wing

The wing was designed to sustain a 2.5g turn in flight which is simulated by placing 7.5 lbs of force on one wing tip. In the Preliminary Design Phase, the wing was rated to fail where it meets the fuselage. The failure was simulated using a test where weights were incrementally loaded onto one half of the entire wing span until it broke. This test provides an accurate representation of bending and shear forces experienced during a 2.5g turn near the root of the wing. Below are photos of the test set up and the wing after failure.



Figure 47: Wing Loading Test

The wing failed once a 17lb load was placed on the wing tip. Failure occurred in the forward shear web where the wing mates with the fuselage and confirmed the failure point predicted in Section 5. It propagated through the rest of the root spars due to the crushing force present. Results rate the wing to be 19% stronger than the predicted 13 lbs. As a result of the wing's superior performance, unnecessary structural weight will be removed in future designs by removing parts of ribs and tapering the spar caps.



8.1.2 Landing Gear

Five different configurations of the main landing gear were constructed, with the structural weight varied between each design. This was accomplished by constructing the landing gear with differing proportions of carbon fiber, carbon tow, and Kevlar. In Section 5 of the report, the ten ply landing gear documented for the aircraft was designed to resist all forces associated with a hard landing. The goal of landing gear testing was to see if the weight of this design could be reduced while still ensuring the plane consistently lands safely. This test consisted of dropping a ten lb weight on the gear from various heights and observing the results. The figure below shows the setup of the test to the left, and the results of the six ply test to the right.



Figure 48: Landing Gear Testing Pictures

The landing gear should survive a force equivalent to the plane dropping from two feet in the air. For a twelve pound aircraft (full payload), the landing gear must withstand a 10lb weight dropped from two feet. Figure 48 below summarizes the testing results.

Test	Weight	Number of Plies	Observations
1	0.10	2	Broke after a 10-lb drop from 6 inches
2	0.24	4	Broke after a 10-lb drop from 24 inches
3	0.32	6	Bent but did not break after 10-lb at 24 inches
4	0.36	8	Did not bend after 10-lb drop from 24 inches
5	0.40	10	Did not bend after 10-lb drop from 24 inches

Figure 49: Landing Gear Test Results

As a result of testing, the ten ply landing gear was replaced with a six ply landing gear that is 0.08lb lighter and reduced the overall system weight of the aircraft.

8.1.3 Propeller and Motor

After determining the optimal propeller diameter for each mission possibility in Preliminary Design and documenting its performance using the mission plots of Section 5, tests were conducted to find the optimal pitch to diameter for each propeller. Tests were conducted in the wind tunnel as the pitch over



diameter (P/D) for different propellers was varied. The efficiency, thrust coefficient, and power coefficient were recorded as a function of advance ratio. Results are shown in the image below.

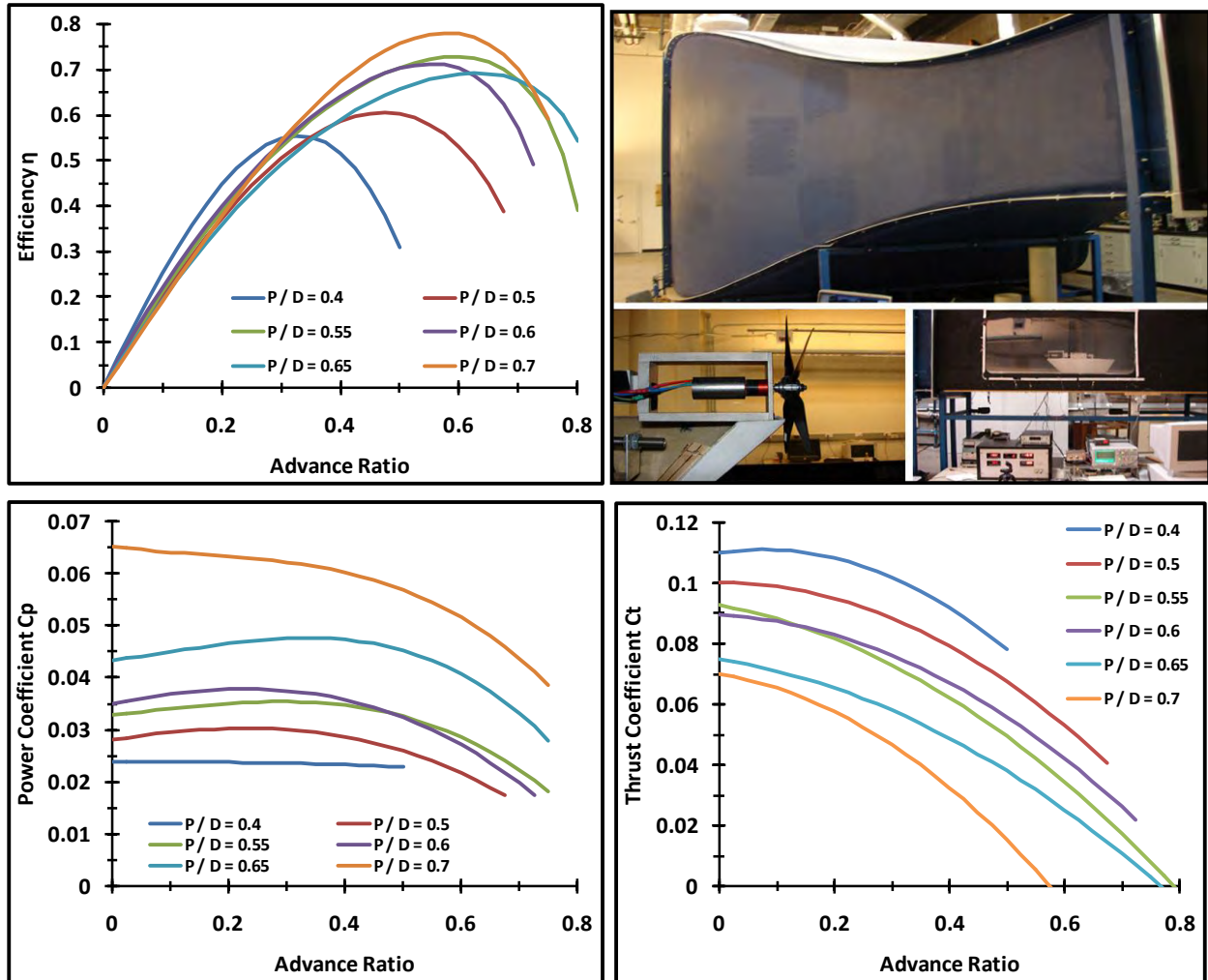


Figure 50: Prop with Motor Test Curves

The results allow the team to determine what power, thrust, and efficiency is associated with different pitches. A propeller with high thrust can be sized for the Payload Mission (rate of climb and take-off limited) while the propeller for the Delivery Mission may be sized for efficiency by choosing the proper pitch. The motor was tested with the propeller and performed within 5% of the manufacturer's listed parameters. The results of the propeller and motor tests improved the aircraft's performance because the propeller pitch was adjusted to 12 degrees for the Delivery Mission and 8 degrees for the Payload Mission.

8.1.4 Battery

During the preliminary design phase, two Elite 1500 batteries were tested. Their capacities were roughly 1000mAh, but a slight discrepancy between the two existed. In order to determine how one Elite 1500 cell's performance varies from another, Fifty Elite 1500 batteries were purchased and their



capacities were measured and recorded. Figure 50 shows the benchmarked predicted value and the capacity demonstrated. The pie chart shows the expected distribution of capacities by percentage.

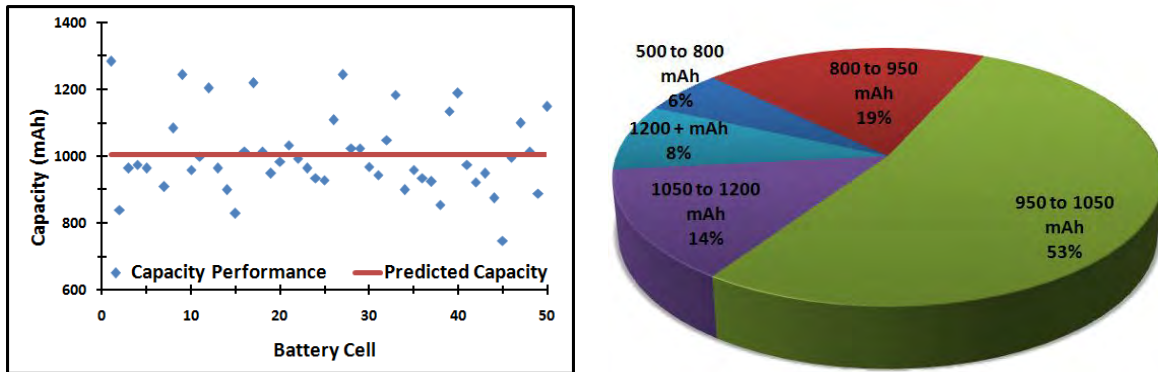


Figure 51: Distribution of Batteries

The demonstrated capacities of the batteries improved aircraft performance by allowing the team to use only the highest capacity batteries available. Batteries with higher capacities are able to provide a given current to the propulsion system for a longer period of time.

8.1.5 Results for other Key Subsystems

The results of testing all other sub-systems are displayed in the table below. The chart briefly summarizes the demonstrated performance of a sub-system during testing and how it compares to the predicted performance in Section 5. The table also describes how the team used the testing results to improve the final design of each key sub-system.

Table 14: Other Key-subsystem Tests and their Effects on the Final Aircraft Solution

Sub-System	Predicted Performance	Demonstrated Performance	Improvement for Final Design
Front Gear	A carbon tow front gear has enough strength	A front gear made from only carbon tow twisted easily	The front gear was reinforced with a carbon fiber weave
Airframe	The internal restraints would carry most loads	The hull of the aircraft carried almost no loads	Twenty two small "windows" were cut out of the fuselage
Hatches	An hatch made of balsa can support payload	The hatch easily supported the payload after plane was tipped	The hatch weight was reduced and still held the payload
Airfoil	Theoretical C_{lmax} of airfoil is 2.00	The airfoil actually achieved a C_{lmax} closer to 1.75	Optimization programs were updated to give more accurate predictions
Payload	Optimum payload is tolerance 4.5inches	Optimum spatial tolerance was 4.3inches	Smaller grid compartments were made to reduce aircraft size and weight



8.2 Aircraft Performance

The primary goal of the aircraft performance testing was to emulate contest conditions and compare demonstrated performance with the predictions documented in Section 5. Testing results are used to improve the complete aircraft solution. To ensure the aircraft was eligible for the competition, check-in tests were simulated and then the aircraft was tested for general flight characteristics. Its overall mission performance was rated by simulating the ground crew loading time, documenting system weight reduction (RAC), and analyzing flight performance data.

8.2.1 Aircraft Check-in Testing

Four key tests are performed during check-in as shown below in the series of four images. The images (starting at the top left and continuing in a clockwise direction) depict the aircraft fitting in a 4' by 5' box, accommodating a combination of fourteen payload elements, passing the 2.5g wing loading test and using the restraining hatch to hold the payload.

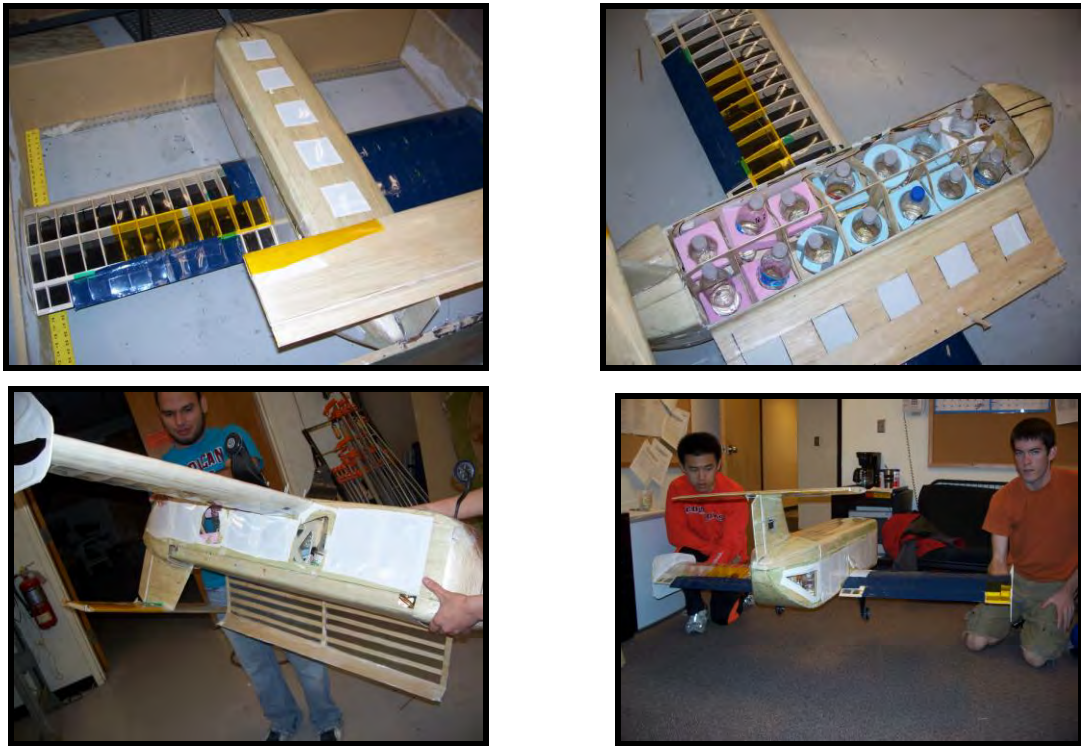


Figure 52: Aircraft Performing Check-in Tests

8.2.2 Taxi and Stability and Control Performance

Before attempting any flights, the aircraft had to pass a taxi test. The nose gear servo was found to give adequate control, and the main gear was properly attached to the aircraft in relation to the CG. An excess battery power was loaded into the plane to provide a safety cushion during its first flight when general stability and control performance were rated. The rudders exhibited low effectiveness because the vertical tail was attached at a slight angle and flutter in the endplates damped yawing motion. The first issue was a construction problem and the tail was fixed by removing the tail and correctly reattaching



it. After the vertical tail was placed correctly on the aircraft, the endplates were still damping the rudder's effectiveness, so the rudder was sized larger to improve its effectiveness.



Figure 53: Aircraft Before, During, and After Take-off

8.2.3 Propulsion Performance

After flight testing, propulsion data was obtained to allow for a comparison between the demonstrated performance of the complete aircraft propulsion system and the documented predictions in Section 5.3. Demonstrated performance for the Delivery Mission in terms of thrust and current is plotted against the predicted results in the figure below.

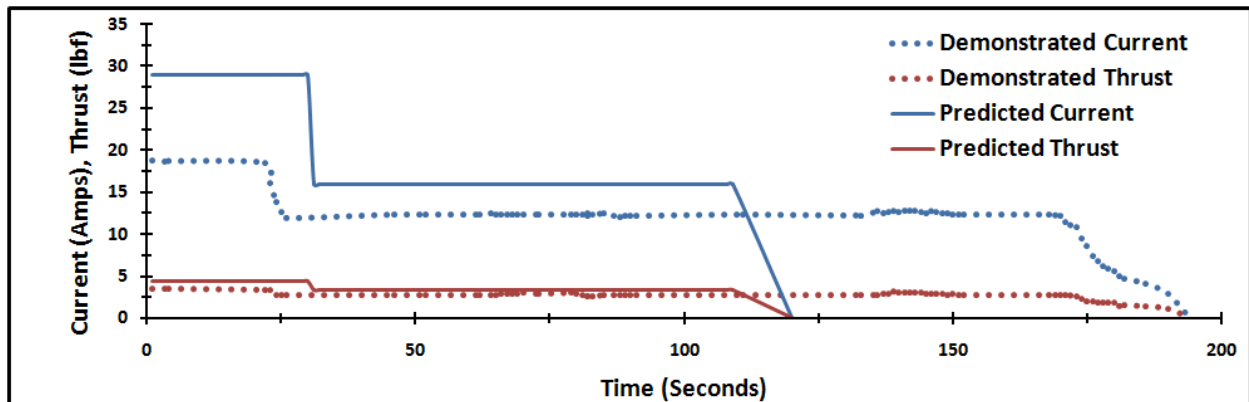


Figure 54: Propulsion Performance

The demonstrated current and thrust in the system was lower than the predicted values. To improve performance, the propulsion system was reconfigured to pull more current from the same number of batteries. An increased current drawn from the batteries resulted in a drop in voltage and overall power from the system, but the trade-off allowed for the aircraft to utilize a larger propeller. After the propeller diameter of the system was increased from 17" to 19" the aircraft achieved a higher thrust. This improvement in the propulsion system allowed the aircraft to match the performance capabilities predicted in section 5.

8.2.4 Ground Crew Performance

The first step in mission simulation compares predicted performance and demonstrated performance during the ground portions of the Payload mission, using the completed aircraft prototype. A ground crew was assembled and timed for how quickly they could load each of the payload configurations. Just as determined in the Preliminary Design investigation, the fourteen bottle configuration took the longest to



load. Practice runs performed by the ground crew assumed the same distances between the aircraft and payload elements as in the Preliminary Design phase to ensure an accurate performance comparison. The initial loading time was about sixteen seconds. According to the documented performance in Section 5 and Preliminary Design, the predicted loading performance was seventeen seconds. Performance improved once the complete aircraft was assembled because the bulkhead restraint system was stiffer than the prototype used for preliminary analysis. More practice resulted in a higher score and performance improved to about fourteen seconds as shown in the graph below.

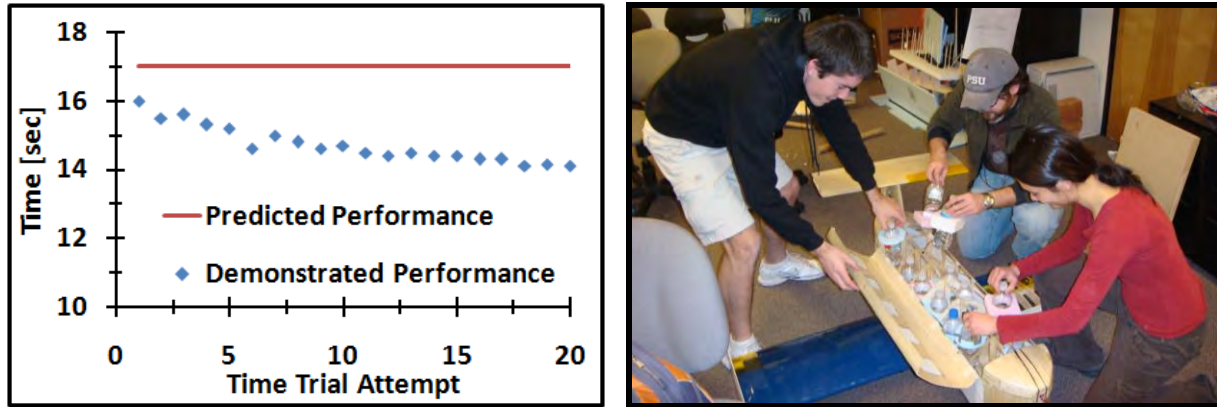


Figure 55: Ground Crew Performance

8.2.5 RAC Performance

Each aircraft component weight is shown below and compared to the Section 5.4 documented weight. Total system weight decreased by about 12% and reflects improvements made after testing.



Figure 56: Difference between System Weight before and after the Testing phase

8.2.6 Overall Mission Performance

The Delivery and Payload Missions were both attempted and after recording data from in-flight performance was recorded. Mission scores were calculated and compared to the documented performance in Section 5. All the following tables assume a 5 mph wind speed. An RAC comparison is shown in Table 15 on the following page.



Table 15: RAC Performance

	SYSTEM WEIGHT X	BATTERY WEIGHT	= RAC
Predicted	4.26 lb	0.6 lb	2.39
After Improvements	3.80 lb	0.6 lb	2.31

The battery weight installed is the same as the 0.6lb predicted from Section 5.6, but because the system weight of the aircraft was reduced by 12%, the overall RAC improved by 3.5%. Table 16 shows a calculation for the Delivery Mission Score and its comparison to the Section 5 prediction:

Table 16: Delivery Mission Performance

	Nlaps	÷	Wbatt	= Score
Predicted	3		0.3lb	10.0
After Improvements	3		0.3lb	10.0

Although the aircraft completes the three laps more easily than the predictions in Section 5.7, the score is identical because 0.3lb of batteries are required to meet voltage requirements in the propulsion system and only complete laps are counted. Switching to smaller batteries does not improve score.

Table 17: Payload Mission Performance

	1 ÷ (Loading Time * RAC) = Score		
Predicted	17 seconds	2.39	0.025
After Improvements	15 seconds	2.31	0.029

The aircraft's Payload mission score increased by 16% compared to Section 5.7's prediction. Score increase is a result of system weight reduction and loading time improvement. After testing and evaluating all key sub-systems and the complete aircraft solution, improvements were made to the performance of each sub-system and the aircraft's performance as a whole. Improvements helped the aircraft's stability and control characteristics, increased propulsion system thrust, decreased loading difficulty, and reduced system weight. The RAC and Payload Mission score increased significantly as a result of these improvements.

References

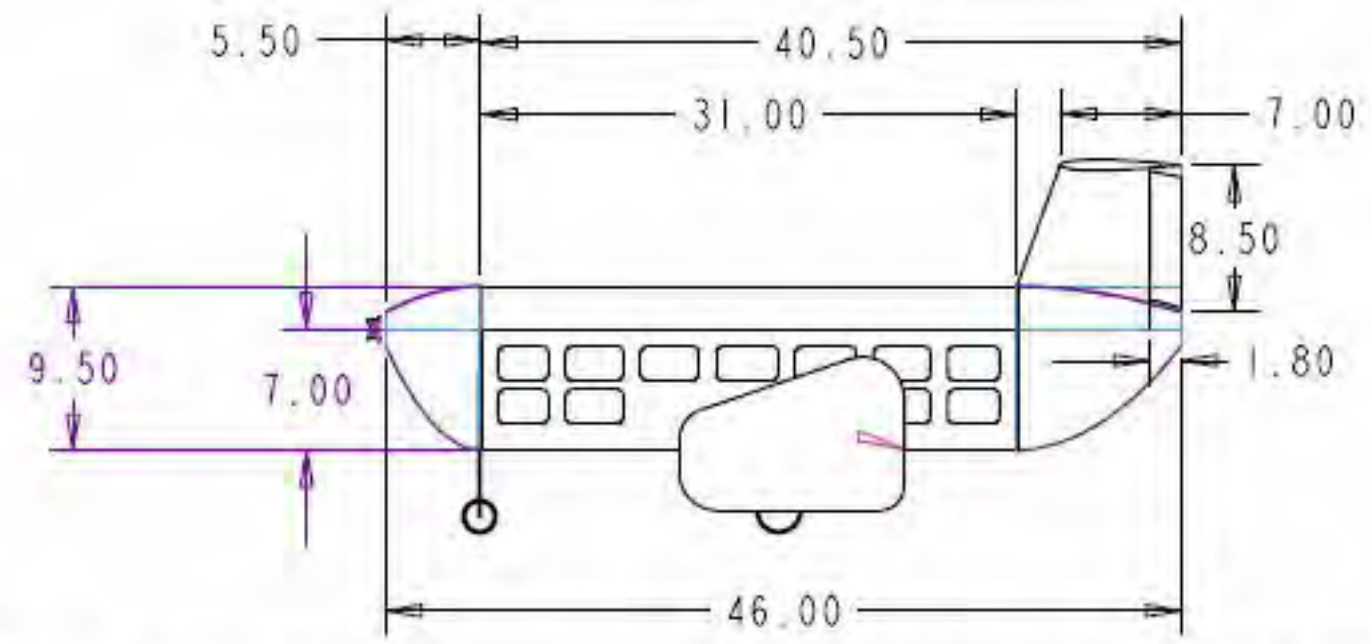
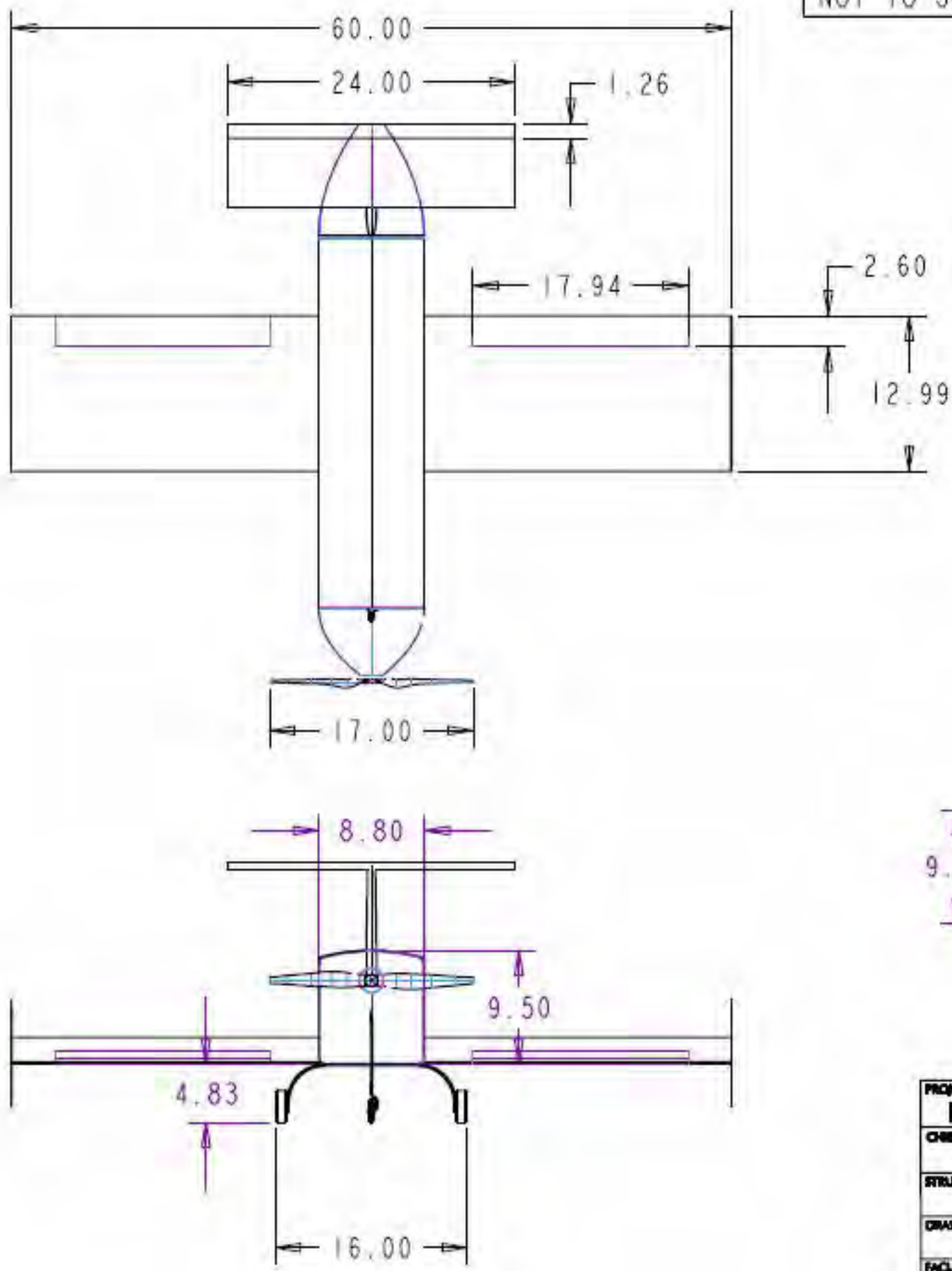
Budynas, Richard G. and Warren C. Young. *Roark's Formulas For Stress And Strain*. 7th Edition. New York: McGraw Hill, 2002.

Nelson, R. C., *Flight Stability and Automatic Control*, 2nd Edition, McGraw-Hill, Boston, 1998.

Raymer, D.P., *Aircraft Design: A conceptual Approach*, 3rd Edition, AIAA, Reston, VA, 1999.

NOT TO SCALE

OKLAHOMA STATE UNIVERSITY BLACK TEAM



PROJECT TITLE
BLACK TEAM
 CHIEF ENGINEER
P. EGAN
 STRUCTURE LEAD
H. BEEM
 DRAWN BY
C. SLATER
 FACULTY ADVISOR
DR. A. ARENA

NOTE: ALL DIMENSIONS
ARE GIVEN IN INCHES

OKLAHOMA STATE UNIVERSITY BLACK TEAM
AIAA DESIGN/BUILD/FLY 2008

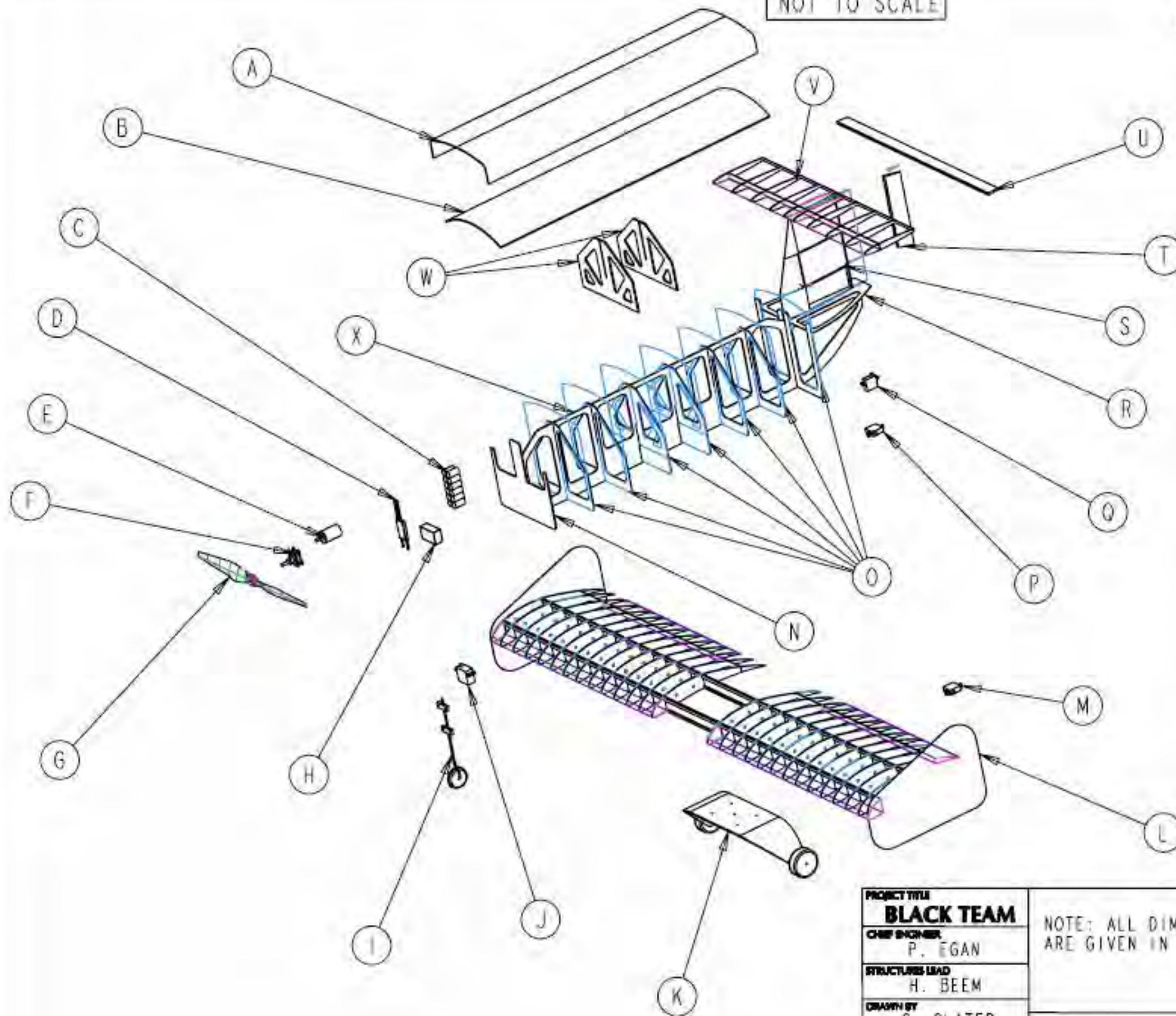
3-VIEW DRAWING

SHEET A-1 DATE OF APPROVAL 2-20-08

DRAWING PACKAGE PAGE 1 OF 5

NOT TO SCALE

OKLAHOMA STATE UNIVERSITY BLACK TEAM



	COMPONENT	MATERIAL
A	HATCH	FIBERGLASS/BALSA
B	PAYLOAD RESTRAINT	FIBERGLASS/BALSA
C	BATTERY	ELITE 1500 12 CELL
D	SPEED CONTROLLER	KONTRONIK JAZZ 40
E	MOTOR	NUE 1107 2.5Y
F	GEAR BOX	MEC 6:1
G	PROPELLER	APC 17 INCH
H	RECEIVER	SPEKTRUM AR9000
I	NOSE GEAR ASM	CARBON
J	NOSE SERVO	HI-TEC HS-475
K	MAIN GEAR ASM	CARBON/BALSA
L	WING ASM	BALSA/CARBON
M	AILERON SERVO	HI-TEC HS-81
N	FOWARD BULKHEAD	LIGHT PLYWOOD
O	PAYLOAD BULKHEADS	FIBERGLASS/BALSA
P	RUDDER SERVO	HI-TEC HS-81
Q	ELEVATOR SERVO	HI-TEC HS-81
R	TAIL BULKHEAD	LIGHT PLYWOOD
S	VERTICAL TAIL ASM	FIBERGLASS/BALSA
T	RUDDER	FIBERGLASS/BALSA
U	ELEVATOR	FIBERGLASS/BALSA
V	HORIZONTAL TAIL ASM	BALSA
W	WING SPAR BULKHEADS	LIGHT PLYWOOD
X	BACKBONE	LIGHT PLYWOOD

PROJECT TITLE
BLACK TEAM
 CHIEF ENGINEER
P. EGAN
 STRUCTURE LEAD
H. BEEM
 DRAWN BY
C. SLATER
 FACULTY ADVISOR
DR. A. ARENA

NOTE: ALL DIMENSIONS
ARE GIVEN IN INCHES

OKLAHOMA STATE UNIVERSITY BLACK TEAM
AIAA DESIGN/BUILD/FLY 2008

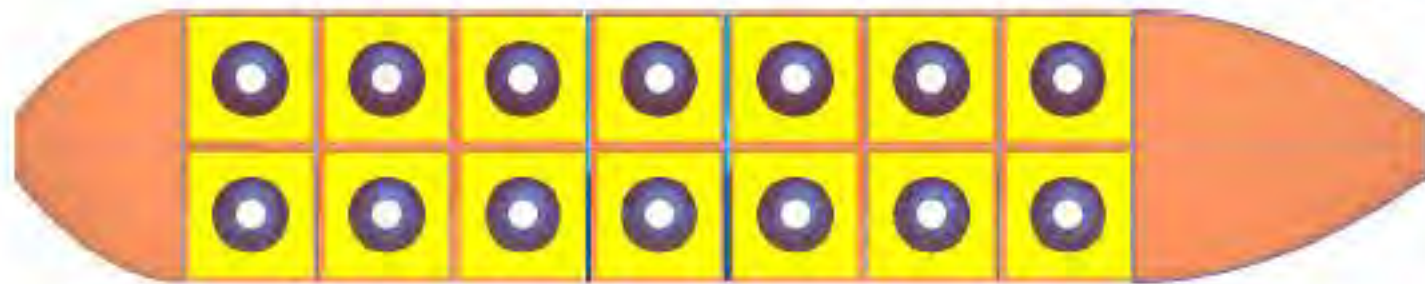
STRUCTURAL ARRANGEMENT

REVISION A-1 DATE OF APPROVAL 2-20-08

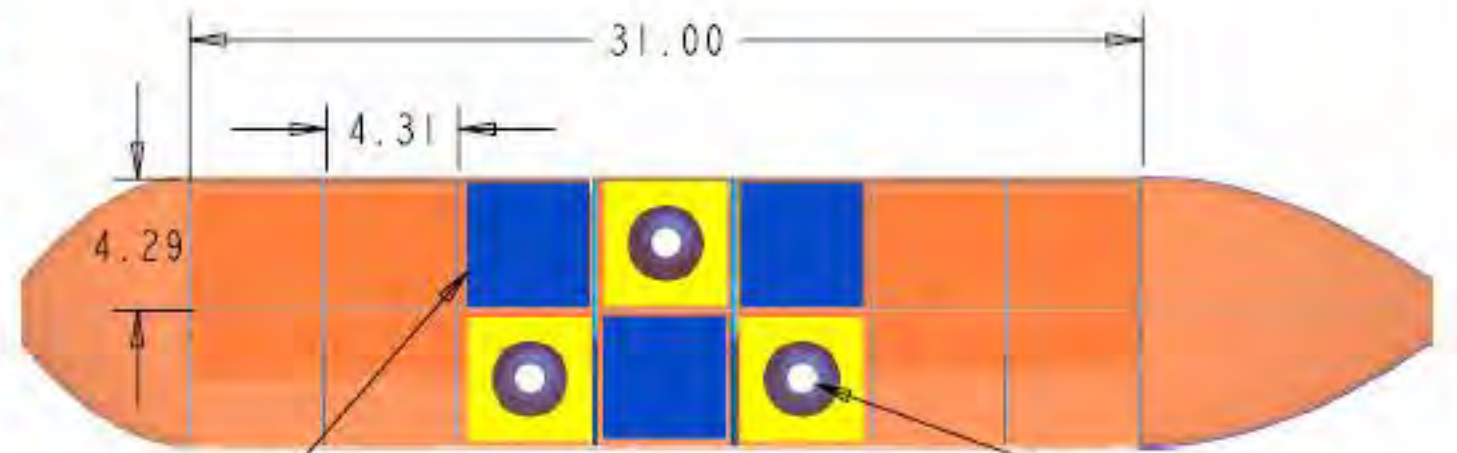
DRAWING PACKAGE PAGE 2 OF 5

NOT TO SCALE

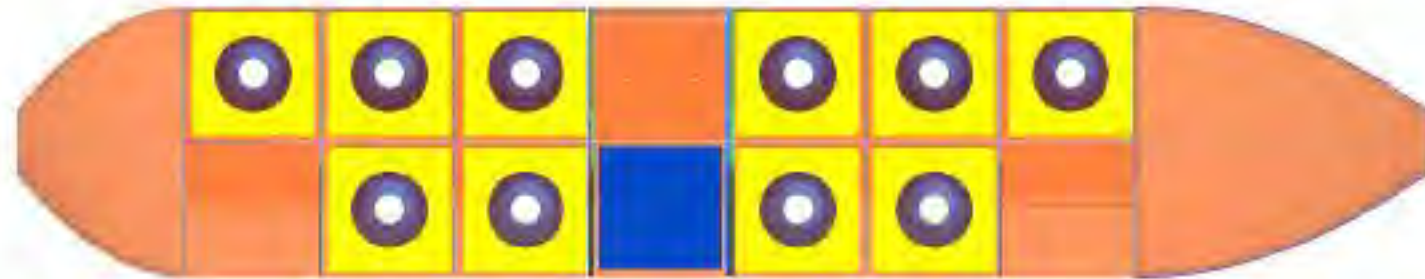
OKLAHOMA STATE UNIVERSITY BLACK TEAM



PAYLOAD CONFIGURATION 1
14 PASSENGERS x 0 CARGO



PAYLOAD CONFIGURATION 4
3 PASSENGERS x 3 CARGO



PAYLOAD CONFIGURATION 2
10 PASSENGERS x 1 CARGO



PAYLOAD CONFIGURATION 5
0 PASSENGERS x 4 CARGO



PAYLOAD CONFIGURATION 3
7 PASSENGERS x 2 CARGO

PROJECT TITLE
BLACK TEAM

CHIEF ENGINEER
P. EGAN

STRUCTURES LEAD
H. BEEM

DRAWN BY
C. SLATER

FACULTY ADVISOR
DR. A. ARENA

NOTE: ALL DIMENSIONS ARE GIVEN IN INCHES

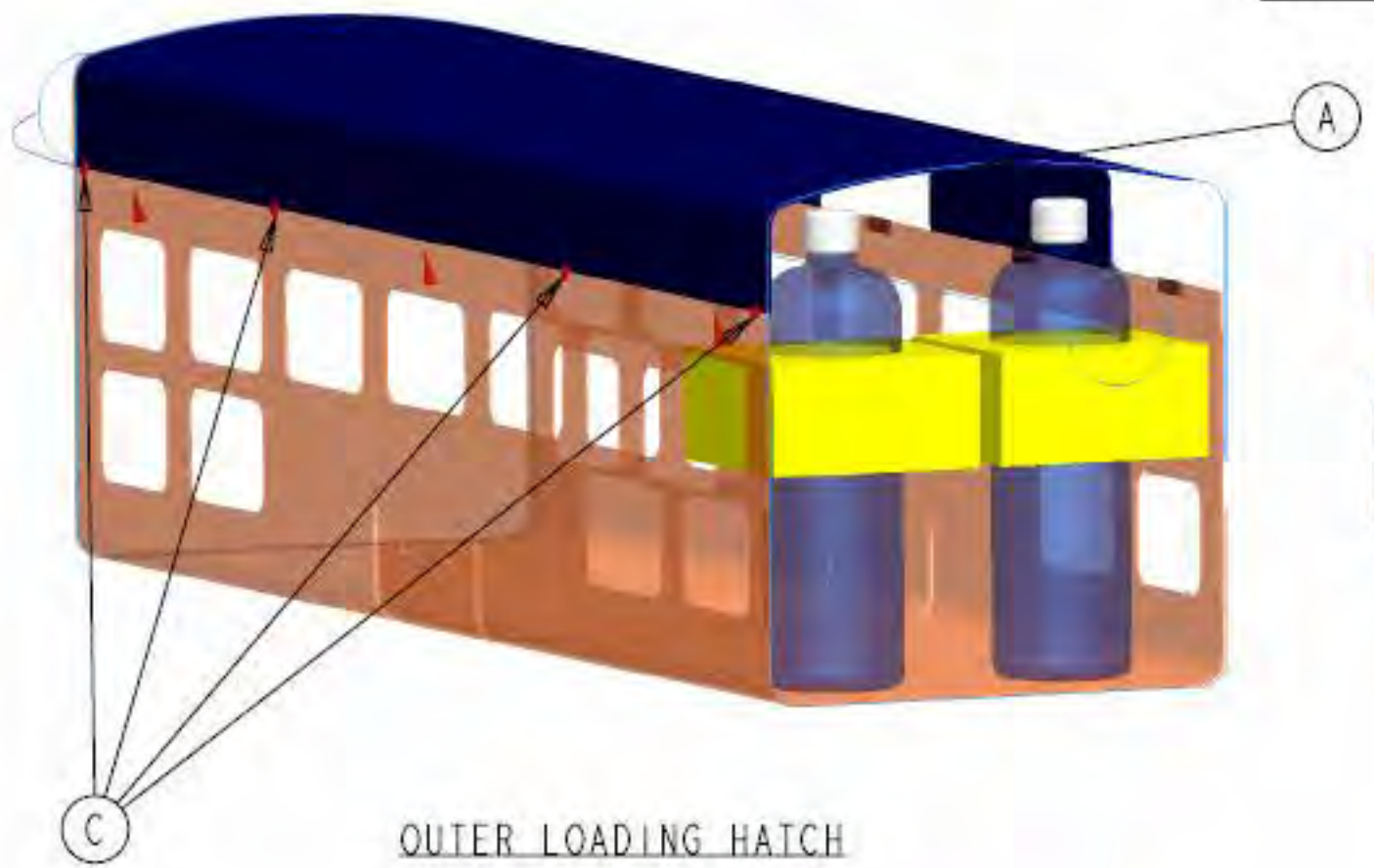
OKLAHOMA STATE UNIVERSITY BLACK TEAM
AIAA DESIGN/BUILD/FLY 2008

PAYLOAD ACCOMMODATION I

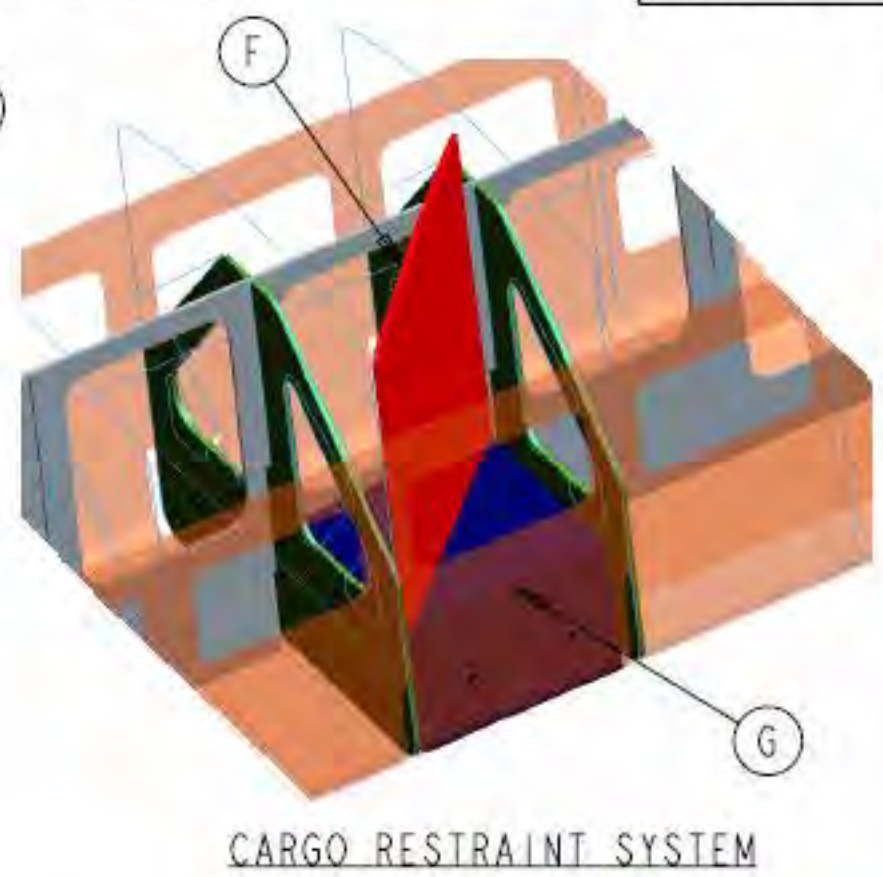
SERIES A-1 DATE OF APPROVAL 2-20-08

NOT TO SCALE

OKLAHOMA STATE UNIVERSITY BLACK TEAM

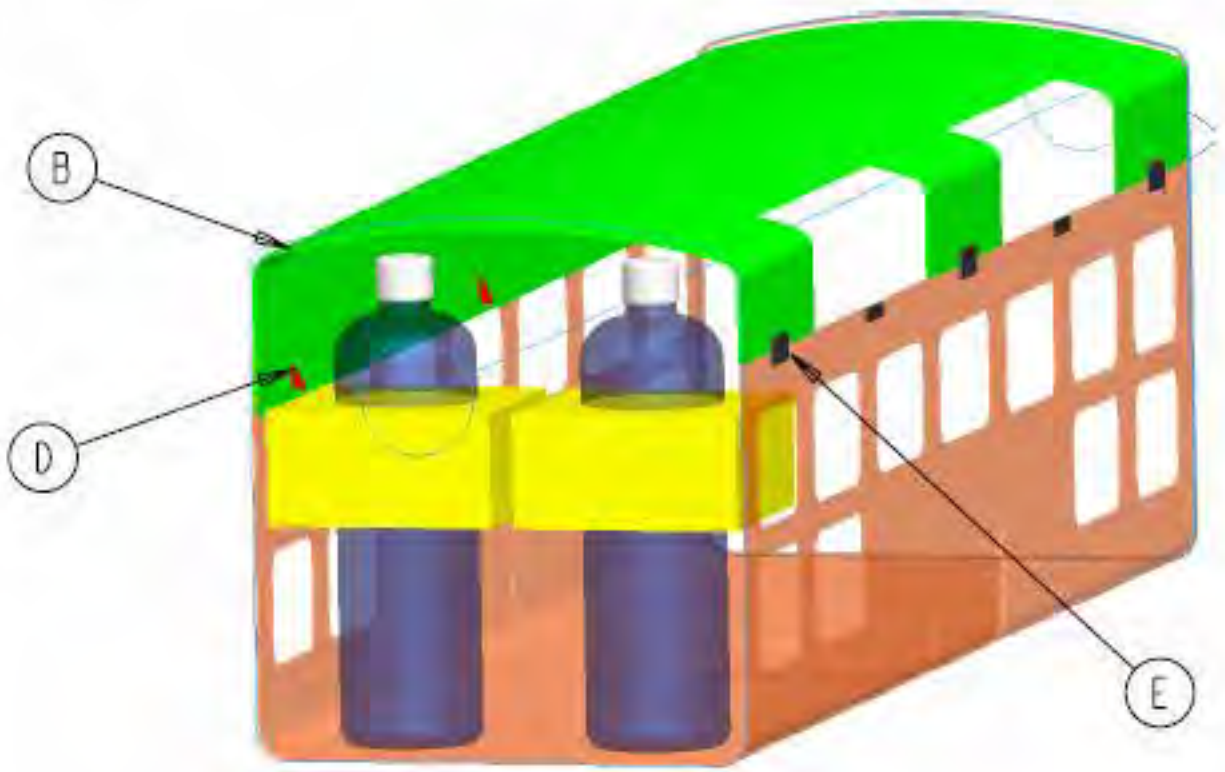


OUTER LOADING HATCH

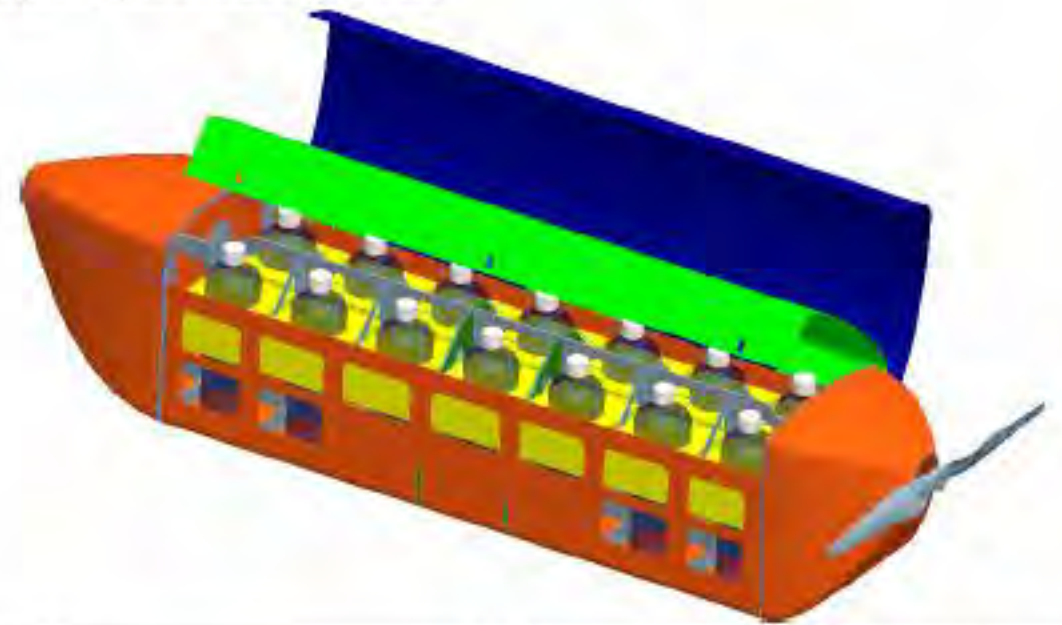


CARGO RESTRAINT SYSTEM

COMPONENT	MATERIAL	
A	LOADING HATCH	FIBERGLASS/BALSA
B	RESTRAINT HATCH	FIBERGLASS/BALSA
C	OUTER LATCHES	MAGNETS
D	INNER LATCH	FIBERGLASS/BALSA
E	HATCH HINGES	PLASTIC
F	CARGO RESTRAINT	FIBERGLASS/BALSA
G	CARGO	BRICK



INNER RESTRAINT HATCH



PROJECT TITLE
BLACK TEAM
 CHIEF ENGINEER
P. EGAN
 STRUCTURE LEAD
H. BEEM
 DRAWN BY
C. SLATER
 FACULTY ADVISOR
DR. A. ARENA

NOTE: ALL DIMENSIONS ARE GIVEN IN INCHES

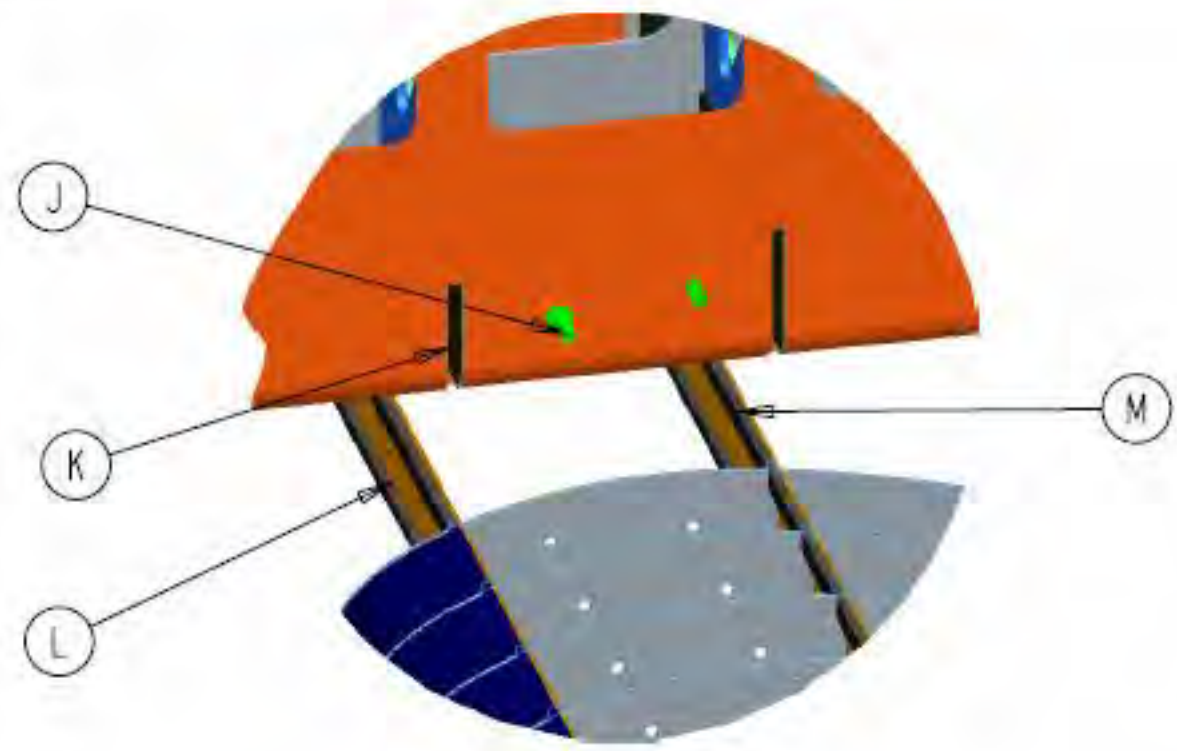
OKLAHOMA STATE UNIVERSITY BLACK TEAM
AIAA DESIGN/BUILD/FLY 2008

PAYLOAD ACCOMMODATION II

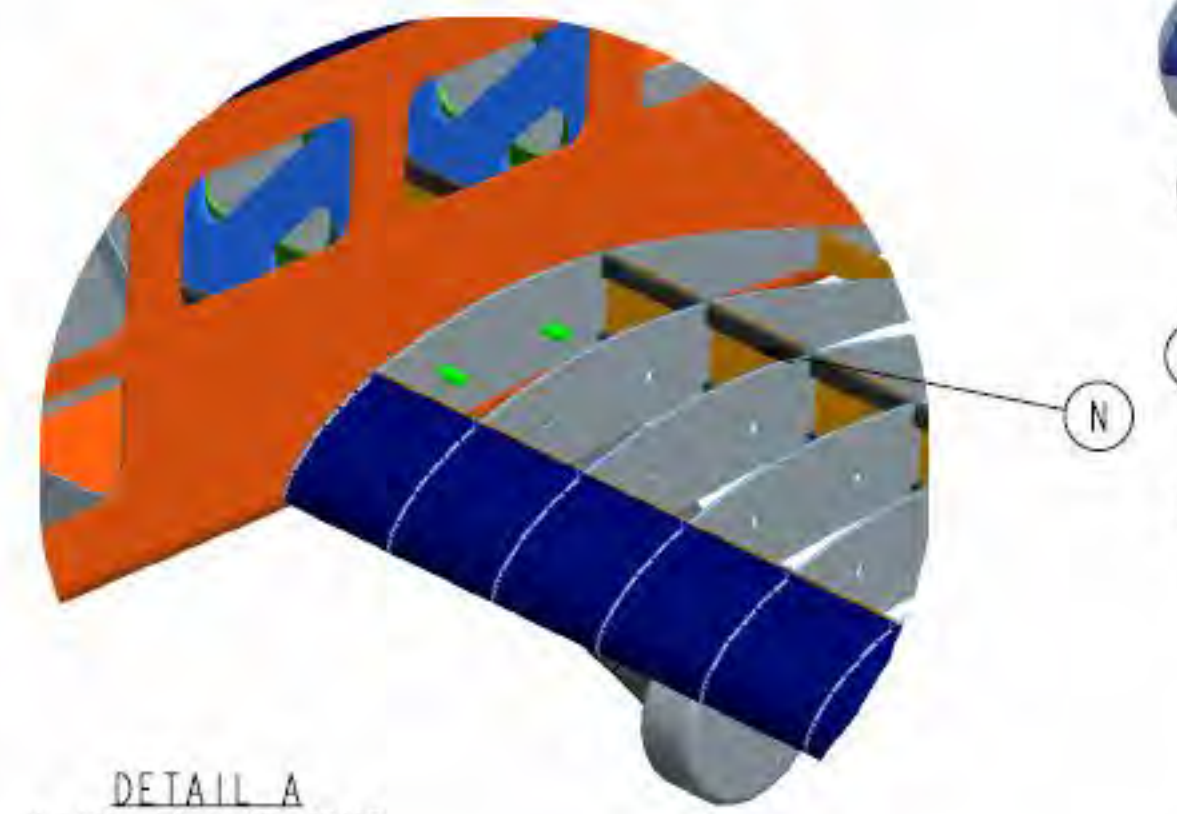
SERIES A-1 DATE OF APPROVAL 2-20-2008

NOT TO SCALE

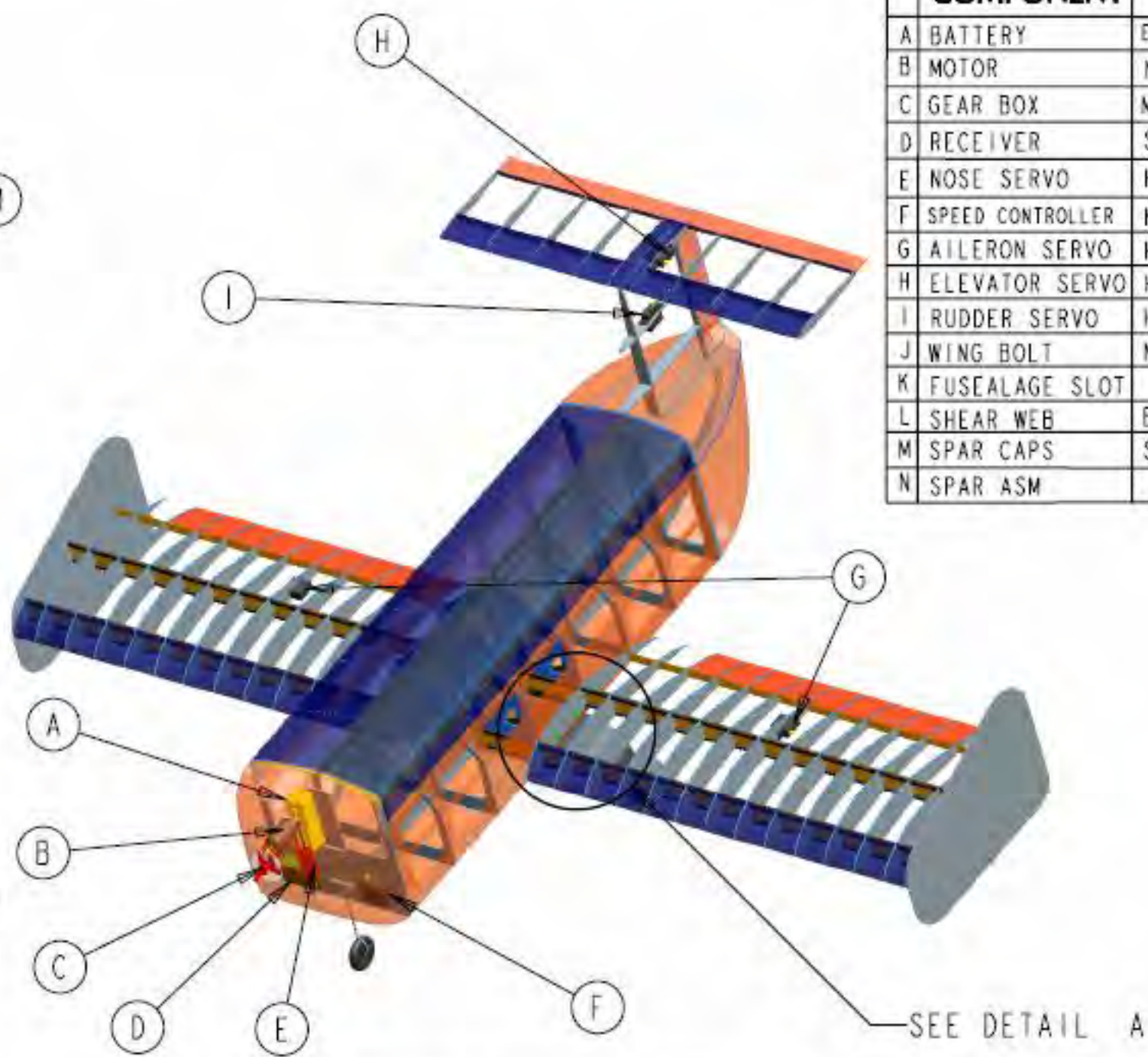
OKLAHOMA STATE UNIVERSITY BLACK TEAM



DETAIL A
WING ATTACHMENT



DETAIL A
WING ATTACHMENT



COMPONENT	MATERIAL
A BATTERY	ELITE 1500 12 CELL
B MOTOR	NUE 1107 2.5Y
C GEAR BOX	MEC 6:1
D RECEIVER	SPEKTRUM AR9000
E NOSE SERVO	HI-TEC HS-475
F SPEED CONTROLLER	KONTRONIK JAZZ 40
G AILERON SERVO	HI-TEC HS-81
H ELEVATOR SERVO	HI-TEC HS-81
I RUDDER SERVO	HI-TEC HS-81
J WING BOLT	NYLON BOLT
K FUSEALAGE SLOT	
L SHEAR WEB	BALSA
M SPAR CAPS	SPRUCE/CARBON
N SPAR ASM	

SEE DETAIL A

PROJECT TITLE
BLACK TEAM
CHIEF ENGINEER
P. EGAN
STRUCTURE LEAD
H. BEEM
DRAWN BY
C. SLATER
FACULTY ADVISOR
DR. A. ARENA

NOTE: ALL DIMENSIONS ARE GIVEN IN INCHES

OKLAHOMA STATE UNIVERSITY BLACK TEAM
AIAA DESIGN/BUILD/FLY 2008

SYSTEMS LAYOUT/LOCATION

SHEET A-1	DATE OF APPROVAL 2-20-08
DRAWING PACKAGE	PAGE 3 OF 5



2007/2008 Design/Build/Fly Competition



HORNWORKS
THE UNIVERSITY OF TEXAS AT AUSTIN

Design Report



Table of Contents

FIGURES	5
TABLES	6
1 EXECUTIVE SUMMARY	7
2 MANAGEMENT SUMMARY	8
2.1 TEAM DIAGRAM	8
2.2 MILESTONES	9
3 CONCEPTUAL DESIGN	11
3.1 MISSION REQUIREMENTS	11
3.1.1 <i>Delivery Mission</i>	11
3.1.2 <i>Payload Mission</i>	11
3.1.3 <i>Configuration Mission</i>	12
3.2 ANALYZING DESIGN REQUIREMENTS FROM MISSION REQUIREMENTS	12
3.2.1 <i>Design Requirements from Flight Score Analysis</i>	13
3.3 INITIAL DESIGN CONCEPTS	14
3.3.1 <i>Wing Configurations</i>	14
3.3.2 <i>Payloads</i>	16
3.3.3 <i>Propulsion</i>	18
3.3.4 <i>Empennage</i>	19
3.3.5 <i>Wing Structure</i>	20
3.3.6 <i>Fuselage Structure</i>	21
3.3.7 <i>Landing Gear Configuration</i>	22
3.4 CONCLUSION	23
4 PRELIMINARY DESIGN	24
4.1 DESIGN AND SIZING TRADE STUDIES	24
4.1.1 <i>Aerodynamics</i>	24
4.1.2 <i>Propulsion Optimization</i>	29
4.1.3 <i>Payload Configuration</i>	33
4.2 MISSION MODEL CAPABILITY	35
4.3 MISSION MODEL UNCERTAINTIES	36
4.3.1 <i>Site Analysis</i>	36
4.4 ESTIMATE OF LIFT CHARACTERISTICS	37
4.5 ESTIMATE OF DRAG CHARACTERISTICS	38



4.6	ESTIMATE OF AIRCRAFT STABILITY CHARACTERISTICS	39
4.7	ESTIMATE OF MISSION PERFORMANCE	40
5	DETAIL DESIGN	40
5.1	DIMENSIONAL PARAMETERS OF FINAL DESIGN.....	40
5.2	PAYLOAD	41
5.2.1	<i>Methods of Payload Restraint</i>	41
5.2.2	<i>Testing</i>	42
5.2.3	<i>Conclusion</i>	42
5.3	PROPULSION.....	43
5.4	WEIGHT AND BALANCING	44
5.5	FLIGHT PERFORMANCE PARAMETERS FOR FINAL DESIGN	45
5.6	RATED AIRCRAFT COST.....	45
5.7	FINAL DESIGN MISSION PERFORMANCE	45
5.8	DRAWING VIEW	46
5.8.1	<i>Three View</i>	46
5.8.2	<i>Structural Arrangement Drawing</i>	47
5.8.3	<i>System Layout Isometric View</i>	48
5.8.4	<i>Payload Configurations</i>	49
6	MANUFACTURING PLAN AND PROCESSES	50
6.1	MANUFACTURING PROCESSES METHODOLOGY	50
6.2	CUTTING OF RIBS.....	50
6.3	WEIGHT OPTIMIZATION.....	50
6.4	MANUFACTURING MILESTONES	50
7	TESTING PLAN	51
7.1	TEST OBJECTIVES.....	51
7.1.1	<i>Propulsion</i>	51
7.1.2	<i>Structure</i>	51
7.2	AERODYNAMICS TEST PLAN AND DATA.....	52
7.3	PROPULSION TEST PLAN AND DATA	52
7.4	STRUCTURAL TEST PLAN.....	52
7.5	WEIGHT AND BALANCE TEST PLAN.....	53
7.6	MISSION PERFORMANCE TEST PLAN.....	53
7.7	TEST CHECKLIST.....	53
7.8	TESTING SCHEDULE	54



8	PERFORMANCE RESULTS	55
8.1	PROPULSION TESTING.....	55
8.1.1	<i>Propeller Testing</i>	55
8.1.2	<i>Battery Testing</i>	56
8.1.3	<i>Fuse Testing</i>	56
8.2	STRUCTURAL TESTING	56
8.3	AERODYNAMICS TESTING	57
9	REFERENCES.....	58



Figures

Figure 1 - Hornworks Organizational Chart 9

Figure 2 - Gantt chart for Project Planning 10

Figure 3 - C_L vs. C_D 25

Figure 4 - C_L/C_D vs. Angles of Attack..... 25

Figure 5 - Estimated Score 26

Figure 6 - Required Static Thrust..... 27

Figure 7 - Drag Buildup for Delivery Mission 28

Figure 8 - Drag Buildup for Payload Mission 28

Figure 9 - Motor and Wing Weight vs. Wing Area 29

Figure 10 - Energy Density Score Chart..... 31

Figure 11 - Thrust vs. Airspeed of Various Propeller Sizes 33

Figure 12 - Average Wind Speed in Wichita..... 36

Figure 13 - Cumulative Distribution Function for Headwind Velocity..... 37

Figure 14 - Payload Mission Drag Polar 38

Figure 15 - Cruise Drag for Payload Mission..... 39

Figure 16 - Cruise Drag for Delivery Mission..... 39

Figure 18 - Manufacturing Gantt Chart 51

Figure 19 - Static Test Stand 52

Figure 20 - Wing Construction Method Structural Test..... 57



Tables

Table 1 - Morphological Chart.....	14
Table 2 - Wing-Body Decision Matrix.....	15
Table 3 - Loading Scheme Decision Matrix	17
Table 4 - Number of Motors Decision Matrix	19
Table 5 - Empennage Decision Matrix.....	20
Table 6 - Wing Structure Decision Matrix	21
Table 7- Fuselage Structure Selection.....	22
Table 8 - Landing Gear Decision Matrix	23
Table 9 - Battery Comparisons	30
Table 10 - Motors and Gearbox Configurations.....	32
Table 11 - CG Locations for payload configurations.....	34
Table 12 - Payload Configuration Decision Matrix.....	35
Table 13 - Cruise Drag for Payload Mission	39
Table 14 - Cruise Drag for Delivery Mission	39
Table 15 – Mission Performance Prediction	40
Table 16 - Final Design Parameters	41
Table 17 - Foam Grid Testing Results	43
Table 18 - Motor Comparison	43
Table 19 - Final Propulsion Design.....	44
Table 20 - Weight and Balancing.....	44
Table 21 - Final Design Flight Performance	45
Table 22 - Motor Test 1	55
Table 23 - Motor Test 2.....	55
Table 24 - Battery Test with Elite 1500 Cells.....	56



1 **Executive Summary**

Every year, Cessna Aircraft Company, Raytheon Missile Systems, and the AIAA Foundation sponsor the Student Design/Build/Fly Competition. The contest provides a real-world aircraft design experience for engineering students by giving them the opportunity to validate their analytic studies. The design requirements and performance objectives change every year to encourage innovation and to provide a fresh design challenge. The 2007-2008 mission involves “Reconfigurable Short Field Transport”. To meet this year’s challenge, the Hornworks team from The University of Texas at Austin presents an aircraft that is conventional in design, and yet, truly pushes the envelope through careful analysis and meticulous construction.

As stated above, the overall design of the aircraft is fairly traditional. It is a monoplane with a low wing, conventional tail, top hatch, tricycle landing gear, centrally mounted tractor motor, and low drag Selig airfoil. The team considered more complex solutions such as, using multiple motors or designing a bi-plane. However, through careful trade studies, the team determined that a simple, more optimized and conventional design is better. To reach this solution, the team first performed score analysis. The delivery mission score reduces down to $\text{Score}=1/\text{Drag}$. The payload mission score is not easily reduced, but it depends strongly on system weight of the aircraft, battery weight, and the payload loading scheme. Therefore, to maximize the score, the design of the aircraft should be prioritized first based on drag reduction, then battery weight reduction, and lastly, system weight of the aircraft.

The low wing design sacrifices some stability for reduced drag during takeoff due to ground effects. From past experience in DBF, low wing design can be successfully flown. The conventional tail was selected because other tail configurations require additional structure or a complex control system. The top hatch configuration was chosen for faster payload loading. Top hatch configuration has a very successful track record in past DBF competitions and with this year’s complex cargo combination makes having an easily accessible cargo area essential. The tricycle landing gear was picked for its rock solid stability during ground roll. With the short field takeoff requirement, it is necessary for the pilot to put the “pedal to the metal” and accelerate quickly without any ground steering issues. Additionally, for the propulsion system, the team analyzed two motor and three motor configurations, but settled on the conventional one motor system because the amount of battery saved does not justify the added motor weight. The Selig S2091 airfoil was selected from a pool of 34 airfoils because it gave the best score in the simulated mission profile. The aircraft design was also optimized for the competition site. The wind conditions for Wichita, Kansas during competition week for the past five years were tabulated hour by hour. Statistical analyses generated a cumulative distribution function which allowed the team to optimize the aircraft for a headwind knowing the exact amount of risk involved.



The team also pushed the envelope on construction methods. The wing will be constructed using built-up balsa ribs with basswood spars and Mono-cot. Kevlar and carbon sheets will be used to strengthen critical areas. The team decided against Carbon fiber spar due to weight considerations. The fuselage will be completely composite in nature. Composite construction gives better strength to weight ratio, durability, and reduced drag compared to wood built-up, but at the cost of greatly increased construction complexity.

The empty aircraft is predicted to weigh slightly over two pounds. This is an extremely aggressive design with minimal margin for error. For the delivery mission, the aircraft will fly two laps with 6.5 ounces of battery at a cruising velocity of 26 ft/s. During the payload mission, the aircraft will fly two laps with 10.8 ounces of battery at a cruise velocity of 46 ft/s.

2 Management Summary

The Hornworks team consists of current undergraduate aerospace engineering students who attend the University of Texas at Austin. The team was split into several areas of research, including: aerodynamics, propulsion, and payload configuration. These groups were responsible for the analysis, design, and testing of their various areas. Based on research and testing, a prototype aircraft was built on which the final contest aircraft is based.

2.1 Team Diagram

Figure 1 shows the organization of The Hornworks team. Each team division was appointed a sub-lead. The sub-lead was in charge of dividing tasks for research, design, and testing. While the primary responsibility of each lead was in their area of research, communication between all groups was very important because several cases required one group to depend on another.

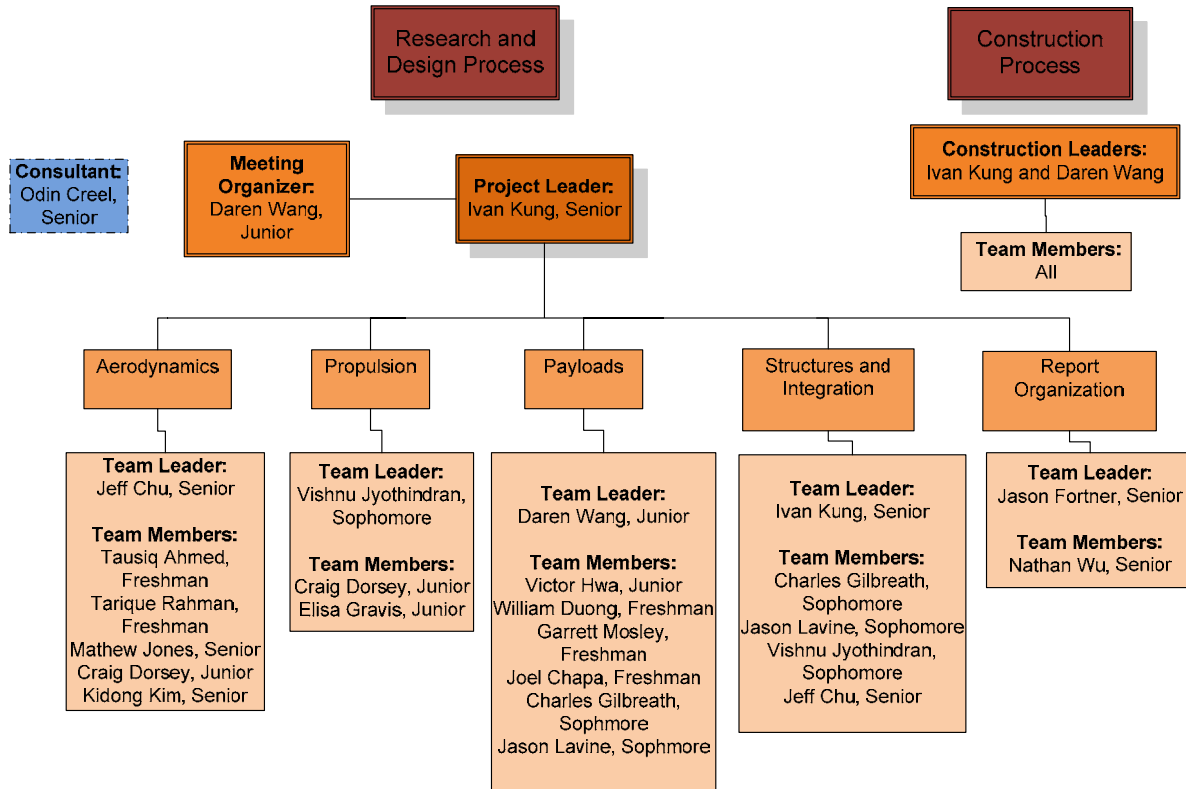


Figure 1 - Hornworks Organizational Chart

Since a large element of the score is devoted to the design report, a leader was assigned to help divide writing tasks and organizing the report. There was an overlap between the design teams and the construction team for the construction process.

2.2 Milestones

A projected timeline of events was created in August of 2007 to help organize the project. All members of the team tracked the deadlines of the project using the Gantt chart in Figure 2. Projected milestones are shown in color bars and actual milestones are shown in black.

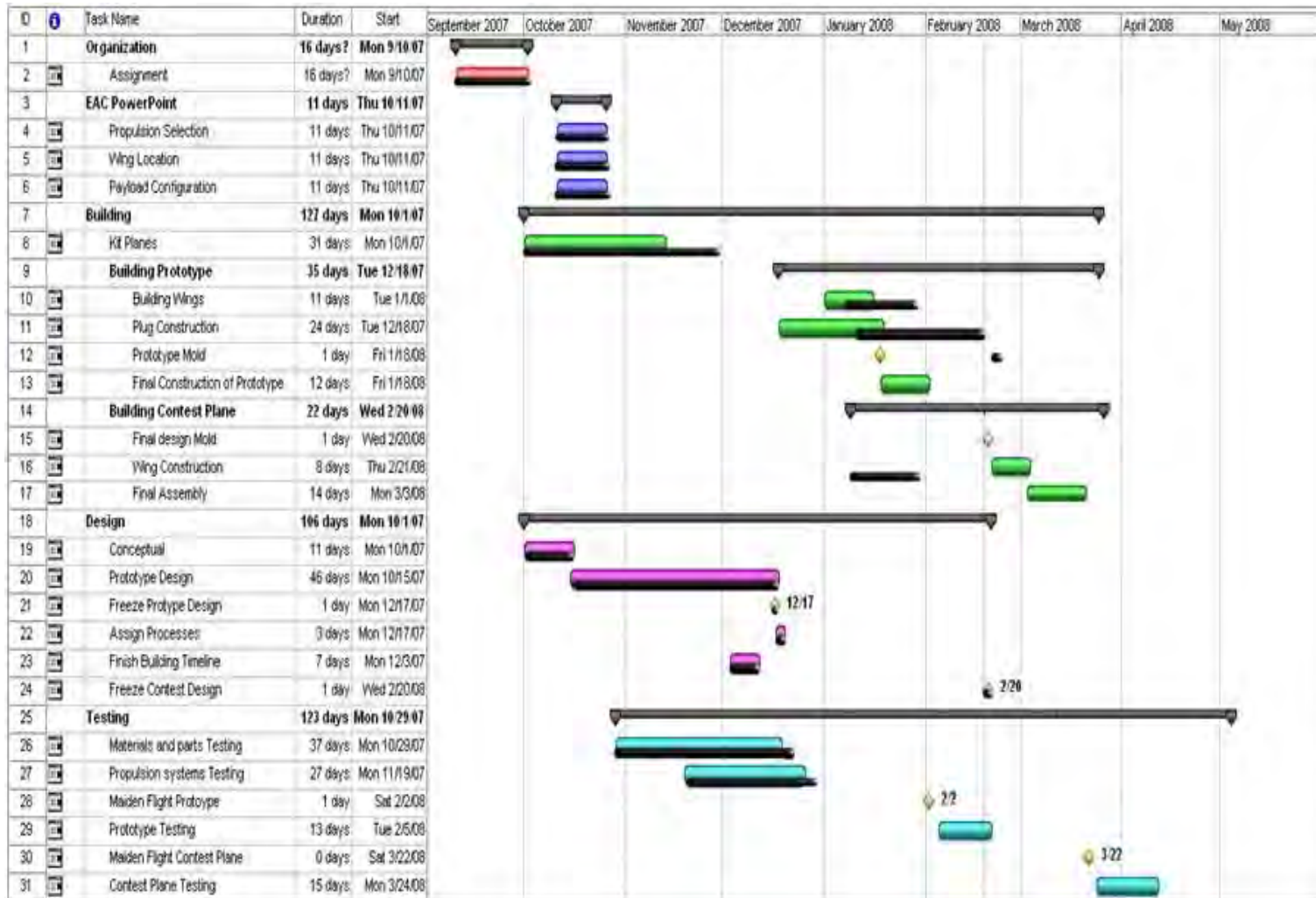


Figure 2 - Gantt chart for Project Planning



Team meetings were held twice a week to update all members of the current progress of all groups and to let everyone know of upcoming deadlines. The team met all of its preliminary and conceptual design deadlines. However, the building of the prototype aircraft and actual contest aircraft fell behind schedule. Flight testing of the actual contest plane is projected to start in mid March.

3 Conceptual Design

The conceptual design phase focused on analyzing the mission and design requirements to determine an aircraft configuration that would likely achieve the maximum score.

3.1 Mission Requirements

The scoring for this year's competition depends on two main components: the written report score and the total flight score. The total competition score is determined by:

$$\text{Total Score} = \text{Written Report Score} \cdot \text{Total Flight Score} \quad (1)$$

The total flight score is calculated by summing up the scores of the delivery flight and the first two successful payload flights.

3.1.1 Delivery Mission

This mission does not require a payload, and the team is given a maximum of five minutes to fly as many laps possible. Even though the aircraft will not carry any cargo in the delivery mission, all payload restraints needed for the payload mission must be carried during flight. The score is calculated as:

$$\text{Score} = \text{Number of Completed Laps} / \text{Battery Weight} \quad (2)$$

Only the first successful flight will be used for scoring and no additional flights for improvements are allowed.

3.1.2 Payload Mission

This mission requires the team to fly two laps carrying a specified payload consisting of a mix of "passengers" and "cargo pallets". The "passengers" are represented by half-full ½ liter plastic bottles fitted with round collars up to four inches in diameter or square collars up to 4"x4" in size. The "cargo pallets" are US ½ size clay bricks. The "passengers" must remain upright within the aircraft during flight and all of the cargo must be mechanically restrained such that the aircraft can be turned over with the cargo hatch open and not lose any "passengers" or "pallets." Additionally, the weights of the "passengers" are not fixed, presenting an added challenge of maintaining a stable center of gravity. All portions of the cargo, "passengers" and "pallets" must be completely enclosed within the aircraft. Finally, the exact cargo configuration will not be known until the moment of loading, so the aircraft must be designed to accommodate the all possible payload configuration. The payload configurations are as follows:



- 14 passengers (nominal 7 lb)
- 4 cargo pallets (nominal 7.2 lb)
- 10 passengers and 1 cargo pallet (nominal 6.8 lb)
- 7 passengers and 2 cargo pallets (nominal 7.1 lb)
- 3 passengers and 3 cargo pallets (nominal 6.9 lb)

The score for the payload mission is calculated by:

$$\text{Score} = 1 / (\text{Loading Time} \cdot \text{RAC}) \quad (3)$$

Loading Time is determined from the configuration mission and the Rated Aircraft Cost (RAC) is found from

$$\text{RAC} = \text{System Weight} \cdot \text{Battery Weight} \quad (4)$$

The system weight is the weight of the empty aircraft without batteries or payload. The first two successful payload flights will be counted towards the total flight score and no additional flights for improvements will be allowed.

3.1.3 Configuration Mission

This is a ground mission is performed after the delivery flight but before the payload mission can be flown. Three ground crews will be timed on how fast they can configure their plane for the specified payload. At the start of the mission (and timer), the team will be given a sheet with their assigned payload combination for which they will have to gather the number of “passengers” and “cargo” and load them securely into the plane. At the end of the mission, the restraints will be tested to determine if the payloads are secure by turning the plane upside down with the hatch open. The time for this mission is the Loading Time (see section 3.1.2) in Eq. (3).

3.2 Analyzing Design Requirements from Mission Requirements

The final competition score is based on two components, the flight score and the written score. Because the composite score is determined by multiplying the two component scores, high scores in both sections are imperative. The flight component score can be further broken down into specific dimensions directly applicable to the aircraft design. The major dimensions of immediate interest are the RAC, aircraft sizing restrictions, payloads and takeoff requirements.



RAC – As described in Eq. (4), the RAC is found by multiplying the system weight with the battery weight. A competitive RAC requires a light aircraft and minimal battery consumption. The battery weight is determined by the specific pack used for the mission and may not exceed four pounds.

Sizing and Takeoff - The aircraft must fit in a four feet by five feet space. The space is defined as a rectangular outline projected on the ground. While deployed and ready for flight, no part of the aircraft may sit outside of the outline. The takeoff restriction for the contest is 75 feet. This means that the aircraft must takeoff within 75 feet or less for a flight to be scored.

Payload - The five payload configurations demand that the aircraft be fitted with a flexible restraint system that allows for any given combination while not altering important properties like aircraft center of gravity.

3.2.1 Design Requirements from Flight Score Analysis

A total of five attempts are allowed for completion of the each flight missions. Battery packs are chosen in the staging box where loading time for the second mission is measured.

3.2.1.1 Delivery Flight Mission

The fundamental relation for a competitive score was found using a string of simplified calculations shown in Eq (5) below.

$$Score = \frac{\text{Laps}}{\text{Battery Weight}} \propto \frac{\text{Distance}}{\text{Power} \cdot \text{Time}} \propto \frac{\text{Velocity} \cdot \text{Time}}{\text{Velocity} \cdot \text{Drag} \cdot \text{Time}} \propto \frac{1}{\text{Drag}} \quad (5)$$

This relation formed the basis of the design of all components of the airplane. It indicates that minimizing drag will maximize the score.

3.2.1.2 Payload Flight Mission

No one dimension influences the score with a direct proportionality, so the specific design points for this mission focused on minimizing the impacts of negative dimensions while creating a stable aircraft capable of handling all five payload packages. The emphasis on weight in the score meant that everything from construction material and methods to integrated systems were considered. Design of the restraint system and loading method required reduced complexity and short loading times.



3.3 Initial Design Concepts

Conceptual ideas for all major design components were collected into a morphological chart, as shown in Table 1, and evaluated using figures of merit.

Table 1 - Morphological Chart

Component	Type					
Body	Conventional	Blended	Lifting			
Wing	Conventional	Biplane	Joined	Delta		
Empennage	Conventional	T-Tail	H-Tail	Bronco	V-Tail	Y-Tail
Landing Gear	Tail Dragger	Single Main	Bicycle	Tricycle	Quad cycle	
Propeller Configuration	Pusher	Puller				
Propulsion	Single Prop	Dual Prop	Triple Prop			

Figures of Merit

Figures of merit were then used in a decision matrix to systematically analyze the pros and cons of each design. Each figure of merit was assigned a weight of importance in the decision matrix. To rate the concepts in each figure of merit, a scale of -2 to +2 was adopted. The conventional concept was rated a neutral 0. As compared to the conventional concept, a component was rated a +1 if is better and +2 if it was significantly better. Likewise, a -1 and -2 scale was used for worse and significantly worse as compared to the conventional design.

3.3.1 Wing Configurations

The initial configuration evaluated was the wing-body design. Several design choices were deemed unsuitable using qualitative reasoning and analysis of practical past experiences. The lifting and blended bodies were eliminated because the mission required the bottles to stand upright. The wing would have to be unreasonably thick to meet this design requirement. The multiple body design was ruled out due to center of gravity concerns with the flexible payload requirement. The tandem, joined, and delta wings were also eliminated as possible design choices because the benefit of each design is minimal at the low speeds and Reynolds number of this competition. They also have higher complexity in design and construction.

The following figures of merit were used to evaluate the remaining concepts:

Loading Time – This is a measure of how the design component affects the amount of time required to load a specified payload into the aircraft. Loading time is a component of the payload mission score.

Drag – This is an evaluation of how the design component affects of the amount of drag on the aircraft. Drag directly correlates to battery usage and the amount of thrust required for flight. Since battery weight is counted for both delivery and payload mission, drag is an extremely important factor.



System Weight – This is a measure of the effect of the design component on the system weight of the plane. System weight encompasses the entire weight of the aircraft not including batteries.

Takeoff Distance – The aircraft must be able to take off within 75 feet of runway. This is a major driver of the aerodynamics and propulsion design.

Stability and Control – This is a measure of how the design components affect the stability and control both in the air and on the runway. The aircraft must be stable enough to complete the mission in normal Wichita weather.

Ease of Construction/Repair – This is a measure of the ease of building in accordance to the design. Easier construction will allow more prototypes to be built and tested. Easier repair will be important during competition.

Table 2 shows the decision matrix used to select the wing-body decision matrix.

Table 2 - Wing-Body Decision Matrix

Figures of Merit: Wing-Body	Weight	Conventional	Bi-plane	Canard	Blended
Loading Time	0.15	0	-1	0	0
System Weight	0.3	0	-1	0	-1
Drag	0.2	0	-1	1	1
Takeoff Distance	0.15	0	2	-2	0
Stability and Control	0.125	0	0	-1	0
Ease of Construction/Repair	0.075	0	-1	-1	-1
Total	1.000	0	-0.425	-0.3	-0.175

Bi-plane – The biplane was thought suitable for the mission due to the 4 ft by 5 ft size restriction and heavy payload. However, the top wing restricts top loading schemes and increases loading time. Another drawback is the decreased L/D of the bi-plane compared to a well-designed monoplane. Bi-planes also have increased weight from additional structures needed to support both wings, therefore increasing the RAC.

Canard – The canard design has two main advantages. First, the canard is designed to stall before the main wing. As the canard stalls, the nose of the aircraft pitches down, preventing the main wing from stalling. Second, unlike the conventional wing body configuration, canards create upward lift. This



reduces the amount of lift required from the main wing, reducing induced drag. However, the canard has the disadvantage of a longer take off distance because the wing's maximum lift coefficient cannot be achieved without the canard stalling.

Blended – The blended wing design is similar to the conventional wing design but allows for a more streamlined design. This decreases the drag at the cost of increased weight and complexity. The blended design was the runner-up in the decision matrix.

Conventional – The conventional design was the design chosen. It offers the best combination of the drag, control, RAC, and allows for efficient top loading schemes.

3.3.2 Payloads

Design of the fuselage began with consideration for the multiple payloads that the aircraft might have to carry. Of the five possible payloads, the most challenging is the 14 passenger configuration. The loading scheme was decided upon first and then the overall layout of the payloads within the fuselage was determined.

3.3.2.1 Hatch Configurations

Included in the score for the payload mission is the loading time of the payload items. The three methods of loading considered were frontal hatch, top-loading hatch, and rear hatch. Factors of interest considered when selecting the hatch design were:

Speed of Loading – The loading speed of the payloads is of the utmost importance. Faster loading directly correlates into a better score.

Ease of Construction – Constructability and reliability of the design is important to the overall performance of the plane. A complicated system often leads to an increase in chances of mission failure. Also, a complex system would be less amenable to fixes during the competition.

Subsystem Impact – A front-loading hatch will displace the propulsions package and require checks to insure that the package is re-installed correctly once the payload is put in place. Top loading schemes will often overlap with a top-wing design to allow full access to the fuselage. Rear loading is the least invasive as the only major aircraft component it could interfere with is the tail assembly, which can easily be avoided by careful hatch design.



Precision of Payload Placement – The payload missions all include a payload package consisting of several items. The placement of these items is important to the stability of the aircraft as they greatly affect the aircraft’s center of gravity. The ability to precisely place and secure the payload items will give accurate control and placement of the aircraft’s center of gravity when loaded.

Table 3 shows decision matrix used to select the loading scheme.

Table 3 - Loading Scheme Decision Matrix

Figure of Merit: Hatch Design	Weight	Front Load	Top Load	Rear Load
Speed of Loading	0.35	-1	0	-1
Ease of Construction	0.2	0	1	1
Subsystem Impact	0.1	-1	-1	0
Precision of Payload Placement	0.35	-1	1	-1
Total	1.00	-0.8	0.45	-0.5

The decision matrix indicates top loading as the optimal hatch configuration. Top loading scheme offered the best speed of loading and precision of item placement at the cost of the increased subsystem impact. The wing structures inside the fuselage must be carefully designed as to not be interfered by the dloading scheme.

3.3.2.2 Payload Arrangement

The competition constrains the placement and restraining methods for the payload. The two following options determined to be the most feasible are:

Single layer – This arrangement would place all items of the payload within the same layer of the fuselage. Having a single plane in which the payloads are placed simplifies access to the entire payload and construction. However, this arrangement requires that the fuselage to have a large footprint in the top-down view and potentially takes up a large section of the wing’s lifting area.

Two or more layers – This arrangement places the payload in layers within the fuselage. This allows for a potentially smaller area taken away from the wing and a much more compact design. The height of the payload items, however, creates a very tall frontal footprint and could result in a high drag fuselage.

The team selected the single layer payload arrangement because of the reduced complexity in construction and ease of payload access.



3.3.3 Propulsion

The inclusion of battery weight in the aircraft RAC calculation meant that there was a *direct* relationship between performance of the propulsion package of the aircraft and the score achieved in each mission. This requires a propulsion system that is:

- a. Powerful: Sufficient amount of static thrust is produced to takeoff in the limited takeoff distance (75 feet)
- b. Speedy: Attains relatively high cruise velocities to achieve lower lap times (Delivery Mission).
- c. Efficient: Efficient use of its batteries.

The placement of the propulsion package was first decided upon and then a motor configuration was determined.

3.3.3.1 Number of Motors

After it was decided that the propulsion package would be a puller, configurations of one, two and three motors were proposed and analyzed.

One motor - In this conventional system, one motor is mounted on the nose. This arrangement is simple and efficient.

Two motors - In this system, two identical motors are mounted on each wing. This arrangement uses lighter motors, and in some cases, uses fewer batteries than the one motor system. Motors placed above the wing allow for power lifting, but also increase the weight of the motor supports and add drag. However, because the motors are near the sides of the fuselage, the sizes of the propellers are limited.

Three motors - In this system, two identical motors are mounted on each wing and a third, more powerful motor, is mounted on the nose. The reasoning behind this configuration is as follows:

- o The large motor is used only at the time of takeoff to generate the static thrust required to takeoff in 75 feet. It is then switched off during cruise.
- o The two wing motors remain switched on during the entire flight. Since the large central motor supplies the majority of the static thrust needed for takeoff, the two wing motors could theoretically use a much smaller propeller with higher, enabling more efficient cruise.
- o This approach, in theory, yields a much smaller consumption of batteries, and a higher mission score.

Using the applicable figures of merit, a decision matrix was developed to assist in selecting the propulsion system configuration. The areas of interest considered were:



Power – The power of the propulsion package must be enough to produce the amount of thrust needed to take off and fly. This parameter was deemed to be of relatively high importance.

Efficiency – Because of the high sensitivity that battery weight has on the flight scores of both missions, the efficiency of the propulsion package must be optimized. Thus this parameter was deemed to be of high importance.

Propeller Size – A safety margin for the size of the propellers must be taken into consideration in order to keep propeller tips from hitting the ground.

Effect on Aerodynamics – Due to the tractor configuration for the motors, the propeller wash from the propulsion package creates large disturbances in the flow field about the wings. This disturbance can cause small negative effects on the aerodynamics of the plane.

Table 4 - Number of Motors Decision Matrix

Figures of Merit: Number of Motors	Weight	1 Motor System	2 Motor System	3 Motor System
Power	0.25	2	2	2
Efficiency	0.35	0	1	2
Propeller Size	0.08	1	-1	-1
Familiarity with Design	0.08	2	1	0
Effect on Aerodynamics	0.08	2	0	-1
Complexity	0.16	0	-1	-2
Total	1.00	0.9	0.69	0.72

The three motor system suffered in the figure of 'complexity' as it required a more complicated electrical wiring system. The two and three motor systems were also detrimental to the aircraft's aerodynamics. The single motor system design was deemed the best because it is simpler and more efficient.

3.3.4 Empennage

The key design parameters for choosing the empennage are:

System Weight – The weight of the empennage is a factor in the system weight which directly influences the payload mission score. Decreasing the weight will directly increase our payload mission score as shown by Eq.(3) and Eq.(4). This parameter was weighted moderately high.



Drag – The drag of the empennage indirectly influences the amount of batteries required. Because the battery weight is a factor in both mission scores, this parameter was weighted heavily. Decreasing the drag will indirectly decrease the number of batteries we use and directly increase the scores for both missions. As shown by Eq.(5), drag is the central element of scoring.

Stability and Control – The stability of the aircraft and relative ease of control dictate the flight capabilities of the aircraft. This parameter was rated moderately.

Ease of Construction – The time that it would take to construct the empennage was another factor that we considered; although, this parameter was rated moderately low.

Table 5 shows the decision matrix for empennage selection.

Table 5 - Empennage Decision Matrix

Figures of Merit: Empennage	<u>Weight</u>	<u>Conventional</u>	<u>T-Tail</u>	<u>H-Tail</u>	<u>Bronco</u>	<u>V-Tail</u>	<u>Y-Tail</u>
System Weight	0.3	0	-1	-2	-1	0	-1
Drag	0.4	0	0	-1	0	0	1
Stability and Control	0.2	0	0	-1	-1	-2	-1
Ease of Construction	0.1	0	0	-1	0	0	-1
Total	1.000	0	-0.3	-1.3	-0.5	-0.4	-0.2

The main disadvantage of the T-tail, H-tail, and Bronco tail was the need for increased structural support. The V-tail and Y-tail required a complex control system due to the ruddervator. Therefore the conventional tail was selected.

3.3.5 Wing Structure

Three basic wing structures were considered in the search for the lightest structure that is reasonable easy to build. Several types of composite wing structure are available. They tend to be stronger and heavier than necessary at this scale. They also come at a high construction cost. It is not possible to make a composite structure that is thin enough to be lighter than a balsa structure, but thick enough to withstand handling loads.

Foam core wings are easy to build and form into an accurate airfoil shape. The structure is usually reinforced with carbon fiber spars or tubing. However, the density of the foam adds significantly to the weight of the wing.



Standard built-up balsa construction is the lightest method we know of at the scale used in these missions. A balsa-D-tube structure utilizes light, optimally placed materials. Carbon fiber can be used in the spar caps if needed, and Kevlar roving can be used to effectively distribute loads from landing gear and other structures.

Table 6 shows the decision matrix used to select a wing structure.

Table 6 - Wing Structure Decision Matrix

Figures of Merit: Wing Structure	Weight	Composite	Foam Core	Built-up
Weight	0.5	-1	-1	0
Strength	0.2	2	0	0
Ease of Construction	0.2	-1	1	0
Cost of Materials	0.1	-1	0	0
Total	1.00	-0.4	-0.3	0

The balsa built-up wing structure was chosen for ease of construction and light weight. Previous experience and comparison of past contest aircraft support this decision.

3.3.6 Fuselage Structure

Three basic fuselage structures were considered to determine the lightest structure that could enclose the payload, incorporate a large access hatch, and provide the necessary stiffness.

Composite with Balsa Core - This method uses a balsa wood layer sandwiched between thin layers of fiberglass. It creates a strong and light structure that can be formed into almost any shape. Construction requires two sets of intermediary molds before the final part is built. The process includes vacuum bagging lay-ups that are both difficult, and time consuming. Cutting and forming the balsa into compound curves adds an additional level of sophistication.

Composite with Stringers - Rather than sandwiching a layer of balsa throughout, strips of balsa or foam can be strategically placed to create an even lighter structure than a solid balsa core. Additional reinforcement can be added around the large hatch opening with a minimum addition of weight. Alternatively, a carbon fiber tube could be run through the length of the structure to the tail, negating most of the structural requirements of the fuselage at an even lighter weight. Construction with this method is similar to construction with balsa core, but compound curves are more easily formed and the forming of the balsa is vastly easier. The main drawback to this structure is its flexibility.

Built Up - A standard balsa structure is usually light. However, internal reinforcements would not work well around the payload, and significant weight would be added by the structure around the hatch area.



Table 7 shows the decision matrix used to select the fuselage structure.

Table 7- Fuselage Structure Selection

Figures of Merit: Wing Structure	Weight	Composite Balsa Core	Composite Stringer	Built-up
Weight	0.4	1	1	0
Loading Time	0.3	0	0	0
Drag	0.2	1	1	0
Ease of Construction	0.1	-2	-1	0
Total	1.00	0.4	0.5	0

The composite stringer structure was selected. While a wing structure is sized well for a wooden structure with internal supports, the size of the payload makes a self-supporting composite structure lighter and more practical. A carbon fiber tube could be used as the bottom stringer and would support the wings, landing gear, motor, and empennage efficiently.

3.3.7 Landing Gear Configuration

Various landing gear configurations were analyzed and selected using a decision matrix. The following figures of merit were used in landing gear analysis.

System weight – System weight directly affects the Rated Aircraft Cost (RAC). Reducing the system weight increases the payload mission score and decreases induced drag on the aircraft during flight. This figure of merit was weighted moderately high.

Drag – Drag directly affects battery usage. As shown in Eq. (5), the score of the delivery mission can be simplified to approximately $1/\text{drag}$. Battery usage is also a part of payload mission RAC calculations. This figure of merit was weighted very high.

Stability and Control – Good stability and control capability during takeoff and landing run is important for a successful takeoff. The aircraft wobbling uncontrollably or veering off the runway could cause failure. This figure of merit was weighted moderately low in the decision matrix.

Ease of Construction – A simpler construction would allow faster and more accurate manufacturing of parts. This figure of merit was weighted low in the decision matrix.

Using these three figures of merit, the decision matrix for landing is shown in Table 8.



Table 8 - Landing Gear Decision Matrix

Figures of Merit	Weight	Tail Dragger	Single Main	Bicycle	Tricycle	Quadricycle
System Weight	0.2	0	1	-1	-1	-2
Drag	0.3	0	1	1	-1	-2
Stability and Control	0.2	0	-2	-1	1	2
Take Off Distance	0.3	-1	-1	-1	1	1
Total	1.000	-0.3	-0.2	-0.4	0	-0.3

Tail Dragger – A tail dragger configuration was considered for its light weight and reduced drag due to the small aft wheel. However, from past experience, tail dragger designs suffer from instability during the first 10-20 ft of takeoff when the direction of the aircraft cannot be controlled easily. Because takeoff distance is a large limitation of the of the payload mission, this was a fatal flaw.

Single Main – A single main configuration consists of a large main gear and three small wheels. The single main configuration should be lighter and have less drag than any other configuration. However, it suffered severely from stability problems during the takeoff run which increased takeoff distance.

Bicycle – The bicycle configuration was rated slightly worse than the tail dragger in the weight parameter due to the required outrigger on the wings. It has better drag characteristics because of the reduced frontal surface. However, the large aft wheel behind the CG decreases takeoff performance since it is harder for the plane to rotate during takeoff.

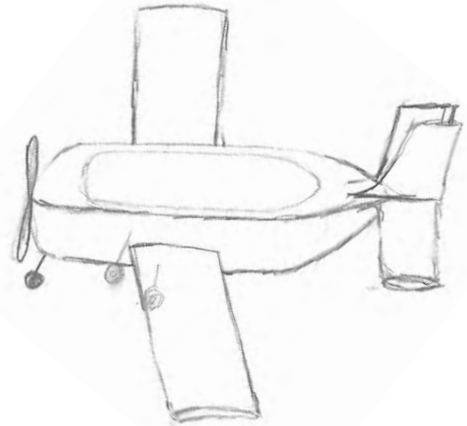
Tricycle – The tricycle configuration suffers from a system weight penalty due to having three wheels. There is also increased drag from the increased frontal area. However, three wheels increase the stability of the aircraft greatly during takeoff which shortens the takeoff distance by allowing the motor to run at full throttle without wobbling and veering off course. The configuration is the selected design.

Quadricycle - Similar to the tricycle configuration, but with slightly better stability and control at the cost of increased weight and drag. The decision matrix suggested that the drawbacks of additional weight and drag do outweigh the stability benefit.

3.4 Conclusion



After a series of configuration selections using qualitative reasoning and decision matrices, a conceptual design was chosen. The aircraft shall be a monoplane with top hatch, one centrally mounted tractor motor, conventional tail, and tricycle landing gear. The fuselage will be made of composite with stringers, and the wings will be made of a balsa built-up construction.



4 Preliminary Design

After deciding upon the basic configuration from the conceptual design phase, further development was performed to optimize the aircraft components.

4.1 Design and Sizing Trade Studies

Trade studies were performed to determine the optimal wing geometry, propulsion system, and payload configuration design.

4.1.1 Aerodynamics

The aerodynamics preliminary design consisted of optimizing airfoil, size wing area, and wing taper.

4.1.1.1 Airfoil Selection

The airfoil optimization process occurred in three stages. The first was to collect a large number of airfoils and rank them using a weighted score of lift over drag (L/D), maximum coefficient of lift ($C_{L_{Max}}$), and ease of construction. Second, the aerodynamics team picked the best airfoils from list by evaluating the drag polar, coefficient of moment curves, and C_L versus angles of attack (α) curves. The third and last stage was to run each airfoil through a simulated delivery and payload mission to obtain an approximate score. The best scoring airfoil was then selected.

Stage One

A total of 34 airfoils were tested in stage one of the optimization process. These airfoils were ones that UT and other successful DBF teams had used in the past, as well as other commonly used airfoils. The figures of merit in ranking were L/D , $C_{L_{max}}$, and ease of construction, with L/D being the most important and ease of construction the least.

A low drag, medium lift airfoil used by UT last year was set as the baseline with a score of 100. Using a merit chart, seven airfoils scored between 96 and 110 which warranted further investigation. The



seven airfoils were: PSU-94-097, Chuch Holliger ch 10-48-13, Davis 3r, Selig S4320, Cody Robertson cr001, Selig S2091, and Selig S7075.

Stage Two

From examining the drag polar and C_L/C_D versus α curves shown in Figure 3 and Figure 4, the team picked out the three best airfoils for further analysis. The three airfoil chosen were CH10, Davis 3r, and the Selig S2091. The CH10 had the highest C_{Lmax} . The Davis 3r was an interesting airfoil because it had small drag bucket, but had the best C_L/C_D of all the airfoils. The Selig S2091 had a very wide drag bucket but a relatively low maximum C_L/C_D .

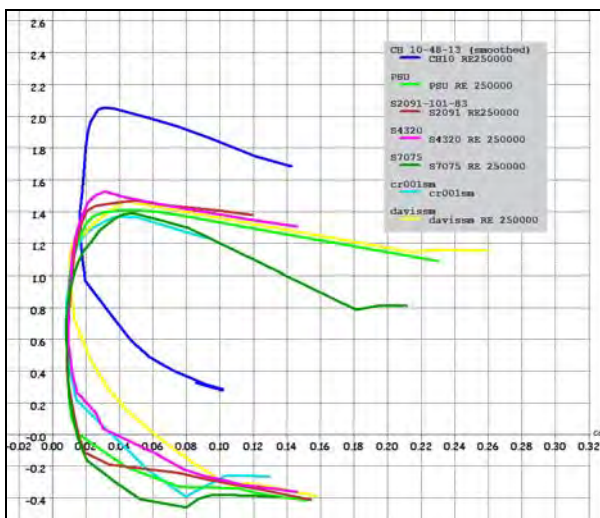


Figure 3 - C_L vs. C_D

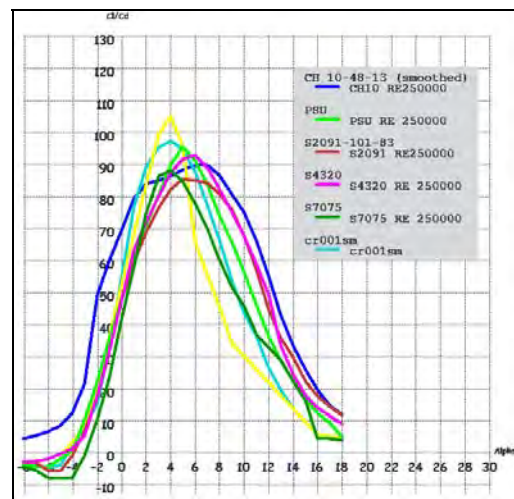


Figure 4 - C_L/C_D vs. Angles of Attack

Stage Three

To evaluate the effect of the airfoil on the mission scores, an energy based approach of simulating the mission and battery usage was developed. The premise of the approach was

- Energy Used per Lap = Lap Length · Drag
- Laps in Delivery Mission = 300 sec/ cruise velocity (rounded down)
- Battery Usage (lb) = Energy / Energy Density of Batteries
- Scaled Delivery Mission Score = Laps/Battery Usage
- Scaled Payload Mission Score = 1/Battery Usage

Some assumptions were made to simplify the analysis. The simplifications were:



- **Ignore battery used in takeoff** - The high lift CH10 airfoil has better flight characteristics in high C_L condition. This analysis will slightly decrease CH10's score. However, since takeoff run is a small segment of the mission profile, its impact on battery usage is minimal.
- **Loading time and system weight is constant** – The high lift CH10 airfoil should be lighter since less wing area is needed. However, since the wing is going to be built out of balsa, the difference in weight will be very small.
- **The propulsion package is 100% efficient** – This will underestimate the amount of battery needed to complete the mission. However, the purpose of this analysis was to compare the airfoils qualitatively; this assumption does not affect the rank of the three airfoils.

The wings analyzed are rectangular and sized to match stall velocity for payload mission. The 75' takeoff distance for the payload mission will be the driver for propulsion and wing sizing. The wingspan was set at 60 inches to maximize aspect ratio. The CH10 had the least amount of wing area due to its high C_{Lmax} , the Davis 3r and Selig S2091 had similar size wings.

The estimated scores are normalized to Davis 3r airfoil. Figure 5 identifies the relative scores of each airfoil. For the total, the scores for the payload mission were weighed double since the payload mission will be flown and scored twice.

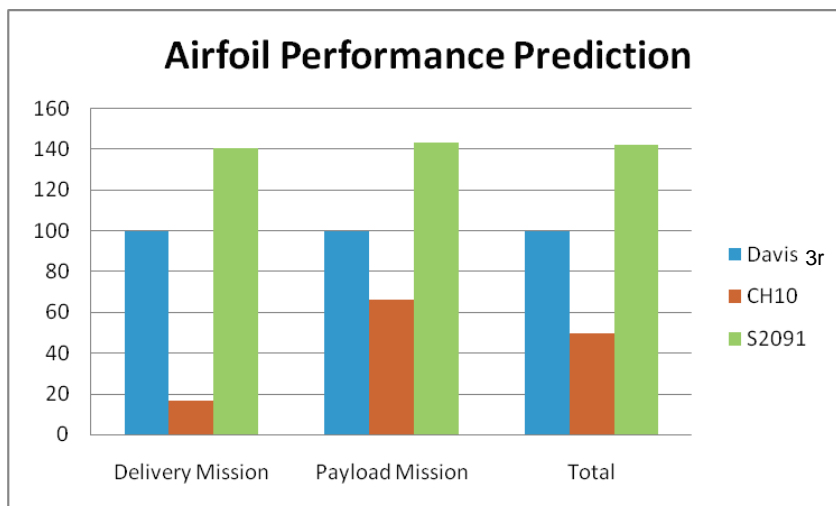


Figure 5 – Estimated Score

The analysis shows that high lift CH10 airfoil is undesirable due to its high drag characteristics during cruise conditions. This is especially apparent in the delivery mission at which the CH10 airfoil is drastically worse than the other two airfoils. The S2091 scored the best due to its large drag bucket. The large drag bucket is important because the two missions have very different aerodynamic requirements on the aircraft.



4.1.1.2 Wingspan

The wingspan of the aircraft was limited by the 4 feet by 5 feet size restraint. The team decided to orient the aircraft with fuselage parallel to the 4' direction and the wing to the 5' direction. The longer 5' direction allows the wing to have a larger wingspan which reduces induced drag on the wing.

4.1.1.3 Wing Area

Wing area is an especially important parameter in this year's competition due to the short takeoff distance requirement and the goal of minimizing battery usage. Since the wingspan is set at 5 feet, wing area must be adjusted by changing the MAC (mean aerodynamic chord). Decreasing wing area increases stall speed which increases the required static thrust to takeoff in 75 feet. Figure 6 shows the static thrust required versus MAC.

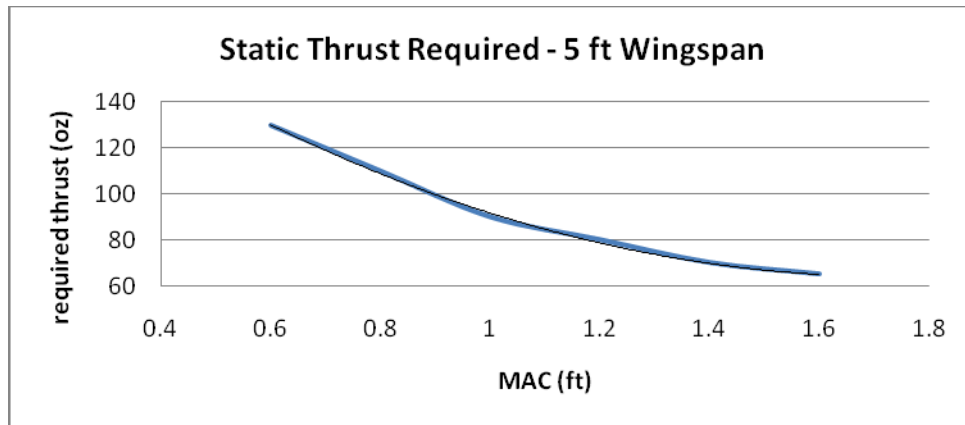


Figure 6 - Required Static Thrust



Increasing the MAC also changes the drag buildup for the aircraft as shown in figure 7 and 8.

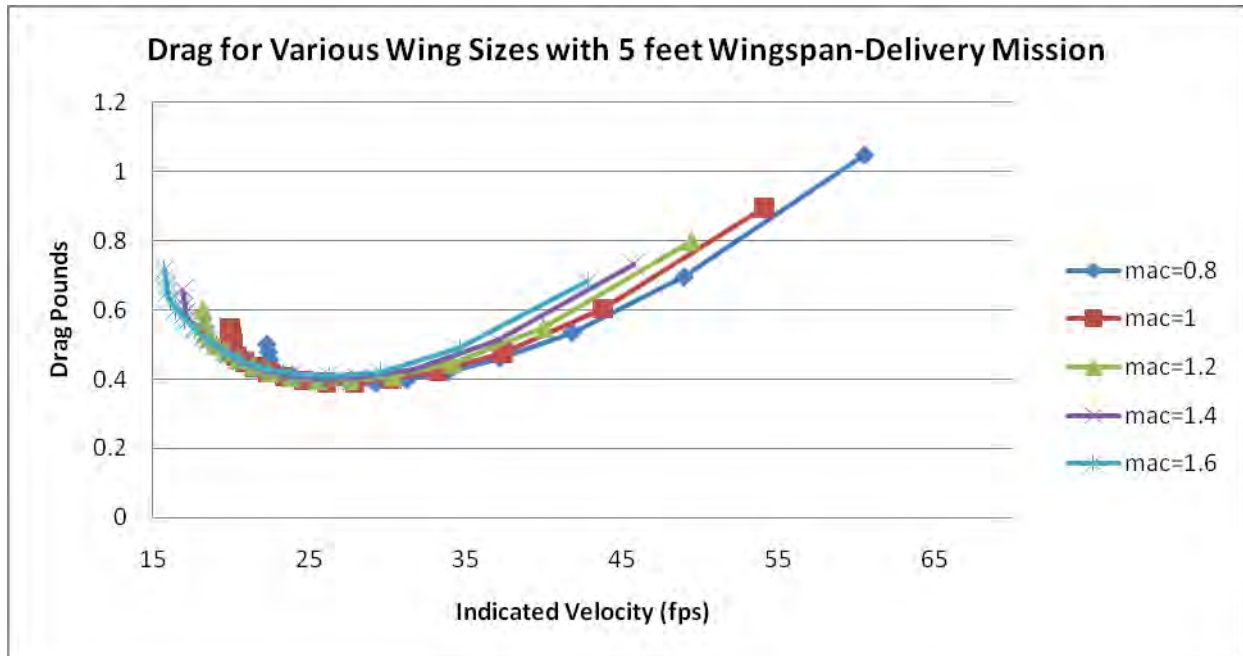


Figure 7 - Drag Buildup for Delivery Mission

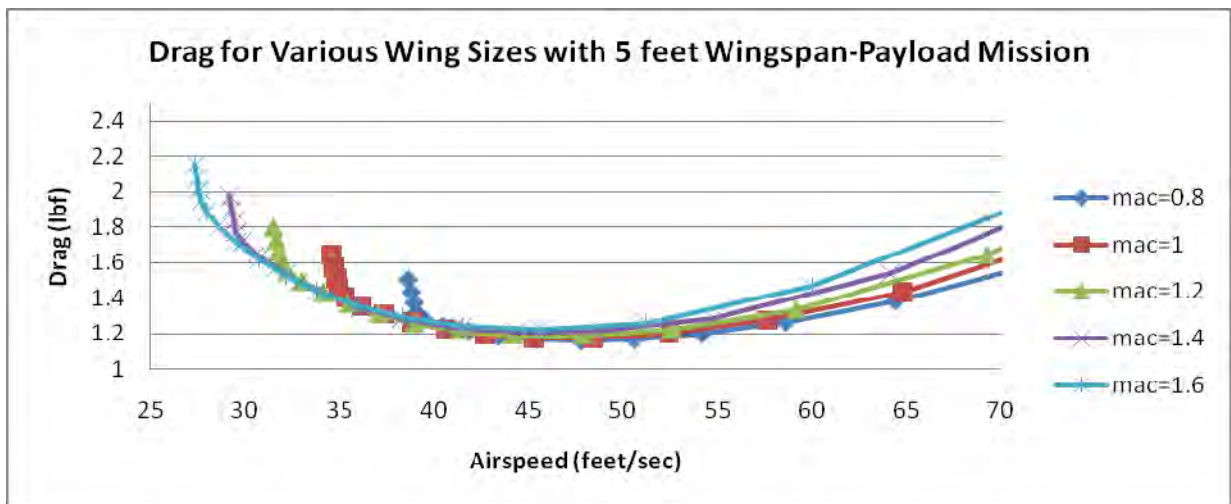


Figure 8 - Drag Buildup for Payload Mission

The minimum drags for the various wing sizes are very similar which suggests that the difference in battery usage is negligible. The loaded mission score can be simplified as a trade between motor weights required for the additional thrust versus additional wing weight required for the extra wing area. Figure 9 shows the sum of motor weight and approximate wing weight.

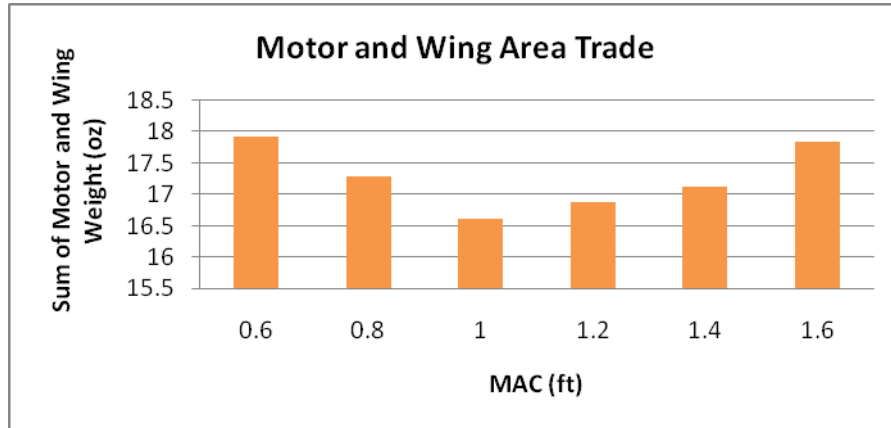


Figure 9 - Motor and Wing Weight vs. Wing Area

The wing with MAC of 1 ft feet and area of 5 ft² was the best in terms of minimizing the weight. The score analysis performed earlier and shown in Eq. (5) reduced the delivery mission score to being inversely proportional to drag. Since the minimum drag term for all of the wing sizes are essentially the same, the delivery mission does not drive wing sizing optimization. The results of the wing sizing optimization study suggest that a 5 ft² is optimal.

4.1.1.4 Taper Ratio

Wings with taper have reduced induced drag since the wing better approximates the ideal elliptical lift distribution. However, our calculation suggests the reduction in drag is at best three percent. The team decided the reduction in drag was not worth the higher costs in construction time.

4.1.2 Propulsion Optimization

An optimization program was used to help determine the most efficient propulsion system. The program, Motocalc, makes use of an extensive database of motors, batteries, gear boxes, propellers, and controls, allowing the user to select one type of each, while having the option of using more than one of each item. The selections are then analyzed by Motocalc as an entire configuration and a table which contains in-flight data calculated from the constants in the database corresponding to the user's selections is produced.

Data obtained and analyzed by the aerodynamics team showed that a static thrust of at least 120 oz. would be needed for the plane to take off well within 75 feet, the required takeoff distance. For the preliminary designs, emphasis was placed on the payload mission since it counted twice as much as the delivery mission.

The process began with a choice of possible brushless motors based predominately on brand and weight. A gear box was then selected. Batteries, typically six to start, were then chosen. Speed controls were selected based on current and their compatibility with a brushless motor. Typically, a small



size propeller would initially be analyzed with the configuration, with the size changing based on further analysis. Once the initial parts of the test configuration were selected, the propulsion system was analyzed by the program. The table of results typically showed a desirable static thrust, current draw, or flight time. The challenge was in discovering, through an iterative process, what changes needed to be made in the number/type of batteries, motor weight, and propeller size to have satisfactory value for flight time, thrust, and current.

4.1.2.1 Batteries

When choosing batteries, the priority was striking a balance between available battery energy and total weight of all batteries combined, in addition to following contest regulations prohibiting the use of LiPo batteries. An obvious consequence of increasing the number of batteries, and thereby the energy available to the motor, is increasing the weight. More than 20 oz. of batteries proved to be inefficient and uncompetitive based on previous DBF experience. Therefore, configurations relying on battery weights of 20 oz. or more were discarded. The propulsion team's first goal was to choose the type of battery. The contest rules only allow NiCd (nickel-cadmium) or NiMh (Nickel Metal-hydride) cells. From previous years' tests, the team determined that NiMh had more energy per weight than NiCd, and so NiMh batteries were selected. Our next goal was to analyze different NiMh cells and find a suitable candidate. Based on previous experience, the capacity of a good cell should be between 1500 and 2300 mAh. Table 9 shows the specifications and current draw test results of various cells candidates.

Table 9 - Battery Comparisons

Battery Comparison Test				
	Capacity (mAh)	Weight (oz.)	Maximum Steady Current (A)	Maximum Peak Current (A)
Elite 1500 AA	1500	0.81	25	35
Elite 1700 AA	1700	1	25	35
HR 1700 AUP	1700	1.2	25	30
Elite 2000	2000	1.16	30	35
GP 2000	2000	1.23	35	50
GP 2200	2200	1.62	35	50

Using Table 9, an energy density score was calculated Eq. (6) and shown in Figure 10:



$$\text{Energy Density Score} = \frac{\text{Capacity}}{\text{Weight}} \quad (6)$$

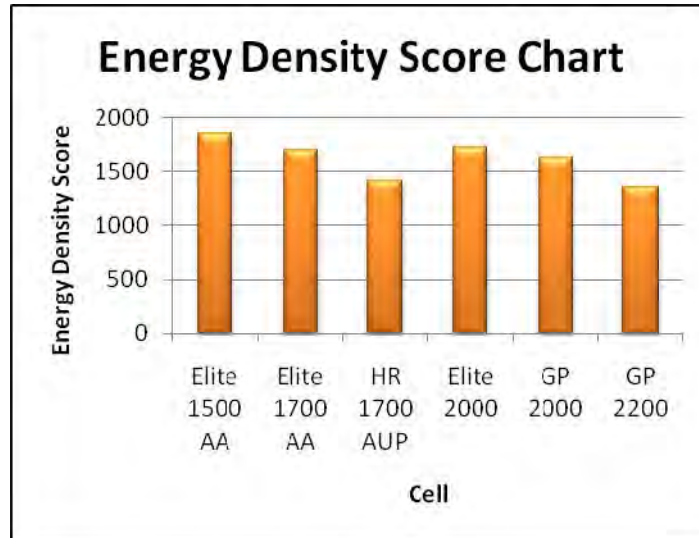


Figure 10 - Energy Density Score Chart

Figure 10 shows that the Elite 1500 AA cell had the highest energy density. Therefore, it was considered to be the ideal candidate. However, the consequence of running such a lightweight cell was that it could handle a peak current of only 35 A. Our next goal was to find a motor/gearbox system that could meet such parameters.

4.1.2.2 Motor/Gear Box/Speed Controls

Due to their known reliability and efficiency, either Hacker or Neu brushless motors were used for all proposed propulsion systems. Motors were chosen based on their weight, optimally less than 11 ounces. Weight was not a large factor in choosing a corresponding gear box and speed control. The gear box was typically chosen based on the motor manufacturers' recommendations.



Table 10 - Motors and Gearbox Configurations

Motor/Gearbox Configurations (Predicted)					
	Static Thrust	Peak Current	Number of Cells	Battery Weight (oz.)	Total Weight of System (including motor/gearbox)
1. Neu 1506/3Y-1700 (5.3:1)	134.6	40.8	15	12.15	20.45
2. Neu 1902/3Y (5.3:1)	140.1	34.1	18	14.58	21.28
3. Hacker B50 18S (6.7:1)	138.6	38.8	16	12.96	21.94
4. Neu 1905/1.5Y (5.3:1 gearbox)	131.2	31.7	17	13.77	22.47
5. Neu 1506/3Y-1700 (6.7:1)	138.4	33.1	18	14.58	22.88
6. Neu 1902/3Y (6.7:1)	136.4	26.5	21	17.01	23.71
7. Hacker B50 13L (6.7:1)	133.7	34.9	16	12.96	24.01
8. Hacker B50 10XL (4.4:1)	134.9	34.7	15	12.15	25.15
9. Neu 1905/1.5Y (6.7:1)	134.7	26	21	17.01	25.71

After detailed review and analysis, the propulsion team determined that the Neu 1905 with 5.3:1 gear ratio and Neu 1506 with 6.7:1 gear ratio were the best candidates because of their low weights. Candidates 1 and 3 were rejected because they operated at currents greater than the capabilities of the Elite 1500 AA. Candidate 2 was rejected after detailed analysis because it was not rated to handle such high input power (≈ 650 Watts). The remaining candidates were discarded because of their high weights or peak currents.

4.1.2.3 Propeller

The propeller was tested based predominantly on its pitch and diameter. With the ideal motor/gearbox candidates selected, the propulsion team’s next goal was to find the ideal propeller to use for the payload mission. After discussions with the aerodynamics team, the team concluded that 19 inches was the highest diameter propeller that could be used. Propellers with larger diameters were discarded because of ground clearance issues.

Several propellers with diameters ranging from 18 to 19 inches were tested with the following settings to ensure consistent results:



Motor: Neu 1905/1.5Y motor
Gear ratio: 5.3:1

Cell: Elite 1500 AA
Number of cells: 17

The results are detailed in Figure 11:

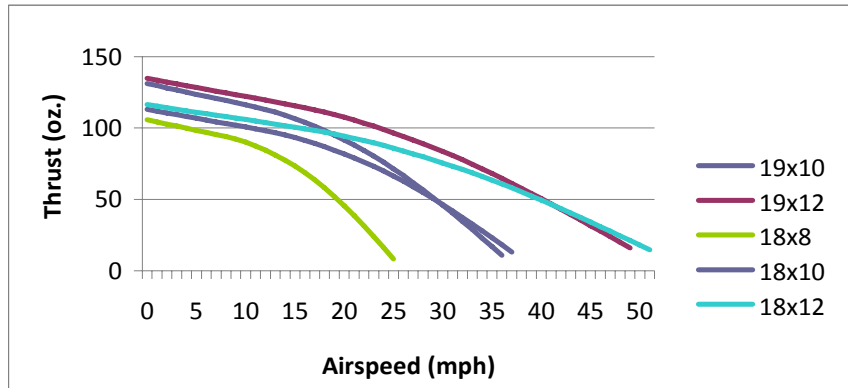


Figure 11 - Thrust vs. Airspeed of Various Propeller Sizes

The 19x12 and the 19x10 propeller were the best candidates because they produced the static thrust required (≈ 135 oz.). However, the 19x12 was favored because the aircraft could fly at much higher airspeeds before thrust approached zero.

4.1.3 Payload Configuration

The competition rules are very specific about the payload restraint system. Keeping the payload from shifting excessively in flight is also a stability concern crucial to completing the missions. The payload items all have similar profiles in the top-down view as the cargo pallets are 4"x4"x2 1/3" and the passengers have a maximum radius or length of 4". The team determined that an individualized compartment for each item was the simplest and most secure restraint configuration. Plans for the placement of the items were then drawn up.

Figures of merit considered when selecting the configuration were:

Center of Gravity – The mission to fly 14 passengers encompasses the largest volume, filling all the item compartments. Since there is no leeway in the weight placement, the 14 passenger configuration was used as the standard for measuring the center of gravity (CG) of each configuration. Each of the five possible payloads was fitted in the configurations with the goal of obtaining a CG as close as possible to the CG of the 14 passenger mission. This ensures that the aircraft's CG does not shift radically from one mission to another. Item placement was also selected with roll equilibrium in mind so that there would be balanced forces about the centerline of the fuselage.



Fuselage Footprint – The footprint of the fuselage, as taken from a top-down perspective, is an important factor to consider. Having the fuselage with too large a footprint creates a fat fuselage that reduced lifting area from the wings as well as creating higher drag.

Fuselage Frontal Area – As with the footprint, the frontal area of the fuselage must be kept to a minimum to reduce the drag of the aircraft.

Ease of Streamlining – While the fuselage is not the exact shape of the payload configuration, the fuselage is contoured very close to create the smallest footprint and frontal area possible. This factor was selected based on how easily a streamlined fuselage could be fitted over the configuration.

Table 11 shows the CG location for every item combination in each payload configuration.

Table 11 - CG Locations for payload configurations

Calculated Optimal CG (inches from front of configuration)						
	Diagram 1	Diagram 2	Diagram 3	Diagram 4	Diagram 5	Diagram 6
14 Passengers	14	14.29	14.57	12.57	10.86	13.43
4 Pallets	14	14	15	13	11	13
10 Passengers 1 Pallet	12.94	14.24	14.64	14.24	10.76	13.47
7 Passengers 2 Pallets	14	14.28	14.56	12.48	10.73	13.44
3 Passengers 3 Pallets	15.39	14.29	14.64	12.72	10.41	13.42
Maximum CG Shift	2.45	0.29	0.44	0.42	0.59	0.47

The payload configuration with two rows of six compartments and one row of two compartments had the least amount of shift in CG. Table 12 shows the decision matrix for the different payload configurations.



Table 12 - Payload Configuration Decision Matrix

Figures of Merit	Weight						
		0	1	1	0	1	1
CG	0.25	0	1	1	0	1	1
Fuselage Footprint	0.2	1	1	1	0	0	0
Frontal Area	0.35	1	1	0	0	0	0
Ease of Streamline	0.2	1	1	0	0	0	1
Total	1.00	0.75	1	0.45	0	0.25	0.45

The payload configuration of two rows of six compartments and one row of two compartments was selected because it had the least amount of CG shift, minimal fuselage footprint, small frontal area, and was easy to streamline.

4.2 Mission Model Capability

In order to optimize the aircraft for the competition, a mission model of the two in-air and on-ground operations were developed and analyzed. While flying the set course, the aircraft would perform an upwind leg, two 180° degree turns, one 360° turn, and a downwind leg. This mission-model imposes a maneuverability and performance requirement on the aircraft. The aircraft must have enough thrust to overcome the headwind and produce enough positive ground speed to complete the mission.

The ground operations consist of several takeoffs and landing criteria. Before entering the staging box, the ground crew is allowed to select the propeller and battery pack to be used for that flight. Battery and propeller combinations should be varied to successfully complete the mission in any weather condition. The aircraft should be fully flight-ready as soon as the team arrives at the flight line. During takeoff, the aircraft is required to leave the ground within 75 feet of the starting line, and the flight crew has five attempts to complete the mission. This mission model imposes strict requirements on the aerodynamics and propulsion performances; the aircraft must accelerate to takeoff velocities in a relatively short amount of time. During landings, the aircraft must be able to touchdown on the runway without major structural failure. Therefore, the landing gear must be able to absorb a significant amount of shock without failing. During the configuration mission, the ground crew will be timed on loading the



specified payload combination. Reducing the loading time will further increase the payload mission score; thus, the payload restraint system must be quick and efficient.

4.3 Mission Model Uncertainties

One unpredictable aspect of the mission profile model is the weather. Wind conditions could significantly alter aircraft performance. Therefore, the site must be analyzed to maximize mission scores for the likely weather conditions.

4.3.1 Site Analysis

The theme for this year's competition is reconfigurable short field transport. The fully-loaded aircraft must be able to lift off within 75 feet of runway while carrying up to 7.2 pounds of payload. The takeoff distance is a function of thrust, total aircraft weight, maximum C_L , wing area, and headwind velocity; higher head wind decreases the planform area required. Decreased planform area has the benefit of lowered induced drag, parasitic drag, and system weight. The team found and averaged wind speeds at Wichita, KS from the last five years from April 15-21 during the hours of the competition. Figure 12 shows the average wind speed and ± 1 standard deviation error bars.

The data suggests that it is very unlikely to have no wind during competition. Since the time of flight is not known nor is the runway orientation given, the wind may not be blowing in the desired direction. The average wind speed and standard deviation are corrected by a factor of $\cos(45^\circ)$.

Type	Value
Sample Size	314
Avg (mph)	16.17
StdDev (mph)	7.47
Avg-cos(45°) (mph)	11.43
StdDev-cos(45°) (mph)	5.28

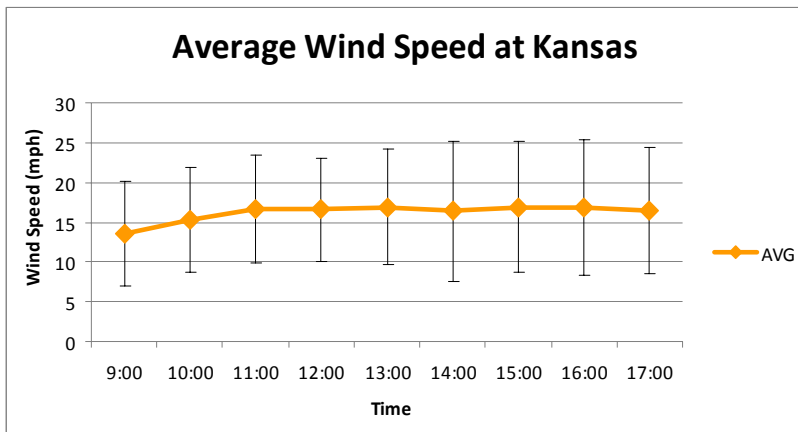


Figure 12 - Average Wind Speed in Wichita



By assuming a normal distribution of wind speeds, the cumulative distribution function of the headwinds was found. Figure 13 shows the cumulative distribution plot.

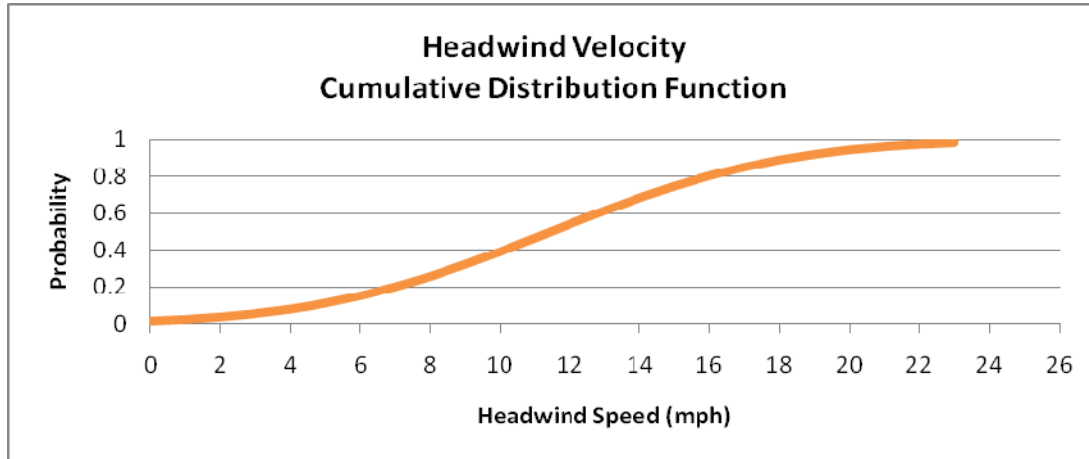


Figure 13 - Cumulative Distribution Function for Headwind Velocity

The analysis suggests that there is an approximately 50 percent chance that the headwind will be less than 12 mph and a 10 percent chance that the headwind will be less than 5 mph. This analysis is inherently conservative because the wind was assumed to be blowing 45° relative to the runway, which is most likely constructed to face the predominant wind direction in Wichita.

Using this analysis, the team decided to design the aircraft assuming a 5 mph headwind during takeoff. This design choice is conservative while still maintaining a competitive edge.

4.4 Estimate of Lift Characteristics

The drag polar of the wing can be obtained by introducing an induced drag term into the 2D drag polar. This will be discussed in more detail in the next section on drag characteristics. The wing drag polar is shown in Figure 14.

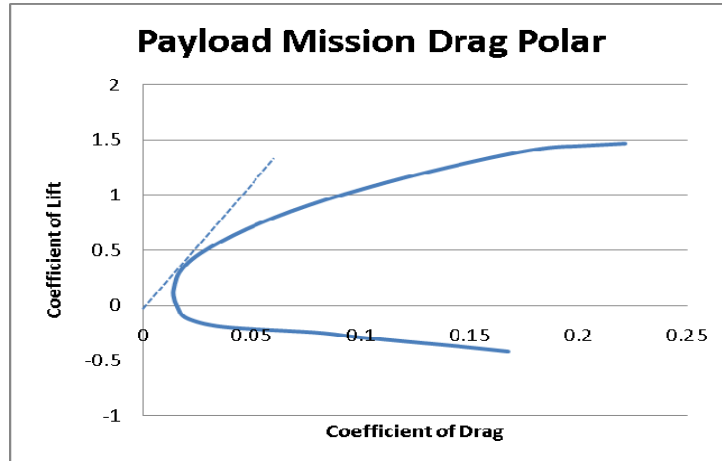


Figure 14 - Payload Mission Drag Polar

The drag polar indicates the drag bucket occurs at a C_L range of between -0.1 and 0.3. The best lift to drag position is shown by the intersection of the dashed line and the drag polar. The best L/D is 8.82 at 2 degrees angle of attack and C_L of 0.63. The drag polar for the delivery mission is similar to the payload mission's.

4.5 Estimate of Drag Characteristics

The overall drag of the aircraft at different angles of attack for the two missions was analyzed. The aircraft has four main drag contributing components: wing, fuselage, tail, and landing gear. Drag on the wing is divided into two parts, a profile or parasitic term and an induced term due to generated lift. The 3D drag buildup of the wing utilizes the parasitic term, C_{D0} , from the 2D drag polar analysis with an additional induced term that is a function of aspect ratio and planform efficiency factor. This is shown in Eq. (7) and Eq. (8) below.

$$C_D = C_{D0} + C_{Di} \quad (7)$$

$$C_{Di} = \frac{C_L^2}{Ar \cdot \varepsilon} \quad (8)$$

where C_D , C_{Di} , and C_{D0} are coefficient of total drag, induced drag, and parasitic drag respectively. C_L is the coefficient of lift. Ar is the aspect ratio, and ε is the planform efficiency factor.

For a flat plate, ε is about 0.92, a good tapered wing is about 0.95, and for an elliptical wing, $\varepsilon=1.00$. The fairly streamlined fuselage C_D is approximated as 0.03. The tail C_D is approximated as 0.015 and the landing gear is approximated as skinny tubes with C_D of 1.3. The drag calculations for cruise conditions are shown in Table 13 and Table 14.



Table 13 - Cruise Drag for Payload Mission

Component	Drag (lbs)
Wing Induced	0.53
Wing Profile	0.15
Fuselage	0.25
Tail	0.06
Landing Gear	0.19

Drag Buildup at Cruise - Payload Mission

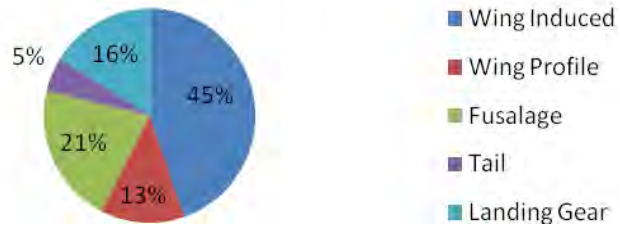


Figure 15 - Cruise Drag for Payload Mission

Table 14 - Cruise Drag for Delivery Mission

Component	Drag (lbs)
Wing Induced	0.05
Wing Profile	0.22
Fuselage	0.08
Tail	0.02
Landing Gear	0.06

Drag Buildup at Cruise - Delivery Mission

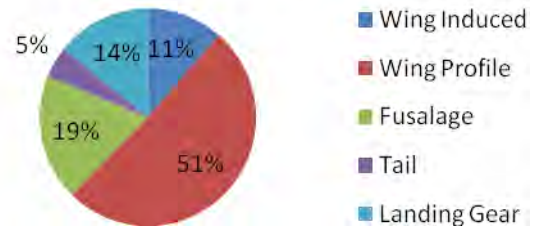


Figure 16 - Cruise Drag for Delivery Mission

The induced drag term dominates in the payload mission. In the unloaded mission, wing profile drag dominates.

4.6 Estimate of Aircraft Stability Characteristics

For the aircraft to be statically stable, the center of gravity of the aircraft must be located ahead of the neutral point of the aircraft. The distance between the CG and the neutral point, normalized by MAC, is the static margin. A large static margin is required for stability because the pilot will not be flying from the aircraft's point of view. Past experience has shown that the static margin of the aircraft should be at least 0.15.

The CG location of the aircraft is fixed relative to the front of the aircraft due to the heavy payload. The static margin then can only be moved by shifting the neutral point. The neutral point was found by using an equation given in Simon's Model Aircraft Aerodynamics. The aircraft did not have a large



enough static margin when CG was placed directly at the wing's quarter chord. The MAC quarter chord was placed .7 inches behind the CG, creating a static margin of 0.164.

4.7 Estimate of Mission Performance

Table 15 below shows the predicted mission performance. For the delivery mission, the aircraft is predicted to weigh 2.53 lb, takeoff in 20 ft, cruise at 46 ft/s, and complete 4 laps in 4 minutes with 6.5 oz. of battery. For the delivery mission, the aircraft is predicted to weigh 10 lb, takeoff in 70 ft, cruise at 46 ft/s, and an have an estimate RAC of 367.2 oz.².

Table 15 – Mission Performance Prediction

	Delivery Mission	Payload Mission
System Weight (oz.)	34	34
Battery weight (oz.)	6.5	10.8
Payload Weight (oz.)	0	115.2
Total Weight (oz.)	40.5	160
Expected Loading Time (s)	-	35
Static Thrust (oz.)	40	100
Takeoff Distance (ft)	20	70
Maximum Rate of Climb (ft/s)	10.5	12
Estimated Cruise velocity (ft/s)	26	46
Maximum Cruise Velocity (ft/s)	38	51
Expected Mission Time (min)	4	1.83
Expected Laps	2	2
Estimated RAC (oz²)	221	367.2
Expected Score (laps/oz.)	0.307	-
Expected Score (1/(sec*RAC))	-	0.0000778

5 Detail Design

This section specifies the final detailed design of the aircraft including aircraft sizing, payload restraint design, propulsion package selection and performance, weight and balancing, flight performance, rated aircraft cost, and aircraft schematics.

5.1 Dimensional Parameters of Final Design

Table 16 below shows the aircraft parameters for the final design.



Table 16 - Final Design Parameters

Geometry							
Fuselage		Wing		Vertical Stabilizer with Rudder		Horizontal Stabilizer with Elevator	
Length (in)	46	Airfoil	Selig 2091	Airfoil	Flat Plate	Airfoil	Flat Plate
Max Width (in)	10	Aspect Ratio	4.16	Aspect Ratio	1.5	Aspect Ratio	3
Max Height (in)	10	Chord-root(in)	14.4	Chord-root(in)	6.75	Chord-root (in)	8.5
		Chord-tip(in)	14.4	Chord-root (in)	4.5	Chord-tip(in)	8.5
		Span (in)	60	Height (in)	11.75	Span (in)	25.375
		Area (ft²)	6	Area (in²)	66	Area (in²)	193

5.2 Payload

Overall, the payload restraint system chosen must be light and sturdy in order to maximize the score for system weight. It must also have a mechanical component to it and be easy to work in order to minimize loading time. The actual restraint method must be able to hold the fixed height bricks and must be able to vary by 5/8 inch to accommodate the varying heights of the water bottle. Also, due to the varying placements of the collar, the device must not be higher than 1/8 inch on the floor or protrude deeper than 1/8 inch on the top.

The team selected a payload configuration that would optimize air flow over the body and weight of materials. Additionally, the many combinations of payloads made making sure the center of gravity is in the right place easy. This system consists of a bank of 4 in x 4 in x 9 in cells that easily accommodates both the bottles and bricks.

5.2.1 Methods of Payload Restraint

Two main methods of payload restraints were decided on due to their optimization of the requirements and were investigated.

Foam Grid - The foam grid is similar to the latex grid in that it relies on a similar core frame work; however, 2" thick foam blocks replace the latex grid as seen in Figure 17. The grid supports are closer together because the foam doesn't need to be kept taut resulting in less material weight. Also, there is 1/8 in thick balsawood beneath the foam block with a 1-1/4 in diameter hole in it to hold the top of the bottle in place. This grid is attached to the fuselage with snap clips, and is mounted so that the top of bottle sits in the hole in the balsawood.



The downside to this plan is that system as a whole, weighs more than the bottle part of the latex grid. Also, the foam size requires more height within the body of the aircraft.

5.2.1.1 Materials

The two factors that determine the material to be used are weight and strength.

Frame - The frame needs be light but able to resist both the pressure from the bottles, pallets, and materials. For that reason, carbon fiber rods were selected over wood or other materials. The carbon fiber is both lighter and stronger than wood and is fairly easy to work with.

Foam Types - In general, open cell foam was favored over closed cell because of compression requirements. Open cell foam has both high density and low density options. High density was chosen because of its flexibility in compression, making the foam push back like latex. Low density was not very good in holding the shorter bottles where there was less compression.

5.2.2 Testing

A single 5 in by 5 in by 9 in cell was constructed from plywood in order to create a test bed. The cell was made wider than the 4 in by 4 in maximum collar width in order to eliminate support assistance from the collars. Both restraint systems were made with multiple materials to satisfy that single cell. A high friction surface was applied to the bottom of the cell and the restraints were attached to the sides to simulate the snap clasps.

First, the carbon fiber support structure was tested and proved it could take all forces applied to it. Next, the latex grid was tested. The latex squares often broke when loaded by either becoming unglued from the frame or ripping in the middle due to high tension. The foam grid secured bottles very well, and after 24 hours of drying, the foam held well to the balsawood section at the bottom. The foam also performed very well in holding stacked bricks. The downside to the foam was that if unsupported by the collar, the foam held poorly without a friction surface holding the bottle at the bottom.

5.2.3 Conclusion

The results from testing are shown in Table 17 below. The parts of the restraint system directly pertaining to the score (weight and speed of use) represent 60% of the final score to reflect their

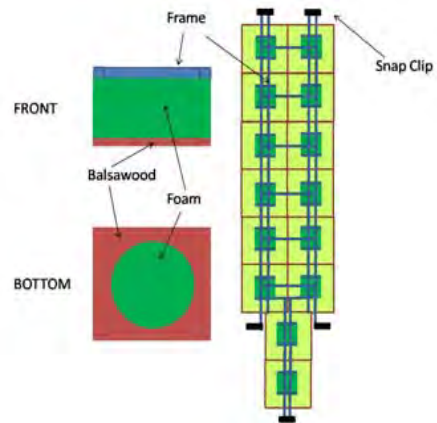


Figure 17 - Foam Grid Layout



importance on final score. The remaining components, pertaining to the final 40% of the score, deal with other important parts of the score.

Table 17 - Foam Grid Testing Results

Figures of Merit	Weight	Foam Grid	Latex Grid
Frame Weight	0.2	0	-1
Restraint System Weight	0.2	0	1
Loading Speed	0.3	0	0
Effectiveness of Holding Bottles	0.1	0	-1
Effectiveness of Holding Pallets	0.1	0	-1
Durability	0.1	0	-2
Total	1	0	-0.4

The results of testing and analysis showed that the foam grid was the best system for payload restraint in our aircraft. The foam system was found to be more sturdy and better at securing all types of payloads. The latex grid, though having a fairly good primary sub-score, was not chosen because it often ripped or broke down and was unreliable.

5.3 Propulsion

After completing static tests, shown in Table 22, the team concluded that the propulsion system had to be redesigned. The new system was designed to supply approximately 100 oz. of thrust while maintaining a pitch speed of 48 mph. Since the number of cells was an important factor in the score, increasing the number of cells while using the same propeller and motor decreased the score. Using the same methodology as discussed in the preliminary design section, a new motor system was found. The results are shown in Table 18.

Table 18 - Motor Comparison

Comparison of Motor Systems Before and After Testing		
	Old	New
Motor	Neu 1506-3Y	Neu 1110-2Y
Gear Ratio	6.7:1	5.3:1
Cells Used	17	12
Max Current draw (A)	24	44
Total Weight (oz.)	21.77	15.72



The new propulsion system is ~30% lighter than the old system. The disadvantage is that the new system puts a greater load on the cells. It drew 44 A at full throttle and required a fuse test to ensure that the fuse would not blow at the time of takeoff. A concentrated effort was put into sizing the new system for the delivery mission because our preliminary testing focused on the payload mission only,

Table 19 - Final Propulsion Design

<u>Comparison of Motor Systems for Missions</u>		
	Delivery Mission	Payload Mission
Motor	Neu 1110-2Y	
Gear Ratio	5.3	
Cell Type	KAN 700	Elite 1500
Cells Used	10	12
Propeller	15x10	19x10
Max Current draw (A)	22	44
Total Weight (oz.)	11	15.72

5.4 Weight and Balancing

Table 20 below shows the weight and balancing of the aircraft for all payload combinations.

Table 20 - Weight and Balancing

<u>Weight Balancing for Different Cargo Configurations</u>						
Configuration	Empty	14 Passenger	4 Cargo	10 Passenger 1 Cargo	7 Passenger 2 Cargo	3 Passenger 3 Cargo
Center of Mass of Entire Aircraft (in)	16	18.84	18.64	18.82	18.84	18.85



5.5 Flight Performance Parameters for Final Design

Table 21 below shows the predicted flight performance for the final design of the aircraft.

Table 21 - Final Design Flight Performance

Performance Data				
	Delivery Mission	Payload Mission	Common Systems	
Propeller	15x8	19x12	Motor	Neu 1110:2Y-2500
Batteries (oz.)	6.5 Oz	10.8	Gear Ratio	5.3:1
Payload (oz)	0	115.2	Speed Controller	Castle Creations 45 Amp
Center of Gravity (in)	16	18.64-18.85	Receiver	JR R790 PCM
CL_{Max}	1.33	1.33	Servos	Hitec hs-81
Stall Speed (ft/s)	19.1	33	System Battery	KAN 700/Elite 1500
Takeoff Speed (ft/s)	21.01	36.3		
Cruise Speed (ft/s)	26	46		
Max Speed (ft/s)	38	51		
Takeoff Distance (ft)	20	70		

5.6 Rated Aircraft Cost

The rated aircraft cost (RAC) can be found using Eq. (4). The predicted weight of the aircraft without batteries and payload is 34 oz. The delivery mission requires 6.5 oz. of battery which gives a RAC of 221 oz². The payload mission has a 10.8 oz. of battery which gives a RAC of 367.2 oz².

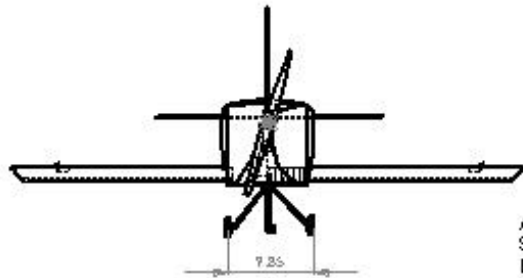
5.7 Final Design Mission Performance

The final design mission performance prediction did not change from preliminary design. See section 4.7 for more detailed prediction of mission performance. The aircraft is predicted to cruise at 26 ft/s and fly for two laps in 4 minutes for the delivery mission. This gives an expected score of 0.307 laps/oz. For the payload mission, the aircraft is expected to cruise at 46 ft/s and complete the 2 lap mission in 1.83 minutes. The estimated RAC is 367.2 oz². The expected score is 0.000778 [1/sec*RAC].

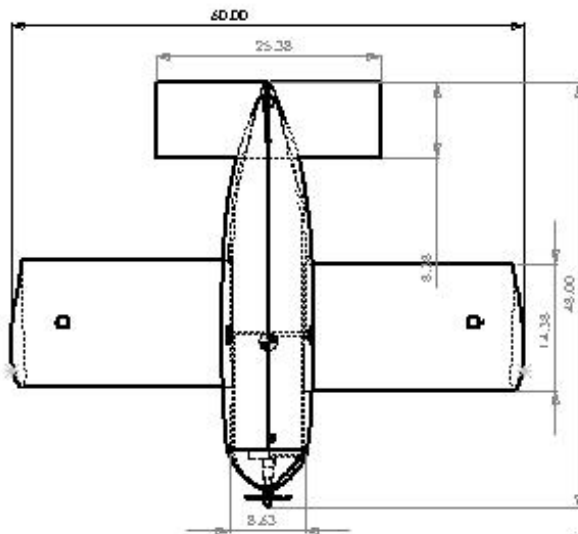
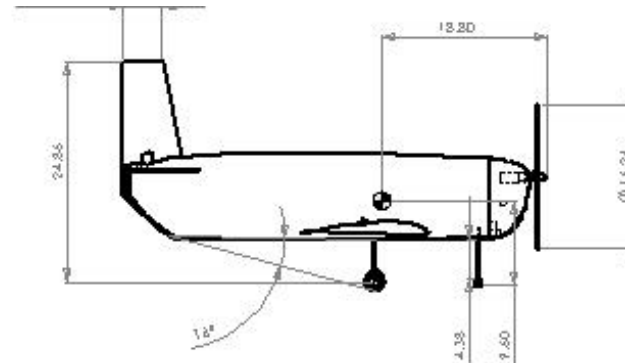


5.8 Drawing View

5.8.1 Three View



All Units in Inches
Scale 1:13
Date: 2/29/08

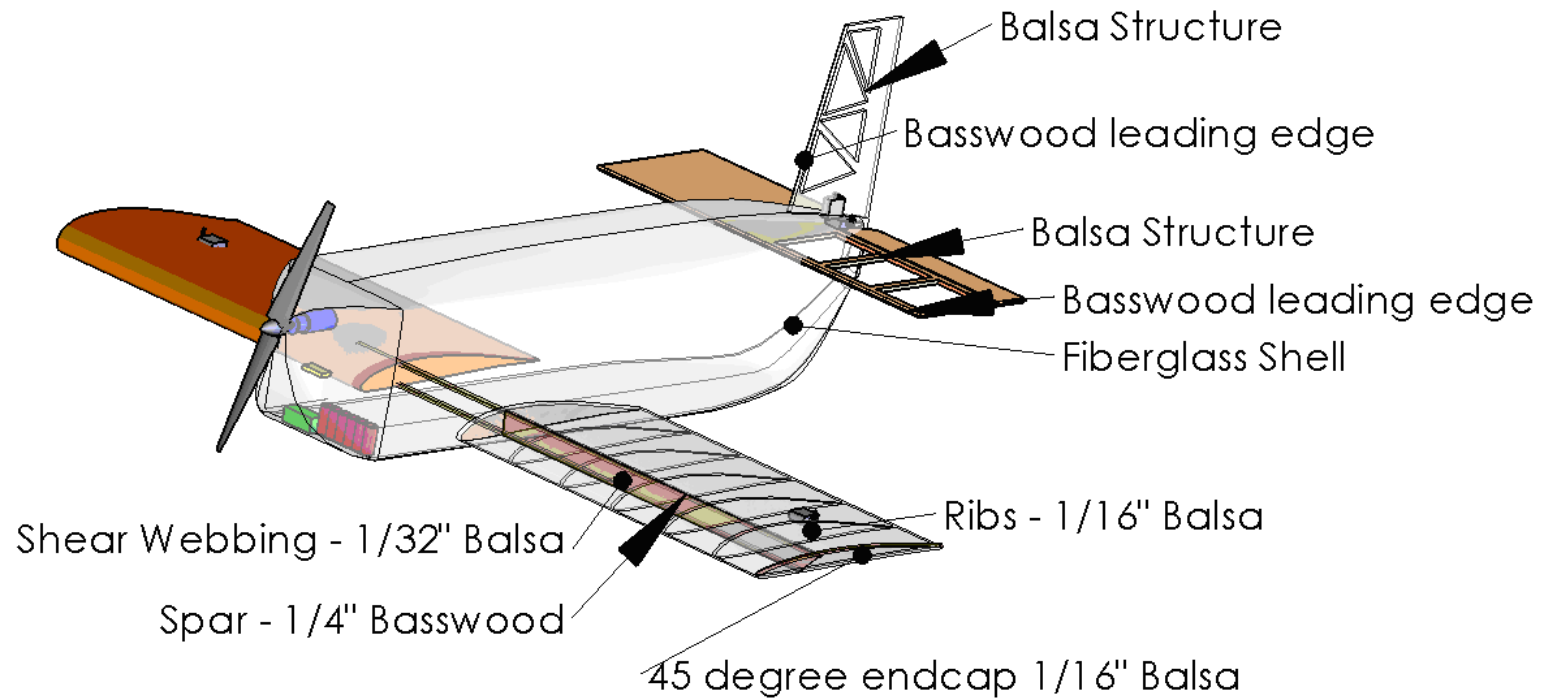


Geometry							
Fuselage		Wing		Vertical Stabilizer with Rudder		Horizontal Stabilizer with Elevator	
Length (in)	46	Airfoil	Selig 2091	Airfoil	Flat Plate	Airfoil	Flat Plate
Max Width (in)	10	Aspect Ratio	4.16	Aspect Ratio	1.5	Aspect Ratio	3
Max Height (in)	10	Chord-root (in)	14.4	Chord-root (in)	6.75	Chord-root (in)	8.5
		Chord-tip (in)	14.4	Chord-tip (in)	4.5	Chord-tip (in)	8.5
		Span (in)	60	Height (in)	11.75	Span (in)	25.38
		Area (ft ²)	6	Area (in ²)	66	Area (in ²)	193

Three-view



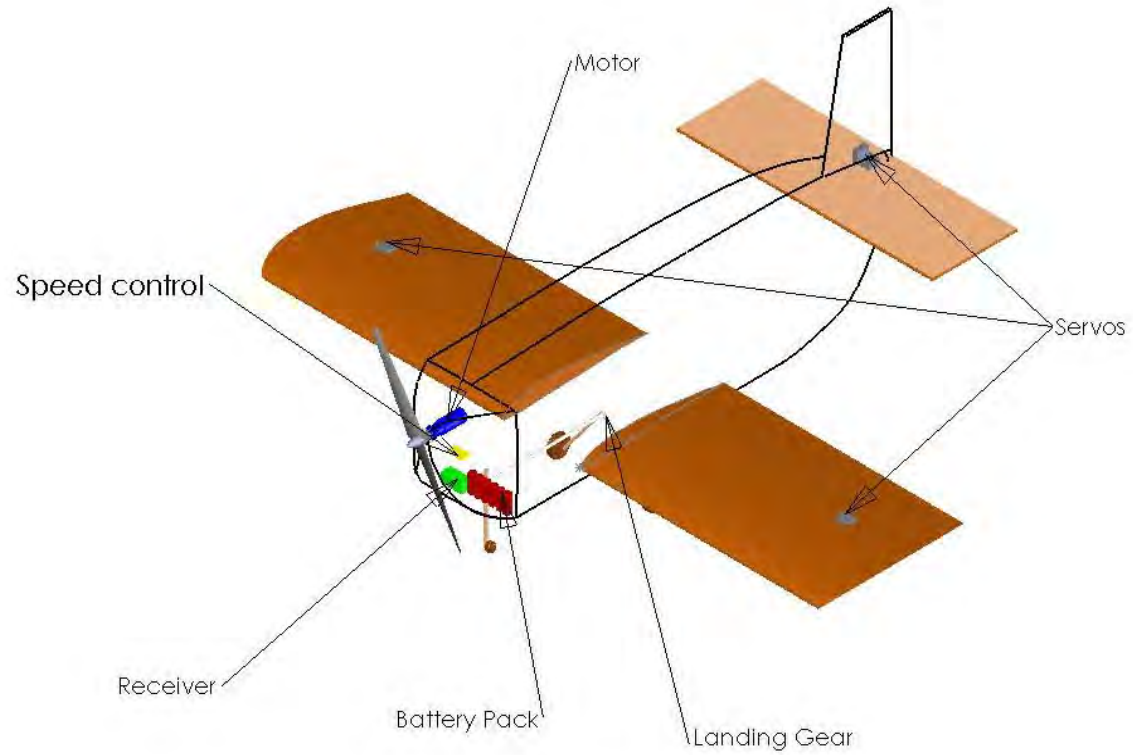
5.8.2 Structural Arrangement Drawing



Structural Arrangement Drawing



5.8.3 System Layout Isometric View

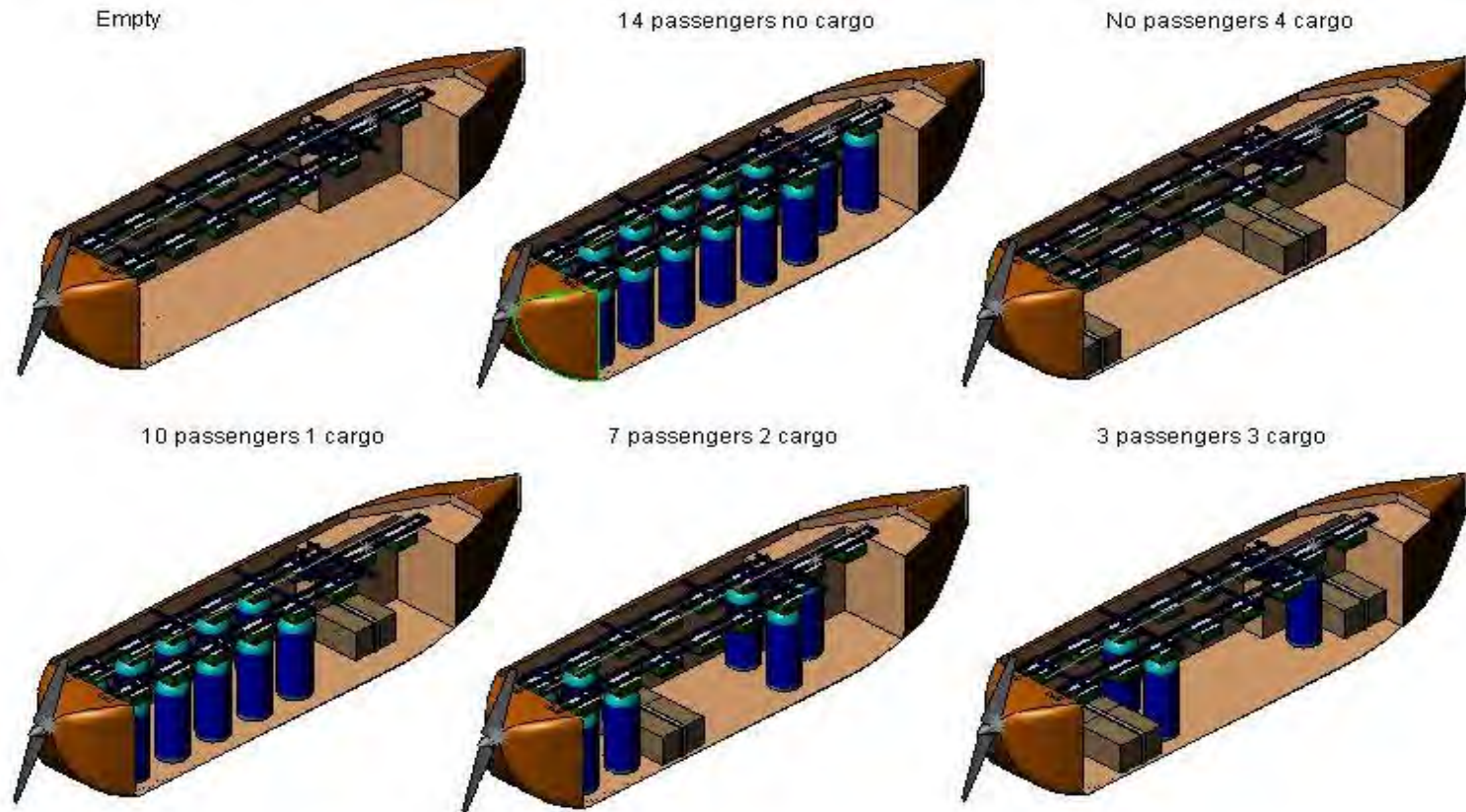


System Layout



5.8.4

5.8.5 Payload Configurations



Payload Configurations

Cargo is restrained by tie downs
Passengers are restrained by top grid
and high friction floor



6 Manufacturing Plan and Processes

6.1 Manufacturing Processes Methodology

All built-up construction was done on full-sized plans much like those found in model aircraft kits. Creating these plans required additional time to draw, but saved time in many other areas because team members had past experience with this construction method. Scaled measurements were taken for components that could not easily be built on top of a set of plans. The landing gear assembly followed this method.

Past experience led to the decision that a fiberglass fuselage is lighter, stronger, and easier to construct than a built-up. This process involved creating a plug from wood and foam. The plug was then used to cast molds. The molds allow for fast and accurate production of the fuselage.

6.2 Cutting of Ribs

The cutting of the wing and empennage ribs was the primary focus of the aircraft's construction that differed from previous experiences, and thus warrants specific consideration. The ribs for the wing and tail can be individually drawn and cut. This is a time-consuming but relatively simple process. Another option is to have the ribs commercially laser cut, but is expensive; it also limits the ability to pick through stock and to find wood with the best density for a particular task. The option chosen was to cut two airfoil section templates, stack the rest of the ribs in between, and sand them all to the particular shape. Maintaining the shape of the ribs is difficult, but faster than cutting the ribs individually and less expensive than professional laser cutting.

6.3 Weight Optimization

Weight was reduced by cutting holes in the center of the wing ribs where the material does not significantly add to the structure of the aircraft. Lightweight structural integrity was added in the form of rib caps. This is advantageous because the caps turned each rib into an I-beam.

6.4 Manufacturing Milestones

Figure 18 shows the Gantt chart for the planned and actual (shown in black) time schedules for the manufacturing process.

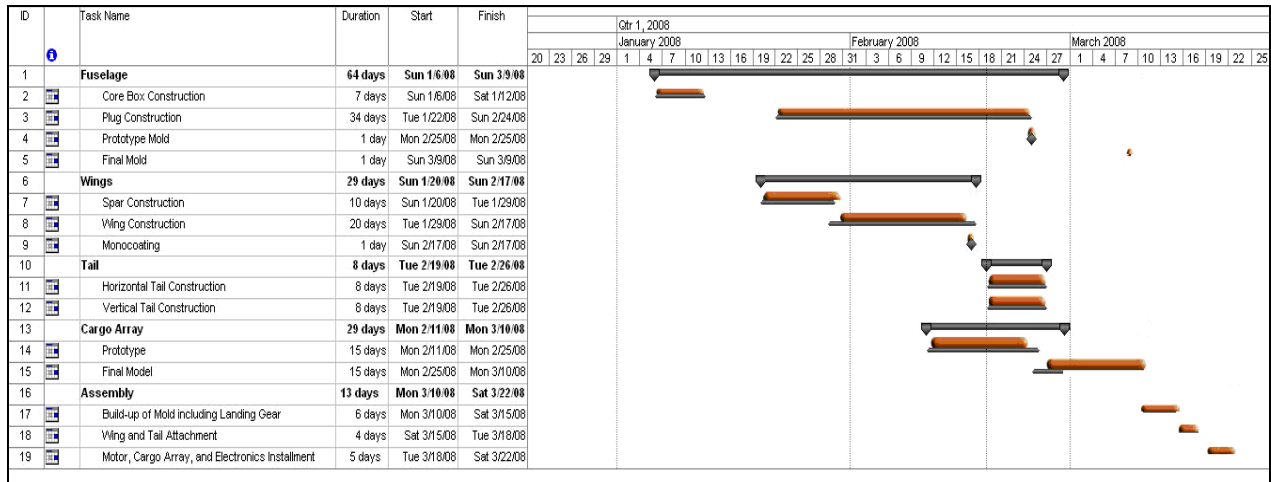


Figure 18 - Manufacturing Gantt Chart

7 Testing Plan

7.1 Test Objectives

Once constructed, all components of the aircraft will be tested to ensure that they meet design expectations and requirements. As of the submittal date of this report, 60% of the test objectives have been completed.

7.1.1 Propulsion

The propulsion package includes the motor and gearbox, propeller, batteries, and speed controllers. Extensive calculations provided a number of packages projected to meet design requirements and all were tested accordingly. Each motor was tested with various propeller sizes and battery packs to ensure that the required amount of thrust can be obtained. All of the electronic equipment will be examined to ensure that regulations are met. The battery packs will be put through a regimen of charge/discharge cycles to verify that each pack holds its charge under operating conditions.

7.1.2 Structure

The structure will be tested to ensure that it can withstand the strains and stresses of operational flight. The wings will also be tested to ensure they produce the expected amount of lift to takeoff and keep the aircraft flying at the expected thrust and speed. Joints will be tested for rigidity so that they do not fail. The landing gear must be tested to guarantee stability during taxi and integrity during landing. The fiberglass fuselage, fabricated from the fewest possible sheets, needs to be tested for integrity while



loaded so that the payload does not cause hull failures. Finally, the payload restraint devices will be tested to make sure that the payload remains fixed for any given aircraft orientation.

7.2 Aerodynamics Test Plan and Data

The team plans to assess the aerodynamic performance of the aircraft by conducting test flights. The stability of the wings and the aircraft will also be evaluated during flight. The flight will also demonstrate whether or not the controls of the plane function efficiently.

7.3 Propulsion Test Plan and Data

The next step in the testing process is to test the propulsion system in a static testing rig, as pictured in Figure 19. The testing will be divided into three phases:

- I. Motor/Propeller testing
- II. Battery testing
- III. Fuse testing



Figure 19 - Static Test Stand

In addition to the conventional propeller and battery tests, a fuse test will be conducted to estimate the amount of time of current overdraw that fuse can endure without blowing.

7.4 Structural Test Plan

Each wing configuration was identically built as a 3 ft x 1.2 ft rectangular wing. Each wing configuration was held by its tips and loaded across its span. Loads and deflections until fracture were recorded. The following wing configurations were created and tested:

1. Foam core with fiberglass shell
2. Balsa wood ribbed core with fiberglass shell



3. Balsa wood ribbed wing

From previous experience, it was noted that the average maximum wing loading was 1-2 lb/ft². The ideal wing configuration should be able to sustain these loads while minimizing weight. The structure selected will also be verified during flight tests.

7.5 Weight and Balance Test Plan

For the aircraft to be statically stable, it is necessary for the center of gravity to be placed in the intended location. Testing each payload configuration will involve holding a rod across the bottom of the aircraft at the calculated center of gravity. If the plane stays steady, the center of gravity is at the correct location; however, if the plane rocks, the design is incorrect and adjustments must be made.

7.6 Mission Performance Test Plan

The mission performance can only be tested by flying the airplane. The following categories need to be evaluated at the time of flight:

- Takeoff Distance: The takeoff distance must be measured because the rules stipulate a maximum takeoff distance of 75 feet.
- Endurance: The endurance of the propulsion system requires testing for both missions. The delivery mission and the payload mission call for the battery pack to last five minutes and two minutes (approximate time required to complete the 2 required laps), respectively.
- Stability: The stability of the aircraft can only be determined visually or through the opinion of the pilot.

7.7 Test Checklist

- Pre-Flight
 - Electrical
 - Make sure fuse is not armed
 - Check all connections
 - Ensure all servos, wires, and fuse are securely fastened
 - Check signal reception and electrical responses
 - Test signal loss response
 - Controls
 - Ensure all control surfaces and control rods secured
 - Check for control surface response and trim
 - Propulsion
 - Check balance and integrity of propeller



- Check motor response
 - Check speed controller programming
 - Structures
 - Ensure CG is located properly
 - Test wing loading
 - Inspect all surfaces for tears and cracks
- In-Flight
 - Take-off
 - Check taxi stability
 - Measure take-off distance and speed
 - Flight
 - Determine Rate of Climb
 - Determine cruise speed
 - Inspect stability
 - Determine maneuverability
 - Check for proper trim
- Post-Flight
 - Check for damages inflicted during flight

7.8 Testing Schedule

- January 13th – Static test of competition motor and propeller
- February 26th – Initial testing of all electrical systems and control motors
- March 1st – Initial round of tests on prototype including static thrust, airframe stability, and in-flight electrical systems operation; maiden unloaded flight and testing of all relevant attributes of the aircraft: takeoff distance and velocity, structural integrity, flight performance, and out-of-range default control system; mock competition run
- March 2nd – First loaded flights and testing of all systems of the prototype aircraft including payload restraint assembly, location of center of gravity, structural integrity with payload, landing gear strength, flight performance with payload, takeoff distance and velocity; series of mock competition runs with each configuration
- March 8th – Final flight tests of prototype with all modifications based on the aircrafts prior performance
- April 1st – Initial static testing of final competition model including airframe integrity, electrical systems operation, control motor testing, loaded structural integrity with all possible payload configurations, landing gear stability under load, and testing of the payload restraint assembly



- April 5th – Maiden unloaded flight of final competition model and testing of all important attributes of the aircraft
- April 6th – First loaded flights of final model and testing of all relevant attributes
- April 12th – Second round of flight testing on final competition aircraft with all modifications based on prior flight performance

8 Performance Results

8.1 Propulsion Testing

8.1.1 Propeller Testing

The first motor configuration tested was the Neu 1506/3Y-1700 with a 6.7:1 gearbox. A 19x10 propeller was used with Elite 1500 battery cells. The data found was 20% lower than expected.

Table 22 - Motor Test 1

<u>Motor Test - Neu 1506/3Y with 6.7 Gearbox - 19x10 Propeller</u>		
	Static thrust (oz.)	Peak Current Draw (A)
Actual	94	24
Predicted	115.3	30
Percentage Error (%)	18.4	20

In order to ensure that the data were not skewed by a faulty motor, a second test was done with a different motor configuration. The results were approximately the same.

Table 23 - Motor Test 2

<u>Motor Test - Neu 1506/3Y with 5.3 Gearbox (Control Test) – 16x10 Propeller</u>		
	Static thrust (oz.)	Peak Current Draw (A)
Actual	81	18
Predicted	97.3	28.1
Percentage Error (%)	16.7	35.9

The next step was to find out the cause behind the error given by the optimization program. It was determined that the batteries may not have performed up to manufacturer specifications. In order to confirm that theory, a battery test was performed.



8.1.2 Battery Testing

Using the static testing rig, the actual capacity and internal resistance of the battery in question was estimated. The results were drastically different from the manufacturer's specifications.

Table 24 - Battery Test with Elite 1500 Cells

Battery Test with the Elite 1500 Cells			
	Internal Resistance(mΩ)	Capacity(mAh)	Peak Current
Actual	0.008	1400	45
Predicted	0.004	1500	35
Percentage Error(%)	100	6.6	28.5

The battery test confirmed that the batteries were not functioning properly. However, the tests showed that the batteries can handle much higher currents than specified by the manufacturer. Because the error in the preliminary designs was significant, the propulsion system required a redesign. The new propulsion system draws much higher currents so a fuse test was performed.

8.1.3 Fuse Testing

To facilitate the fuse test, a fuse was connected to a power source and the time required to blow the fuse was recorded. The propulsion system is estimated to run at 50 A at the time of takeoff(~30 seconds). For that reason, the fuse was tested at a current of 50 A. The fuse required more than 50 seconds to blow, validating the feasibility of such a propulsion system.

8.2 Structural Testing

Mock up wings of three structural configurations were made and loading tests were done. The results are shown below, in Figure 20.

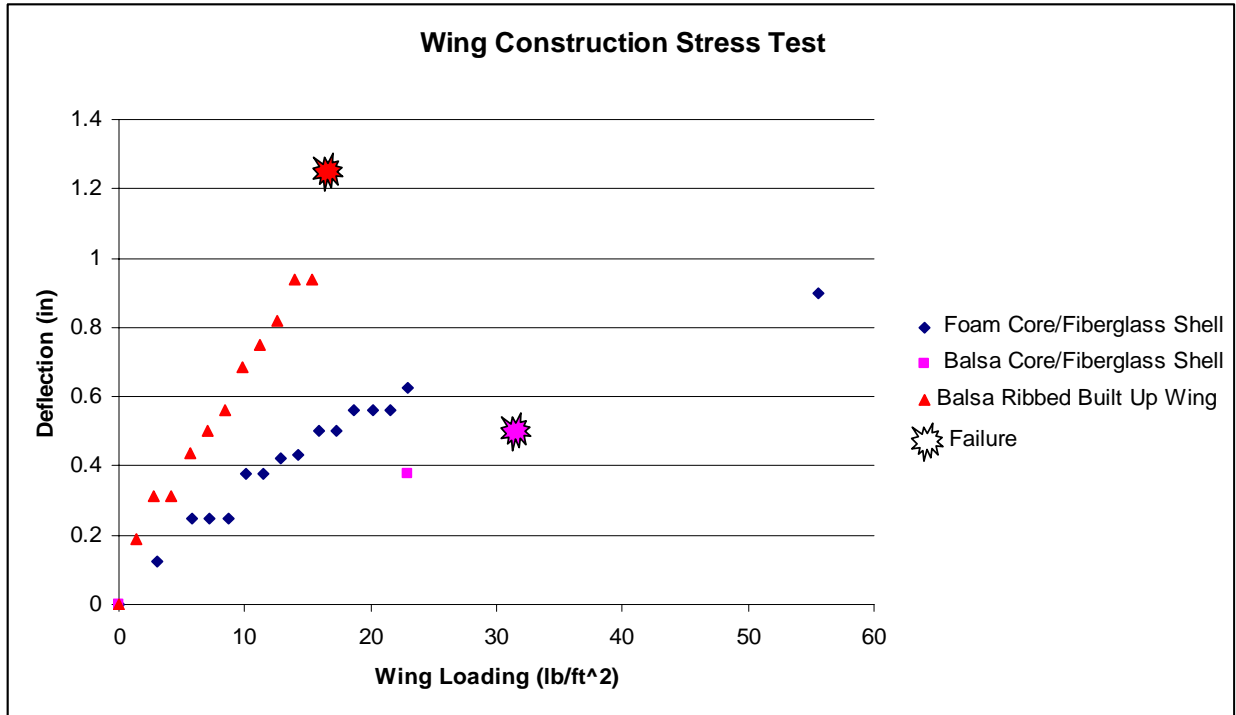


Figure 20 - Wing Construction Method Structural Test

The results show that the plain balsa wing is appropriate since it can withstand 700% of the target wing loading (~2lb/ft²). The other configurations would result in an inefficient use of resources.

8.3 Aerodynamics Testing

At the time of the report submittal, the team has not performed any test flights. There was a steep learning curve in composite fuselage construction which caused the delay. The projected maiden flight date is March 7th. The goals of the first flight are:

- Verify the aircraft takes off within 75 ft with headwind greater than 5 mph.
- Verify the aircraft is stable during ground roll at full throttle
- Verify the aircraft is stable in flight in both loaded and unloaded condition.

The subsequent flights will focus on optimizing the wing and tail angle of incidence to minimize drag as well as verifying the aircraft exhibits the predicted cruise, climb, and loiter performance.



9 References

- [1] Raymer, D. P. *Aircraft Design: A Conceptual Approach*, 3rd ed., AIAA Education Series, Reston, Virginia, 1999.
- [2] Nicolai, L. M. *Fundamentals of aircraft Design*, Mets, San Jose, California, 1975.
- [3] Selig, M. *Summary of Low Speed Airfoil Data: Volume 2*, SoarTech Publications, 1996.
- [4] Simons, M. *Model Aircraft Aerodynamics*, 4th ed., Martin Simons, London, UK, 2002.
- [5] Katz, A. *Subsonic Airplane Performance*, SAE, Warrendale, Pennsylvania, 1994.
- [6] Nelson, R.C. *Flight Stability and Automatic Control*, 2nd ed., McGraw-Hill, New Jersey, 1997.
- [7] McCormick, B. W., *Aerodynamics, Aeronautics, and Flight Mechanics*, John Wiley & Sons, New York, 1994.
- [8] AIAA, "Design, Build and Fly Competition 2007/2008", URL: <http://www.ae.uiuc.edu/aiaadb/>. [Cited 05 of September 2007].
- [9] Nicolai, L. M. *Estimating R/C Model Aerodynamics and Performance*, Paper for SAE Aerial Competition, June, 2002.
- [10] Demasi, L. "Induced Drag minimization: a Variational Approach Using the Acceleration Potential". *Journal of Aircraft*, AIAA, June, 2006, Vol 43, pp 669-680.

2007/2008 AIAA Foundation

Cessna Aircraft/Raytheon Missile Systems

Student Design / Build / Fly Competition • Wichita, KS • April 18-20th, 2008

Design Report “Flying Nemo”

Oklahoma State University Orange Team



**FLYING
NEMO**

OKLAHOMA STATE UNIVERSITY



Table of Contents

1.0.	Executive Summary	3
1.1.	Design Summary Description	3
1.2.	Design Features Keyed to Significant Mission Requirements.....	4
1.3.	Performance and Capabilities.....	4
2.0.	Management Summary.....	4
2.1.	Team Organization	5
2.2.	Schedule / Milestones.....	5
3.0.	Conceptual Design.....	6
3.1.	Mission Requirements Summary.....	6
3.2.	Initial Aircraft Design Concepts.....	10
3.3.	Conceptual Aircraft Summary.....	20
4.0.	Preliminary Design	21
4.1.	Mission Modeling and Analysis Methodology.....	21
4.2.	Design and Sensitivity Studies	24
4.3.	Aircraft Sizing and Trade Studies	28
4.4.	Mission Model Capabilities and Uncertainties	32
4.5.	Estimates for Lift, Drag, and Stability	34
4.6.	Aircraft Mission Performance Estimates.....	39
5.0.	Detail Design.....	40
5.1.	Dimensional Parameters	40
5.2.	Structural Characteristics / Capabilities.....	40
5.3.	Systems and Sub-Systems.....	42
5.4.	Weight and Balance.....	43
5.5.	Flight Performance	46
5.6.	Rated Aircraft Cost (RAC)	47
5.7.	Mission Performance	47
5.8.	Drawing Package.....	47
6.0.	Manufacturing Plan and Processes	52
6.1.	Component Manufacturing Processes	52
7.0.	Testing Plan	55
7.1.	Propulsion and Structural Testing	55
7.2.	Flight Testing	56
8.0.	Performance Results.....	56
8.1.	Propulsion Performance	57
8.2.	Structural Performance.....	58
8.3.	Demonstrated Aircraft Performance	59

1.0. Executive Summary

The techniques used to design and build Oklahoma State University Orange Team's entry in the 2007/2008 Cessna/Raytheon Missile Systems student Design/Build/Fly competition are outlined in this report. The aircraft was optimized to fly two missions: an empty delivery mission and loaded passenger / cargo mission. The overall contest score is computed from the written report score, the total flight score, and the rated aircraft cost, all of which will be outline in the sections that follow.

1.1. Design Summary Description

At the start of the conceptual design phase, aircraft approximations and figures of merit (FOM) were developed, including system weight, loading time, aerodynamic efficiency, and propulsion weight. A nonlinear, multidimensional optimization program was developed to analyze the entire flight profile for each mission and aided in the development of sensitivity studies for screening the figures of merit. From in-depth sensitivity studies, the passenger / cargo combination mission was found to be of higher importance than the delivery mission. The payload mission is scored twice, and the delivery mission is only scored once. Also a plane optimized for high payload weight and short takeoff distance is more easily adapted to the unloaded endurance mission than the reverse.

Sensitivity studies showed the design should be aerodynamically efficient, have a low structural and propulsion weight, and have a quick load time. The driving aspect of the design was a lightweight, quick-loading payload restraint system. The payload restraint system is required to store and secure combinations of passengers (water bottles with spacing collars of various heights) and cargo (clay bricks). A system was devised that uses a double hatch to engage the restraint system concurrently with the closing of the main payload door. A high aspect ratio biplane was chosen for high aerodynamic efficiency. The plane was placed diagonally in the 4 ft by 5 ft spot size, which yielded a maximum wing span of 5.85 ft. The diagonal placement of the plane restricted the horizontal tail to an asymmetric planform, which allowed for enough tail area for an adequately stable design. A single motor was chosen for efficiency and weight. The motor and propeller were setup as a tractor system for simplicity and reliability over a pusher or pod mounted system.

The preliminary design stage continued with aerodynamic trade studies and sizing, optimization of the propulsion system, and estimation of component strengths and weights. A study was conducted to find the best wind speed to design around. A wing with 6.5 sq. ft of effective area was shown to out perform any other configuration from 0 to 15 mph winds. An airfoil was chosen based on the best combination of aerodynamic performance, structural efficiency, and manufacturability. The horizontal, vertical, and all four control surfaces were sized to give adequate stability and control at all flight speeds. The propulsion system was optimized using component testing and overall system modeling. A Medusa 1700 motor and 20 in. propeller were chosen to meet the take off requirements. Twelve Elite 1500 batteries were selected to provide enough endurance for the payload mission. The structure was optimized through appropriate load paths and repeated construction and testing components.

The detail design phase integrated the aerodynamic, structural, and propulsive work done in preliminary design. Sizing dimensions were frozen at optimum values, system and sub-system component was specified to meet performance requirements, and every structural component was built and tested to establish the final RAC, which was determined to be 2.14. Performance analysis determined the maximum lift-to-drag ratio was 8.7 and the cruise speeds were 30 ft/s for the delivery mission and 40 ft/s for the payload mission, from which the minimum energy required was found. This design is the best solution because it is the most efficient configuration possible and is built to the limits of material strength and required energy.

1.2. Design Features Keyed to Significant Mission Requirements

The payload loading scheme was designed to both minimize the load time and maximize system redundancy to ensure easy repetition and safety in loading. The remaining aircraft systems were designed around the payload mechanism, so that no design decisions were made to compromise the integrity of the loading system.

The wing was placed diagonally in the spot size to maximize aspect ratio and thus aerodynamic efficiency. The effective aspect ratio was further increased through the use of a biplane with endplates. The asymmetric tail fits diagonally in the spot size, provides adequate stability, and helps counter the motor torque while allowing more payload loading access on the opposite side of the fuselage.

The propulsion system was optimized by bench testing motors and batteries to find the most efficient combination and through dynamics testing of propeller in the OSU wind tunnel. The propulsion system was designed to minimize weight while maintaining a high efficiency.

The plane is constructed using carbon fiber, fiberglass, and balsa to distribute the aircraft loads in order to minimize the system weight. Computer numerical control (CNC) molds and templates, generated with detailed drawings, were used to construct aerodynamic surfaces precisely and quickly.

1.3. Performance and Capabilities

The final aircraft has superior characteristics in both the ground loading missions and in flight handling qualities. Performance predictions for the first mission indicate a score of 13.16 before normalization. The aircraft in the first mission flies 4 laps cruising at 30 ft/s with 12 KAN 700 batteries weighing 0.412 lbs. If the second mission has a payload loading time of 0.33 minutes then the mission score will be 0.816. This mission is flown with the heaviest payload and 12 Elite 1500 batteries weighing 0.612 lbs cruising at 40 ft/s. The system weight for the aircraft was 4 lbs.

2.0. Management Summary

The Orange Team modeled most of its operations after a small company. Managers balanced their own workloads as well as delegating tasks throughout their teams in order to maintain a tight time schedule determined before the project's beginning. The team organization and function is detailed in this section.

2.1. Team Organization

The Orange Team was separated into groups which focus on primary design areas of the aircraft. This hierarchy is illustrated in Figure 2.1. The chief engineer oversees all aspects of the design, construction, and flight testing, followed closely by group leads for aerodynamics, structures, and propulsion. To aid in the design of the aircraft, a computer-aided design (CAD) lead was also appointed to complete all the technical drawings. This team arrangement provides an effective solution so key team members can specialize in certain elements of the design and construction.

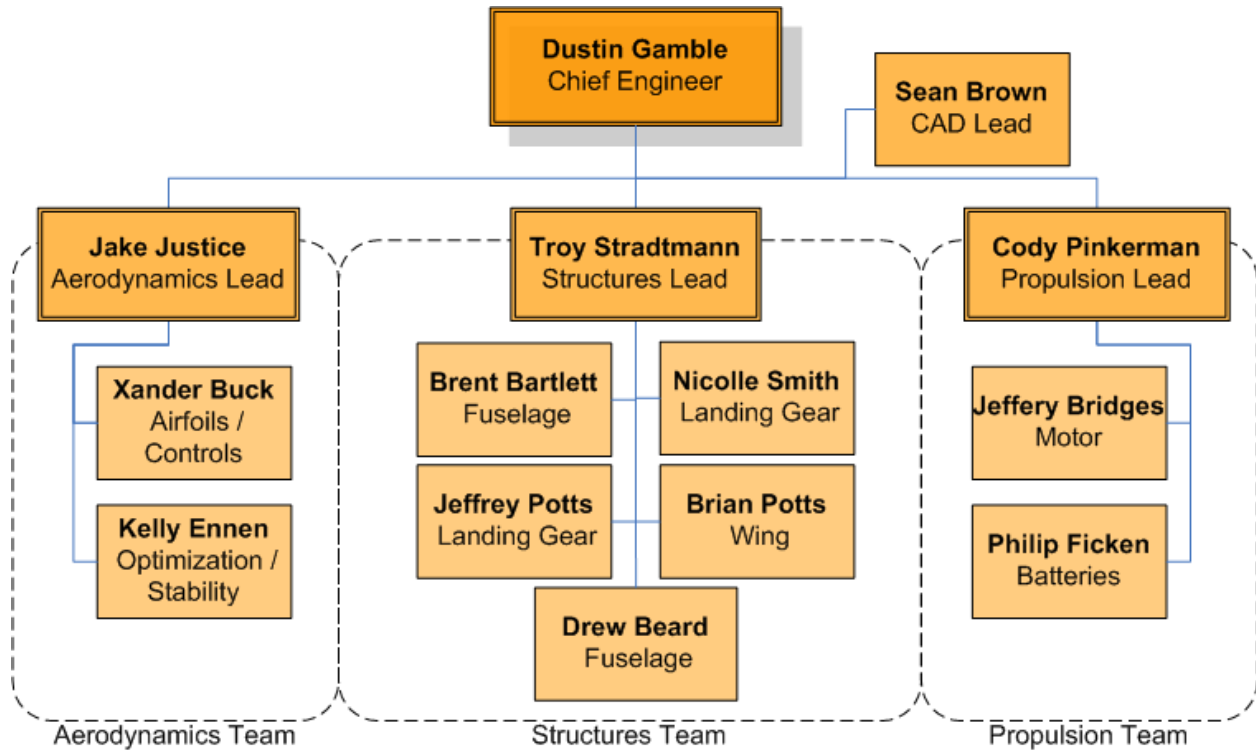


Figure 2.1: Orange Team Organizational Chart

2.1.1. Technical Groups

In order to complete a project of this magnitude, the members of this team were divided into three task-specific groups: Aerodynamics, Structures, and Propulsion. This helped encourage specialization of tasks and facilitated higher quality results. Each team was primarily responsible for developing criteria to evaluate design options during the conceptual phase. Additionally, the teams were in charge of selecting components and subcomponents as they related to their individual fields as well as sizing any and all systems required for performance. Finally, each team facilitated specific tests and simulations that led to the optimization and tuning of the final aircraft performance.

2.2. Schedule / Milestones

The overall project was broken down in to three phases. The first phase consisted of the conceptual design, where overall airplane concepts are discussed and several different ideas were analyzed. The next step was the preliminary / detailed design where the general concept of the aircraft was dimensioned

in preparation for construction. After the detailed design of the aircraft was complete, the construction phase began. This started with a prototype airplane which was used for the final phase of the flight testing. Once flight testing had begun, minor changes were made to complete the final aircraft. A Gantt chart, shown in Figure 2.2, was created to help complete the aircraft on time.

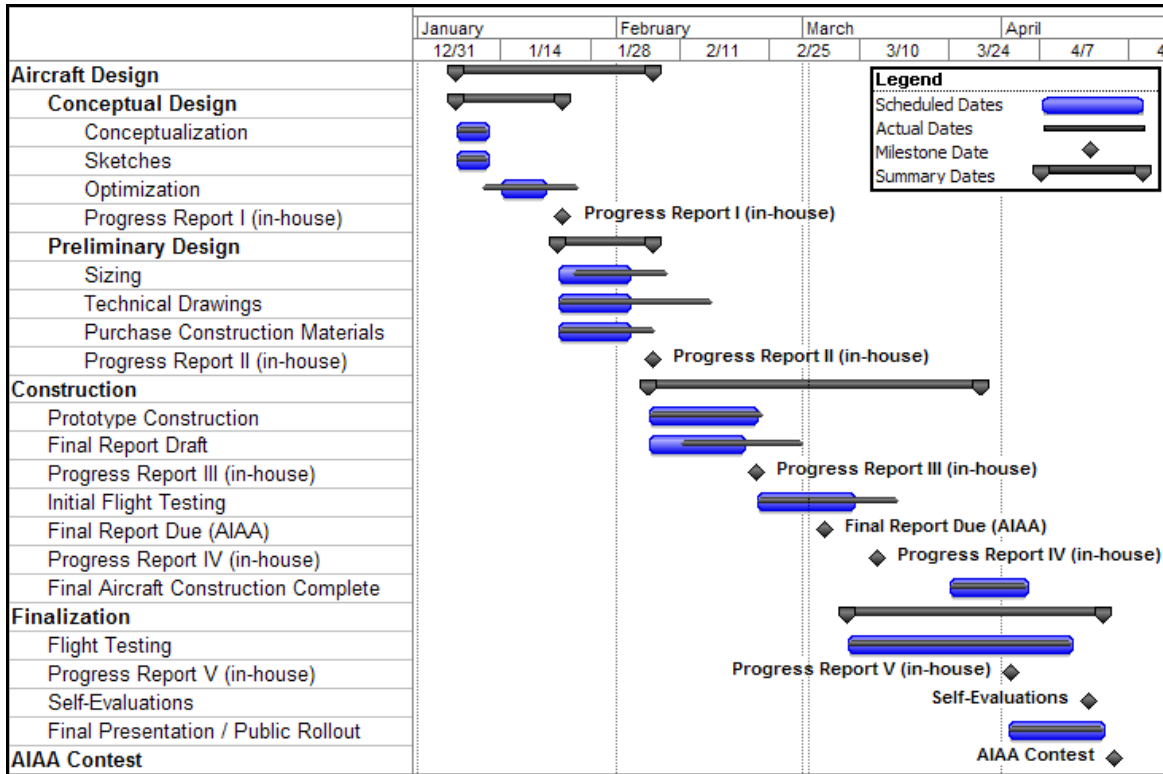


Figure 2.2: Project Schedule

3.0. Conceptual Design

During the conceptual design phase, the team started with as many ideas for ways to complete the various tasks stipulated by the rules. All ideas brought forth were divided amongst the members and technical teams to be researched and evaluated. The concepts were evaluated using morphological charts and weighted decision matrices. Once each idea was discussed and evaluated, they were brought back together and their ability to coalesce into a cohesive design was assessed. Subsystem and component potential was again divided amongst the teams and evaluated for strengths and weaknesses. Once all relevant decisions had been made, the team once again convened to assemble the ideas into a consistent conceptual design.

3.1. Mission Requirements Summary

The contest consists of two missions, one delivery mission and one payload mission. The delivery mission will be completed once and the payload mission will be completed twice, which may only be attempted after successful completion of the first mission. In both missions, the plane must fit in a spot size of 4 ft by 5 ft. This led the team to creatively analyze the geometry within the box size. Also, the

plane must takeoff within 75 ft for both missions. This resulted in the analysis of several methods of obtaining a short takeoff. One 360°-turn in the opposite direction of the flight pattern is required on all missions. Unlike previous years, teams will not be required to call out a battery pack until they enter the stage box for the specific mission. In addition, the team is only allowed to complete one successful delivery mission and two successful payload missions. No subsequent runs may be flown in order to increase score beyond that obtained during the first successful attempts.

3.1.1. Delivery Mission Requirements

The delivery mission will test the plane emptied of all payload, containing only the payload restraint system needed for the second mission. The plane must fly as many laps around the course as possible in a 5 minute time period. The time will start at the beginning of take-off, and the aircraft must land successfully on the runway for any score to count.

3.1.2. Delivery Mission Score Analysis and Design Requirements

In the scoring function for the first mission, shown in Equation 3.1, no factor bears more importance than another. Obviously, as battery weight increases, the number of laps should increase due to more available energy. But, at some point, the required average cruise speed for so many laps would decrease efficiency, so a maximum case of 5 laps was established. Figure 3.1 shows the delivery mission score function, with the various lines representing different numbers of completed laps. Table 3.1 shows a few possible battery cell and lap combinations with corresponding scores.

Equation 3.1: Delivery Mission Score

$$Score_{ferry} = \frac{laps}{weight_{battery}}$$

Table 3.1: Delivery Mission Scores

		Number of Elite 1500 Cells (0.051 lbs per cell)			
		10	14	18	22
Number of Laps	1	1.96	1.40	1.09	0.89
	2	3.92	2.80	2.18	1.78
	3	5.88	4.20	3.27	2.67
	4	7.84	5.60	4.36	3.57
	5	9.80	7.00	5.45	4.46

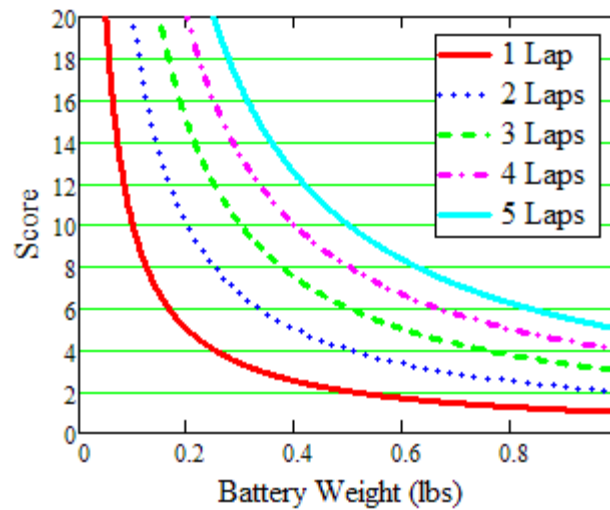


Figure 3.1: Delivery Mission Score Function Analysis

This mission is a trade off between speed and efficiency. A fast plane will require more power and more batteries but will complete more laps. On the other hand an efficient airplane will have a lighter battery weight but will complete fewer laps.

3.1.3. Payload Mission Requirements

The payload mission will require the teams to perform a timed loading of their aircraft with a specified payload combination. The possible configurations for this contest presented a unique challenge. One half liter plastic water bottles and clay bricks were used to simulate passengers and cargo pallets to be stowed within the aircraft during the required 2-lap flight. Each payload element's dimensions and weight are shown in Table 3.2.

Table 3.2: Payload Items with Size and Weight Approximations

	<u>Width (in)</u>			<u>Height (in)</u>			<u>Weight (lb)</u>		
	<i>Min</i>	<i>Nominal</i>	<i>Max</i>	<i>Min</i>	<i>Nominal</i>	<i>Max</i>	<i>Min</i>	<i>Nominal</i>	<i>Max</i>
Bottles	2.400	2.50	2.600	7.600	7.95	8.300	0.475	0.50	0.525
Blocks	3.800	4.00	4.200	2.533	2.67	2.800	1.530	1.80	2.070

The water bottle —“passengers” are also outfitted with a foam collar to limit their spacing. The collars have a maximum spot size of 4 in by 4 in. The collars may not overlap, and each passenger is required to stay upright during flight. The passengers must be restrained within the cabin securely with the hatch open. The team members will be required to invert the loaded aircraft just before flight to demonstrate the payload restraint system's security. None of the restraints can make use of the collar, that is, no restraint system may hold or attach to the collar itself. The cargo pallets may be oriented in any way or stacked for flight, but passengers can only be stacked if there is structural non-removable floor between each level.

In addition to the variability of the individual payloads, any one of five possible combinations of bottles and bricks will be given to the team during flight preparation. The list of the possible payload combinations and their approximated weights is shown in Table 3.3.

Table 3.3: Payload Configurations with Weight Ranges

<u>Payload Configuration</u>				<u>Weight (lb)</u>		
				<i>Minimum</i>	<i>Nominal</i>	<i>Maximum</i>
14	Passengers			6.650	7.00	7.350
10	Passengers	1	Cargo Pallet	6.280	6.80	7.320
7	Passengers	2	Cargo Pallets	6.385	7.10	7.815
3	Passengers	3	Cargo Pallets	6.015	6.90	7.785
		4	Cargo Pallets	6.120	7.20	8.280

3.1.4. Payload Mission Score Analysis and Design Requirements

The payload mission score function is shown in Equation 3.2 and Equation 3.3, and is graphed in Figure 3.2 as a function of battery weight, with various loading time and system weights.

Equation 3.2: Payload Mission Score

$$Score_{payload} = \frac{1}{(RAC) \cdot (time_{load})}$$

Equation 3.3: Payload Mission RAC

$$RAC = (weight_{system}) \cdot (weight_{battery})$$

This large score difference shows the high importance that loading time plays in the score function, especially at lower battery weights. As system weight decreases score increases, with more of an increase occurring at quick loading times and low battery weight. As illustrated, a plane that can be loaded in 30 seconds benefits much more from lower overall system weight than one that takes 100 seconds to load. Therefore, payload loading must be a quick motion to keep the loading time to a minimal and allow the aircraft weight minimization process to be as effective to the score as possible.

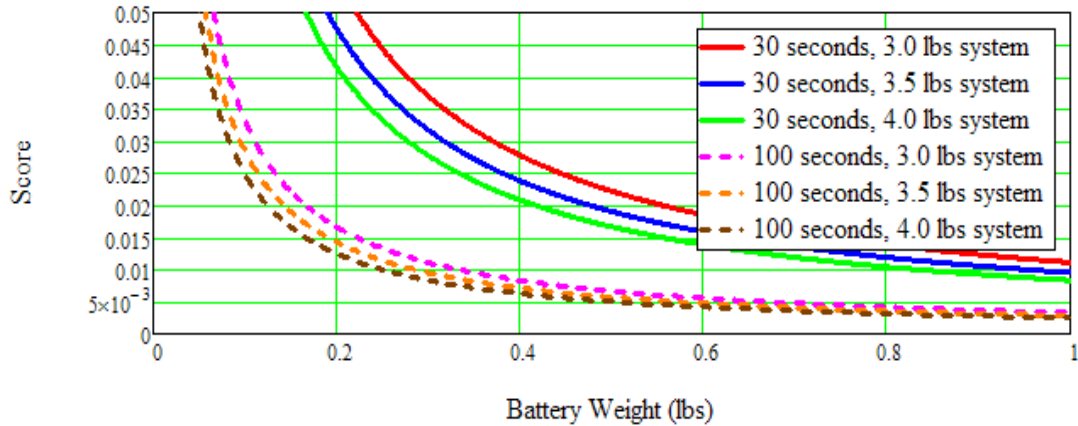


Figure 3.2: Payload Mission Score Function Analysis

3.1.5. Design Requirements Summary

The total score function for the entire contest is shown in Equation 3.4. The delivery mission is summed with the two payload missions and multiplied by the report score to yield the overall score. Aside from stressing the importance of a very high scoring report, the function shows that the payload performance is approximately twice as important as the delivery mission score.

Equation 3.4: Overall Scoring Function

$$Score = (Score_{report}) \cdot (Score_{ferry} + Score_{payload1} + Score_{payload2})$$

The battery pack may be changed for each mission. Just prior to approaching the starting line, the team could choose a battery pack based on any number of conditions, such as wind speed or approximate weight of the clay bricks due to moisture variance. Therefore, the team can prepare several battery packs for various flight conditions and payload combinations, thus using any unforeseeable variance to the team's advantage.

In order to design the best possible scoring plane, the team sought to find a design which would yield the highest total score. The team decided that the most important task would be designing a payload restraint system that could be loaded in as little time as possible, thus providing the maximum benefit from system and battery weight reduction throughout the design. The team also identified the payload mission as the main design focus due to the loaded 75-ft takeoff, coupled with its greater influence on score. The appearance of high efficiency in both mission's analysis indicated that a plane designed for high efficiency in the payload mission could be better adapted for high efficiency in the delivery mission.

3.2. Initial Aircraft Design Concepts

Once payload securing research and analysis was performed, the team moved their focus onto designing the structures and aerodynamics of the final airplane. The following sections detail the concepts and arrangements / integration of major components into the design. Initially, the team developed certain figures of merit (FOM's) with which to evaluate the concepts. For each portion of the design, the team identified which of the FOM's were relevant in the examination of the ideas, in addition to possibly defining additional FOM's for assessment. After defining specifics about each concept, an objective comparison was made via a weighted decision matrix.

3.2.1. Morphological Chart

The conceptual design of the main aircraft components began with general brainstorming and the creation of the morphological chart shown in Table 3.4 in order to maximize the number of concepts for each of the major components and overall aircraft configurations. This is crucial to the team's success because it ensures that an optimal and feasible design that could have the potential to win will not go overlooked. The concepts tabulated below will be explored in more detail in the following sections and concepts will be eliminated based on FOM's derived from the scoring function.

Table 3.4: Morphological Chart of Conceptual Ideas

Loading Scheme	Removable "Efficiency Loading" Tray			Grab-And-Carry Technique		
Payload Restraints	Rubber Band Collar	Double Hatch	Flex-Wall	The Wedge		
	Straw Lid	Press Fit Foam	The Accordion	Safe-T-Wire		
Fuselage Shape	"The Ice Cube Tray"		"The Blue Catfish"		"The tuna"	
Aircraft Type	Conventional	Blended	Lifting Body	Flying Wing		
Wing Configuration	Monoplane	Biplane	Canard / Tandem			
Spot Size Orientation	5' wing, 4' fuselage		4' wing, 5' fuselage		Diagonal Wingspan	
Empennage	Conventional	T-Tail	V-Tail	Cruciform Tail	Y-Tail	H-Tail
Landing Gear	Tail Dragger		Tricycle		Bicycle	
Propulsion Mounting	1 Tractor	2 Tractor	1 Pusher	2 Pusher	1 Pod	2 Pod

3.2.2. Figures of Merit

Based on the design requirements translated from the performance requirements and score function analysis, the team derived several FOM's that encompassed the desired qualities of the aircraft.

- **Battery Weight** – The weight of the battery packs has strong influence on mission scores and must be minimized to earn the highest score.
- **System Weight** – The system weight of the aircraft was defined as the weight of the aircraft including any payload-loading devices or restraint components but without any payload or batteries. System weight must be minimized to achieve the highest score.
- **Loading Time** – The time to load the aircraft with the specified payload combination was considered, as well as secure all components and close the aircraft to ready it for flight.
- **Aerodynamic Efficiency** – Due to the repeated appearance of the battery weight in both the payload mission RAC as well as the delivery mission score, an FOM depicting a design's propensity for efficient battery usage and flight was created.

The main figures of merit mentioned above helped the team organize and score conceptual ideas for each of the major systems incorporated into the aircraft. These FOMs are broad to keep the main goals of the aircraft's performance at the forefront of the design process. However, more specific FOMs will be assigned as each system is evaluated. The more specific FOM's will fall under some or all of the main FOM's shown bulleted above depending on relevance to the system.

3.2.3. Payload Loading Scheme

In order to design a fast and efficient loading system, the team first considered two schemes based on Lean Six Sigma. In Lean Six Sigma, the methodology is to provide quality products with the least amount of wasted time and resources. By counting the number of actions and the distance traveled from the starting line to the aircraft for the three loading crew members, the two loading schemes were assessed for their merits of time, actions (or chances for human error), and efficiency (both with payload-procuring and restraint).

The first system involves using a speed-loading device, or —efficiency loader”, that accelerates payload retrieval, organization, and restraint by incorporating the system into one manageable tray. This system is illustrated in Figure 3.3a. The Removable —Efficiency Loading” Tray scheme allows the loading crew to perform three independent actions in tandem, so that a bottleneck does not form in the loading process. The tray acts both as a speed-loader, which could be loaded with payload and quickly secured into the airplane, and as a grid system to control the center of gravity location and keep the components separated in the fuselage. The number of actions for one crew member is kept to a minimum. An important negative aspect of this scheme is Person 2, shown in blue. At the end of action two, the person must run to the airplane and properly secure a fully-loaded tray (in the fourteen bottle combination). The chances for human error are significant; the entire outcome of the contest is places on one person's ability not to trip or drop a cumbersome tray during transport. There are wasted actions by both the person prearranging the payload and then moving those items to the tray.

The Grab-And-Carry technique, shown in Figure 3.3b, involves simply running to the table and grabbing as many payload components as possible, running to the airplane and then loading and

restraining the payload. In this manner, the payload items are touched only once before arriving at the airplane. The Grab-And-Carry will be optimized for speed and error minimization. For the worst case of fourteen bottles, the first two people grab four bottles each and the last person grabs the remaining six bottles. Persons 2 and 3 work in parallel while Person 1 is staggered by the payload manifest so that all three people are not trying to grab payload items and load the airplane at the exact same time. Persons 2 and 3 may also aid Person 1. Due to the low number of actions required, as well as the efficiency and redundancy of the staggered ground crew members, the Grab-And-Carry scheme was selected as the most effective loading scheme.

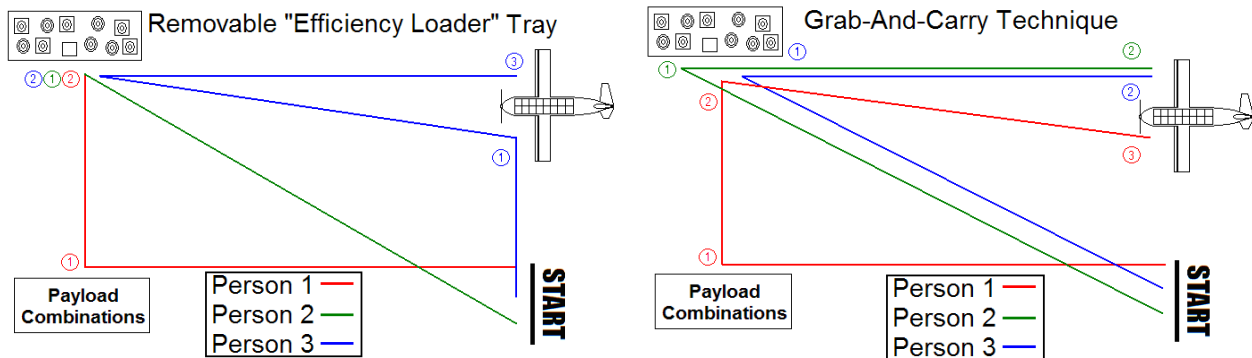


Figure 3.3: Loading Diagrams for "Efficiency Loading Tray" [a] and "Grab-And-Carry" [b]

3.2.4. Payload Restraint System

Brainstorming payload restraint ideas began at the onset of the team meetings. The team decided that the best payload restraint system would be one that combined quick and simple loading while reliably securing the payload. The group members individually brainstormed ideas before bringing them to a group concept meeting where they were presented to the team and coalesced into a few cohesive ideas.

- **The Rubber Band Collar** – This concept utilizes the tension of rubber bands attached to the fuselage to restrain the payload. This design featured an independent restraint for each element.
- **The Double Hatch** – The double hatch uses a single closing action to simultaneously secure all payloads. A secondary hatch mechanism secures independently when the outer hatch is closed.
- **The Flex Wall** – The flex wall uses string or zip-ties to provide the necessary force to keep the payload stationary. The flex wall works by squeezing the walls of the fuselage against the payload until the normal force is large enough to secure the payload.
- **The Wedge** – This configuration utilizes a large wedge running length-wise down the aircraft, which presses down on top of the payload acting to restrain the payload against the fuselage. The wedge relies completely on its ability to fit between the payloads.
- **The Straw Lid** – The straw lid design is literally modeled after a plastic drinking cup lid, adapting the perforation where the straw pokes through the lid into a design to restrain a payload. This configuration is based upon the desire to utilize the action of loading to also restrain the bottles or

blocks. The straw lid works by allowing the elements to be pushed in, but not allowing the elements to back out the same way.

- **Press Fit Foam** – The press fit foam idea restrains the payload elements using foam with enough separation to allow objects to be shoved in the plane, but not fall out when turned upside down.
- **The Accordion** – This design utilizes a set of movable dividers which can be pulled taut by a string at the end of the fuselage. The dividers, which were tall enough to accommodate all possible collar locations on the bottles, contracted to restrain the payload.
- **Safe-T-Wire** – The Safe-T-Wire concept operated by securing the payload using individual restraints. One variation used pieces of split cardboard, the other used strips of carbon fiber or Kevlar to imparted tension to the system, tightening the “wire” around the elements.

The flex wall raised major concerns within the team regarding the contest rules in that it effectively and intentionally altering the external profile of the aircraft. A modified design was considered which placed a secondary flexible wall inside the fuselage; however, such a design would increase weight, negating one of the primary benefits of the design. Therefore the flex wall concept was dismissed. The press fit foam was also dismissed because the concept does not work well with collars. The accordion was ruled out early on because the CG drifts dramatically between the 14-bottle and the 4-block payloads without major manipulation on the flight line.

The specific figures of merit for the payload restraint system are described below and the concepts are rated on a scale of +1 to -1, where +1 represents an improvement of and -1 a degradation of the baseline case, measured as 0.

- **System Weight** – The weight of the payload restraint system must be minimized to reduce aircraft weight but the restraint system must be robust enough to withstand heavy use.
- **Center of Gravity** – The center of gravity is very important to the static stability of the aircraft and therefore its location must remain as constant as possible. The more forward the CG is ultimately the smaller the tail can be, which has major aerodynamic benefits.
- **Loading Efficiency** – The payload loading is timed during the contest so maximum loading efficiency is most likely to be achieved by avoiding ‘bottle necking’ during the loading process
- **Flexibility** – The payload will not be known until just prior to the starting time so the payload floor plan must show ample flexibility whether the payload is bottles, bricks or both.

Using these FOM's, the restraint systems were evaluated in the decision matrix shown in Figure 3.4. The rubber band collar is considered the baseline for comparison and received all zeros in the decision matrix. The Straw lid scores the lowest because the concept might violate the rules by moving or gripping the collars. The Safe-T-Wire concept also scores low for the same reason. The Wedge scored second highest because the design may not need a grid system to separate the passengers and therefore may weigh the lightest. The passengers are also simultaneously restrained in one closing motion. The Wedge might move or grip the collars on the passengers. This leaves the Double Hatch concept with the highest

score. The team determined that the Double Hatch will restrain the passengers without interfering with the collars; the concept also restrains all passengers with one closing motion.






Payload Restraint Concept Weighted Decision Matrix		Rubberband Collar	Double Hatch	The Wedge	The Straw Lid	Safe-T-Wire
Figures of Merit	FOM Weight					
Structural Weight	0.25	0	1	1	-1	0
Center of Gravity	0.2	0	0	0	0	-1
Loading Efficiency	0.25	0	1	0	1	1
Versatility	0.3	0	-1	-1	-1	0
Score	1	0	0.2	-0.05	-0.3	0.05

Figure 3.4: Weighted Decision Matrix Comparing Different Payload Restraint Concepts

The hatch used to allow the payloads to enter the aircraft must be a robust design. The hatch must open fully and be clear of the ground crew during the loading process. Weight is always a concern so the hatch will most likely have one hinge and one latch. The hatch when fully opened will expose every spot designated for a passenger. This will allow the payloads to be dropped in from the top without the need to navigate around internal systems inside the fuselage.

3.2.5. Fuselage Shape

The team brainstormed many different payload layout options. For each case the fourteen bottle combination is used as the design point, as this will be the maximum amount of volume in the fuselage. The most obvious was a narrow bodied fuselage with the bottles running two wide along the length of the fuselage. In addition, the team developed a set of wide body fuselages that would have three bottles at its widest point, tapering to a point in the aft section of the fuselage. This leads to Figure 3.5 which shows the decision matrix and the total score for each concept using the FOM's from Section 3.2.2.



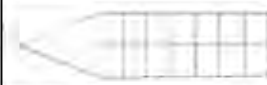
Payload Layout Weighted Decision Matrix		"The Blue Catfish"	"The Tuna"	"The Ice Cube Tray"
Figures of Merit	FOM Weight			
Drag	0.25	0	0	1
Center of Gravity	0.2	1	0	0
Loading Efficiency	0.25	0	0	0
Versatility	0.3	1	0	1
Score	1	0.5	0	0.55

Figure 3.5: Payload Layout Weighted Decision Matrix

Versatility is given the highest weight because all possible payloads must be able to fit. Loading efficiency and drag are both given the next highest weight because drag translates to more batteries and loading efficiency translates to loading time both of which must be optimized to maximize mission score.

Center of gravity is given the lowest weight because if the battery packs are strategically placed, the center of gravity movement due to changes in payload could be negated.

As can be seen —the Ice Cube Tray” achieved the highest score. This concept is determined to be the best due to its narrow shape and spread out floor plan which will help reduce ‘bottle necking’ or clutter when the plane is loaded. However, the drag was assumed to be less only when considering the smaller frontal profile. Due to the small difference in score, further drag quantification and comparison that would definitively show advantages and disadvantages is scheduled for the initial sizing phase.

3.2.6. Aircraft Body Types

The following aircraft body styles were investigated during the conceptual design phase. The aerodynamics team was primarily responsible for the evaluation of the lift and drag characteristics, while the structures team gave input in constructability and weight.

- **Conventional** – This concept was appealing because it is easy to manufacture in modular form and can be simpler to design. However, conventional body types have more interference drag at the fuselage-wing joint.
- **Blended** – A blended fuselage and wing concept has favorable lifting characteristics and reduced in but blended bodies tend to have an increase in wetted surface area and a more complex and restricting assembly process.
- **Lifting Body** - Pure lifting body concept has a relatively low L/D and can be destabilizing in pitch.

The team researched aircraft with all types of bodies and determined the manufacturing, stability and frontal area all are problematic with blended and lifting bodies. The conventional body type has the most potential for optimization given the team’s resources and schedule.

3.2.7. Wing Configuration

The following aircraft wing styles were investigated during the conceptual design phase. Using the morphological chart derived during the earliest portion of the project, the team brainstormed and evaluated the wing styles discussed below.

- **Monoplane** – This configuration is used as a reference to which other configurations are compared. A monoplane is appealing because of the historical success and its short takeoff potential.
- **Biplane** – A biplane has very favorable aerodynamic characteristics especially with span restrictions. This design also has great structural benefits if the team takes advantage of the high moment of inertia generated the spacing between the wings.
- **Canard** – The canard is considered in case the CG is too far aft. Multiple lifting surfaces had potential for better performance in the payload mission.
- **Tandem** – Similar to the canard, a tandem configuration shows promise due to its multiple lifting surfaces and higher effective aspect ratio from its multiple wings.

- **Flying Wing** – The flying wing has high aerodynamic efficiency from the lack of a fuselage, which translates to low battery weight which was very influential to the mission scores.

To compare the design choices to one another, the overall FOM's from Section 3.2.1 were adapted and redefined to include specifics relating to the component being designed. These FOM's for the wing configuration are detailed below.

- **Aerodynamics** – This FOM attempts to quantify aerodynamic parameters such as span, aspect ratio, L/D and wetted surface area in a way that will give the team insight into an over optimal design that performs highly in both the delivery mission and the payload mission.
- **Stability and Control** – Some concepts better handling qualities than others but the more control systems the aircraft requires will ultimately effect the RAC poorly. Reliably and consistency affect the pilot's ability to fly the plane and must be considered when exploring stability and control.
- **Short TO Potential** – Since the payload weight is not exactly consistent, the plane must be able to takeoff in zero wind conditions with some takeoff distance factor of safety
- **RAC** – The rated aircraft cost must be a FOM because it is directly in the payload mission score function. The RAC will help the team finalize a design that is structurally light and can carry a minimum amount of power.

Once the specific FOM's were defined, a weighted decision matrix was constructed to objectively compare and score the concepts. This weighted decision matrix is shown in Figure 3.6.

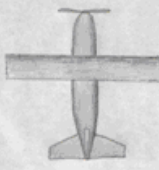


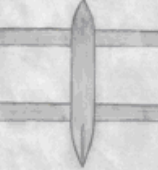

Wing Configuration Weighted Decision Matrix		Mono-wing	Bi-Wing	Canard	Tandem	Flying Wing
						
Figures of Merit	FOM Weight					
Stability & Control	0.25	0	0	-1	-1	-1
Short TO Potential	0.2	0	0	-1	-1	-1
Aerodynamics	0.25	0	1	-1	-1	-1
RAC	0.3	0*	0*	-1	-1	1
Score	1	0*	0.25*	-1	-1	-0.4

Figure 3.6: Weighted Decision Matrix Comparing Different Types of Wing Concepts

The RAC was given the highest weight due to its strong influence on the mission score. Short takeoff was given the lowest rating even though it is a strict requirement because short takeoff performance can be improved with optimized planform area, span, airfoil characteristics, and high lift devices. When assigning scores for the various FOM's, the aerodynamics and structures team could not resolve the discussion of which wing configuration could be build lighter. While a biplane required more connection points and possibly more weight, its larger moment of inertia due to the separation between the wings could result in more strength for the wing's weight. This led to the asterisk shown in the monoplane and biplane columns. Further quantitative study would be required to definitively prove that the biplane would outperform and outscore the monoplane. In the interest of one solid concept, however, the team decided

that a biplane should be designed, with the stipulation that the first step in the preliminary phase detail the performance of the two designs.

3.2.8. Spot Size Orientation

When initially devising design constraints, the team did several calculations to see if orienting the plane diagonally within the spot size limitation would be beneficial. For an initial estimate however, a 12 in chord was used, and the nearly 6.4 ft of diagonal length would only provide about 5.15 ft of possible span, for an increase of less than 2 in. A biplane could potentially have half of the chord of the monoplane, reducing the corner-to-corner loss of inserting a rectangular wing into the box. Essentially, the largest benefit of this atypical orientation would be with a biplane configuration. The main concept was amended so that the span line was oriented with the wing along the box's diagonal. Since any possible monoplane configuration would not benefit from this orientation, it was only examined oriented with the span along the 5 ft box dimension.

3.2.9. Empennage

Based on the wing and body styles under consideration, the team studied various types of tails.

- **Conventional** – A conventional tail is a low horizontal stabilizer centered below the vertical tail.
- **T-Tail** – A T-Tail is a high-mounted horizontal tail.
- **V-Tail** – A V-Tail is two dihedral surfaces in a “V” shape.

The team also considered an H-tail, Y-tail, cruciform tail, and fuselage-centered tail, but were immediately eliminated due to manufacturing and spot size restraint concerns.

To compare these concepts, the overall FOM's from Section 3.2.2 were adapted and redefined to include specifics relating to the component being designed.

- **RAC** – The rated aircraft cost must be a FOM because it is directly in the payload mission score function. The RAC will help the team finalize a design that is structurally light and can carry a minimum amount of power.
- **Stability and Control** – This FOM measures the proficiency of a tail to cleanly contribute to the stability of the aircraft.
- **Drag** – Each tail was sized that provided the same aspect ratio and effective lift per degree of angle of attack, and then the drag was calculated based on the geometry. This gave a comparison of the drag given the same required lift.
- **Ease of Construction** – This FOM assesses the simplicity of construction.

Once the FOM's were defined, a weighted decision matrix, shown in Figure 3.7 was constructed. The T-tail received a high stability score because the horizontal stabilizer is above the fuselage flow. The RAC for the T-Tail takes a hit because the vertical would need to be stronger to handle the horizontal's loads. Although the V-Tail only has 2 surfaces, it would be very difficult to construct. A conventional tail is the only empennage configuration that could easily be adapted for asymmetry without causing unorthodox fuselage torque. The biplane configuration oriented diagonally within the spot size would

therefore utilize an asymmetric conventional tail, while a monoplane modification could easily incorporate a similar symmetric conventional tail.




Empennage Weighted Decision Matrix		Conventional	T-Tail	V-Tail
				
Figures of Merit	FOM Weight			
Drag	0.1	0	0	1
Stability & Control	0.2	0	1	0
RAC	0.4	0	-1	0
Ease of Construction	0.3	0	-1	-1
Score	1	0	-0.5	-0.2

Figure 3.7: Weighted Decision Matrix Comparing Different Empennage Concepts

3.2.10. Landing Gear Concepts

The landing gear conceptualization phase came after the main fuselage had begun to take shape. Based on rough estimates of amount of rotation required as well as impact loading during a full landing, several concepts were developed and assessed.

- **Bicycle** – This configuration uses two wheels mounted on the center line of the plane with stabilizing outriggers on the wing tips. This gear configuration is the most stream-lined but also the most troublesome with respect to ground handling.
- **Tricycle** – A tricycle configuration uses two wheels as the main gear mounted underneath the wing with one steerable wheel at the nose. This configuration has the most potential for good ground handling and allows for lots of rotational freedom depending on the tail configuration.
- **Tail Dragger** – A tail dragger is similar to the tricycle gear, only the steerable wheel is located at the tail, limiting the rotation angle at take off. The motor torque can also compromise steering.
- **Tandem** – A tandem arrangement is similar to a car’s wheels. Tandem gear requires two steerable wheels and may have a much larger turning radius during taxi. This configuration can be more incline to withstand hard landings since the impact forces can be distributed over a larger area, and have increased drag since more components are exposed to the air flow.

To compare these design choices to one another, the overall FOM’s from Section 3.2.2 were adapted and redefined to include specifics relating to the component being designed.

- **Structural Weight** – The landing gear needs to be strong enough to with stand a rough landing but light enough to not excessively add to the RAC.
- **Drag** – The selected gear must minimize drag thus reducing the required battery power.
- **Rotational Freedom** – The short takeoff requirements are strict so the landing gear should be considered to optimize plane incidence and rotation during takeoff.
- **Taxi Control** – Ground control must be ample enough so the plane can take off easily, even in the event of unfavorable cross winds.

Once the FOM's were defined, a weighted decision matrix, shown in Figure 3.8 was constructed. When the weighting and scoring were summed, the tricycle gear scored the highest. Due to the mission requirements the tricycle gear shows the most potential for optimization with respect to both structural weight and drag without sacrificing ground handling and rotation angle.



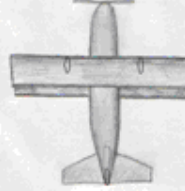
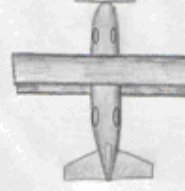
Landing Gear Weighted Decision Matrix		Bicycle	Tricycle	Tail Dragger	Tandem
					
Figures of Merit	FOM Weight				
Structural Weight	0.3	1	0	0	-1
Drag	0.3	0	0	0	-1
Rotational Freedom	0.25	-1	0	0	-1
Taxi Control	0.15	-1	0	-1	-1
Score	1	-0.1	0	-0.15	-1

Figure 3.8: Weighted Decision Matrix for Different Landing Gear Configurations

3.2.11. Propeller / Motor Mounting

The group first researched different motor placement configurations. Multiple configurations were initially sketched and discussed to optimize the best concept. The different concepts are discussed below.

- **Single Tractor-** This concept uses a single motor mounted at the nose. A single tractor allows the propeller to operate more efficiently since the propeller is in the undisturbed free stream. This can also move the center of gravity farther in front of the wing increasing stability.
- **Twin Tractor-** A twin tractor configuration puts the motors towards the tips of the wings, possibly causing an increase in weight due to increased requisite wing strength.
- **Single Pusher -** A pusher is a single motor mounted at the tail of plane, allowing the upsweep angle of the fuselage to be higher, helping to shorten the fuselage. This design also has center of gravity problems as well as takeoff angle restrictions. This will operate less efficiently since the propeller is in the disturbed flow coming off the wing and fuselage.
- **Twin Pusher-** A twin pusher has similar problems to the single pusher however the RAC may be even worse with two motors.
- **Pod Mounted-** Pod mounted motors are very flexible to placement and can almost always place the propeller in a high quality airstream. Pod mounted motors however add drag since the pod increases the wetted surface area.

Each motor concept is evaluated using FOMs described below with the single tractor concept being the baseline for comparison.

- **RAC-** Motors add a very significant amount of weight which directly effects the RAC and therefore must be minimized

- **Air Stream Quality-** Motor and propeller location will affect the quality of the airstream the propeller sees. To make sure the propeller is operating under optimal conditions the airstream quality must allow the propeller to be efficient.
- **Center of Gravity-** Motor placement can shift the center of gravity a significant amount must be controlled so that the aircraft can be balanced easily.
- **Propeller Clearance-** Propeller ground clearance it important because large rotational freedom may be needed for short takeoffs.

A weighted decision matrix, shown below in Figure 3.9, was created for the decision making process.






Propulsion System Mounting Weighted Decision Matrix		Single Tractor	Twin Tractor	Single Pusher	Twin Pusher	External Pod
						
Figures of Merit	FOM Weight					
RAC	0.3	0	-1	0	-1	-1
Air Stream Quality	0.2	0	0	-1	-1	0
CG	0.25	0	0	-1	-1	0
Prop Clearance	0.25	0	-1	-1	-1	1
Score	1	0	-0.55	-0.7	-1	-0.05

Figure 3.9: Decision Matrix Weighting and Scoring

The weighted decision matrix shows that a single engine tractor scores the highest. The tractor mounting gives the propeller proper clearance for takeoff and landing and allows the propeller to blow over the root section of the wing which could help with takeoff and roll control. The single tractor improves the center of gravity location by placing the propulsion system at the nose of the aircraft.

3.3. Conceptual Aircraft Summary

Once the individual component selection processes had completed, the team convened in order to assemble the selected concepts into one final conceptual aircraft, shown in Figure 3.10. The plane concept is a narrow-body fuselage with a single tractor propulsion system and tricycle landing gear. The fuselage also has a double-hatch system to effectively restrain the payloads.

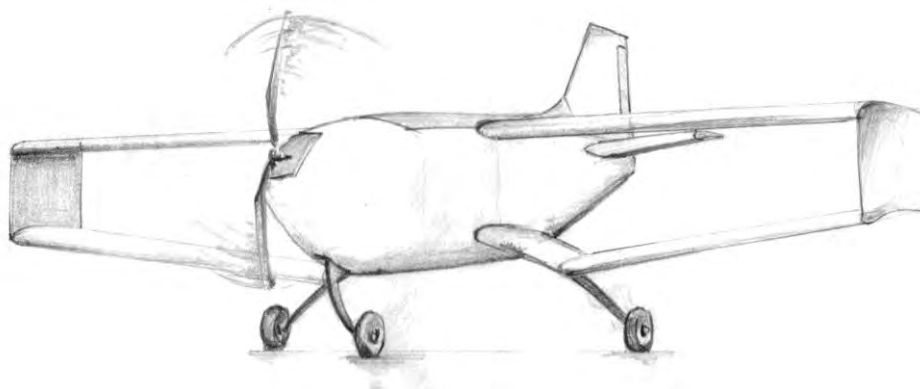


Figure 3.10: Final Conceptual Configuration

One final configuration decision awaited detailed investigation immediately at the start of preliminary design however. Although the biplane outscored the monoplane, the decision on the number of wings is finalized in the first stages of the preliminary design phase. A monoplane placed in the spot size traditionally with a conventional tail will be compared quantitatively with a biplane oriented diagonally with an asymmetric tail.

4.0. Preliminary Design

After completion of the conceptual design phase, the team transitioned into the preliminary design and sizing portion of the project. The aerodynamics team sized the wings, tail, and controls for stability and performance. The propulsion team gathered actual component test data to design an optimized propulsion system. The structures team used historical data to predict an initial weight model and then tested various construction techniques to refine the weight model.

4.1. Mission Modeling and Analysis Methodology

The three technical groups utilized different design tools and methodologies to their respective subsystems. The design tools are outlined first, followed by an overview of the design and analysis methodology for each group.

4.1.1. Design Tools

Various tools were used to design and analyze the aircraft and various subsystems. The aerodynamics team utilized a performance optimization, airfoil design, and stability and control codes. The propulsion team combined data from dynamometer and bench tests in a system optimization code. The structures team used ProEngineer as well as various Excel programs to calculate the center of gravity and cross section properties while designing the structural components of the plane.

- **Aerodynamic Optimization** – The aerodynamic optimization program was developed in Mathcad to simulate all phases of the two missions. The user inputs include a weight model, airfoil data, wing configuration, wind speed, and battery type. The program then executes a series of nonlinear, multidimensional solvers with such constraints as the maximum takeoff distance, battery usage limits, and the spot size limitations. The program allows the aerodynamic team to estimate speed, time, and power required for the different phases of the missions. The program outputs several parameters for high scoring aircraft, such as planform, span, battery weight, and optimum cruise velocity and power. These values can be used to estimate the score for the mission, as well as specific aircraft characteristics like lift coefficients and trim angles.
- **XFoil** – XFoil is an inviscid / viscous panel method code written by Dr. M. Drela. The program also creates lift curves and drag polars, as well as calculating hinge moment. . User-defined blends of multiple airfoils were created to further improve possible performance.

Lift, drag, and moment characteristics of possible airfoils were computed and inputted into the optimizer program. Data for airfoils at varying Reynolds numbers and detailed analysis on airfoil defects was also used to study performance

- **Stability and Control Program** – The stability and control program, also developed in Mathcad, used aircraft geometry and mass properties to estimate static and dynamic stability, along with control sizing. The program returns eigenvalues and eigenvectors for the full eight degree-of-freedom system that models coupled longitudinal and lateral motion.
- **Propulsion Optimization** – The propulsion optimization was built in Mathcad to simulate combined performance of the entire propulsion systems. The program combines test data in the form of propeller curves (thrust, power, and efficiency), motor performance curves, and battery efficiencies. When supplied with accurate coefficients and speeds, the program generates realistic estimates for takeoff distance and mission energy usage.
- **Dynamometer and Wind Tunnel** – The propulsion dynamometer measures the thrust and torque on the propeller, RPM of the motor, voltage and current seen by the motor. The system can be used for static testing or placed in the wind tunnel to provide dynamic propeller data. The data can be used to generate propeller and motor performance curves.
- **Computerized Battery Analyzer (CBA)** – This tester measures the real battery capacity and maximum discharge rate of individual cells and battery packs. The tester is used to determine deviations from the manufacturer's data and identifying the best batteries for final packs.
- **ProEngineer** – In the preliminary design phase, ProEngineer was used for lofting, system integration and component and assembly drawings. ProE was also used to ensure that entire aircraft fit within the spot size limitation as changes were made to the wings, fuselage and tail.
- **CG Estimation Tool** – The center of gravity (CG) estimator was built in Microsoft Excel and was used to track the total weight and location of the CG as elements were added and modified within the design. The CG estimation tool was used to arrange the payloads so that the does not change for empty and loaded configurations.
- **Cross Sectional Properties Tool** – The cross sectional properties tool was also built in Microsoft Excel and was used to analytically predict the structural loads and cross sectional properties to help minimize structural weight through material tapering.

4.1.2. Design Methodology

The three technical groups worked independently through their own design methodologies, as well as interacting with each other at key points in the overall process. The group methodologies are shown in Figure 4.1 along with the appropriate interaction points and shared information.

- **Aerodynamics Group** – The aerodynamic group used the aerodynamics optimization to perform sensitivity studies on monoplane and biplane configurations, wind speed around which to design, airfoil for the wing, and useful battery types. XFOIL was used to design the optimal airfoil and to generate airfoil drag polars for the aerodynamic optimization. The aerodynamics optimization

program was used to size the fuselage and wing dimensions to obtain the highest scoring configuration. The stability and control program was used to size the horizontal and vertical tail surfaces for appropriate static stability characteristics and necessary control sizing. The stability program also calculated the full eight degree-of-freedom and dynamic stability for the design.

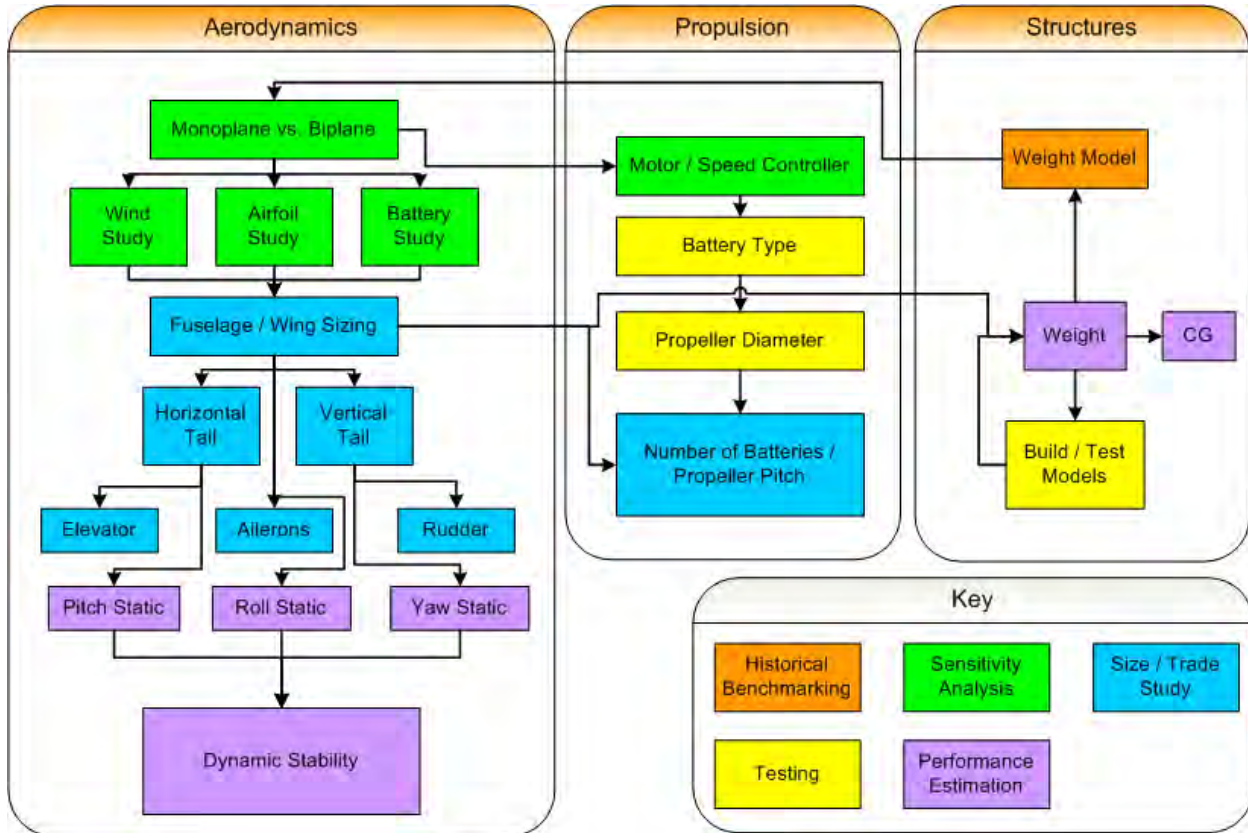


Figure 4.1: Design Methodology of the Technical Groups

- Propulsion Group** – The propulsion group used manufacturer’s data along with information from the aerodynamics groups to decide on an appropriate takeoff power and the necessary requirements for motor and speed controller. The motor and speed controller were further selected from a list of possible components, using sensitivity studies and weight comparisons. The group then tested batteries and propellers using the battery tester, dynamometer, and wind tunnel. The group analyzed propeller diameter, gear ratio, specific battery type and their effect on the overall system. Finally, the group refined their design using the propulsion optimization program with test data to select the optimal number of batteries and propeller pitch to give the best performance for each mission under various wind conditions.
- Structures Group** – The structures group used historical data to generate a weight model for use in the aerodynamics optimization program. The group then improved their weight model by building wings, tails, and fuselages in the desired methods and weighing the actual parts. The build-ups were refined using the cross-sectional properties tool and rebuilt for weighing and strength testing. Near the end of the preliminary phase, the structures team was able to construct

accurate weight models for the major components and assemble the overall weight model and CG estimate. ProEngineer was used throughout the preliminary phase to model the outer mold lines of the plane and ensure that the entire plane fits inside of the spot size limitations as well as providing full accommodations for the required payloads and necessary flight systems.

4.2. Design and Sensitivity Studies

Once the mission models and optimization codes were developed, the teams began running sensitivity studies and trend analyses to quantitatively evaluate which specific design parameters resulted in the largest score increases. The aerodynamics team ran simulations to determine if a monoplane or biplane was superior, and each team ran sizing trade studies to establish key design elements.

4.2.1. Monoplane vs. Biplane

The team first sought to identify whether or not the larger wingspan of a diagonally oriented biplane would increase scores enough to offset the more unique geometric constraints for the aft section of the plane. The payload optimization code was modified to include a chord limit based on span, effectively eliminating planes that will not fit in the spot size restriction. In order to isolate all possible variables, airfoils were selected that were appropriate for the Reynolds number regime. For the monoplane optimizations, an Eppler 423 airfoil was used at higher Reynolds numbers, and for the biplane optimizations an MVA 227 is used at lower Reynolds numbers. After several runs, the data was sorted as a carpet plot in Figure 4.2. The equation used to limit the chord based on span is plotted for reference.

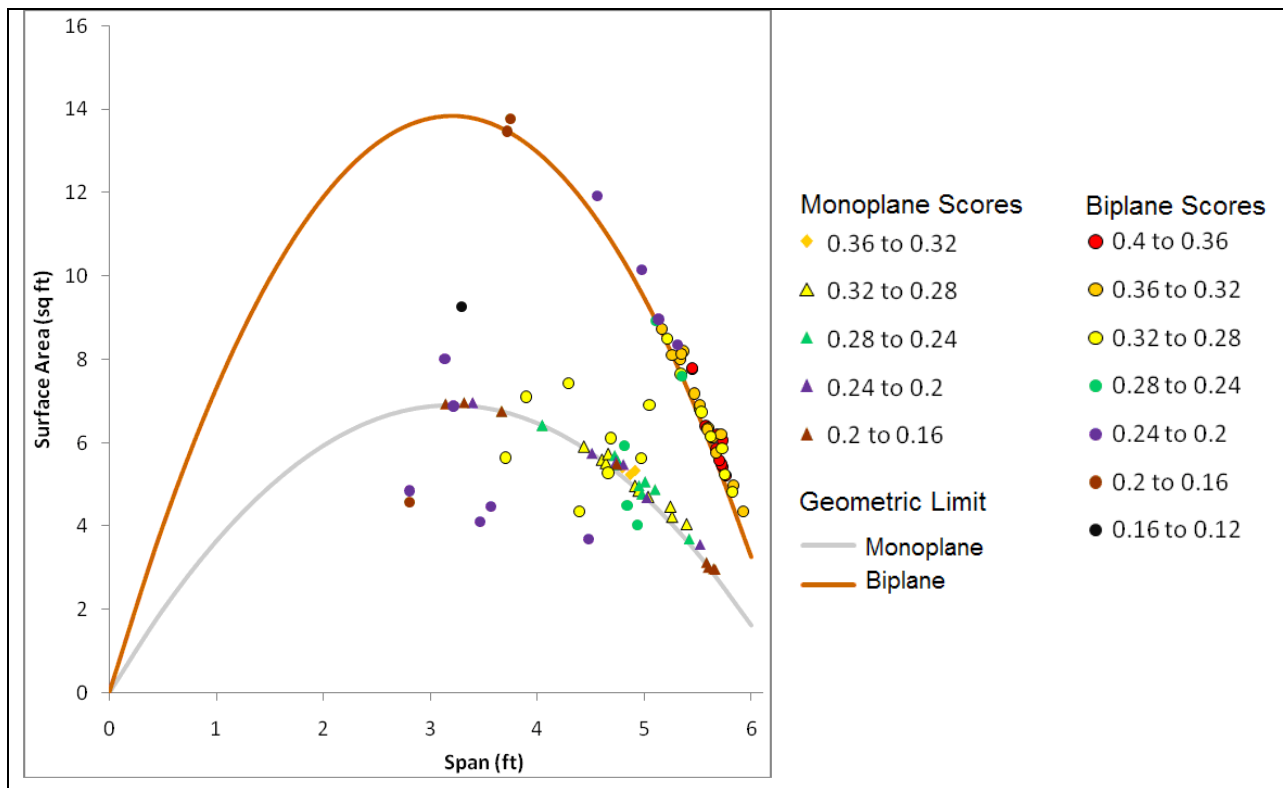


Figure 4.2: Carpet Plot of Monoplane vs. Biplane

Figure 4.2 shows payload mission scores for different monoplanes and biplanes. The mission scores shown are not normalized nor do they include loading time. From the graph, most of the monoplanes are easily defeated by even the worst of the biplane scores. A large set of biplane data values fall in an acceptable range at a high score and high span, which means these planes have higher aspect ratios. This data shows that a biplane configuration would be superior to a monoplane in scoring. Additionally, the original constraint function was overlaid on the data in Figure 4.2, showing that the constraints were not only adhered to, but that the optimizer tried to reach maximum score limits. Also, the scores tend to be higher for biplanes with spans between 5 and 6 ft².

During the conceptual design phase, the team was unable to predict whether a monoplane and a biplane could be built to the same weight model. Rather than undertake complicated monoplane and biplane strength and weight tests, a weight study was done to understand which configuration would score higher as construction methods improved. The aerodynamics team manipulated the weight model within the aerodynamic optimization code, again holding the airfoils constant. Figure 4.3 [a] shows the data collected for a biplane and monoplane while varying the weight model. The monoplane is more sensitive to changes in weight but the biplane scores higher in the weight range in which the design is predicted to follow. The scatter plot suggests a biplane will be superior for weights above 0.07 lbs per ft² of planform, the minimum weight model achieved through initial structural tests.

The team also studied the aspect ratio of possible biplanes and monoplanes. Assuming a 6.5 ft² planform area, the aspect ratio of a monoplane and the effective aspect ratio of a biplane with 8 in wing spacing were graphed as shown in Figure 4.3 [b]. The monoplane could only fit in the box up to a span of 5.15 ft; however the biplane was able to fit with a 7 in chord and a 5.85 ft span. This results in a 57% larger effective aspect ratio for a maximum-span biplane. The biplane effective aspect ratio was calculated using the equation shown in Figure 4.3 [b], where h is the wing spacing and b is the span. The data from the weight model study coupled with the biplane's higher aspect ratio resulted in the team choosing a biplane configuration for the aircraft.

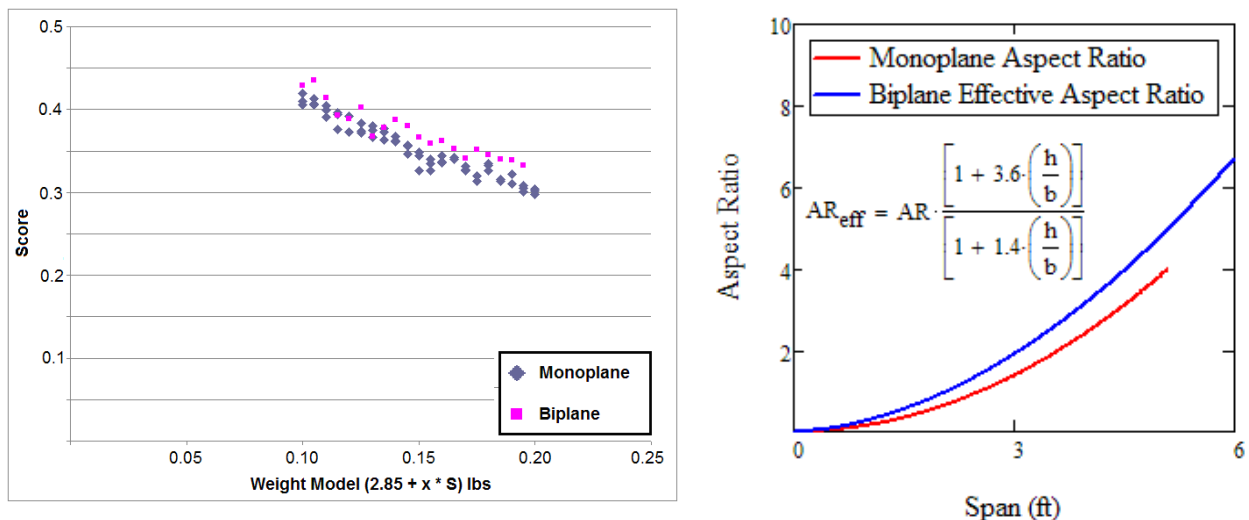


Figure 4.3: Weight Model Study [a] and Effective Aspect Ratio (AR_{eff}) Increase for Biplane [b]

4.2.2. Wind Speed Sensitivity Study

Minor aerodynamic changes could require an additional 1 or 2 batteries, rapidly increasing the battery weight and ultimately lowering the score. Since this power optimization plays such a key role in determining the score for a flight, a more thorough investigation was required. The main “flight condition” studied was wind speed, which showed the largest performance changes.

Using the aerodynamic optimization program, several aircraft configurations were generated for various wind conditions, while holding all other variables constant. The team investigated the possibility that an optimal planform area exists that is capable of completing both missions in all wind conditions. Figure 4.4 shows the wind study results of a biplane using only Elite 1500 NiMH cells to maintain consistency. Once the outliers were removed, many of the highest scoring planes were located around 5.0 – 7.0 ft² of planform. Once this was further analyzed, a plane of about 6.5 ft² of planform scored the highest at 5 mph. Planes with 6.5 ft² outscored planes of different planforms at most other wind speeds.

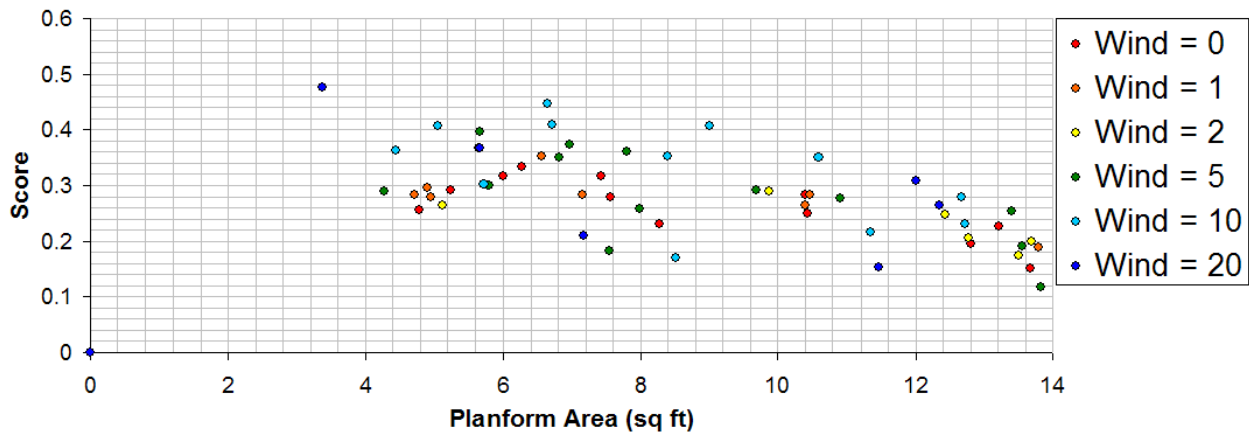


Figure 4.4: Wind Speed Sensitivity Study

From Figure 4.4, a planform area range that contains the most versatile aircraft with respect to wind speed was estimated. A plane optimized for both zero wind and the average April wind in Wichita (7 mph) exists within these bounds. A 7 mph wind is deemed the “design point” for planform area.

4.2.3. Airfoil Sensitivity Study

The first thing the team considered when choosing an optimum airfoil was the Reynolds number regime. With the chord length estimated at 7 in, the Reynolds number is estimated to fall in the range 10^5 to 4×10^5 . High lift, low Reynolds number airfoils were ran in the aerodynamic optimization. A scatter plot of the three best scoring airfoils and bar chart of their average scores is shown in Figure 4.5. The MVA 227 shows many high scores in the planform range dictated by the wind study.

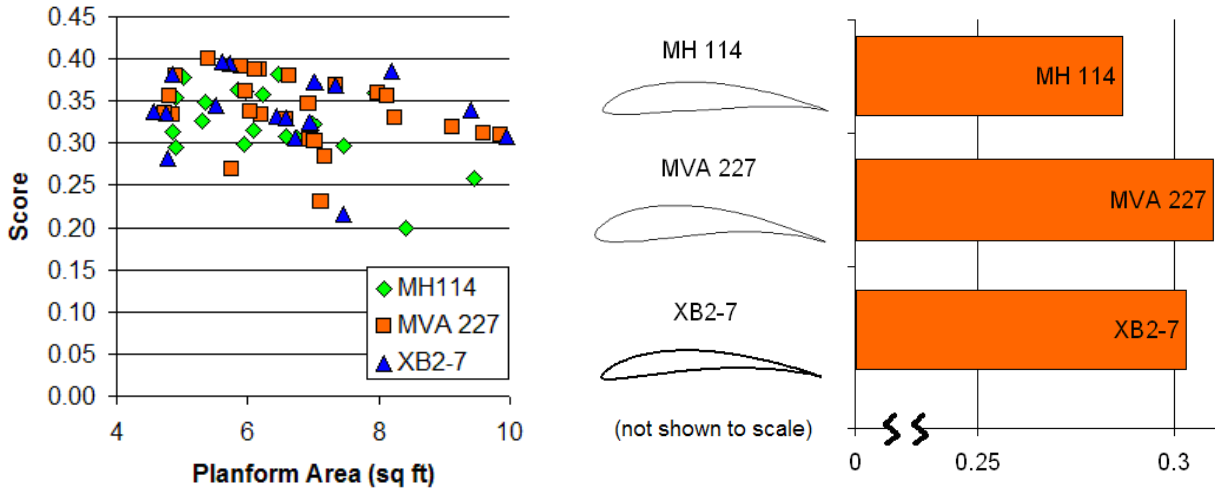


Figure 4.5: Airfoil Sensitivity Study Data [a] and Average Payload Mission Scores [b]

An average of the top three highest-scoring airfoils is taken and shown in the Figure 4.5 [b]. The MVA 227 outscored all of the MH 114 airplanes. The XB2-7 is a MH 114 and MVA 227 blend with reduced thickness and is competitive with the MVA 227 but the trailing edge of the XB2-7 was too thin to manufacture lightweight. The MVA 227 lift curve is shown in Figure 4.6 [a] and the drag polar is shown in Figure 4.6 [b] at Reynolds numbers in the predicted range. Maximum lift is slightly affected by low Reynolds numbers. The drag polar however is more susceptible to Reynolds number changes. Figure 4.6 shows the MVA 227 can perform adequately even during the lowest Reynolds number predictions.

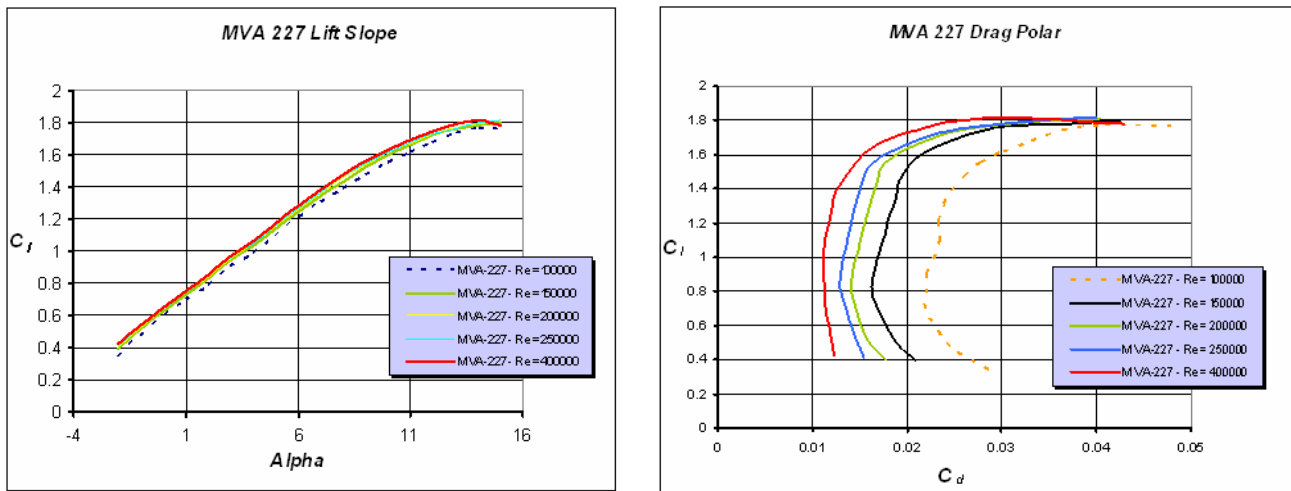


Figure 4.6: Lifting Curve and Drag Polar for the MVA 227 at Different Reynolds Numbers

4.2.4. Battery Sensitivity Study

In addition to the dimensional and configuration-specific inputs that the aerodynamic optimization program accepted, battery performance was used in the program to calculate available takeoff power total battery usage. In order to gain a better understanding of the mission's optimization points, the aerodynamics team performed several studies that changed battery types used in the missions. The

propulsion team would spend most of their time optimizing battery backs during preliminary and detail design, but this investigation could identify how sensitive performance was to battery weight changes.

The aerodynamics team initially ran several identical configurations in the simulation, varying only the battery type used. A graph of several optimized planes for both Elite 1500 and KAN 400 parallel cells is shown in Figure 4.7. The scores are for the payload mission.

In the battery sensitivity study shown in Figure 4.7 [a], the Elite 1500-powered aircrafts outscored KAN-powered planes of the same basic configuration. In fact, no KAN outscored a similarly-sized Elite 1500 aircraft. Figure 4.7 [b] utilized the wind study data from Section 4.2.2. The highest-scoring airplane for each wind speed is shown, one point representing an optimized aircraft powered by Elite 1500's and the other powered by KAN 400 in parallel. Again, at all wind speeds, the best Elite 1500 configuration outscored the best KAN configuration.

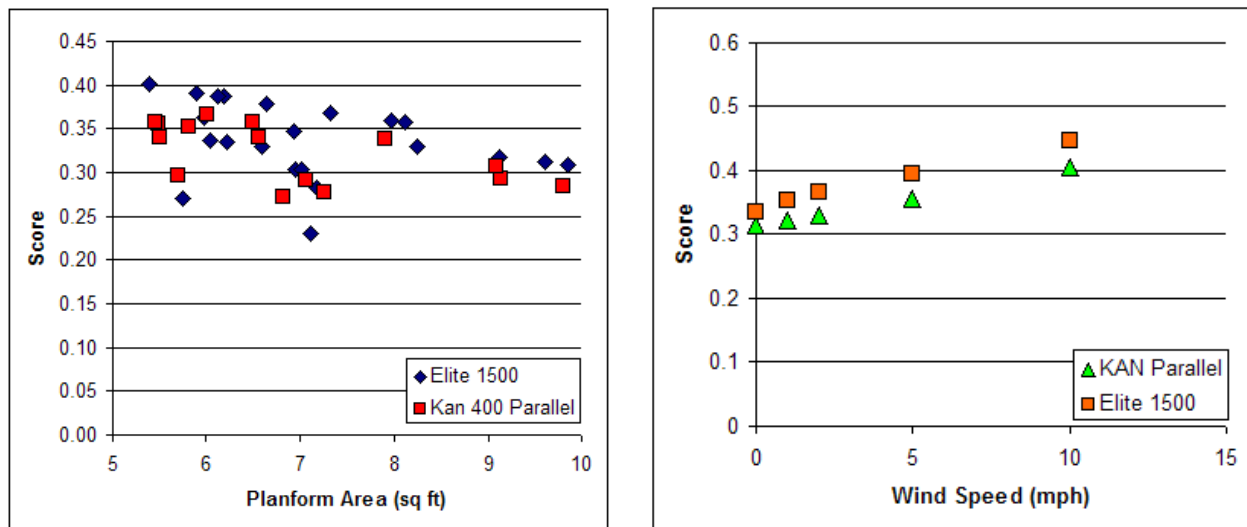


Figure 4.7: Elite 1500 / KAN 400 Parallel Scatter Plot [a] and Wind / Battery [b] Studies

Using this data, the aerodynamics team began investigating the possibility of drawing more current than specified by the manufacturer. Though the scores were much higher, the propulsion testing showed that higher currents resulted in much higher resistance, eliminating the benefit of the higher current draw.

Ultimately, however, this battery sensitivity study helped the aerodynamics team to understand that the mission scores were very sensitive to battery weight. One or two cell addition or subtraction could yield vastly different optimized planes, as well as much higher or lower scores.

4.3. Aircraft Sizing and Trade Studies

The next step in the preliminary design was to evaluate how the size of certain elements would affect the performance and score of the aircraft. The aerodynamics team investigated fuselage sizing as well as wing and tail dimensions while the propulsion team studied battery types, speed controllers, and gear ratio / propeller size. Also, the structures team benchmarked wing weight models and built test wings in an attempt to reduce the predicted weight model.

4.3.1. Aerodynamic Sizing

For all fuselage arrangements, the aerodynamics team calculated a value of drag divided by dynamic pressure, or D/q . Rather than a drag coefficient, which is nondimensionalized based on fuselage reference area, D/q is not referenced to any specific area. Several fuselage parameters were investigated to evaluate whether the narrow or wide bodied fuselage would be more aerodynamically efficient.

For each payload layout, the fuselage shape was analyzed for major flow separation points. Form factors and fineness ratios shapes were calculated and used to derive D/q . Each layout required a different upsweep of the fuselage. A graph of the D/q for the entire fuselage based on the distance to the first payload row is shown in Figure 4.8.

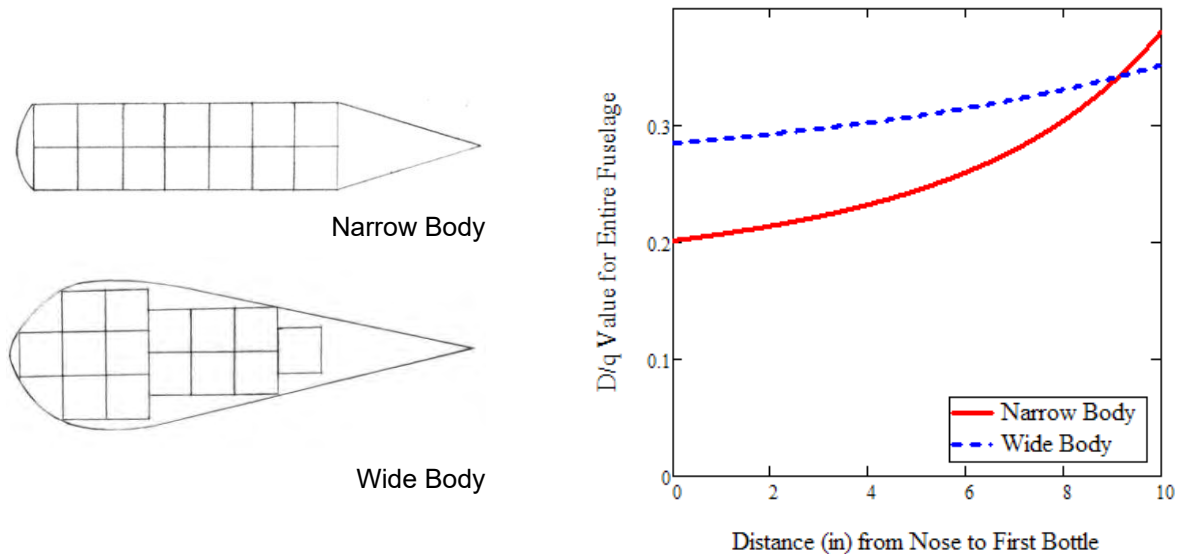


Figure 4.8: D/q Value for the Entire Fuselage

A tip-to-payload distance of 4 in is estimated based on the propulsion system requirements. At this distance the narrow-bodied fuselage had about 30% less drag than the wide body fuselages. For this reason, the aerodynamic recommendation was the narrow body fuselage.

Originally the wing spacing was set at 9 in, the exact height of the payload. However due to difficulties with payload loading the wing gap was reduced to 7.8 in. The wind sensitivity study indicates that the most versatile wings have planform areas between 5-7 ft^2 approximately. Planform areas in this range produced the highest scoring planes in the wide window of possible gross take-off weights and wind conditions. The two wings therefore have a chord of 7 in, a span of 5.8 ft, a planform area of 6.7 ft^2 and an aspect ratio of 6.3.

Placement of the horizontal stabilizer presented a unique challenge due to the configuration and the space available in the box. Increasing the horizontal stabilizer surface area decreases the moment arm which further increases the horizontal stabilizer planform area. However, due to an abundance of free space on a single side of the fuselage an asymmetrical L-tail was designed. The L-tail has a longer moment arm than the symmetric tail. The longer moment is allows for less surface area.

One problem with the side tail configuration is the roll moment it produces. At trim the tail is producing approximately 0.8 lbs of down force and a roll moment of 0.57 lb-ft. This moment could potentially produce problems with excessive aileron deflections. However, torque from the propeller was initially estimated to also be 0.5 lb-ft. Additional strategies for reducing the horizontal tail's roll moment were investigated and include adding taper to shift the lift distribution closer to the fuselage and reducing the static margin to lessen the amount of lift the tail needs to produce.

The final tail has a root of 12 in, a tip chord of 6.38 in, and a half span of 17 in. These dimensions were selected to maintain a moment arm of 2 ft. This moment arm requires a surface area of 1.08 ft² once the portion of the tail the fuselage occupied is subtracted. To obtain the additional area required, a short tail was added to the port side of the fuselage that follows the boundary of the box at the trailing edge and has a tip chord of 4 in. The half span of that stab was set at 8.6 in. The final result was a tail with 1.22 ft² of area. A diagram of the horizontal tail layout can be seen in Figure 4.9.

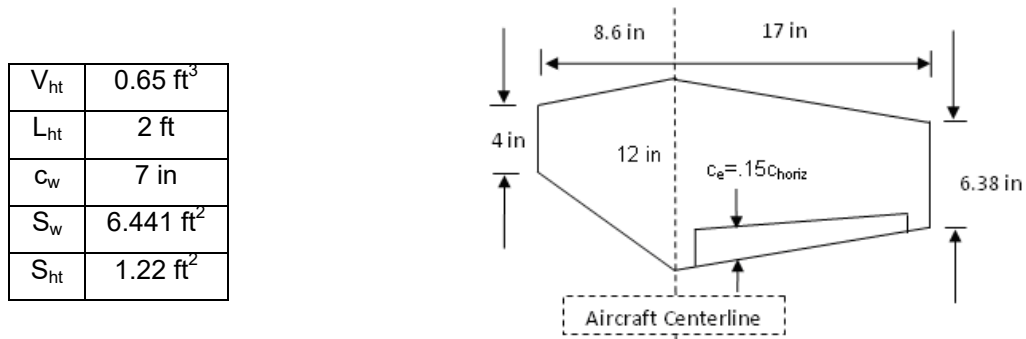


Figure 4.9: Horizontal Tail Sizing

Vertical stabilizer sizing was approached using the tail volume coefficient method. A required value of 0.04 ft³ was determined for the vertical tail volume coefficient, and later increased to 0.047 ft³ in order to meet rudder power requirements in a typical crosswind. The vertical stabilizer was given a mean aerodynamic chord of 10 in, a taper ratio of 0.82, and no sweep. This maintained the vertical tail's moment arm at 2 ft. The taper shifts the force distribution closer to the fuselage, which lessens the yaw-roll coupling. The half span of the vertical was set at 1.06 ft to obtain the required area. A NACA 0012 was chosen for both tail surfaces because of its low drag, lack of pitching moment and ease of construction. A diagram of the vertical tail layout can be seen in Figure 4.10.

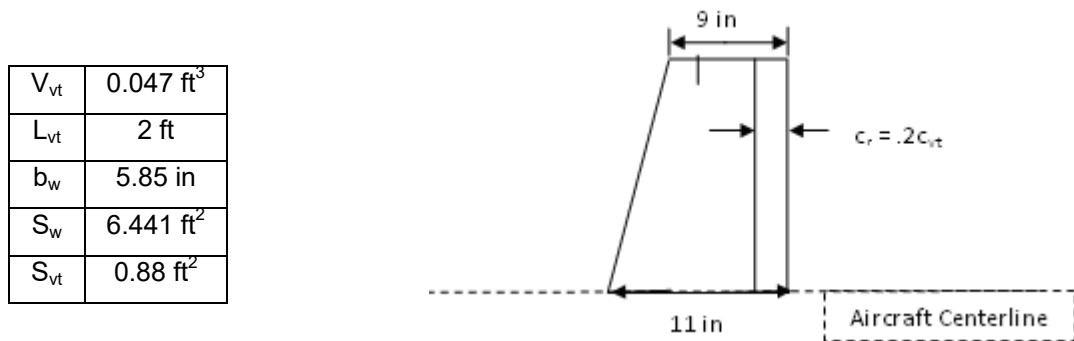


Figure 4.10: Vertical Tail Sizing

4.3.2. Propulsion System Selection and Sizing

Using the power requirements as a starting point, the Propulsion team began searching through a number of possible propellers, motor and gear box combinations to find an optimal propulsion system.

- **Motor Selection** – Power and weight are the most important parameters for motor selection. Brushed and brushless motors were investigated and selected based on power, weight, and ability to withstand the high current. Several motors were selected from initial power to weight ratio benchmarking. Motors were narrowed down by analyzing their mission performance such as obtaining a 75 ft takeoff distance. The remaining motors were analyzed while varying the gear ratio, propeller, and batteries. The Medusa 028-040-1700V2 was selected for its performance: 350 Watts / 27 Amps max, and 100-g weight.
- **Battery Selection** – Capacity and weight are the parameters optimized in battery selection. Nickel-metal hydrides and nickel-cadmium batteries were researched. NiMH batteries were chosen based on higher energy densities compared to the NiCd. The batteries were required to have high capacity, low resistance, and low weight. Battery type and number of cells were varied to determine the best combination for both missions with varying wind conditions. The aerodynamics group provided the propulsion team with data relating score to battery capacity and weight. Testing was done on the batteries to observe actual power capacity and output instead of using the manufacture's data. Battery weight, current, takeoff distance, and endurance were considered when choosing the battery combinations. The KAN 700AA was chosen for the delivery mission along with the Elite 1500s for the payload mission. Battery selection was made using the test results along with sensitivity studies in the aerodynamics optimization.
- **Speed Controller Selection** – The most important parameters to select the speed controller are programmability, efficiency, and the peak current. The speed controller needs to be capable of handling the current through the propulsion system as well as have a variety of settings to optimize the system performance. The Kontronik Jazz 40-6-18 Brushless ESC was selected due to the speed controller's light weight, 40 Amp carrying capability, and the 7.2 to 21.6 Volt range.
- **Gear Ratio / Propeller Selection** – The propeller has specific criteria that needs to be met to accomplish the missions. The propeller needs to provide enough thrust to get the heaviest possible payload off the ground in 75 ft. A large range of diameters were researched as well as varying pitch angles. The propeller has to be smaller than 24 in to prevent a propeller strike. The team noticed that the larger propellers (17 to 20 inches) provided the most thrust with the least amount of batteries. The propulsion system was designed to be most efficient at cruise. As shown in Figure 4.11 [a], the 18x10 and the 20x11 allowed for the least number of batteries to be used because of increased cruise efficiency. The gear ratio was decided based on the shortest takeoff distance with the fewest number of batteries. Two types of gear boxes are available for the motor; planetary and offset. For the selected motors, the offset gear boxes allow better flexibility and lower weight. When gear combinations were analyzed, the team discovered there was an optimal

gear ratio to achieve the lowest takeoff distance for any given propeller. An APC 20x11 propeller with a 4.75:1 gear box ratio was chosen, which gave the team ample thrust for take off while using the least number of batteries. This trend is shown in Figure 4.11 [b].

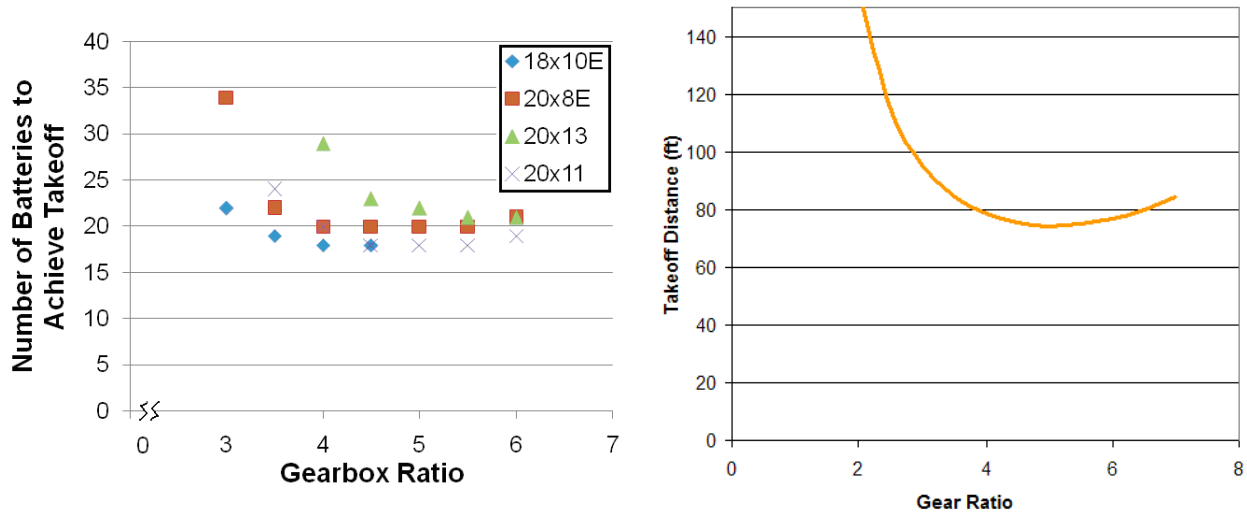


Figure 4.11: Cells vs. Gearing Ratio [a] and Takeoff Distance for Gearing Ratios [b]

4.3.3. Structures Development and Sizing

Since weight is a very high priority in this year's competition, the team wanted to make sure that they built the lightest plane that Oklahoma State has ever built. The target weight model for the plane given by the team is shown in Equation 4.1. Components that were available from the prototypes of past planes were weighed and compared with the aero design site to roughly determine the weight models used for those planes. Table 4.1 depicts the weight models that were found from the available data and components. The weight models found from the historical data show that the proposed weight model for the fuselage section is conservative compared to years past and that the wing model is more aggressive.

Equation 4.1: Target Weight Model

$$weight = 2.85 + 0.17 \cdot (area_{wing})$$

Table 4.1: Historical Weight Model

Team	Weight Model
Black 2006	2.63+0.242(S)
Black 2005	2.87+0.451(S)
Orange 2005	3.26+0.451(S)

Once the target weight model was defined, the structures team began constructing various types of wings that could potentially beat the targeted weight model. This testing is further discussed in Section 7.0. As lighter and lighter wing construction techniques were tested, the structures team, the data was passed along to the aerodynamics and propulsion teams to refine their performance estimations.

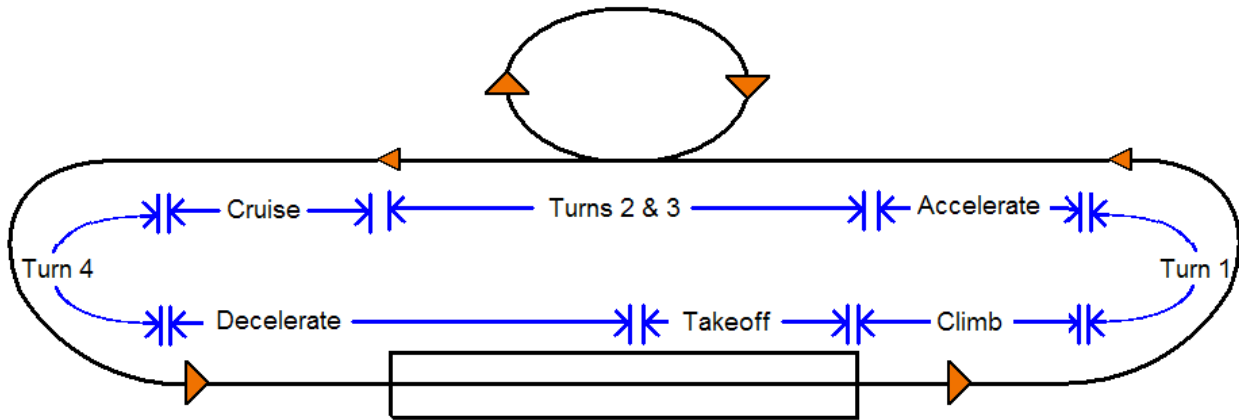
4.4. Mission Model Capabilities and Uncertainties

The team broke the mission model down into several main stages of flight in order to approximate the performance of the aircraft. Figure 4.12 shows these different flight stages.

The team identified the critical values that needed to be calculated during each stage of the mission.

These values are listed in Table 4.2. Some were calculated to estimate a design's ability to fly the mission based on practical limits and others were used in the scoring functions to rank the designs.

Figure 4.12: Mission / Flight Stages



Mission Leg	Flight Assumptions	Calculated Values	
		Aircraft Performance	Mission Performance
Takeoff	<ul style="list-style-type: none"> • Full Power • Full Flaps 	<ul style="list-style-type: none"> • Lift / Rotation Angle • Power Required 	<ul style="list-style-type: none"> • Distance • Time • Energy Used
Climb	<ul style="list-style-type: none"> • Full Power • Full Flaps 	<ul style="list-style-type: none"> • Velocity • Rate of Climb • Power Required 	<ul style="list-style-type: none"> • Time • Energy Used
Turn 1	<ul style="list-style-type: none"> • Full Power • Full Flaps 	<ul style="list-style-type: none"> • Altitude Loss • Power Required 	
Accelerate	<ul style="list-style-type: none"> • Full Power • Zero Flaps 	<ul style="list-style-type: none"> • Full Power • Power Required 	
Turns 2 & 3	<ul style="list-style-type: none"> • Full Power • Zero Flaps 	<ul style="list-style-type: none"> • Altitude Loss • Power Required 	
Cruise	<ul style="list-style-type: none"> • Cruise Power • Zero Flaps 	<ul style="list-style-type: none"> • Angle of Attack • Power Required 	
Turn 4	<ul style="list-style-type: none"> • Full Power • Zero Flaps 	<ul style="list-style-type: none"> • Altitude Loss • Power Required 	

Table 4.2: Mission Model Capabilities

4.4.1. Mission Model Limitations and Uncertainties

The optimization code written includes several areas of uncertainty with reported results. A brief analysis of the mission model led to the uncertainties and remedies listed in Table 4.3.

Table 4.3: Mission Model Uncertainties

Uncertainty		Solution
Optimization	Model assumes constant environmental conditions, perfect pilot execution, etc.	Pilot will attempt to minimize power usage; propulsion provides “cushion” energy
Structures	Optimal design cannot feasibly be built (small chord, thin airfoil, etc)	Structures team defined chord limits, construction / installation tolerances
	Weight model only a function of wing area	Structures built and tested wings of varying weight models, aero wind study
Aerodynamics	Resulting design cannot achieve theoretical aero performance	Factors of Safety during design, regarding maximum lift and angle of attack precision
Propulsion	Resulting design does not consume energy at constant rates	Factors of Safety during battery pack sizing; flight testing to refine batteries

4.5. Estimates for Lift, Drag, and Stability

The stability program that was developed was used to calculate the lift and drag parameters of the aircraft. This data was then utilized in control sizing by illustrating the control response curves for the aircraft as well as investigating the unique static and dynamic stability that the asymmetric tail induces.

4.5.1. Lift and Drag

Figure 4.13 shows the estimated aerodynamic characteristics of the entire aircraft. On the left, the drag polar shows a zero lift drag coefficient of 0.057. On the right, the lift to drag ratio is seen to be at an optimum value of 8.7 at an angle of attack of 4°, which the whole aircraft is design to fly at during the payload mission,

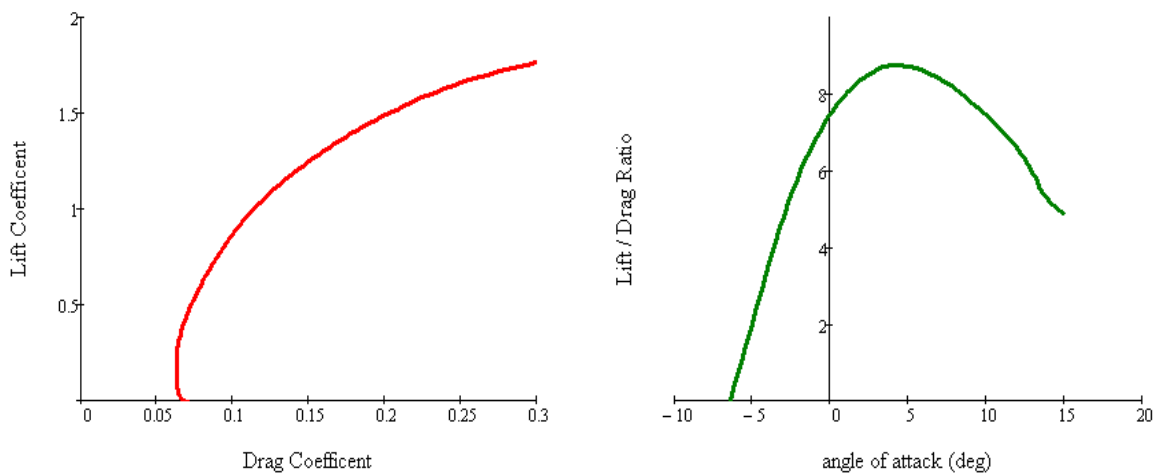


Figure 4.13: Performance Curves - Drag Polar [a] and Lift to Drag Ratio [b]

The required lift coefficient for each mission can be found with the weight, wing area, and cruise velocity. The delivery mission requires a lift coefficient of 0.67 which corresponds to a lift to drag ratio of 8 and a glide angle of 7.13° . Performing the same analysis for the payload mission confirms that the aircraft is flying at peak efficiency and a glide angle of 6.56° . Additionally, the aerodynamic efficiency can be used to find the total energy required for each mission.

4.5.2. Static Stability

The stability and control code was used in the analysis static stability. The airfoil data of the wing and tail were obtained in tabular format with XFOIL. This data was linearized and corrected for three dimensional flow. The neutral point was then calculated to be 1.36 inches behind the quarter chord. To arrive at a static margin of 20%, the center of gravity was placed on the quarter chord, which provided a sufficient compromise between stability and efficiency. The final result is the stability curve shown in Figure 4.14. Each component is represented individually as a dotted line and the entire aircraft is shown by the solid line.

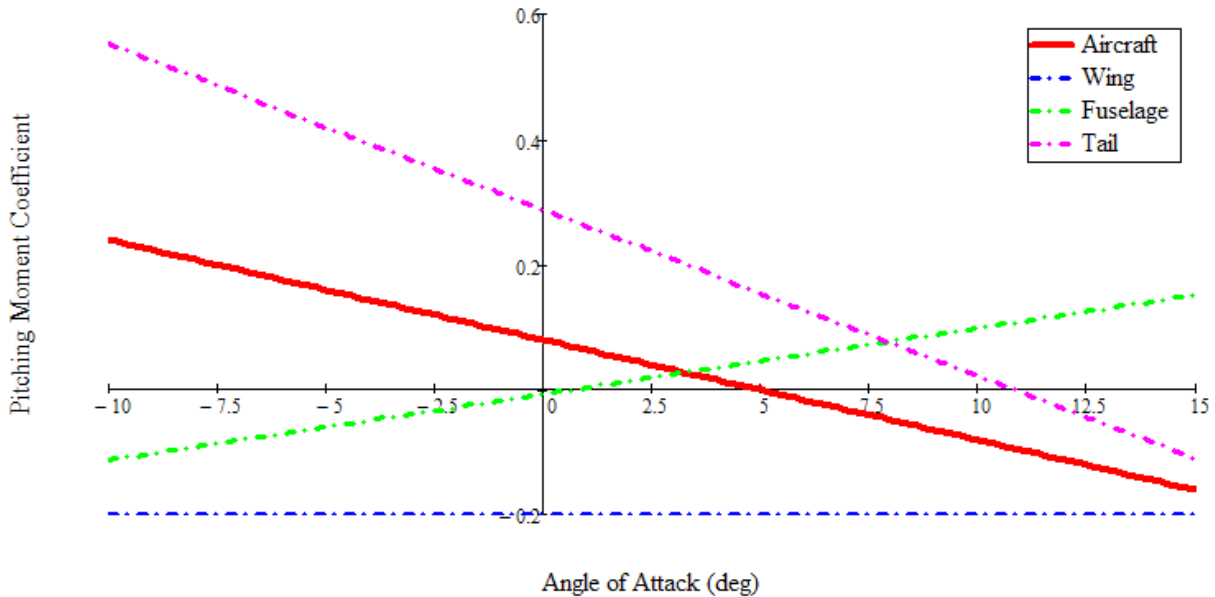


Figure 4.14: Static Stability Diagram

The aircraft's trim point is estimated by observing at what angle the aircraft pitching moment coefficient curve crosses the horizontal axis. The tail incidence was set to 1° , and the wing incidence to 2° for an efficient cruise. The lift coefficient for the wing at the trim angle of attack needed to be about 1.02 (fully loaded 40 ft per sec cruise), and so the incidence angles were used to try to obtain this lift. Based on Figure 4.14, the aircraft trims at about 5° . At cruise velocity of 40 ft/s, the aircraft trims for L/D max at 4° . The trim condition requires minor elevator deflection.

4.5.3. Control Sizing

For a biplane, either both wings could have ailerons or a single wing could. Placing ailerons on both wings will require the additional weight of four independent servos or linkages to join two ailerons to one servo. Instead the ailerons were implemented on the bottom wing. The aileron dimensions can be seen in Figure 4.15 and Table 4.4.

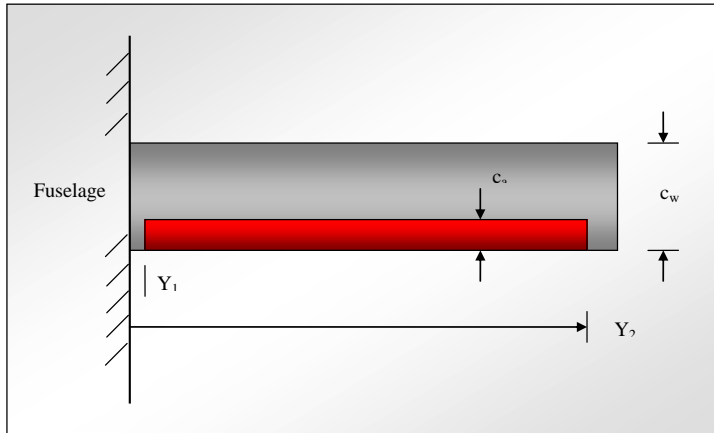


Table 4.4: Aileron Dimensions

C_{aileron}	1.4 in
Total b_{aileron}	4.6 ft
Total S_{aileron}	0.6 ft ²
Y₁	3.5 in
Y₂	31.2 in

Figure 4.15: Aileron Diagram

An aileron chord of 1.4 in and flap effectiveness of 0.35 gives a roll rate of 15° per second. Maximum aileron deflection is set at 5° to avoid flow separation. However, differential aileron deflection was available after production. After the first test flight has been flown, pilot input will be gathered and modifications to the roll control system may be made. This will help give the pilot the control he needs to perform the mission to the best of his ability.

The angle of attack required to take off was found to be approximately 7.4°, and C_{Lmax} occurs at approximately 10°. The elevator was sized to enable the aircraft to reach C_{Lmax} using the relation shown in Equation 4.2.

Equation 4.2: Incremental Moment Coefficient

$$\Delta C_{m_{cg}} = C_{m0} + (C_{m\alpha}) \cdot (\Delta\alpha) = -0.103$$

The maximum elevator deflection angle was fixed at 10° due to the degradation of airfoil performance at large flap deflection angles. The flap effectiveness was then calculated to meet this requirement which yields an elevator length of 15% of the stabilizer's chord. Additionally, using the elevator size information, a plot of moment coefficient for various elevator deflection angles was generated in Figure 4.16.

Rudder sizing was performed based on a maximum side slip angle of 11.5°, which corresponds to a cross wind of 4 mph on take off. At a side slip of 11.5°, the yaw moment coefficient was 0.0124. A maximum rudder deflection angle was assumed to be 15°. The flap effectiveness parameter was solved for and found to be 0.39. The rudder needs to be 20% of the vertical stabilizer's chord.

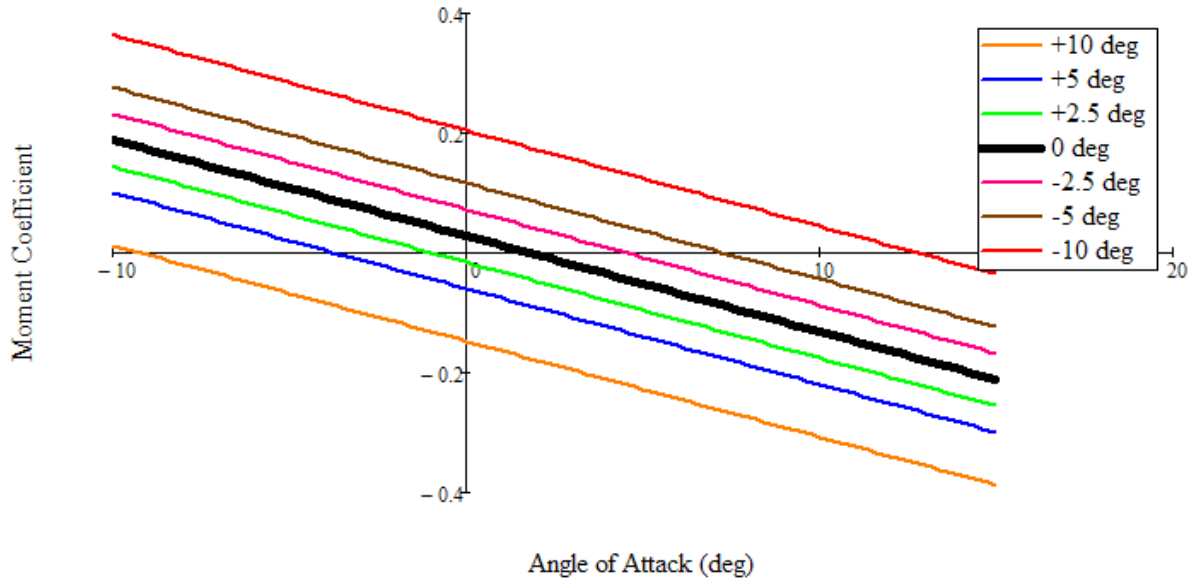


Figure 4.16: Static Stability Curve with Elevator Deflections

4.5.4. Elevator Deflection – Roll Moment Coupling

An asymmetrical tail called for an analysis of the coupling between pitch and roll control. The relationship for was calculated similarly to aileron roll power. The elevator roll moment is $-0.0005/\text{degree}$, which shows that even at maximum elevator deflection, the roll moment should be easily corrected by minimal aileron inputs. Figure 4.17 [a] shows roll moment coefficients versus aileron deflection for multiple elevator deflections and Figure 4.17 [b] shows the aileron deflection required to trim in roll for a given elevator deflection.

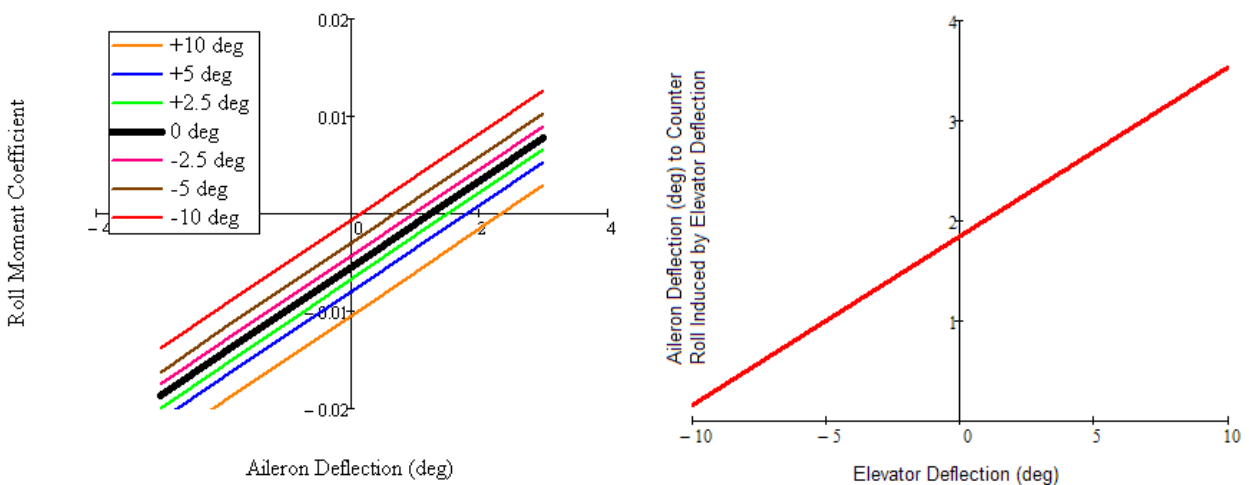


Figure 4.17: [a] Roll Moment Coefficient vs. Aileron Deflection [b] Aileron Deflection to Trim

4.5.5. Dynamic Aircraft Stability

The analysis of the aircraft's dynamic stability was performed to determine if response time was adequate. The asymmetrical tail required the calculation of additional stability derivatives to more precisely predict the aircraft's dynamic response via the coupling of the longitudinal and lateral axes.

Initially, the longitudinal and lateral modes were examined individually. A state-transition matrix that incorporated all the longitudinal and lateral stability derivatives was constructed, including the additional terms that couple the lateral and longitudinal motion of the aircraft. Table 4.5 shows these additional stability derivatives highlighted in yellow along with the derivatives that are typical of conventional stability analyses in orange. Table 4.6 shows the time to half for all stable modes, time to double for the unstable spiral mode and periods of oscillating modes. The eigenvalues are graphed in Figure 4.18.

Table 4.5: Coupled Dynamic Stability Matrix

$$\begin{bmatrix} \dot{u} \\ \dot{w} \\ \dot{q} \\ \dot{\theta} \\ \dot{\beta} \\ \dot{p} \\ \dot{r} \\ \dot{\phi} \end{bmatrix} = \begin{bmatrix} -0.06 & 0.57 & 0 & -32.17 & 0 & 0 & 0 & 0 \\ -1.15 & -4.23 & 45.00 & 0 & 0 & 0.97 & 0 & 0 \\ 0.07 & -0.62 & -7.93 & 0 & 0 & 8.99 & 0 & 0 \\ 0 & 0 & 1.00 & 0 & 0 & 0 & 0 & 0 \\ 0 & 0 & 0 & 0 & -0.14 & 0.01 & -0.99 & 0.72 \\ -0.16 & -0.66 & -0.03 & 0 & 0 & -35.75 & 9.07 & 0 \\ 0 & 0 & 0 & 0 & 23.21 & -1.70 & -1.42 & 0 \\ 0 & 0 & 0 & 0 & 0 & 1.00 & 0 & 0 \end{bmatrix} \begin{bmatrix} u \\ w \\ q \\ \theta \\ \beta \\ p \\ r \\ \phi \end{bmatrix}$$

Table 4.6: Dynamic Response (sec)

	$t_{1/2}$	t_{double}	Period
Roll	0.019	---	---
Short Period	0.116	---	1.077
Dutch Roll	0.645	---	1.328
Long Period	19.25	---	9.119
Spiral	---	4.006	---

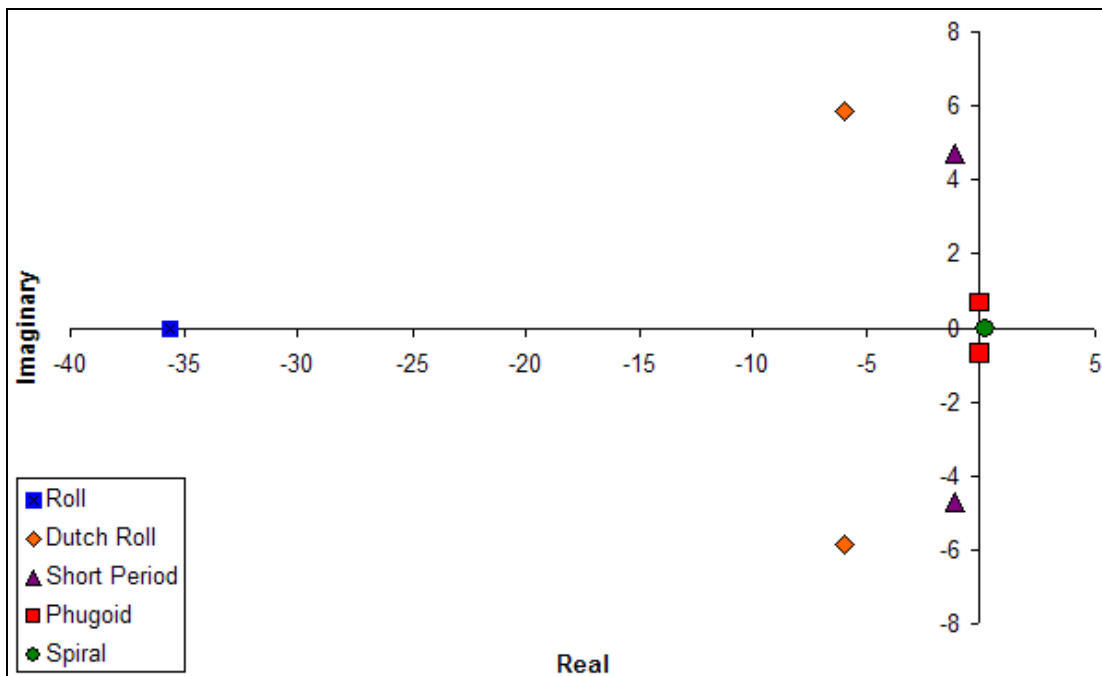


Figure 4.18: S-Plot of Stability Roots

All of the eigenvalues graphed in Figure 4.18 have negative real components except for the lightly unstable spiral mode root, indicating that the movements are stable and damped. The results in Table 4.6 lead to the conclusion that pilot correction should be sufficient to achieve desirable performance.

4.6. Aircraft Mission Performance Estimates

Estimates of the aircraft's performance characteristics were applied to each of the mission models in order to approximate a score for each mission. The mission models were divided into different stages of flight; performance predictions were made for each stage in the mission. The flight stages within the missions include the takeoff stage and the cruise stage. The performance predictions for the different flight stages are summarized in Figure 4.19.

Preliminary estimates for weight, propulsion and aerodynamics were collected from their respective groups and were input into the mission models. The mission model output useful data regarding power, velocities and score. The predicted mission scores are not normalized and the payload loading time was estimated at 30 seconds based on early time trails.

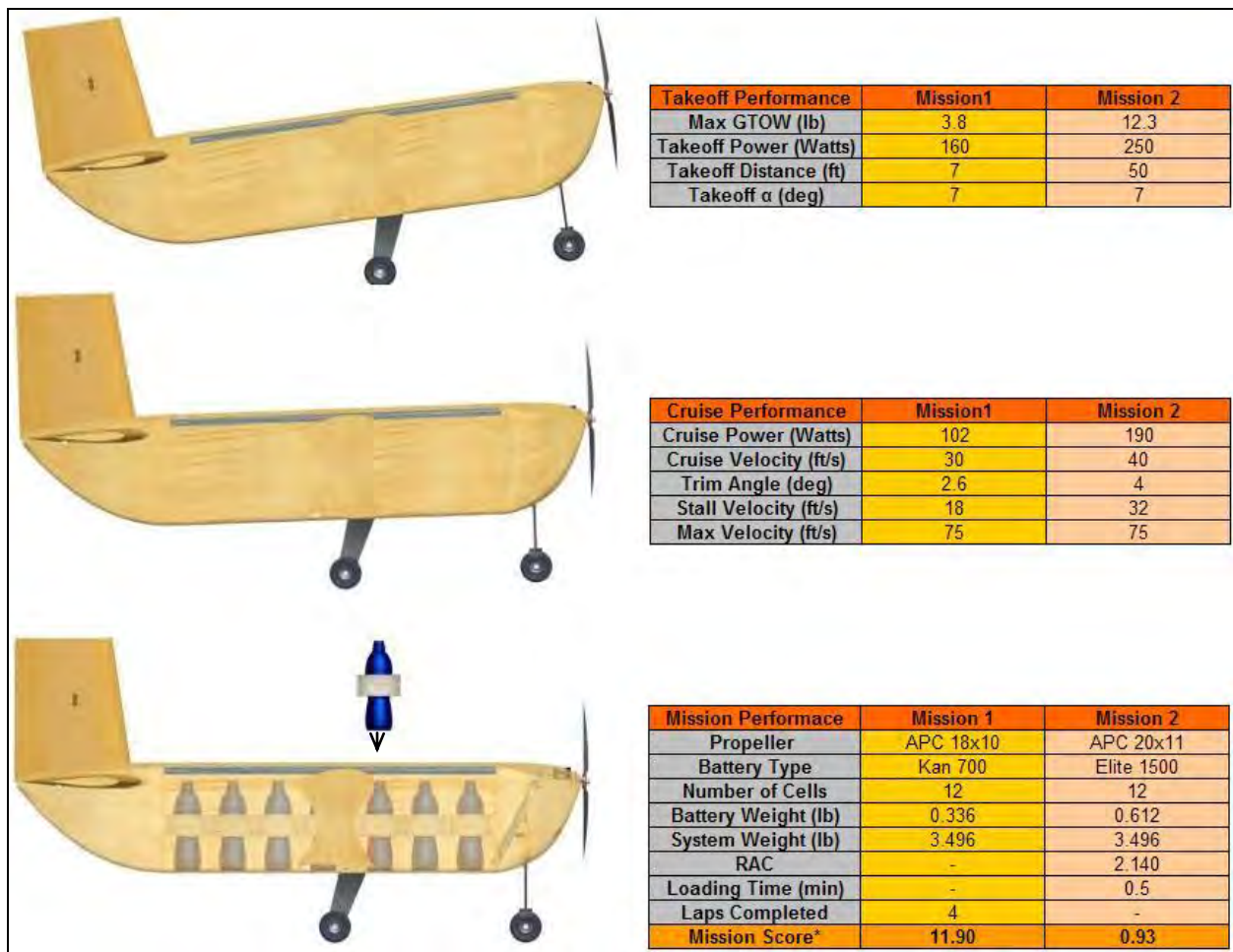


Figure 4.19: Mission 1 & 2 Scores and Performance Predictions

5.0. Detail Design

This phase summarized the aircraft's dimensions, systems, and structural characteristics that resulted from the trade studies performed, as well as identifying predicted aircraft and mission scores.

5.1. Dimensional Parameters

A summary of the dimensions of the aircraft as well as control sizes is shown in Table 5.1.

Table 5.1: Dimensional Parameters Summary

Geometry						
Fuselage		Horizontal Stabilizer			Vertical Stabilizer	
Length (in)	52.00	Airfoil	NACA 0012		Airfoil	NACA 0012
Width x Height (in)	8.52 x 10.5					
Wings			Port	Starbord		
Airfoil	MVA-227	Root Chord (in)	12.00	12.00	Root Chord (in)	11.00
Chord (in)	7.00	Tip Chord (in)	4.00	6.38	Tip Chord (in)	9.00
Span (ft)	5.85	Span (in)	8.60	17.00	Span (in)	1.06
Area (ft ²)	6.50	Area (ft ²)	1.23		Area (ft ²)	0.88
Wing Spacing (in)	8.00	AR	3.70		AR	1.27
AR _{eff}	6.39	Volume Ratio	0.65		Volume Ratio	0.046
Ailerons (lower wing)		Elevator (starbord side)			Rudder	
Chord (in)	1.40	Chord (in)	1.80		Chord (in)	2.20
Width _{aileron} (ft)	2.30	Width _{elevator} (ft)	1.42		Width _{rudder} (ft)	1.06
S _a / S _w	18%	S _e / S _{ht}	17%		S _r / S _{vt}	22%

5.2. Structural Characteristics / Capabilities

The aircraft structure can be broken into four major components: fuselage, wing, empennage, and gear. The components are ordered by the loading capabilities of each, the fuselage being the main support structure that supports the loading of the wings, empennage, and gear.

5.2.1. Fuselage and Hatch

The fuselage is a monocoque structure that is comprised of balsa reinforced with fiberglass layers. The skin of the aircraft is the root of all the transfer of the forces as illustrated in Figure 5.1.

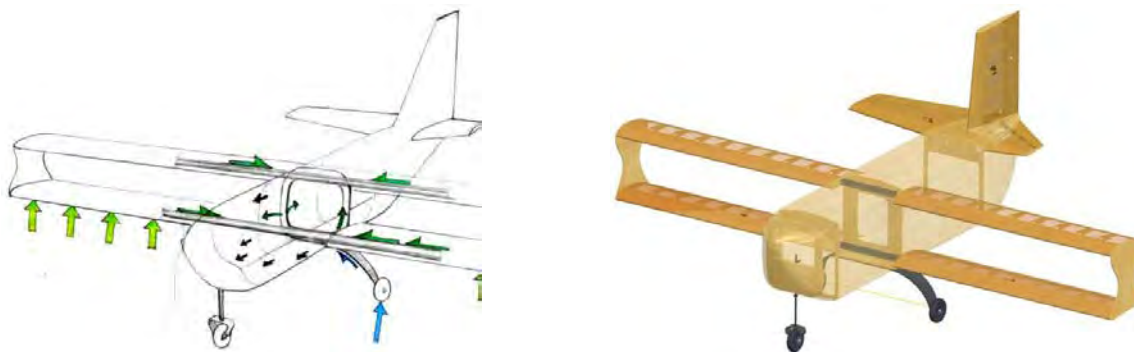


Figure 5.1: Load Paths

At key stress areas, Kevlar is used to help transfer the load and prevent shearing of the fuselage. Light aircraft-grade plywood bulkheads are used to help maintain fuselage shape and transfer landing loads into the fuselage. The forward bulkhead supports the nose gear while the third bulkhead supports the main gear, wings, and the hatch latch. The second and fourth bulkheads are used to support the payload restraint system as well as provide locations for small magnets to seal the hatch. The payload system is a grid of fiberglass reinforced balsa. The grid is covered with a clear, high strength, transparent vacuum film that latches into the bulkheads to restrain the passenger simulate payloads. The cargo pallet payloads are restrained via rubber bands fixed at points in the lower section of the fuselage. The outer hatch is cut from the solid balsa-fiberglass fuselage and reattached and hinged with Kevlar.

The main fuselage capability is to provide a support to tie in all subsystems. The fuselage supports the root of the wing from tearing away from the plane during lifting. The fuselage absorbs and transfers impact forces experienced during landing.

5.2.2. Wing

The wings are composed of 5 main components: carbon fiber C-channel, balsa ribs, balsa leading and trailing edge, and Microlite. The C-channel acts as the wing spar, and is one continuous structure between wing tips. The C-channel is tapered to provide the most strength at the root of the wing and save weight at the wing tips. The ribs give the airfoil shape to the Microlite, and the balsa leading and trailing edge give rigidity to the structure. For the bottom wing the ailerons are formed from a solid balsa piece for the control surface and an aircraft-grade plywood rib is used to support the servo. Ribs and leading and trailing edges were made of 1/16 in balsa. A cross section of the wing layup is shown in Figure 5.2. Balsa end plates reinforced with carbon fiber were placed between the two wings to give torsional rigidity to the wings as well as maintain spacing. This gives an overall lightweight structure still capable of handling the required 2.5-G load.

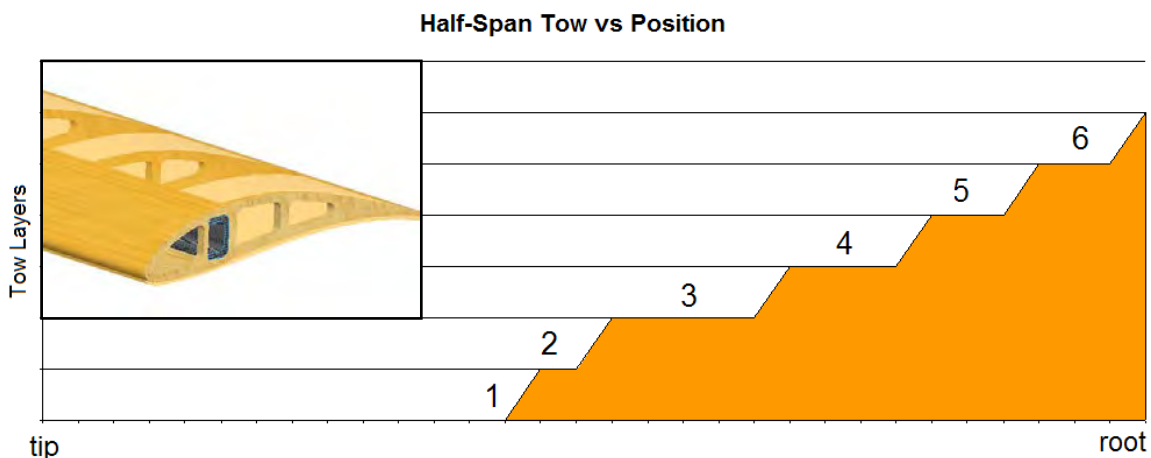


Figure 5.2: Monokote Wing Loading, Tow Build-Up, and Structure

5.2.3. Empennage

The horizontal and vertical tails are made of a frame of 1/16 in balsa ribs with two spars of 3/16 in

balsa. The ribs were bonded to the spars and covered with a balsa skin. Holes were then cut from into the skin and the entire surface was covered in Microlite. The servos were attached into the base of both the horizontal and vertical stabilizer and connected directly to the elevator and rudder respectively. The elevator and rudder are hollow triangles made of 1/16 in balsa and covered in Microlite. Both tails are capable of sustaining the tail loads with a balsa structure. The empennage is shown in Figure 5.3a.

5.2.4. Landing Gear

The main gear of the aircraft utilizes the flexibility and strength of carbon fiber bow gear. Several variations were made and tested until a suitable strength to weight ratio was achieved. A Kevlar flying wire is attached between the wheels to prevent the gear from flexing too far apart. The wheels were attached with 8 gauge screws and fixed with lock nuts and washers. The gear is attached to aircraft-grade plywood floor reinforcement with two 1/4 in nylon bolts and nuts. The floor helps to take the impact of landing. The nose gear is made of a natural spring of formed carbon fiber with a carbon rod bonded to it. The nose gear uses an 8 gauge screw, washers and lock nuts to attach the wheel. A washer was bonded to the carbon rod and a sloped balsa block was formed to transfer the stress from the rod washer evenly to the skin. A servo control horn was fabricated to fit the rod and allow for steering.

The main gear is capable of sustaining a drop from 18 in and also completely supports a fully loaded aircraft. The nose gear can support the static loading of the fully loaded aircraft. The landing gear is shown in Figure 5.3b.

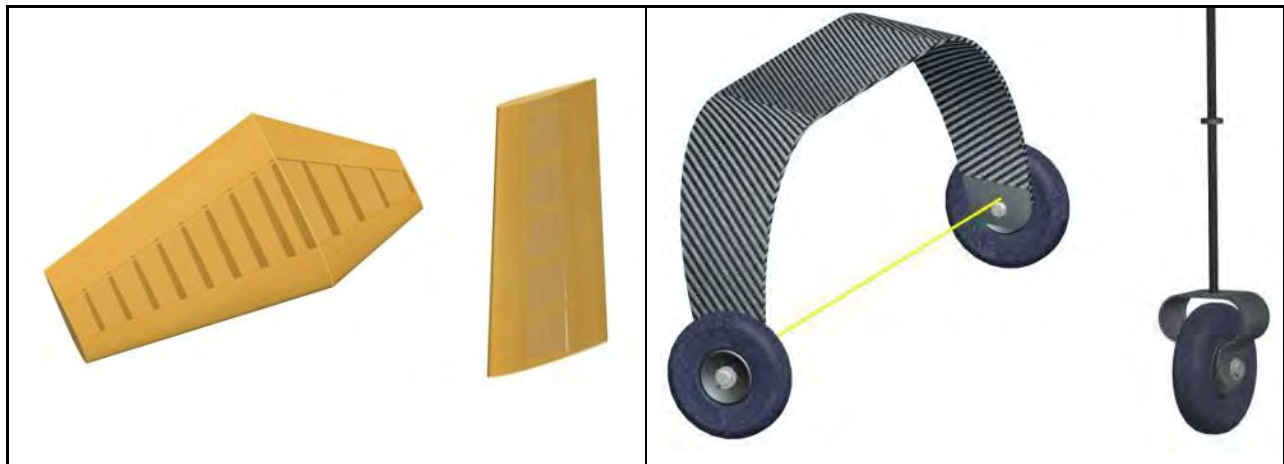


Figure 5.3: Empennage [a] and Landing Gear [b] CAD Drawings

5.3. Systems and Sub-Systems

Control servo requirements were determined by using XFOIL to find hinge moment coefficients for the airfoils. The coefficients were found by assuming a control surface deflection angle of 15° and an angle of attack of 12°. The hinge moment was calculated for an 80 ft/s dive. The rudder moment was calculated for a high crosswind at the take off velocity of 30 ft/s in order to size the servo to handle the take off side slip. The hinge moment data is summarized in Table 5.2.

Surface	Coefficient	Moment
Elevator	0.003643	6.43 oz-in
Rudder	0.061161	8.94 oz-in
Aileron	0.01892	26.6 oz-in

Table 5.2: Hinge Moments

For reliability reasons only servos with metal gears were considered. The Futaba S3156MG met the aileron torque requirements while having a weight low enough to make it desirable. This servo was powerful enough to meet all servo requirements throughout the aircraft. In addition, the other main systems components are listed in Table 5.3. The initial battery pack estimations are shown in Table 5.4.

Table 5.3: Aircraft Systems

Systems	
Radio	Spektrum DX7 2.4 GHz
Servo Motors (5)	Futaba S3156MG
Motor	Medusa 028-040-1700
Propellor	APC 20x11E
Gear Ratio	4.75:1
Receiver	Spektrum AR9000
Speed Controller	Kontronik Jazz 40-6-18

Table 5.4: Predicted Mission Battery Packs

Battery Packs		
	Delivery	Payload
# of Cells / Type	(12) Elite 1500	(12) KAN 700
Pack Weight (lbs)	0.396	0.612

5.4. Weight and Balance

Figure 5.4 shows the system weight broken down into all major systems components.

Sub-Assembly	Estimated Weight (lbs)	Actual Weight (lbs)	Key
Fuselage	0.873	1.180	Green
Wings	0.806	0.897	Red
Empennage	0.346	0.270	Blue
Landing Gear	0.362	0.350	Grey
Payload Restraint	0.048	0.090	Yellow
Propulsion	0.672	0.730	Orange
Systems	0.203	0.171	Purple

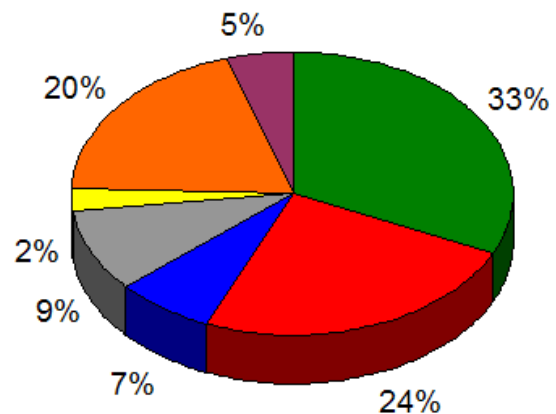


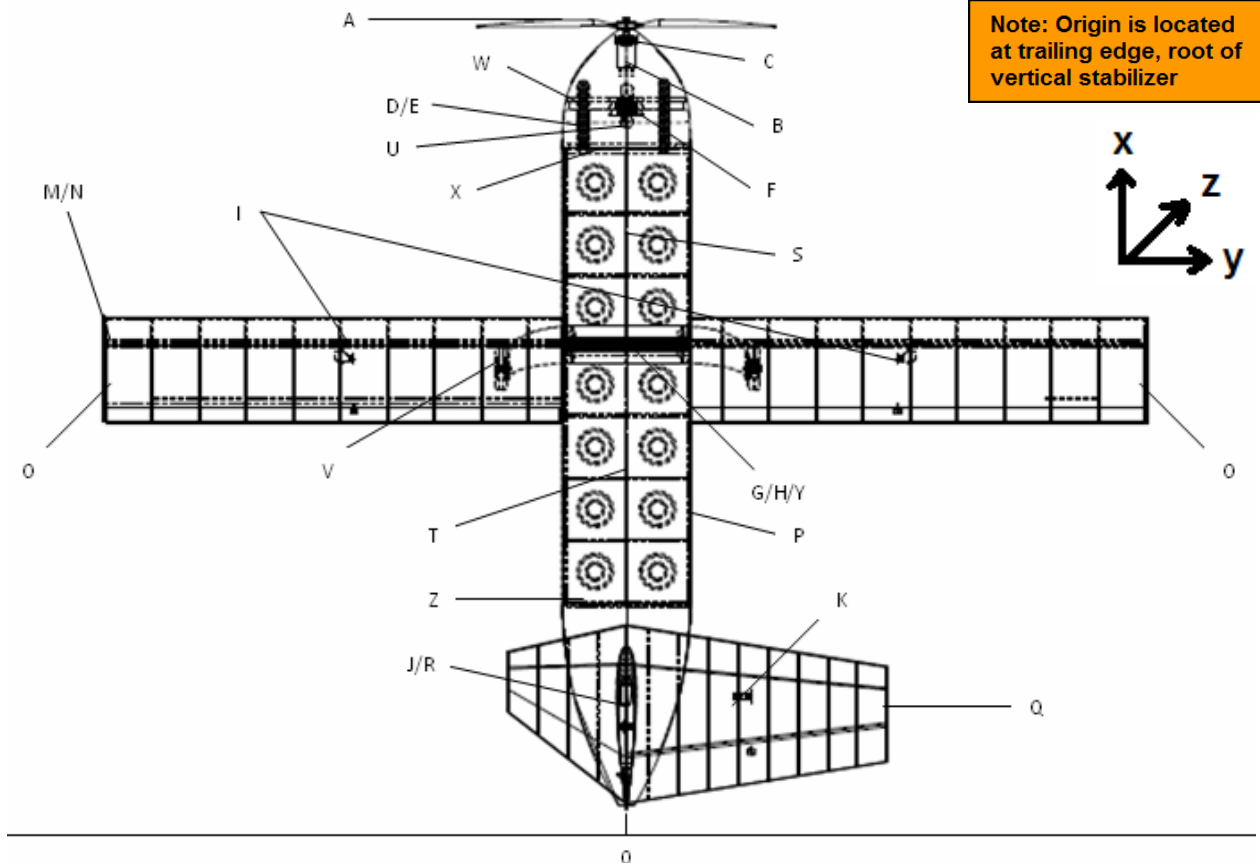
Figure 5.4: System Weight Detail

To simplify the process of calculating the CG an Excel program was constructed that used moment calculations to keep the CG centered over the quarter chord of the wing. Table 5.5 shows the weight and balance detail. Since the payload changes, the combinations can cause the CG to shift. The center of gravity of the aircraft must remain very consistent in order to extract the maximum performance from the

aircraft. The payload arrangements that were derived keep the CG within a ¼ in radius from the empty aircraft CG. The resulting payload arrangements and CG positions are shown in Table 5.6 to Table 5.10.

Table 5.5: Aircraft Weight and Balance Detail

Propulsion				Structures			
Component	Weight (lbs)	CG Station (in)		Component	Weight (lbs)	CG Station (in)	
A Propeller	0.137	x = 53		M Top Wing	0.386	x = 30.5	
B Motor	0.200	x = 51.5		N Lower Wing	0.400	x = 30.5	
C Gearbox	0.077	x = 51		O End Plates	0.020	x = 30.5	
D Motor Battery Pack (loaded)	0.700	x = 50		P Fuselage	0.467	x = 26	
E Motor Battery Pack (ferry)	0.200	x = 48.5		Q Horizontal Tail	0.205	x = 6	
F Speed Controller	0.073	x = 51.5		R Vertical Tail	0.141	x = 6	
G Servo Battery Pack	0.100	x = 31.5		S Restraint System (front section)	0.021	x = 38.25	
H Servo Receiver	0.086	x = 31.5		T Restraint System (rear section)	0.027	x = 23.65	
Servos & Wiring				U Front Gear + Wheels	0.066	x = 50	
Component	Weight (lbs)	CG Station (in)		V Rear Bow Gear + wheels	0.295	x = 28	
I Servo (Wings)	0.066	x = 29		W Front Bulkhead	0.075	x = 50	
J Servo (V-Tail)	0.033	x = 4		X 2nd Bulkhead	0.082	x = 46.2	
K Servo (H-Tail)	0.033	x = 4		Y Wing spar bulkhead	0.167	x = 31.5	
L Total Weight of Wiring	0.071	---		Z Rear Bulkhead	0.082	x = 14.7	
				AA Misc Components (bolts, nuts, etc)	0.200	---	



Gross Weight (w/o batteries)	3.510 lbs
Delivery Mission Weight	3.906 lbs
Payload Mission Weight	11.122 lbs

Table 5.6: Weight and Balance Chart for 14 Bottles

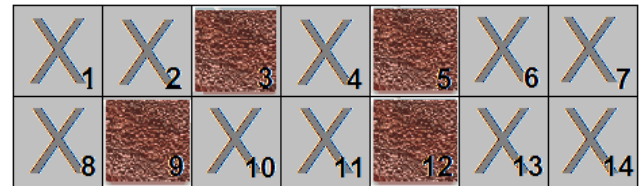
Payload Element	Weight (lbs)	Position (in)
Bottle - 1	0.5	x = 45.1
Bottle - 2	0.5	x = 40.9
Bottle - 3	0.5	x = 36.7
Bottle - 4	0.5	x = 26.7
Bottle - 5	0.5	x = 24.6
Bottle - 6	0.5	x = 20.4
Bottle - 7	0.5	x = 16.2
Bottle - 8	0.5	x = 45.1
Bottle - 9	0.5	x = 40.9
Bottle - 10	0.5	x = 36.7
Bottle - 11	0.5	x = 26.7
Bottle - 12	0.5	x = 24.6
Bottle - 13	0.5	x = 20.4
Bottle - 14	0.5	x = 16.2



CG of Payload	28.828 in
CG of Loaded Aircraft	31.509 in
Weight of Aircraft	11.025 lbs

Table 5.7: Weight and Balance Chart for 4 Bricks

Payload Element	Weight (lbs)	Position (in)
Brick - 3	1.8	x = 36.7
Brick - 6	1.8	x = 20.4
Brick - 9	1.8	x = 40.9
Brick - 13	1.8	x = 20.4



CG of Payload	31.911 in
CG of Loaded Aircraft	31.501 in
Weight of Aircraft	11.726 lbs

Table 5.8: Weight and Balance Chart for 10 Bottles, 1 Brick

Payload Element	Weight (lbs)	Position (in)
Brick - 3	1.8	x = 36.7
Bottle - 4	0.5	x = 26.7
Bottle - 6	0.5	x = 20.4
Bottle - 7	0.5	x = 16.2
Bottle - 8	0.5	x = 45.1
Bottle - 9	0.5	x = 40.9
Bottle - 10	0.5	x = 36.7
Bottle - 11	0.5	x = 26.7
Bottle - 12	0.5	x = 24.6
Bottle - 13	0.5	x = 20.4
Bottle - 14	0.5	x = 16.2



CG of Payload	28.453 in
CG of Loaded Aircraft	31.601 in
Weight of Aircraft	10.826 lbs

Table 5.9: Weight and Balance Chart for 7 Bottles, 2 Bricks

Payload Element	Weight (lbs)	Position (in)
Bottle - 1	0.5	x = 45.1
Bottle - 2	0.5	x = 40.9
Bottle - 3	0.5	x = 36.7
Bottle - 4	0.5	x = 26.7
Bottle - 5	0.5	x = 24.6
Bottle - 6	0.5	x = 20.4
Brick - 9	1.8	x = 40.9
Bottle - 12	0.5	x = 24.6
Brick - 14	1.8	x = 16.2



CG of Payload	25.904 in
CG of Loaded Aircraft	31.536 in
Weight of Aircraft	9.826 lbs

Table 5.10: Weight and Balance Chart for 3 Bottles, 3 Bricks

Payload Element	Weight (lbs)	Position (in)
Brick - 3	1.8	x = 36.7
Brick - 5	1.8	x = 24.6
Bottle - 9	0.5	x = 40.9
Bottle - 10	0.5	x = 36.7
Brick - 11	1.8	x = 26.7
Bottle - 14	0.5	x = 16.2



CG of Payload	28.806 in
CG of Loaded Aircraft	31.547 in
Weight of Aircraft	10.926 lbs

5.5. Flight Performance

The performance of the aircraft was estimated using the stability program. Maximum lift coefficient and zero-lift drag coefficient were derived obtained from the airfoil data, and the induced drag parameter K was estimated using the effective computed aspect ratio. Velocity and rate of climb estimates were made using the loaded and empty aircraft parameters and are shown in Table 5.11.

Table 5.11: Flight Performance Estimates

Performance			
C_{Lmax}	1.80	C_{D0}	0.056
L/D_{max}	7.25	K	0.050
Empty		Loaded (maximum payload)	
R/C_{max} (ft/s)	14.5	R/C_{max} (ft/s)	2.3
Cruise Speed (ft/s)	30.0	Cruise Speed (ft/s)	40.0
Stall Speed (ft/s)	18.0	Stall Speed (ft/s)	32.0
Maximum Speed (ft/s)	75.0	Maximum Speed (ft/s)	75.0
Takeoff Distance (ft)	5.0	Takeoff Distance (ft)	50.0

5.6. Rated Aircraft Cost (RAC)

The RAC for the contest is only defined for the payload mission, and is shown in Equation 5.1.

Equation 5.1: Payload Mission RAC

$$RAC = (\text{weight}_{\text{system}}) \cdot (\text{weight}_{\text{battery}}) = (3.71) \cdot (1.0) = 3.71$$

5.7. Mission Performance

Errors were expected in the mission performance predictions made in the preliminary analysis. This was because the preliminary analysis was completed using mathematical models that relied on several assumptions. Experimental data pulled from the dynamometer, wind tunnel, and battery bench tester was used in the detail design. This data allowed for a more precise determination of how well the aircraft would score for each mission. Mission performance for the final design is shown in Table 5.12.

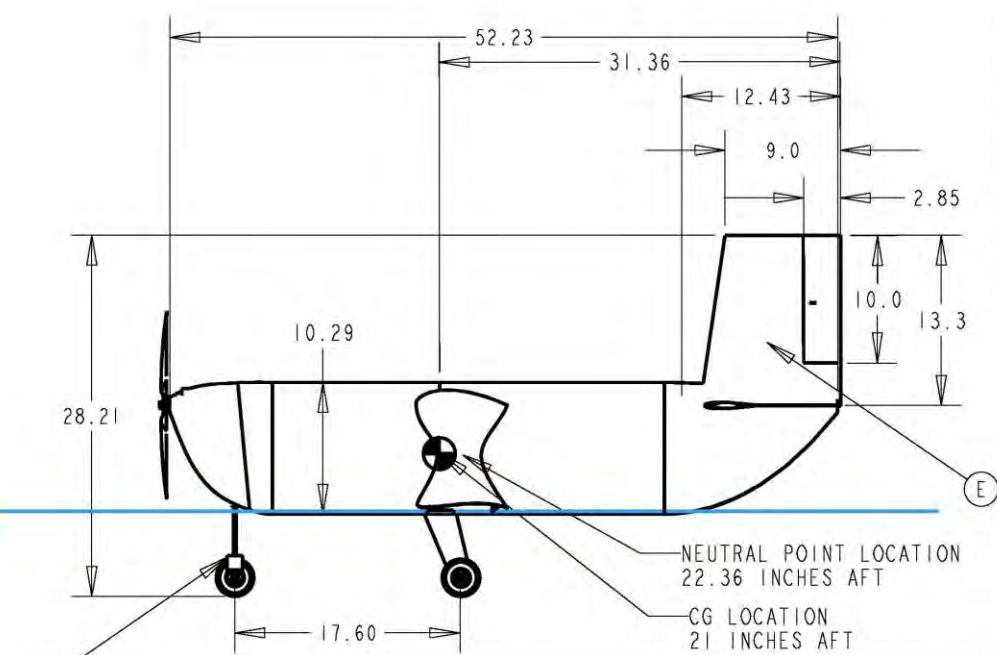
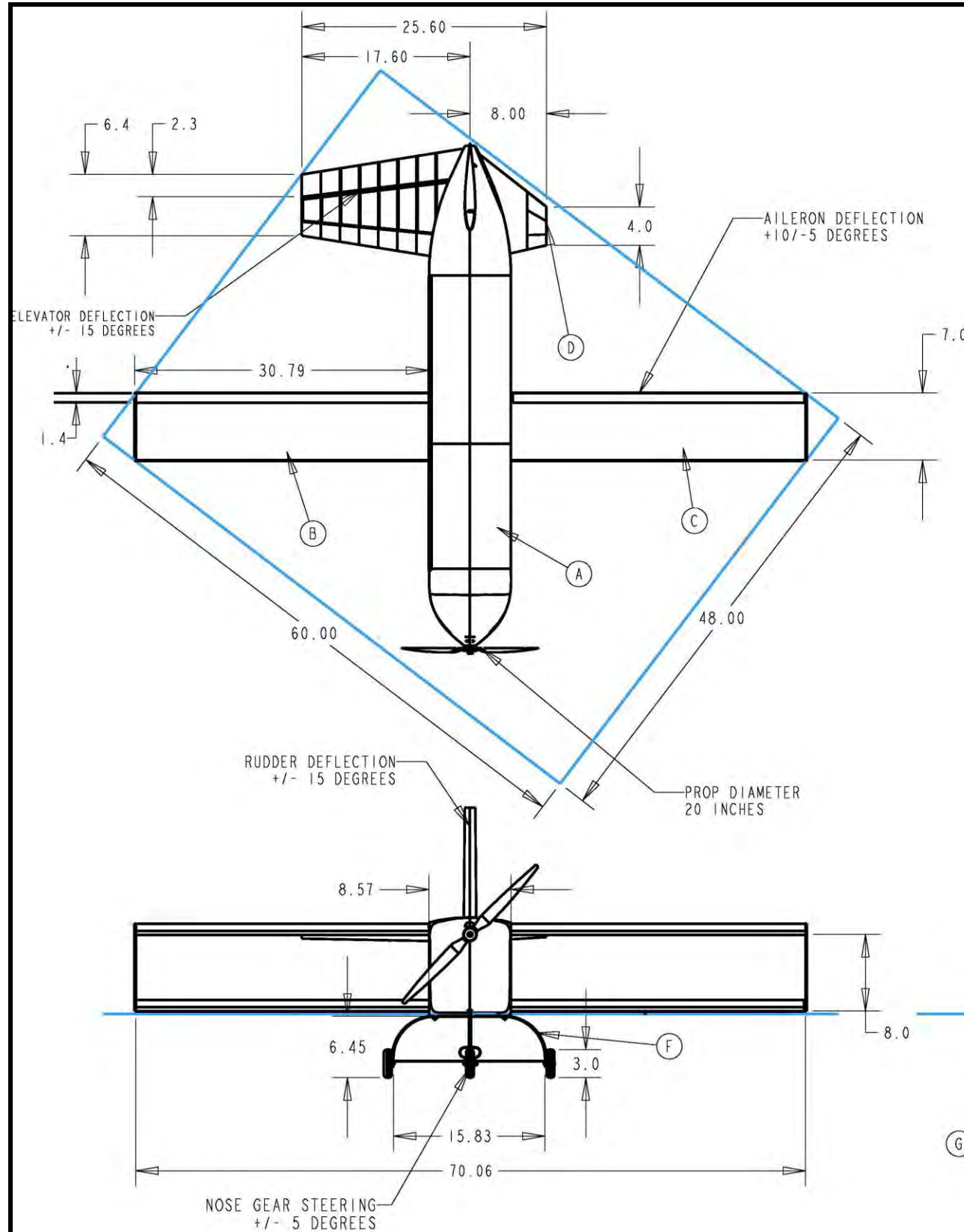
Table 5.12: Final Design Mission Performance

Mission	V _{cruise} (ft/s)	W _{batt} (lb)	N _{laps}	Loading Time (min)	RAC	Score
Delivery	30	0.304	4	---	---	13.16
Payload	39.3	0.935	2	0.33	3.71	0.816

5.8. Drawing Package

The drawing package was developed and created in Pro-Engineer. The drawing package contains the Flight Configuration (three-view), Structural Arrangement, Systems Layout, and Payload Accommodation. The drawings are on the four following pages:

- Page 48 – Flight Configuration (three-view)
- Page 59 – Structural Arrangement
- Page 50 – Systems Layout
- Page 51 – Payload Accommodation

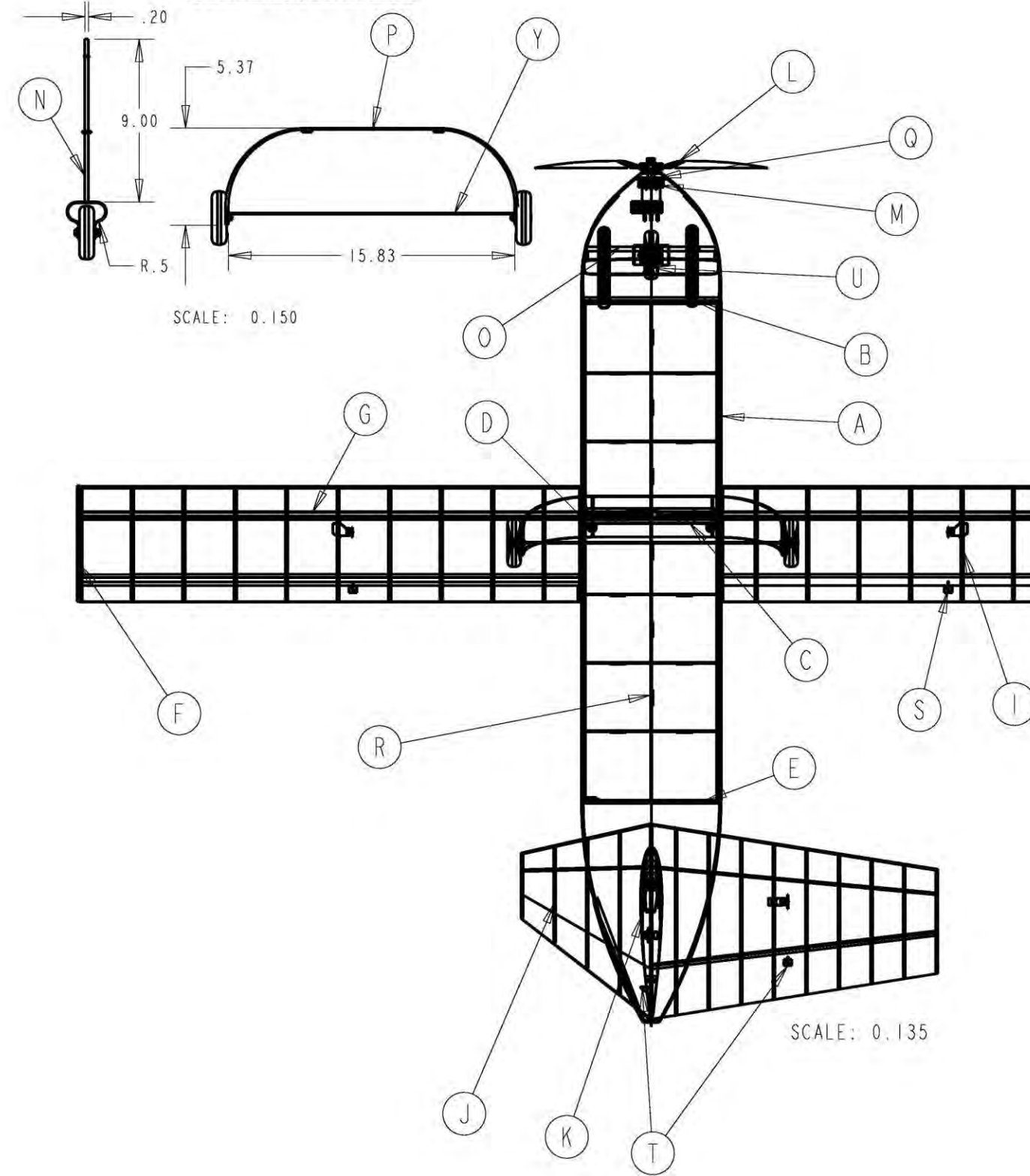


PRIMARY COMPONENT LIST	
A	FUSELAGE
B	STARBOARD WING ASSEMBLY
C	PORT WING ASSEMBLY
D	HORIZONTAL STABILIZER ASSEMBLY
E	VERTICAL STABILIZER ASSEMBLY
F	MAIN LANDING GEAR
G	NOSE LANDING GEAR

SCALE: 0.08

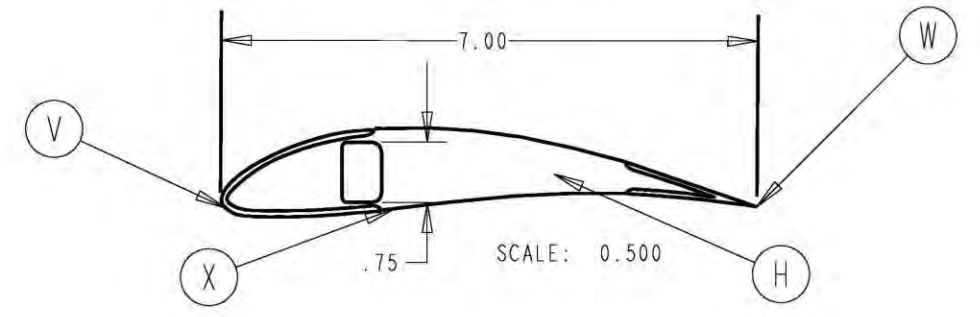
FLYING NEMO		OKLAHOMA STATE UNIVERSITY ORANGE TEAM CESSNA/RAYTHEON MISSILE SYSTEMS DESIGN/BUILD/FLY 2008		
CHIEF ENGINEER D. GAMBLE	NOTE: ALL DIMENSIONS ARE GIVEN IN INCHES	FLIGHT CONFIGURATION		
STRUCTURES LEAD T. STRADTMANN		REVISION 1R		
DRAWN BY S. BROWN		DATE OF APPROVAL 2-13-08	DRAWING PACKAGE	
FACILITY ADMIRAL DR. A. ARENA JR.		PAGE 1 OF 4		

GEAR ASSEMBLIES

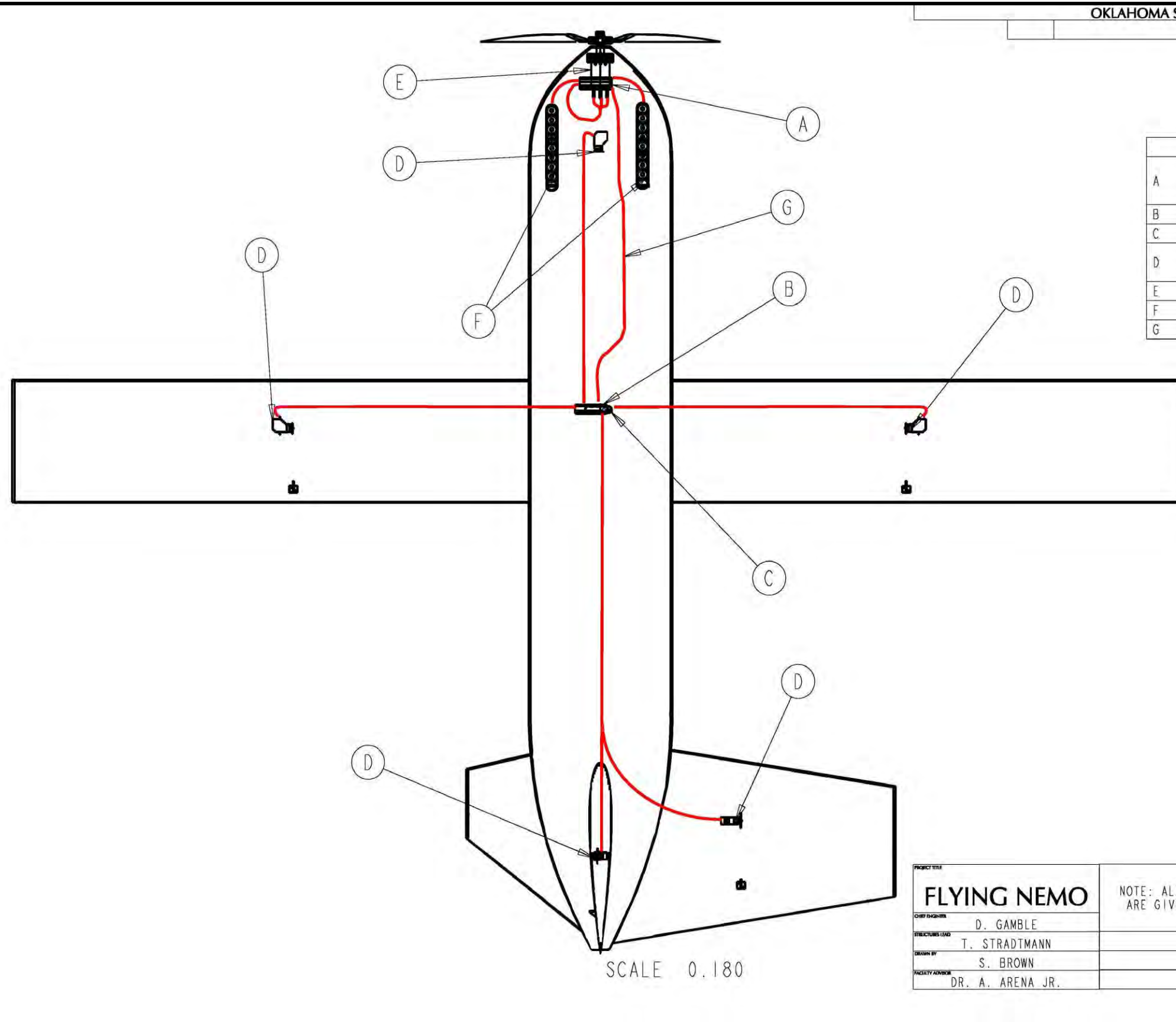


COMPONENT	MATERIAL	QTY	
A	FUSELAGE ASSEMBLY	FIBERGLASS/BALSA	1
B	FWD BULKHEAD	LIGHT PLYWOOD	1
C	CENTER BULKHEAD	LIGHT PLYWOOD	1
D	MAIN GEAR MOUNT	LIGHT PLYWOOD	1
E	AFT BULKHEAD	LIGHT PLYWOOD	1
F	WING ENDPLATE	BALSA/CARBON FIBER	2
G	WING C-CHANNEL SPAR	COMPOSITE	2
H	WING RIB	BALSA	44
I	AILERON SERVO WING RIB	LIGHT PLYWOOD	2
J	HORIZONTAL STAB ASSEMBLY	BALSA/MICROLITE	1
K	VERTICAL STAB ASSEMBLY	BALSA/MICROLITE	1
L	PROPELLER	APC 20 INCH	1
M	GEAR BOX 4.75:1	ALUMINUM/PLASTIC	1
N	NOSE GEAR ASSEMBLY	CARBON FIBER/CARBON ROD	1
O	NOSE GEAR MOUNT BULKHEAD	LIGHT PLYWOOD/BALSA	1
P	MAIN GEAR ASSEMBLY	CARBON FIBER/KEVLAR	1
Q	FIREWALL	LIGHT PLYWOOD	1
R	PAYLOAD RESTRAINT GRID	BALSA/FIBERGLASS	1
S	WING SERVO HORN	NYLON	2
T	TAIL SERVO HORN	NYLON	2
U	NOSE GEAR SERVO HORN	NYLON	1
V	WING LEADING EDGE	BALSA	4
W	WING TRAILING EDGE	BALSA	4
X	WING SKIN	MICROLITE	4
Y	LANDING GEAR WIRE	KEVLAR	1

SIDE WING VIEW



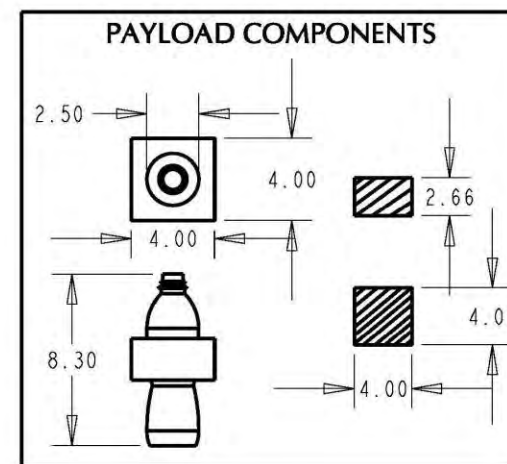
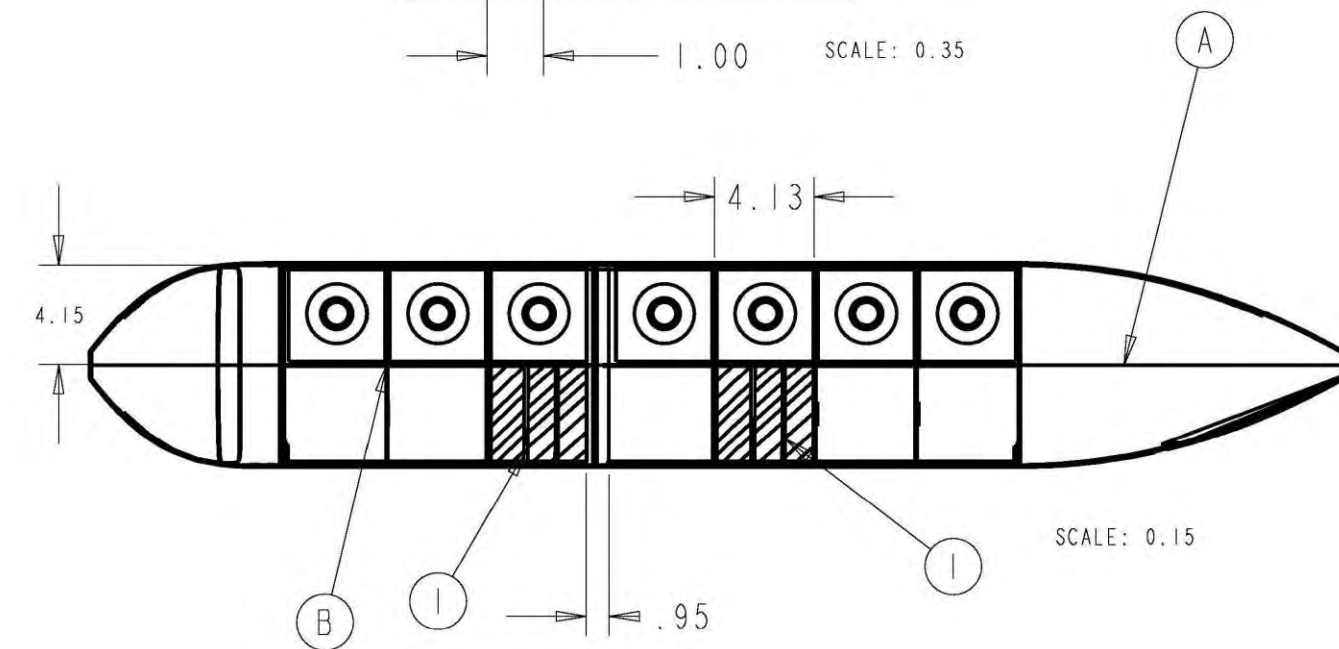
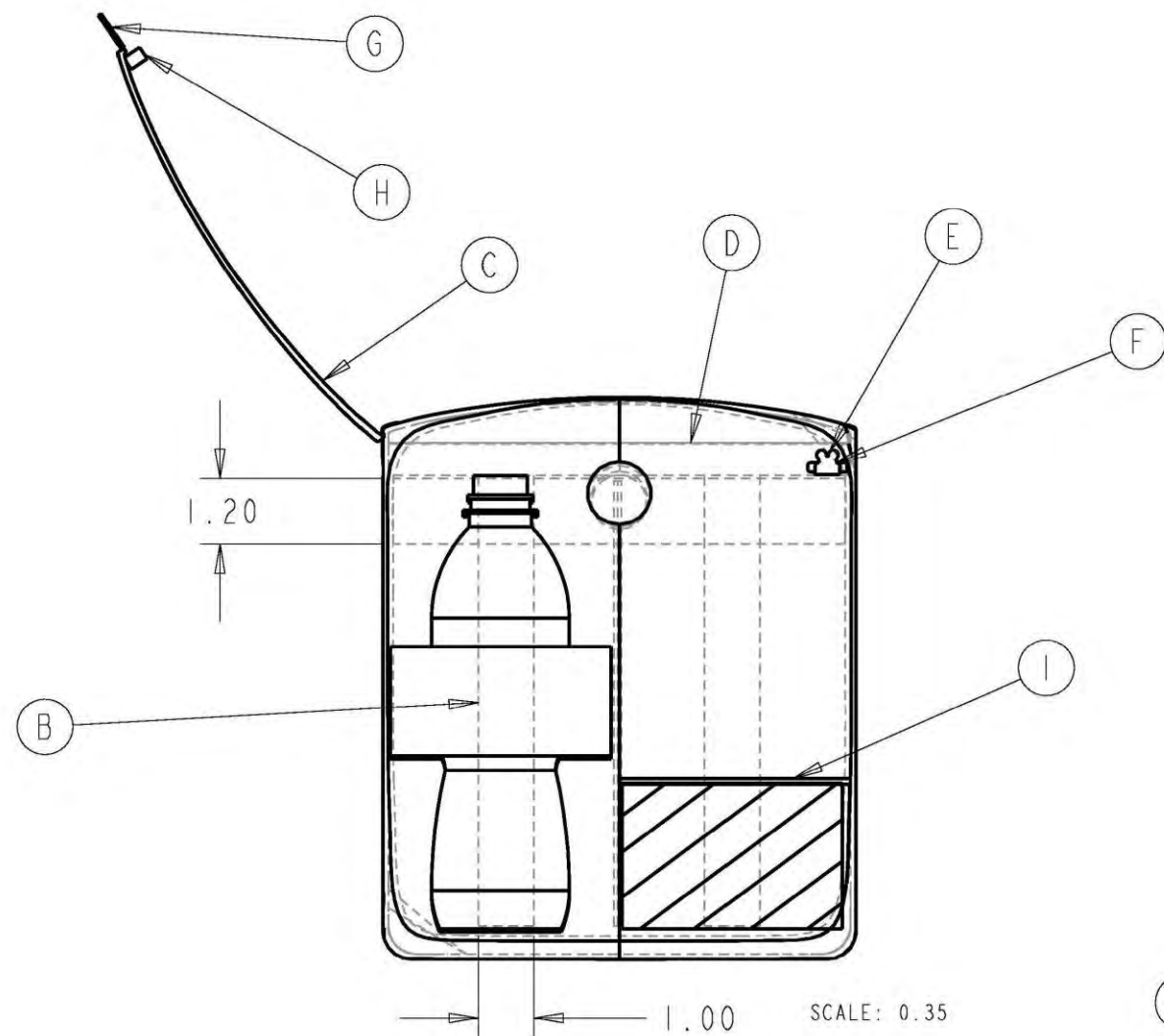
FLYING NEMO		NOTE: ALL DIMENSIONS ARE GIVEN IN INCHES		OKLAHOMA STATE UNIVERSITY ORANGE TEAM CESSNA/RAYTHEON MISSILE SYSTEMS DESIGN/BUILD/FLY 2008	
CHIEF ENGINEER	D. GAMBLE			STRUCTURAL ARRANGEMENT	
STRUCTURES LEAD	T. STRADTMANN			REVISION IR	
DESIGN BY	S. BROWN			DATE OF APPROVAL	2-13-08
FACULTY ADVISOR	DR. A. ARENA JR.			DRAWING PACKAGE	PAGE 2 OF 4



	COMPONENT	QTY
A	KONTRONIK JAZZ 40-6-18 BRUSHLESS ELECTRONIC SPEED CONTROL	1
B	SPEKTRUM AR9000 RECEIVER	1
C	6V 1000 MAH NIMH BATTERY PACK	1
D	FUTABA S3156 MICRO DIGITAL METAL GEAR SERVO	5
E	MEDUSA 028-040-1700 MOTOR	1
F	ELITE 1500 AND KAN 700AA BATTERY PACK	1
G	WIRING HARNESS	1

SCALE 0.180

PROJECT TITLE	FLYING NEMO	NOTE: ALL DIMENSIONS ARE GIVEN IN INCHES	OKLAHOMA STATE UNIVERSITY ORANGE TEAM CESSNA/RAYTHEON MISSILE SYSTEMS DESIGN/BUILD/FLY 2008	
CHIEF ENGINEER			SYSTEMS LAYOUT	
STRUCTURE LEAD	D. GAMBLE		REVISION 1R	
DESIGN BY	T. STRADTMANN		DATE OF APPROVAL	2-13-08
FACILITY ADDRESS	S. BROWN		DRAWING PACKAGE	PAGE 3 OF 4
	DR. A. ARENA JR.			



PRIMARY COMPONENT LIST	
A	FUSELAGE
B	GRID
C	PRIMARY HATCH
D	PAYLOAD RESTRAINT
E	CARBON ROD
F	LATCHES
G	TAB
H	MAGNETS
I	RUBBER BAND

PROJECT TITLE FLYING NEMO		NOTE: ALL DIMENSIONS ARE GIVEN IN INCHES		OKLAHOMA STATE UNIVERSITY ORANGE TEAM CESSNA/RAYTHEON MISSILE SYSTEMS DESIGN/BUILDFLY 2008	
CHIEF ENGINEER	D. GAMBLE			PAYLOAD ACCOMMODATION	
STRUCTURAL LEAD	T. STRADTMANN			DATE OF APPROVAL	REVISION IR
DRAWN BY	S. BROWN			2-13-08	
FACULTY ADVISOR	DR. A. ARENA JR.			DRAWING PACKAGE	PAGE 4 OF 4

6.0. Manufacturing Plan and Processes

Several materials, construction techniques, and assembly methods were considered for each component in order to select the most appropriate, based upon the established FOM's in Section 3.2.2. In some cases, trial components were constructed by different methods to help facilitate a better understanding of the advantages and disadvantages of each technique and material. A manufacturing schedule was also created to establish deadlines and partition tasks to promote completion of deadlines.

6.1. Component Manufacturing Processes

Each FOM from Section 3.2.2 was reassessed for construction applicability. Additional FOM's were generated if needed.

6.1.1. Figures of Merit

To effectively compare the variety of manufacturing techniques, the following figures of merit were analyzed for each alternative. The FOM's discussed in Section 3.2.2 were adapted for specific analysis of construction techniques. No construction technique bore any relevance to fly ability, aerodynamic efficiency or loading time.

- **System Weight** – The system weight appeared in the score function and is directly affected by the results of the manufacturing process. Construction techniques and materials were chosen to minimize weight whenever possible.

In addition to the figures of merit used earlier, the structures team created four new items specifically for evaluating different construction techniques.

- **Construction Time** – Time constraints were a significant concern; construction techniques that allow tasks to be performed in parallel are preferred. Minimization of downtime was a priority concern for each manufacturing process.
- **Construction Cost** – Manufacturing techniques that reduced cost by reducing material waste or using less expensive materials were preferred.
- **Serviceability** – The potential for aircraft damage at the contest necessitated consideration of each component's ability to be replaced or repaired in the instance of failure.
- **Strength** – The component must be strong enough to withstand high loads conditions to prevent failure. Durability is also a concern—the part must not deteriorate appreciably with use.

6.1.2. Fuselage

Three methods were investigated prior to construction: Foam core, mold, and stringer-frame methods. The foam core method allows the fuselage to be made from cut foam, laid up, and the foam is cut away, which makes a fast procedure relative to the other methods. The downside to the foam method is weight. The mold method requires the construction of a plug to make the mold. The stringer-frame method relies on internal framework for its strength. However, stringer-frame takes an extensive amount

of time that does not allow for fast repeatability. Weight savings and time are the compromise that the mold method makes to become the desired choice.

The fuselage must maintain its form during flight and withstand payload insertion. Balsa was selected as the skin material of choice because it met these requirements. The complex form of the fuselage is achieved by constructing within a mold; the mold-making process itself is quite involved and time-intensive. However, some departures from the prior process offered a significant reduction in downtime during construction. To construct the fuselage, 1/16 in thick balsa was formed wet within the mold and dried to retain the shape of each half. After drying, the balsa shell was sandwiched between two layers of 0.7 oz/yd² fiberglass to preserve the shape and enhance rigidity. Each half of the fuselage was bonded with aircraft grade plywood bulkheads.

6.1.3. Wings

A variety of materials and construction techniques were considered for the wings. These configurations are analyzed based upon FOM analysis in Figure 6.1.

Figure of Merit	Weight	Balsa Only	Balsa Skin/ Carbon Spar	Microlite/ Carbon Spar	Microlite/ Balsa Spar
System Weight	0.35	0	-1	1	1
Construction Time	0.15	0	-1	-1	1
Construction Cost	0.05	0	-1	-1	0
Serviceability	0.10	0	-1	-1	0
Strength	0.35	0	1	1	-1
Overall Score	1	0	-0.3	0.4	0.15

Figure 6.1: Weighted Decision Matrix for Wing Manufacturing

In addition, several practice wings were constructed and subsequently tested to failure to provide a more concrete basis from which to judge factors such as strength, construction time and reparability.

The large wingspan created severe bending loads within the main spar; as such, strength and rigidity were of major concern. However, a biplane design necessitates very light wing manufacturing to keep the system weight at or below that of comparable monoplane configurations. The Microlite / carbon spar combination offered the optimal combination of strength and durability while keeping system weight low. There are a few different methods for building the wings, but the carbon spar and Microlite limit it to a traditional build-up over foam wings and molded wings.

The spar strength came from utilizing a C-channel post bonded to a bulkhead. The C-channel was created using sections of 3/4 in tall, 3/16 in thick vertical grain balsa for the shear web, with carbon fiber on the flanges. Based upon prior analysis, carbon fiber content in the web was increased in the vicinity of the fuselage to better accommodate the larger stresses present at the base of the wings. The outer third of the span utilized a pure balsa C-channel. The leading edges of each wing were created from 1/16 in balsa shaped within a precisely cut foam mold. In order to minimize weight and construction time, the ribs were cut from balsa using a CNC machine. The ribs slid onto the C-channel and were arranged atop the shaped foam mold. Three-inch rib spacing was chosen to compromise between weight and tension in the

Microlite. The wings were then covered in Microlite, a thin film which was ironed directly onto the balsa wing structure. A separate structural rib was used in place of a balsa rib to support the servo.

The empennage used similar FOM as the wings for the decision. The lower aerodynamic loads on the tail did not require additional reinforcement. The Microlite / balsa spar choice becomes the best option which also requires the build-up method for construction again similar to the wings.

6.1.4. Landing Gear

The primary focus of the manufacturing plan for the landing gear was on the main bow gear which would see potentially significant impact forces upon landing. FOM analysis in conjunction with the relative ease of creating prototype lay-ups enabled evaluation of manufacturing techniques for the main gear.

Figure of Merit	Weight	Carbon Only	Carbon & Balsa	Carbon, Balsa & Wire	Aluminum Struts
System Weight	0.4	0	1	1	-1
Construction Time	0.05	0	0	0	1
Construction Cost	0.05	0	0	-1	0
Serviceability	0.2	0	0	0	1
Strength	0.3	0	0	1	-1
Overall Score	1	0	0.4	0.65	-0.45

Figure 6.2: Weighted Decision Matrix for Landing Gear Manufacturing

Figure 6.2 shows a weighted decision matrix comparing the techniques. An ideal balance between strength and weight as desired for the main gear—pure carbon fiber designs proved resilient, but also relatively heavy. Incorporating balsa into the lay-up preserved the rigidity of the carbon fiber lay-ups, but reduced weight significantly. The optimal structure was a lightweight design which consisted of 3/16 inch thick balsa fitted between three layers of carbon fiber, featuring a taut wire between the wheels to enhance strength under impact. The gear would be laid up in a shaped mold and utilize Kevlar strips to reinforce bolt contact points. The nose gear construction process consisted of laying up two strips of carbon fiber around Kevlar on top of a shaped mold. A small balsa block sandwiched within the lay-up provided a mount for a carbon fiber tube to connect the gear to the bulkhead within the fuselage.

6.1.5. Manufacturing Schedule

After completion of the design process, a manufacturing schedule was created to establish deadlines. Projected completion times were allotted based upon time to complete practice lay-ups. Figure 6.3 shows a schedule for manufacturing the aircraft and major aircraft components.

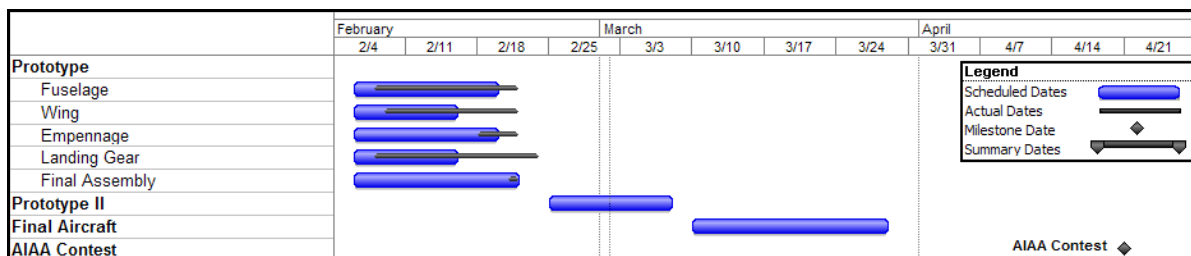


Figure 6.3: Manufacturing Schedule

6.1.6. Project Cost

Figure 6.4 shows a total project cost estimate and Figure 6.5 shows the per-aircraft material and construction cost estimate.

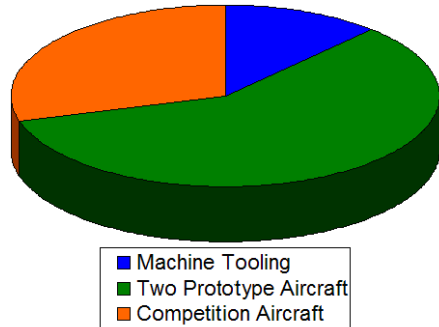


Figure 6.4: Projected Project Cost

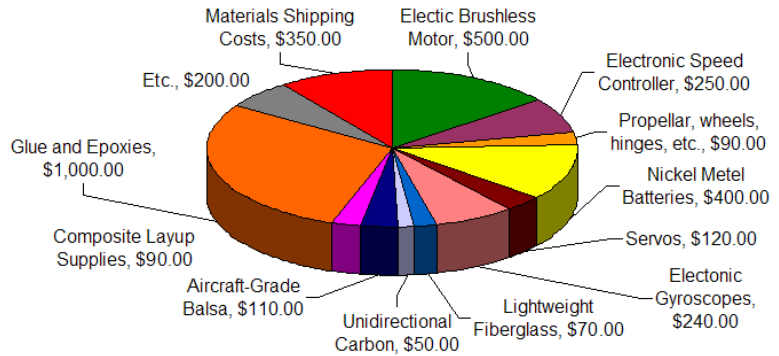


Figure 6.5: Projected Per-Aircraft Cost

7.0. Testing Plan

The time constraints placed on developing the aircraft required the team to schedule testing such that key systems were completed early on. Initial testing of the completed aircraft began in the third week of February, which allowed time for more thorough mission testing and score optimization. The testing schedule is shown in Figure 7.1

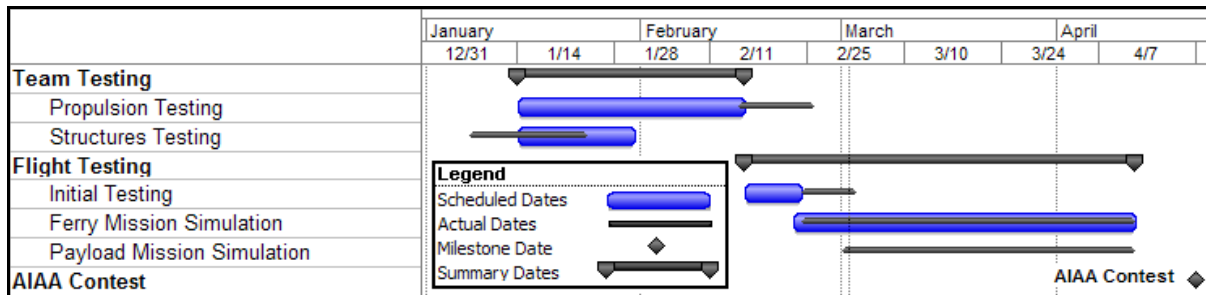


Figure 7.1: Testing Schedule

7.1. Propulsion and Structural Testing

Propulsion system testing was performed to investigate batteries, propellers, and motors and find any discrepancies from predicted performance. Batteries were charged and discharged repeatedly to find their capacity and discharge rates compared with those given by the manufacturer. Propellers were bench tested for take-off (static) performance and cruise efficiency (dynamic, wind tunnel). Objectives of motor testing were to determine if power generation was sufficient, while investigating cooling methods to prevent overheating. Reliably pushing the motor to its limit was the main concern during testing. Propellers were tested on a dynamometer to collect thrust, torque, RPM, and airspeed data, which was used to create thrust, power, and efficiency curves. The results from these tests allowed the implementation of a highly efficient propulsion system in the final design.

The testing goal of the structures group was to validate preliminary calculations and determine the

optimized hardware for the completed aircraft. The testing occurred as soon as construction was completed on each component to learn lessons that could be immediately applied to the next build. The testing plan was to develop one ft test sections of various materials and load them with weight at the center while supported at the ends. Landing gear was tested with a simulated hard landing by being dropped one ft while loaded with the appropriate weight. The landing gear testing goal was to confirm the design strength and reduce the overall weight.

7.2. Flight Testing

Due to the many uncertainties in aerodynamic analysis, flight testing the design was a crucial step in maximizing the aircraft's performance. The initial flight tests were executed in three separate flights, each with unique objectives. A shakedown flight was performed first to verify control functionality, structural integrity, and trim the control surfaces for further testing. Next, a trial run of the delivery mission was flown to verify thrust and drag predictions, observe energy usage, check the completion time, and assess the overall mission competency. The last test flight was a used to evaluate the aircraft's performance with a payload. Flight objectives included making sure take-off power was adequate, verify thrust and drag predictions, measure energy usage, and assess system's overall mission competency. The information gained in these flights was invaluable for maximizing the aircraft's score.

7.2.1. Checklists

Figure 7.2 shows an example of a pre-flight checklist used during the initial test flight section. The team identified key structural and systems checks to ensure that tests were properly prepared.

Structural Integrity				Controls		Propulsion / Electronics					
Visually and physically inspect each component for defects or damage				Verify range of motion		Verify electronics communication / performance					
<input type="checkbox"/>	Fuselage	<input type="checkbox"/>	Horizontal Stabilizer	<input type="checkbox"/>	Hatch Lid	<input type="checkbox"/>	Ailerons	<input type="checkbox"/>	Batteries Charged	<input type="checkbox"/>	Fail-Safe Activated
<input type="checkbox"/>	Wings	<input type="checkbox"/>	Vertical Stabilizer	<input type="checkbox"/>	Hatch Fastener	<input type="checkbox"/>	Elevator	<input type="checkbox"/>	Battery Temperature	<input type="checkbox"/>	Radio Fail-Safe Activated
<input type="checkbox"/>	Landing Gear	<input type="checkbox"/>	Control Surfaces	<input type="checkbox"/>	Payload Restraint System	<input type="checkbox"/>	Rudder	<input type="checkbox"/>	Servos Active (5)	<input type="checkbox"/>	
<input type="checkbox"/>	Bond Lines	<input type="checkbox"/>	Internal Bulkheads	<input type="checkbox"/>	Payload Restraint Fasteners	<input type="checkbox"/>		<input type="checkbox"/>	5 sec. Throttle Run Up	<input type="checkbox"/>	
Systems Integrity					Final Checks						
Visually and physically inspect each component for defects or damage, verify component is secure					Verify final testing parameters are prepared, verbally confirm crew readiness ("go" / "no go")						
<input type="checkbox"/>	Motor	<input type="checkbox"/>	Servo Motors (5)	<input type="checkbox"/>	Control Surface Hinges	<input type="checkbox"/>	Final Visual Inspection	<input type="checkbox"/>	Pilot	<input type="checkbox"/>	Structures Lead
<input type="checkbox"/>	Propeller	<input type="checkbox"/>	Servo Wiring	<input type="checkbox"/>	Bolts and Fasteners	<input type="checkbox"/>	Specific Test Readiness	<input type="checkbox"/>	Spotter	<input type="checkbox"/>	Propulsion Lead
<input type="checkbox"/>	Battery Pack	<input type="checkbox"/>	Connector Rods	<input type="checkbox"/>	Nose Gear	<input type="checkbox"/>	Data Collection	<input type="checkbox"/>	Ground Crew	<input type="checkbox"/>	Chief Engineer
<input type="checkbox"/>	Speed Controller / Gearbox	<input type="checkbox"/>	Hatch	<input type="checkbox"/>	Main Gear	<input type="checkbox"/>		<input type="checkbox"/>		<input type="checkbox"/>	

Figure 7.2: Preflight Checklist

8.0. Performance Results

The results from the performance tests set out in the previous section allowed comparisons to be

made between the predictions contained in the detailed design phase and the actual aircraft performance.

8.1. Propulsion Performance

Performance results for propulsion system components as well as the whole system in flight were obtained during testing. Figure 8.1 shows the discrepancies between the advertised battery performance and the actual battery performance observed during testing.

During testing, new batteries were charged and discharged, allowing them to cycle and charge to their full capacity providing better data. The batteries were tested individually to search for and eliminate batteries with low capacity and poor results. Testing was done at the current that was expected during takeoff and in cruise. The data recorded was used to determine which batteries and how many were needed in each mission to provide the best score.

Propeller testing was done by putting each one on a motor attached to a dynamometer inside of a wind tunnel. This setup allowed for measurement of the RPM, thrust, and torque caused by the propeller at different wind speeds. The team calculated the propeller power coefficient, propeller thrust coefficient, and the overall propeller efficiency. Comparisons between propellers could be made simply by putting a different propeller onto the test stand. Efficiency, thrust, and power were compared to make the decision on which propeller to use in each mission, shown Figure 8.2. The propellers that achieved the highest efficiency were then input into the propulsion system optimization to determine the highest possible score for the missions. Analysis of the efficiency curves generated during testing indicated an 18x10 propeller would perform more efficient for the delivery mission. However, the reduction in battery weight made possible by using a 20x11 for the payload mission merited the efficiency reduction.

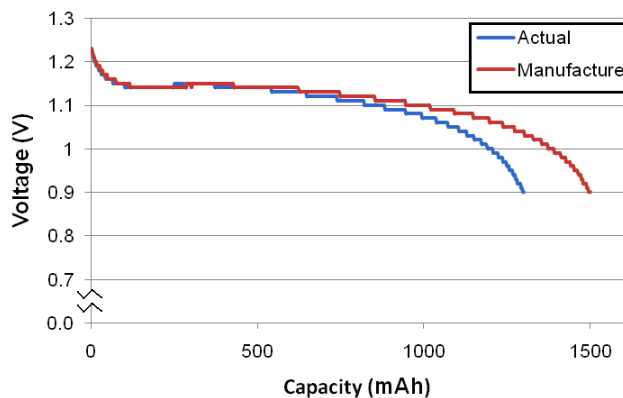


Figure 8.1: Actual vs. Manufacture Battery Data

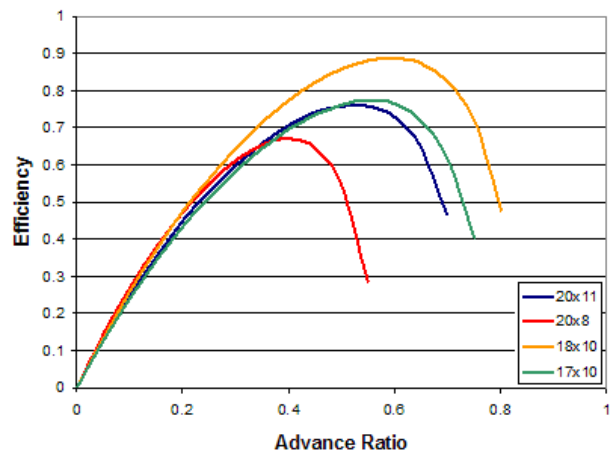


Figure 8.2: Propeller Efficiency Curves

Initial flight testing was used to obtain performance data of the propulsion system in flight. The first flight used an Elite battery pack with no payload present allowed ample flight time to decrease the risk of failure. The delivery mission trial, which was the second of three flights, was flown with KAN batteries. Detailed analysis indicated the aircraft would have been capable of four laps, but enough data was obtained from flying two. The final flight trial was a mock payload mission. Twelve Elite batteries were

used to carry an eight pound payload. The aircraft attempted the short take-off and one lap. Data regarding the battery capacity used and voltage was recorded and documented in Table 8.1.

Table 8.1: Propulsion Flight Test Results

Flight	Time	Battery Pack	Capacity Used	Voltage	Laps
1	3 min 2 sec	12 Elite 1500	337 mAh	15.7 V	N/A
2	3 min 15 sec	12 KAN 700AA	384 mAh	15.16 V	2
3	2 min 13 sec	12 Elite 1500	562 mAh	15.5 V	1

The aircraft successfully completed one lap, along with a 360°-turn upon landing. It did not obtain a 75 ft takeoff, but achieved 85 ft. After analyzing the aircraft the extra measuring equipment added 0.7 lbs of weight. When the propulsion system optimization compensated for the wind conditions and the additional weight, the theoretical take off was 87 ft which matches that of the actual test flight. The number of possible laps was compared with the program data as well. The data did not take into account the power needed for takeoff and landing. The consumption that was recorded from the flight data contained the entire flight (throttle up, takeoff, cruise, and landing). The aircraft is mission capable based on energy usage recorded during the flight test.

8.2. Structural Performance

Post testing results for the structural subsystems were positive results. The fuselage remained intact for all flight missions with full structural integrity. The wings remained fixed to the bulkhead with no stress marks. Multiple landings were endured with no cracks or breaks in the fuselage. The tails caused no damage and maintained correct positioning after flight. The changes planned for the fuselage are creating a separate hatch structure that is not as strong or heavy. As a result bulkheads would have to be trimmed down as well resulting in a significant weight savings.

The wings did not appear to deflect much or at all during flight. All wing connections remained intact and no part of the structure was damaged. The tip test, shown in Figure 8.3, simulated a 2.5-G load which was also successful for a fully loaded aircraft. Due to wing performance, rib spacing will be increased to save additional weight, but holes will be removed to make installation and manufacturing easier.

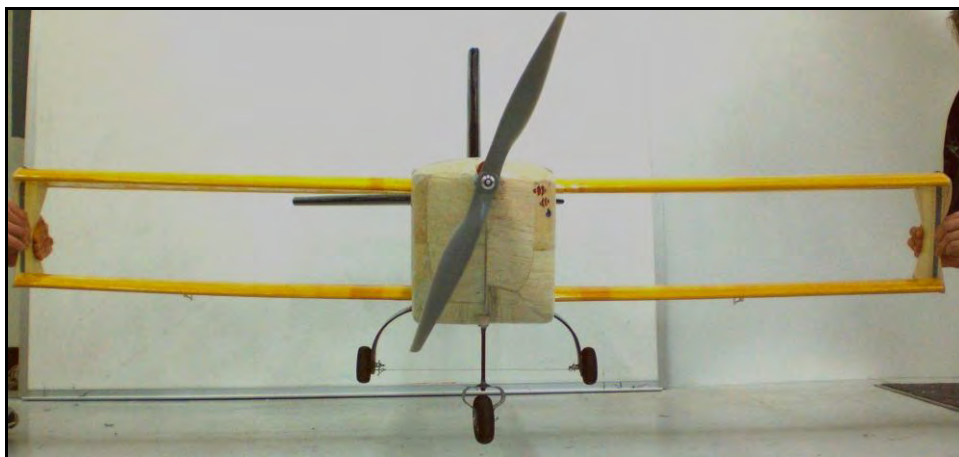


Figure 8.3: Tip-Test (fully loaded)

The tail remained intact. The control surfaces proved to be effective and the servos were able to provide enough support for the torque seen on the control. The adequate strength of the wings gives the possibility to change the tail structure to a lighter structure equivalent to the main wings.

The main gear survived several drop tests from various heights and various angles to simulate crooked landings fully loaded. The nose gear fully functioned during taxi tests and takeoffs according to the design specifications. The improvements would be decreasing the weight of the main gear and sacrifice some strength that might be excessive.

The overall improvements and lessons learned resulted in more precise structural geometries and reduced weight. Wing construction was improved by eliminating the superfluous holes in the rib, which increase weight slightly but greatly improved wing rigidity. Additionally, constructing the hatch out of a balsa frame wrapped in Microlite produced significant weight savings.

8.3. Demonstrated Aircraft Performance

Data collected during flight testing include position, time, average wind speed, and power usage. Data sets were collected for a trial run of the delivery mission and the payload mission. Evaluation of the data was performed by determining the average velocity for each leg of the mission using the position and time data. The ground velocity and average wind speed were then used to approximate the free stream velocity the aircraft was exposed to. Average velocity data for the delivery mission trial can be seen in Table 8.2. Figure 8.4 shows photos taken during the maiden flight.

Table 8.2: Delivery Mission Trial Data

Leg	Time (s)	Distance (ft)	Ground Speed (ft/s)	Wind Velocity (ft/s)	Velocity (ft/s)
Climb Out	31	500	16.13	-10	26.13
Cruise 1	11	537.5	48.86	10	38.86
Cruise 2	10	537.5	53.75	10	43.75
Cruise 3	41	1075	26.22	-10	36.22
Cruise 4	10	537.5	53.75	10	43.75
Cruise 5	8	537.5	67.19	10	57.19
Descent	36	537.5	14.93	-10	24.93

The delivery mission performance trial covered two complete circuits of the course including climb-out and descent in a 10 ft/s wind. To avoid pushing the aircraft to its limits, only half of the four circuits for the mission were completed and total mission performance was extrapolated out. Approximately half of the capacity of the KAN 700 batteries was used. Each leg of the mission shown in the table represents flight in a straight line between pylons and each leg is separated by the appropriate turning maneuver stipulated by the rules. Turning times were recorded but determining turning distances was not possible, so they were excluded from the analysis. The data shows that the majority of the mission was flown off of optimal cruise velocity. Additionally, a similar trial was performed for the payload mission. Data for the payload trial can be seen in Table 8.3.

The payload trial was only conducted for one circuit of the course in a 5 ft/s wind. 12 Elite 1500

batteries were used and approximately half of their capacity was depleted. Again, only half the mission was completed for safety reasons. Total mission performance was extrapolated from the trial result. The results of the payload trial show that it was also flown off optimal.

Table 8.3: Payload Mission Trial Data

Leg	Time (s)	Distance (ft)	Ground Speed (ft/s)	Relative Winds (ft/s)	Velocity (ft/s)
Climb Out	19.0	500	26.32	-5.0	31.32
Cruise 1	8.0	537.5	67.19	5.0	62.19
Cruise 2	9.0	537.5	59.72	5.0	54.72
Cruise 3	19.0	537.5	28.29	-5.0	33.29

Although neither of the missions was flown in full, the aircraft is capable of flying both missions from the energy usage data. The potential for significant improvements is possible by flying closer to the optimal velocity. In section 5 mission scores were projected as 13.16 and 0.816 for the delivery and payload missions, respectively. The actual flight test indicates a delivery mission score of 7.08 due to the greater number of batteries and inability to complete the fourth lap in less than 5 minutes. However, the payload score increased from a projected 0.816 to an actual 1.21.



Figure 8.4: Documented Flight Performance Photos (Flight Test #1 – February 24th, 2008)

References

- Anderson, John D. Jr. Aircraft Performance and Design. New York City, NY: WCB/McGraw-Hill, 1999.
- Arena, A.S. Class notes. Unpublished. 2007
- Budynas, Richard G., and J. Keith Nisbett. Shigley's Mechanical Engineering Design. 8th ed. New York: McGraw-Hill, 2008.
- Hoerner, Sighard F. Fluid-Dynamic Drag. New York City, NY: 1964.
- Hoerner, Sighard F., and Henry Borst. Fluid-Dynamic Lift. 2nd ed.. New York City, New York: 1965.
- Nelson, Robert. Flight Stability and Automatic Control. 2nd ed New York, NY: The McGraw-Hill Companies, Inc., 1998.
- Raymer, Daniel. Aircraft Design: A Conceptual Approach. 3rd ed. Reston, Virginia: American Institute of Aeronautics and Astronautics, Inc., 1999.